THE UNIVERSITY of ADELAIDE

Characterisation and Treatment of Pan-Human Epidermal Receptor Tyrosine Kinase Inhibitor-Induced Gastrointestinal Toxicity

A thesis submitted in fulfilment for degree of

DOCTOR OF PHILOSOPHY

in

The Discipline of Physiology

Adelaide Medical School

The University of Adelaide

by

Ysabella Van Sebille

September 2017

Declaration

"I certify that this work contains no material which has been accepted for the award of any other degree or diploma in my name in any university or other tertiary institution and, to the best of my knowledge and belief, contains no material previously published or written by another person, except where due reference has been made in the text. In addition, I certify that no part of this work will, in the future, be used in a submission in my name for any other degree or diploma in any university or other tertiary institution without the prior approval of the University of Adelaide."

I give consent for this copy of my thesis, when deposited in the University Library, being made available for loan and photocopy, subject to the provisions of the Copyright Act 1968. I acknowledge that copyright of published works contained within this thesis reside with the copyright holders of those works.

I also give permission for the digital version of this thesis to be made available on the web, via the University's digital research repository, the Library Search and also through web search engines.

Ysabella Van Sebille

September 2017

Table of Contents

DECLARATION ..... **II**

TABLE OF CONTENTS ..... **III**

ACKNOWLEDGEMENTS ..... **VI**

PUBLICATIONS ARISING FROM THIS THESIS ..... **VIII**

CONTRIBUTIONS MADE BY CO-AUTHORS ..... **IX**

ADDITIONAL STUDIES AND PUBLICATIONS ..... **XX**

THESIS EXPLANATION ..... **XXIII**

HYPOTHESIS AND AIMS ..... **XXV**

NOMENCLATURE ..... **XXVII**

CHAPTER 1 GASTROINTESTINAL TOXICITIES OF FIRST AND SECOND GENERATION SMALL MOLECULE HUMAN EPIDERMAL GROWTH FACTOR RECEPTOR TYROSINE KINASE INHIBITORS IN ADVANCED NON-SMALL CELL LUNG CANCER **3**

ABSTRACT 3
INTRODUCTION 4
HER TKIS 5
DIARRHOEA 5
MECHANISMS 8
FIRST GENERATION HER-TKI- GEFITINIB 8
SECOND GENERATION HER TKI- DACOMITINIB 10
CONCLUSION 12

CHAPTER 2 ERBB SMALL MOLECULE TYROSINE KINASE INHIBITOR (TKI) INDUCED DIARRHOEA: CHLORIDE SECRETION AS A MECHANISTIC HYPOTHESIS **16**

ABSTRACT 16
INTRODUCTION 16
ERBB RECEPTORS 18
ERBB TKIS AND DIARRHOEA 21
DO ERBB TKIS INDUCE DIARRHOEA VIA A DISTINCTLY DIFFERENT MECHANISM THAN CHEMOTHERAPY-INDUCED DIARRHOEA? 22
CHLORIDE SECRETION AND DIARRHOEA 25
TKI AND CHEMOTHERAPY CONCOMITANT THERAPY 30
CURRENT TREATMENT APPROACHES FOR TKI-INDUCED DIARRHOEA 31
POTENTIAL TREATMENT APPROACHES FOR TKI-INDUCED DIARRHOEA 33
CONCLUSION 34

CHAPTER 3 DACOMITINIB-INDUCED DIARRHOEA IS ASSOCIATED WITH ALTERED GASTROINTESTINAL PERMEABILITY AND DISRUPTION IN ILEAL HISTOLOGY IN RATS **38**

ABSTRACT 38
INTRODUCTION 39
MATERIALS AND METHODS 41

Chemicals *41*
In vitro Model *41*
In vivo Model and Ethics *43*
Experimental Design *43*
Clinical Assessment of Gastrointestinal Toxicity *43*
Tissue Preparation *44*
Blood Biochemistry *44*
Gastrointestinal Histopathological Analysis *45*
Goblet Cell Analysis *45*
Immunohistochemistry *45*
Real Time PCR *46*
Tissue Cytokine Quantification *47*
FITC-dextran Assay *48*
Statistical Analysis *48*
RESULTS 49
Dacomitinib Does Not Cause Direct Cytotoxicity to T84 Epithelial Cells *49*
Dacomitinib Causes Reproducible, Severe Diarrhoea *51*
Dacomitinib Alters Biochemistry and Histology *53*
Dacomitinib Causes Significant ileal Damage *53*
Dacomitinib Did Not Alter Gastrointestinal Apoptosis or Proliferation *57*
ErbB1 Receptor is Highly Expressed in the Ileum *57*
Dacomitinib Treatment Increases Levels of monocyte chemoattractant protein-1 (MCP-1) in the ileum *60*
Dacomitinib Caused Increased Gastrointestinal Permeability *62*
DISCUSSION 64
CONCLUSION 67
SUPPLEMENTARY TABLE 68

CHAPTER 4 DACOMITINIB-INDUCED DIARRHOEA: TARGETING CHLORIDE SECRETION WITH CROFELEMER 72
ABSTRACT 72
INTRODUCTION 73
MATERIALS AND METHODS 74
Chemicals *74*
In vitro Model *75*
Cell Preparation and Maintenance *75*
In vitro Electrophysiological Studies using Ussing Chambers *76*
In vivo Model *77*
Ethics *77*
Experimental Design *77*
Clinical Assessment of Gastrointestinal Toxicity *78*
Tissue Preparation *78*
In vivo Electrophysiological Studies using Ussing Chambers *78*
Serum Drug Analysis *79*
FITC-dextran Assay *80*
Histopathological Analysis *80*
Immunohistochemistry *81*
Tight Junction Analysis *81*
Statistical Analysis *83*
RESULTS 83
Crofelemer Inhibits Dacomitinib-Induced Chloride Secretion in vitro *83*
Crofelemer is ineffective at reducing dacomitinib-induced diarrhoea *85*
Weight loss *87*
Crofelemer did not inhibit chloride secretion in the presence of dacomitinib in this model *89*
Crofelemer does not increase serum absorption of dacomitinib *91*

Dacomitinib induces gastrointestinal permeability *93*
Cytoplasmic redistribution of tight junction proteins contributes to dacomitinib-induced barrier dysfunction *95*
Crofelemer does not attenuate dacomitinib induced histopathological injury *99*
DISCUSSION 101
CONCLUSION 107

CHAPTER 5 USE OF ZEBRAFISH TO MODEL CHEMOTHERAPY AND TARGETED THERAPY GASTROINTESTINAL TOXICITY 110
ABSTRACT 110
INTRODUCTION 111
METHODS 113
Fish Husbandry *113*
Drug Treatment *113*
Imaging and tissue preparation *117*
Histopathological analysis *117*
Goblet Cell Analysis *117*
Immunohistochemistry *118*
Statistics *118*
RESULTS 119
Dose titration *119*
Transgenic zebrafish larvae fluorescence imaging *121*
Histopathological intestinal analysis in adult zebrafish *123*
DISCUSSION 125
CONCLUSION 128

CHAPTER 6 GENERAL DISCUSSION 129
INTRODUCTION 129
HISTOPATHOLOGICAL DAMAGE TO THE ILEUM, BARRIER DYSFUNCTION, AND INFLAMMATION: TRAITS OF DACOMITINIB-INDUCED GASTROINTESTINAL TOXICITY 131
HIGHLIGHTING LIMITATIONS TO THE HYPOTHESIS OF CHLORIDE SECRETORY MECHANISMS FOR TKI-INDUCED DIARRHOEA WITH CROFELEMER 134
BRIDGING THE GAP BETWEEN *IN VITRO* AND WHOLE-ORGANISM MODELS WITH ZEBRAFISH 138
CONCLUSION 142

CHAPTER 7 REFERENCES 143

APPENDIX 1: PUBLICATIONS ARISING FROM THIS THESIS 156

APPENDIX 2: PFIZER REPORT 191

Acknowledgements

I extend my sincere thanks and gratitude to my supervisors, Associate Professor Joanne Bowen, and Professor Rachel Gibson for giving me countless opportunities, unwavering support, and encouragement. I cannot express how lucky I have been to have you as my mentors.

In addition, I would like to thank my dear friend and colleague, Dr. Hannah Wardill for her endless support, guidance, encouragement and friendship. I cannot imagine doing this without you by my side, and I am forever grateful for all this, and so much more.

Thank you to members of the Cancer Treatment Toxicities Group, specifically Dr. Janet Coller, Ms Imogen Ball, Ms Kate Secombe, Ms Romany Stansborough and Mr Anthony Wignall for technical assistance, and support.

Thank you to members of The Adelaide Medical School for their encouragement, support and technical assistance. In particular, sincere thanks to Dr. Danijela Menicanin, Professor Mario Ricci, Mr. Kent Algate, Dr. Viythia Katharesan, Ms Emily Schneider, Mr. Jim Manavis and other members of histology and laboratory animal services.

I would like to thank Associate Professor Tom Carney from The Institute of Molecular and Cell Biology, Biopolois, Singapore for providing me the opportunity to complete research with his zebrafish reporter line in Singapore with his group. In regards to this

research, thanks also to Associate Professor Joanne Bowen, for providing me with the opportunity, to Tom Lynas for his support, and special thanks to Ashley Shu Mei NG and other members of the lab at IMCB, Biopolis Singapore. I would like to thank the Walter and Dorothy Duncan Trust Travel Grant, the Research Abroad Scholarship and the Global Learning Travel Grant for their financial support of this trip.

Thank you to Pfizer Pharmaceuticals for providing funds to carry out my research projects. I would also like to thank The Florey Medical Research Project Grant in Cancer Research and The Doctor Chun Chung Wong and Madam So Lau Lam Memorial Postgraduate Scholarship for their support. In addition, I would like to thank the Channel 9 Young Achiever Award committee for their continued support, the Australian Society for Medical Research and the Multinational Association of Supportive Care in Cancer for recognising my research.

Finally, thank you also to my family for their support and encouragement. I would particularly like to thank Ashley Crocker, Serrin Ainslie, Tom Lynas and my Mum and Dad for their unwavering support.

Publications arising from this thesis

***Van Sebille, Y.Z.,** Gibson, R.J., Wardill, H.R., Bowen J.M., (2016) Gastrointestinal toxicities of first and second-generation small molecule human epidermal growth factor receptor tyrosine kinase inhibitors in advanced non-small cell lung cancer. Current Opinion in Supportive and Palliative Care. 10 (12) 152-156

Van Sebille, Y.Z., Gibson, R.J., Wardill, H.R., Bowen, J.M., (2015) ErbB small molecule tyrosine kinase inhibitor (TKI) induced diarrhoea: Chloride secretion as a mechanistic hypothesis. Cancer Treatment Reviews. 41(7) 646-752

Van Sebille Y.Z., Gibson, R.J., Wardill, H.R., Secombe, K.R., Ball, I.A., Keefe, D.M., Finnie, J.W., Bowen, J.M., (2017), Dacomitinib-induced diarrhoea is associated with altered gastrointestinal permeability and disruption in ileal histology in rats. International Journal of Cancer.140 (12), 2820-2829

Van Sebille, Y.Z., Gibson, R.J., Wardill, H.R., Ball, I.A., Keefe, D.M., Bowen, J.M., (2017), Dacomitinib-induced diarrhoea: targeting chloride secretion with crofelemer. International Journal of Cancer, Accepted, *In Press*

Van Sebille, Y.Z., Bowen, J.M., Gibson, R.J., Wardill, H.R., Carney, T.J., (2017), Use of zebrafish to model chemotherapy and targeted therapy gastrointestinal toxicity, *Submitted to Supportive Care in Cancer*

*Denotes invited review

Contributions made by co-authors

Associate Professor Joanne Bowen

Van Sebille, Y.Z., Gibson, R.J., Wardill, H.R., **Bowen J.M.,** (2016) Gastrointestinal toxicities of first and second-generation small molecule human epidermal growth factor receptor tyrosine kinase inhibitors in advanced non-small cell lung cancer. Current Opinion in Supportive and Palliative Care. 10(12) 152-156.

Van Sebille, Y.Z., Gibson, R.J., Wardill, H.R., **Bowen, J.M.,** (2015) ErbB small molecule tyrosine kinase inhibitor (TKI) induced diarrhoea: Chloride secretion as a mechanistic hypothesis. Cancer Treatment Reviews. 41(7) 646-752

Van Sebille, Y.Z., Gibson, R.J., Wardill, H.R., Secombe, K.R., Ball, I.A., Keefe, D.M., Finnie, J.W., **Bowen, J.M.,** (2017), Dacomitinib-induced diarrhoea is associated with altered gastrointestinal permeability and disruption in ileal histology in rats. International Journal of Cancer. 140 (12), 2820-2829.

Van Sebille, Y.Z., Gibson, R.J., Wardill, H.R., Ball, I.A., Keefe, D.M., **Bowen, J.M.,** (2017), Dacomitinib-induced diarrhoea: targeting chloride secretion with crofelemer. International Journal of Cancer, *Accepted, In Press*

Van Sebille, Y.Z., **Bowen, J.M.,** Gibson, R.J., Wardill, H.R., Carney, T.J., (2017), Use of zebrafish to model chemotherapy and targeted therapy gastrointestinal toxicity, *Submitted to Supportive Care in Cancer*

Associate Professor Joanne Bowen was my co-principal supervisor (with Professor Rachel Gibson) and has therefore been listed on all publications arising from this thesis. Joanne helped design studies and interpret results, provided technical advice, as well as being responsible for obtaining funding for this project. She was also involved in the drafting of all manuscripts in preparation for publication.

Professor Rachel Gibson

Van Sebille, Y.Z., **Gibson, R.J.,** Wardill, H.R., Bowen J.M., (2016) Gastrointestinal toxicities of first and second-generation small molecule human epidermal growth factor receptor tyrosine kinase inhibitors in advanced non-small cell lung cancer. Current Opinion in Supportive and Palliative Care. 10(12) 152-156.

Van Sebille, Y.Z., **Gibson, R.J.,** Wardill, H.R., Bowen, J.M., (2015) ErbB small molecule tyrosine kinase inhibitor (TKI) induced diarrhoea: Chloride secretion as a mechanistic hypothesis. Cancer Treatment Reviews. 41(7) 646-752

Van Sebille, Y.Z., **Gibson, R.J.,** Wardill, H.R., Secombe, K.R., Ball, I.A., Keefe, D.M., Finnie, J.W., Bowen, J.M., (2017), Dacomitinib-induced diarrhoea is associated with altered gastrointestinal permeability and disruption in ileal histology in rats. International Journal of Cancer. 140 (12), 2820-2829.

Van Sebille, Y.Z., **Gibson, R.J.,** Wardill, H.R., Ball, I.A., Keefe, D.M., Bowen, J.M., (2017), Dacomitinib-induced diarrhoea: targeting chloride secretion with crofelemer. International Journal of Cancer, *Accepted, In Press*

Van Sebille, Y.Z., Bowen, J.M., **Gibson, R.J.,** Wardill, H.R., Carney, T.J., (2017), Use of zebrafish to model chemotherapy and targeted therapy gastrointestinal toxicity, *Submitted to Supportive Care in Cancer*

Professor Rachel Gibson was my co-principal supervisor (with Associate Professor

Joanne Bowen) and has therefore been listed on all publications arising from this thesis. Rachel helped design studies and interpret results, and was also involved in the drafting of all manuscripts in preparation for publication.

Dr. Hannah Wardill

Van Sebille, Y.Z., Gibson, R.J., **Wardill, H.R.,** Bowen J.M., (2016) Gastrointestinal toxicities of first and second-generation small molecule human epidermal growth factor receptor tyrosine kinase inhibitors in advanced non-small cell lung cancer. Current Opinion in Supportive and Palliative Care. 10(12) 152-156.

Van Sebille, Y.Z., Gibson, R.J., **Wardill, H.R.,** Bowen, J.M., (2015) ErbB small molecule tyrosine kinase inhibitor (TKI) induced diarrhoea: Chloride secretion as a mechanistic hypothesis. Cancer Treatment Reviews. 41(7) 646-752

Van Sebille, Y.Z., Gibson, R.J., **Wardill, H.R.,** Secombe, K.R., Ball, I.A., Keefe, D.M., Finnie, J.W., Bowen, J.M., (2017), Dacomitinib-induced diarrhoea is associated with altered gastrointestinal permeability and disruption in ileal histology in rats. International Journal of Cancer. 140 (12), 2820-2829.

Van Sebille, Y.Z., Gibson, R.J., **Wardill, H.R.,** Ball, I.A., Keefe, D.M., Bowen, J.M., (2017), Dacomitinib-induced diarrhoea: targeting chloride secretion with crofelemer. International Journal of Cancer, *Accepted, In Press*

Van Sebille, Y.Z., Bowen, J.M., Gibson, R.J., **Wardill, H.R.,** Carney, T.J., (2017), Use of zebrafish to model chemotherapy and targeted therapy gastrointestinal toxicity, *Submitted to Supportive Care in Cancer*

Dr Hannah Wardill is a member of the Cancer Treatment Toxicities Group. Hannah

contributed to publications arising from this thesis by assisting with laboratory and animal work, as well as reading draft manuscripts.

Ms. Kate Secombe

Van Sebille, Y.Z., Gibson, R.J., Wardill, H.R., **Secombe, K.R.,** Ball, I.A., Keefe, D.M., Finnie, J.W., Bowen, J.M., (2017), Dacomitinib-induced diarrhoea is associated with altered gastrointestinal permeability and disruption in ileal histology in rats. International Journal of Cancer. 140 (12), 2820-2829.

Ms. Kate Secombe was a research assistant in the Cancer Treatment Toxicities Group. She assisted with the animal studies presented in this manuscript.

Ms Imogen Ball

Van Sebille, Y.Z., Gibson, R.J., Wardill, H.R., Secombe, K.R., **Ball, I.A.,** Keefe, D.M., Finnie, J.W., Bowen, J.M., (2017), Dacomitinib-induced diarrhoea is associated with altered gastrointestinal permeability and disruption in ileal histology in rats. International Journal of Cancer. 140 (12), 2820-2829.

Van Sebille, Y.Z., Gibson, R.J., Wardill, H.R., **Ball, I.A.,** Keefe, D.M., Bowen, J.M., (2017), Dacomitinib-induced diarrhoea: targeting chloride secretion with crofelemer. International Journal of Cancer, *Accepted, In Press*

Ms Imogen Ball is a research assistant in the Cancer Treatment Toxicities Group. Imogen was listed as a co-author on two publications based on her contribution to the animal study.

Professor Dorothy Keefe

Van Sebille, Y.Z., Gibson, R.J., Wardill, H.R., Secombe, K.R., Ball, I.A., **Keefe, D.M.,** Finnie, J.W., Bowen, J.M., (2017), Dacomitinib-induced diarrhoea is associated with altered gastrointestinal permeability and disruption in ileal histology in rats. International Journal of Cancer. 140 (12), 2820-2829.

Van Sebille, Y.Z., Gibson, R.J., Wardill, H.R., Ball, I.A., **Keefe, D.M.,** Bowen, J.M., (2017), Dacomitinib-induced diarrhoea: targeting chloride secretion with crofelemer. International Journal of Cancer, *Accepted, In Press*

Professor Dorothy Keefe was partly responsible for obtaining funding for research, and was thus listed as an author on these publications.

Professor John Finnie

Van Sebille, Y.Z., Gibson, R.J., Wardill, H.R., Secombe, K.R., Ball, I.A., Keefe, D.M., **Finnie, J.W.,** Bowen, J.M., (2017), Dacomitinib-induced diarrhoea is associated with altered gastrointestinal permeability and disruption in ileal histology in rats. International Journal of Cancer. 140 (12), 2820-2829.

Professor John Finnie is a pathologist for SA pathology, research division. John was involved in giving pathology advice in regards to renal-toxicity, hepatotoxicity, and gastrointestinal toxicity, and was thus included as an author on this publication.

Assistant Professor Thomas Carney

Van Sebille, Y.Z., Bowen, J.M., Gibson, R.J., Wardill, H.R., **Carney, T.J.,** (2017), Use of zebrafish to model chemotherapy and targeted therapy gastrointestinal toxicity, *Submitted to Supportive Care in Cancer*

Assistant Professor Tom Carney is highly specialised in the area of zebrafish transgenic lines, and is listed as co-senior author (with Associate Professor Joanne Bowen) on this manuscript. Tom hosted me in his laboratory in Singapore, and provided the facilities, and reporter zebrafish lines for this publication. Tom provided advice and guidance in this area, and read draft manuscripts.

Additional Studies and Publications

During my PhD candidature, I published several papers that are not presented in this thesis. These publications are listed below:

Van Sebille, Y.Z., Stansborough R., Wardill, H.R., Bateman, E., Gibson, R.J., Keefe, D.M., (2015), Management of Mucositis During Chemotherapy: From Pathophysiology to Pragmatic Therapeutics. Current Oncology Reports 17(11), 50-58.

Wardill H.R., Bowen, J.M., **Van Sebille, Y.Z.,** Gibson, R.J., (2017) Routine assessment of the gut microbiome to promote preclinical research reproducibility and transparency. Gut 66(10), 1869-1871.

Coller, J.K., Bowen, J.M., Ball, I.A., Wardill, H.R., **Van Sebille, Y.Z.,** Stansborough, R.L., Lightwala, Z., Wignall, A, Shirren, J., Secombe, K., Gibson, R.J., (2017) Potential safety concerns of TLR4 antagonism with irinotecan: a preclinical observational report. Cancer Chemotherapy Pharmacology 79(2), 431-434.

Wardill, H.R., Bowen, J.M., **Van Sebille, Y.Z.,** Secombe, K.R., Coller, J.K., Ball, I. A., Logan R.M., Gibson, R.J., (2016) TLR4-Dependent Claudin-1 Internalization and Secretagogue-Mediated Chloride Secretion Regulate Irinotecan-Induced Diarrhoea. Molecular Cancer Therapeutics 15(11), 2767-2779.

Wardill, H.R., Mander, K.A., **Van Sebille, Y.Z.,** Gibson, R.J., Logan, R.M., Bowen, J.M., Sonis, S.T., (2016) Cytokine-mediated blood brain barrier disruption as a conduit for cancer chemotherapy-associated neurotoxicity and cognitive dysfunction.

International Journal of Cancer 139(12), 2635-2645.

Wardill, H.R., Gibson, R.J., **Van Sebille, Y.Z.,** Secombe, K.R., Logan, R.M., Bowen, J.M., (2016) A novel in vitro platform for the study of SN38-induced mucosal damage and the development of Toll-like receptor 4-targeted therapeutic options. Experimental Biology and Medicine 241(13), 1386-1394.

Wardill, H.R., Gibson, R.J., **Van Sebille, Y.Z.,** Secombe, K.R., Coller J.K., White, I.A., Manavis, J., Hutchinson, M.R., Staikopoulos, V., Logan, R.M., Bowen, J.M., (2016) Irinotecan-Induced Gastrointestinal dysfunction and Pain Are Mediated by Common TLR4-Dependent Mechanisms. Molecular Cancer Therapeutics 15(6) 1376-1386.

Wardill, H.R., Logan, R.M., Bowen, J.M., **Van Sebille, Y.Z.,** Gibson, R.J., (2016) Tight junction defects are seen in the buccal mucosa of patients receiving standard dose chemotherapy for cancer. Supportive Care in Cancer 24(4) 1779-1788.

Wardill, H.R.*, **Van Sebille, Y.Z.*,** Bowen, J.M., Gibson, R.J., (2015) Editorial Comment: Does gut derived inflammation enhance pain signalling following chemotherapy in a Toll-like receptor 4-dependent manner? Current Opinion in Supportive and Palliative Care 9(2) 155-156.
*These authors contributed equally to this work

Wardill, HR., **Van Sebille, Y.Z.,** Mander, K.A., Gibson, R.J., Logan, R.M., Bowen, J.M., Sonis, S.T., (2014) Toll-like receptor 4 signalling: A common biological

mechanism of regimen-related toxicities: An emerging hypothesis for neuropathy and gastrointestinal toxicity. Cancer Treatment Reviews 41(2) 122-128.

Thesis explanation

The format of my thesis is as follows: two literature reviews, three research chapters, a general discussion, references and appendices. During my candidature, I made a significant effort to publish my research findings. Each chapter is presented in its **original** publication format, with the exception of spelling changes to keep consistent English spelling, and the references which are listed in the final chapter. This may result in slight repetition between chapters arising from the same study.

My thesis has two distinct themes relating to the pathobiology of gastrointestinal toxicity second to targeted cancer treatment. The first theme aims to characterise gastrointestinal toxicity induced by dacomitinib, a pan-human epidermal receptor (HER) tyrosine kinase inhibitor (TKI) associated with high levels of diarrhoea. This theme gives rise to the first four chapters. Chapter 1 was an invited review introducing dacomitinib, highlighting the increasing incidence of gastrointestinal toxicity seen with second generation small molecule HER-TKIs and incorporating basic information required for understanding of subsequent chapters. Chapter 2 is a detailed literature review proposing chloride secretion as a mechanistic hypothesis for development of HER TKI-induced diarrhoea. Chapter 3 is my first original research chapter, which characterised dacomitinib-induced gastrointestinal toxicity in a novel rat model. Chapter 4, my second original research chapter, advances on this characterisation, and introduces crofelemer, a chloride channel blocker as a therapeutic intervention for the prevention of dacomitinib-induced diarrhoea. During my candidature, I had the opportunity to work with Assistant Professor Tom Carney from the Institute of Molecular and Cell Biology (IMCB), Biopolis, Singapore. This collaboration

comprises Chapter 5, the second theme of this thesis. This chapter attempted to address the need for an innovative model for the study of gastrointestinal toxicity, investigating transgenic zebrafish reporter lines as a novel model for the study of chemotherapy and targeted therapy-induced gastrointestinal toxicity.

Parts of this thesis were funded by Pfizer Pharmaceuticals under an **unrestricted** investigator-initiated grant (Reference #WI175212). The report I generated for this grant, which partly formed the basis of the publications presented in Chapters 3 and 4, is included as an appendix in this thesis.

Hypothesis and Aims

The overarching themes of my thesis are based on the characterisation of pan-HER TKI-induced gastrointestinal toxicity. The initial hypothesis presented in this thesis addressed chloride secretion as the proposed mechanism for pan-HER TKI-induced diarrhoea. This thesis extensively investigated the literature to formulate this hypothesis, which is presented in Chapter 2. This hypothesis drove my first three aims:

1. To characterise second generation pan-HER TKI-induced gastrointestinal toxicity using dacomitinib in *in vitro* and rodent models (Chapter 3).

2. Utilising crofelemer (an antisecretory, antidiarrhoeal), investigate the hypothesis of chloride secretion as a mechanism of HER TKI-induced diarrhoea utilising the previously developed *in vitro* and rodent models (Chapter 4)

3. To determine if crofelemer is an effective prophylactic for dacomitinib-induced diarrhoea using an established rodent model (Chapter 4).

An important feature arising from these chapters was the lack of translatability from *in vitro* to whole organism *in vivo* models. I utilised *in vitro* models as proof of concept, but when translated to rodent models, effects were not seen. This highlighted the need for a bridge between *in vitro* and *in vivo* models that allows for high throughput, time, and cost-efficient screening. The secondary theme of this thesis was therefore to try and address this need, resulting in my fourth aim:

4. Investigate zebrafish as a novel model to study gastrointestinal toxicity to bridge the gap between *in vitro* and *in vivo* models (Chapter 5).

Nomenclature

This thesis contains variations in terminology relating to gastrointestinal toxicity second to cancer treatment. This is in part reflected by the lack of an accurate definition of the pathophysiology in the field. There are also variances in terminology of receptors that are key to this thesis. Inconsistencies within this thesis are due to requests made by reviewers during peer-review of each publication. I did not change this terminology from what was used in the original publications to avoid altering their content.

Please review the following nomenclature.

Gut and *gastrointestinal tract:* the small and large intestine

HER (Human Epidermal Receptor), ErbB, and *EGFR (Epidermal Growth Factor Receptor):* Interchangeable terms pertaining to the same class of proteins, HER is refined to humans, ErbB pertains to all species, EGFR refers to the HER1/ErbB1 receptor.

Mucositis or gastrointestinal toxicity: Mucositis is a term referring to ulceration and inflammation of the alimentary tract (any region from mouth to anus) that is characterised by a 5-phase model, typically induced from traditional chemotherapy. Gastrointestinal toxicity refers to side effects of gastrointestinal origin induced by any drug, and not specifically defined by the 5-phase model.

Statement of Authorship

Title of Paper	Gastrointestinal toxicities of first and second generation small molecule human epidermal growth factor receptor tyrosine kinase inhibitors in advanced non-small cell lung cancer
Publication Status	☒ Published ☐ Accepted for Publication ☐ Submitted for Publication ☐ Unpublished and Unsubmitted w ork w ritten in manuscript style
Publication Details	Invited review in Current Opinion in Supportive and Palliative Care (2016) 10: 152-156

Principal Author

Name of Principal Author (Candidate)	Ysabella Van Sebille		
Contribution to the Paper	First author and main contributor. I developed the concept, did the literature searching and review, wrote the original draft, and was responsible for reviewing and editing.		
Overall percentage (%)	90%		
Certification:	This paper reports on original research I conducted during the period of my Higher Degree by Research candidature and is not subject to any obligations or contractual agreements with a third party that would constrain its inclusion in this thesis. I am the primary author of this paper.		
Signature		Date	September, 2017

Co-Author Contributions

By signing the Statement of Authorship, each author certifies that:

i. the candidate's stated contribution to the publication is accurate (as detailed above);

ii. permission is granted for the candidate in include the publication in the thesis; and

iii. the sum of all co-author contributions is equal to 100% less the candidate's stated contribution.

Name of Co-Author	Rachel Gibson		
Contribution to the Paper	Rachel was involved in conceptualisation, supervision, and reviewing manuscript drafts		
Signature		Date	September, 2017

Name of Co-Author	Hannah Wardill		
Contribution to the Paper	Hannah was involved in reviewing manuscript drafts.		
Signature		Date	September, 2017

Name of Co-Author	Joanne Bowen		
Contribution to the Paper	Joanne was involved in conceptualisation, supervision, and reviewing manuscript drafts.		
Signature		Date	September, 2017

Chapter 1 Gastrointestinal toxicities of first and second generation small molecule human epidermal growth factor receptor tyrosine kinase inhibitors in advanced non-small cell lung cancer

---

This chapter was an invited editorial published in the special issue, Gastrointestinal Symptoms, in Current Opinion in Supportive and Palliative Care (**Van Sebille, Y.Z.,** Gibson, R. J., Wardill, H.R., Bowen, J.M. 2016. Gastrointestinal toxicities of first and second-generation small molecule human epidermal growth factor receptor tyrosine kinase inhibitors in advanced non-small lung cancer. *Current Opinion in Supportive and Palliative Care*, 10, 152-156.)

Abstract

Tyrosine kinase inhibitors (TKIs) against human epidermal growth factor receptors (HER) are the standard of care treatment in non-small cell lung cancer (NSCLC). Gefitinib is a first generation HER1 TKI used first line HER1 mutation-positive NSLC. Initially, oncology end points were promising, however acquired resistance and mutations have occurred, triggering the development of second-generation pan-HER TKIs, such as dacomitinib.

However, with the development of novel targeted therapies has come worsened side effects, in particular diarrhoea. Despite this toxicity being the most common side effect of pan-HER TKIs, it is poorly understood. This editorial discusses this gastrointestinal

toxicity, comparing first generation to second generation HER TKIs for the treatment of NSCLC, using gefitinib and dacomitinib respectively.

Introduction

Lung cancer remains the leading cause of cancer-related death worldwide, with non-small cell lung cancer (NSCLC) representing 85% of all lung cancer diagnoses [1, 2]. Platinum-based chemotherapy is recommended as standard first-line treatment; however, the objective response rate is modest and recurrence eventually occurs for most patients [3]. The landscape of NSCLC therapeutics has changed over the past decade in response to discovery that many tumours overexpress the human epidermal growth factor receptor (HER) family. This has resulted in the introduction of small molecule HER tyrosine kinase inhibitors (TKIs) for the treatment of NSCLC [4]. Many new HER TKIs have since emerged, moving from single HER targets (primarily HER1), such as gefitinib and erlotinib to pan-HER targets such as dacomitinib and afatinib. Additionally, these small molecule therapeutics have moved from first to second generation agents; now resistant to the acquired mutations of the first-generation class of drugs, such as the T790 mutation. It was originally anticipated with the advent of these targeted therapies that patients would experience less toxicity than traditional cytotoxic therapies. While undoubtedly these new agents have improved therapy significantly, they also have downsides, namely, causing unexpected adverse event profiles. This editorial will focus on the predominant HER TKI-related side effect, namely diarrhoea, addressing the change in the gastrointestinal toxicity profiles seen from the single-HER targeted drugs to the second-generation pan-HER targeted drugs using gefitinib and dacomitinib as examples.

HER TKIs

TKIs were first described in 1988, and specifically inhibited the human epidermal growth factor receptor 1 (HER1) [5]. The activity of the HER receptors is dictated by the expression of their ligands, which can be classified into three groups: 1) those binding specifically to HER1; 2) those exhibiting dual specificity binding to HER1 and HER4; and 3) neuregulins sub classified upon their capacity to bind HER3 and HER4 or only HER4 [6] [7]. Currently, no ligand has been identified to be specific for HER2, however it is understood that this receptor forms heterodimers with the other HER receptors. Upon ligand binding to the HER receptor, heterodimerisation or homodimerisation of receptors occurs, leading to a cascade of signalling pathways [8]. Among the pathways activated are ERK, and PI3K/Akt. Pathway activation leads to changes in protein functions and activation of gene transcription [8-10]. Briefly, these complex signalling pathways result in interactions with apoptotic signalling, cell proliferation, differentiation, migration and survival, which can promote tumorigenesis [9, 11].

Diarrhoea

For oral agents administered daily, toxicities of any grade are extremely important as they can determine compliance. Despite this, adverse events remain largely ignored, with the emphasis placed on efficacy. Diarrhoea is a severe, dose-limiting, and the most common adverse event of small molecule HER TKI treatment [12]. HER TKI-induced diarrhoea can become evident as early as 2-3 days after initiation of treatment, and given the daily and continuous manner of HER TKI treatment, can persist for substantial periods of time, significantly impacting on patients' quality of life, resulting in poor compliance and therapy interruption [13]. The severity of diarrhoea is most commonly graded using the National Cancer Institute's Common Terminology Criteria for Adverse

Events (Table 1). Grade 3 (severe) diarrhoea can result in fluid and electrolyte loss, which then can lead to dehydration, electrolyte imbalances, and renal insufficiency. Additionally, alterations in gastrointestinal transit and digestion can lead to nutritional deficiencies that can negatively impact the quality of life of patients. Furthermore, given that therapy with HER TKIs tends to continue for more than 10 months, grade 1-2 toxicities should be considered equally important, and appropriate management of diarrhoea is essential.

Table 1. Diarrhoea grading scale

Grade 1	Grade 2	Grade 3	Grade 4	Grade 5
Increase of <4 stools over baseline	Increase of 4-6 stools over baseline; iv fluids <24 h	Increase of ≥7 stools over baseline; incontinence; iv fluids ≥ 24 h; hospitalisation indicated; limits activities of daily living	Life threatening consequences; urgent; intervention indicated	Death

Mechanisms

The underlying mechanism(s) of HER TKI-induced diarrhoea remain poorly understood. Despite a similar clinical manifestation to traditional chemotherapy treatment-induced diarrhoea, toxicities associated with targeted therapies are hypothesised to have different pathogenic mechanisms [14]. Preclinical studies using targeted therapies have shown diarrhoea is not correlative with intestinal mucosal damage [15], suggestive of pathogenic mechanisms that differ to traditional cytotoxic cancer treatments. Gaining significant momentum is the hypothesis that HER TKI-induced diarrhoea is a result of excess chloride secretion based on the established role of HERs in regulating ion conductance channels in the colon [16]. Currently, treatment for cancer-therapy induced diarrhoea is limited; coupled with increasing cancer prevalence, it is clear that the need for a fuller understanding of the mechanism(s), and subsequently therapeutic targets will not abate. Ultimately, such an understanding should eventually point to safer, more targeted and more effective therapies for cancer sufferers.

First Generation HER-TKI- Gefitinib

Gefitinib (Iressa; AstraZeneca, London, U.K., http://www. astrazeneca.com) was the first oral HER TKI approved in the U.S. Gefitinib reversibly binds to the adenosine triphosphate -binding pocket of the tyrosine kinase domain of HER1 subsequently inhibiting kinase-dependent signal transduction [17-19]. Gefitinib, has demonstrated benefit in terms of response rate and time to progression in adults with metastatic NSCLC who have activating HER1 mutations [20-22]. However, results from multiple clinical trials have demonstrated that between 25 – 55 % of patients receiving gefitinib monotherapy develop diarrhoea (Table 2).

Table 2. Clinical trials of gefitinib

Study	Experimental design	Diarrhoea (all grades)	Diarrhoea grade 3-4
Thatcher et al., 2005 [23]	NSCLC Phase III (n = 1688)	27 %	3 %
Sun et al., 2012 [24]	NSCLC Phase III (n = 135)	26.5 %	0 %
Cufer et al., 2006 [25]	NSCLC Phase II (n = 140)	26.5 %	2.9 %
Kim et al., 2008 [26]	NSCLC Phase III (n = 1466)	35 %	2.5 %
Lee et al., 2010 [27]	NSCLC Phase III (n =161)	25.9 %	1.2 %
Mok et al., 2009 [28]	NSCLC Phase III (n = 1217)	46.6 %	3.8 %
Maemondo et al., 2010 [29]	NSCLC Phase III (n = 161)	34.2 %	0.9%
Goss et al., 2009 [30]	NSCLC Phase II (n = 201)	51 %	3 %
Morère et al., 2010 [31]	NSCLC Phase II (n = 128)	28 %	5 %
Mitsudomi et al., 2010 [32]	NSCLC Phase III (n = 117)	54 %	1.1 %
Zhang et al., 2012 [33]	NSCLC Phase III (n = 298)	25 %	0 %
Crinò et al., 2008 [34]	NSCLC Phase II (n = 196)	25.5 %	4.3 %

Second Generation HER TKI- Dacomitinib

Resistance to reversible HER1 TKIs such as gefitinib has increased, leading to the development of novel target-based therapies such as dacomitinib for the treatment of NSCLC harbouring exon 19 deletions or exon 21 (L858R) mutations [35-37]. Conventional HER TKIs such as gefitinib are reversible: they competitively bind to the HER1 tyrosine kinase domain [38]. However, the simultaneous activation of different HER family members through dynamic hetero- and homo- dimerisation can compromise the therapeutic efficacy by inhibition of a single receptor [39]. Dacomitinib (PF-00299804, Pfizer) was developed to irreversibly (covalently) bind to the ATP domain of each of the three kinase-active members of the HER family (HER1, HER2 and HER4) effectively inactivating them [40]. Subsequently, signal transduction pathways implicated in the proliferation and survival of cancer cells are blocked [41]. Dacomitinib has shown significant therapeutic efficacy in NSCLC, specifically to tumours that have not previously responded to conventional single receptor inhibitors, and also against tumours with mutations developed for acquired resistance of targeted therapies [37-39]. Dacomitinib is currently in phase III clinical trials, and the most commonly reported adverse event among all trials has been diarrhoea (Table 3), commonly resulting in dose reductions and patient withdrawal from clinical trials [38, 39, 42-44].

Table 3. Clinical trials of dacomitinib

Study	Experimental design	Diarrhoea (all grades)	Diarrhoea grade 3-4
Jänne et al., 2011 [45]	NSCLC Phase I (n = 121)	66.7 %	11 %
Reckamp et al., 2014 [44]	NSCLC Phase II (n = 66)	84.8 %	12.1 %
Abdul Razak et al., 2013 [42]	NSCLC Phase II (n = 69)	84.1 %	15.9 %
Ramalingam et al., 2012[46]	NSCLC Phase II (n = 94)	73.1 %	11.8 %
Takahashi et al., 2012 [39]	NSCLC Phase I (n = 13)	92 %	0 %
Ruiz-Garcia et al., 2013 [47]	NSCLC Phase I (n = 14)	14 %	0 %
Ramalingam et al., 2014[48]	NSCLC Phase III (n = 878)	72 %	12 %
Jänne et al., 2016 [49]	NSCLC Phase I (n = 70)	74 %	16 %
Ellis et al., 2014 [50]	NSCLC Phase III (n = 720)	78 %	13 %

Conclusion

Over the past decade, therapies for advanced NSCLC have significantly changed with the development of small molecule TKIs moving from single- to pan- HER targets. The median percentage of patients developing diarrhoea from gefitinib is 27.5 %, with a median of 2.5 % developing grade 3 or higher diarrhoea; compared to a median of 74 % of patients developing diarrhoea from dacomitinib, with a median of 12 % developing grade 3 or higher. Using gefitinib and dacomitinib as examples, it is clear that second generation, pan-HER TKIs induce diarrhoea in a higher proportion of patients, and to a worse degree than first generation single-HER TKIs. The HER family of receptors are mainly expressed on cells of epithelial origin, including those of the gastrointestinal tract, and inhibitors of the HER pathway are therefore associated with gastrointestinal side effects, with diarrhoea constituting the most frequent. Perhaps, the increased incidence and worse diarrhoea seen with pan-HER TKIs vs single-HER TKIs suggests that other members of the HER family, and not only HER1 are important in the mechanism(s) of HER-TKI induced diarrhoea. Whilst understanding of the role of HER1 in growth and repair of the GIT is well understood, little is known of the role of other HER receptors in GIT homeostasis.

Dacomitinib is a novel HER family blocker that has demonstrated anticancer activity in Phase II and III studies in NSCLC patients whose tumours harbor HER mutations. Gefitinib is currently the standard of care for these patients as first-line treatment. Following positive clinical trial data, dacomitinib may replace gefitinib as the first-line choice of treatment for EGFR mutation-positive advanced NSCLC patients. Given the aforementioned concerns associated with dacomitinib-induced diarrhoea, education on the frequency of HER TKI-associated diarrhoea, as well as early diagnosis, timely

management and reassessment and close patient follow-up, will help to prevent adverse event aggravation, dose reductions or therapy discontinuation, thus encouraging patient compliance and allowing patients to obtain the maximum therapeutic benefit from this novel agent.

Statement of Authorship

Title of Paper	ErbB small molecule tyrosine kinase inhibitor (TKI) induced diarrhoea: chloride secretion as a mechanistic hypothesis
Publication Status Published	☒ Published ☐ Accepted for Publication ☐ Submitted for Publication ☐ Unpublished and Unsubmitted w ork w ritten in manuscript style
Publication Details	Literature review published in Cancer Treatment Reviews (2015) 41: 646-652

Principal Author

Name of Principal Author (Candidate)	Ysabella Van Sebille		
Contribution to the Paper	First author and main contributor. I developed the concept, did the literature search and review, wrote the original draft, and was responsible for reviewing and editing.		
Overall percentage (%)	90%		
Certification:	This paper reports on original research I conducted during the period of my Higher Degree by Research candidature and is not subject to any obligations or contractual agreements with a third party that would constrain its inclusion in this thesis. I am the primary author of this paper.		
Signature		Date	September, 2017

Co-Author Contributions

By signing the Statement of Authorship, each author certifies that:

i. the candidate's stated contribution to the publication is accurate (as detailed above);

ii. permission is granted for the candidate in include the publication in the thesis; and

iii. the sum of all co-author contributions is equal to 100% less the candidate's stated contribution.

Name of Co-Author	Rachel Gibson		
Contribution to the Paper	Rachel was involved in conceptualisation, supervision, and reviewing manuscript drafts.		
Signature		Date	September, 2017

Name of Co-Author	Hannah Wardill		
Contribution to the Paper	Hannah was involved in reviewing manuscript drafts.		
Signature		Date	September, 2017

Name of Co-Author	Joanne Bowen		
Contribution to the Paper	Joanne was involved in conceptualisation, supervision, and reviewing manuscript drafts		
Signature		Date	September, 2017

Chapter 2 ErbB small molecule tyrosine kinase inhibitor (TKI) induced diarrhoea: chloride secretion as a mechanistic hypothesis.

This chapter was published in Cancer Treatment Reviews (**Van Sebille, Y.Z.,** Gibson, R. J., Wardill, H.R., Bowen, J.M. 2015. ErbB small molecule tyrosine kinase inhibitor (TKI) induced diarrhoea: Chloride secretion as a mechanistic hypothesis. *Cancer Treatment Reviews*, 41, 646-652.)

Abstract

Diarrhoea is a common, debilitating and potentially life threatening toxicity of many cancer therapies. While the mechanisms of diarrhoea induced by traditional chemotherapy have been the focus of much research, the mechanism(s) of diarrhoea induced by small molecule ErbB TKI, have received relatively little attention. Given the increasing use of small molecule ErbB TKIs, identifying this mechanism is key to optimal cancer care. This paper critically reviews the literature and forms a hypothesis that diarrhoea induced by small molecule ErbB TKIs is driven by intestinal chloride secretion based on the negative regulation of chloride secretion by ErbB receptors being disrupted by tyrosine kinase inhibition.

Introduction

In clinical oncology practice, diarrhoea is a very common and severe side effect of cancer treatments including radiotherapy, chemotherapy, and targeted therapies [51]. Diarrhoea occurs in between 50-100% of patients depending on their treatment regimen [12, 52]. It is a debilitating and potentially life threatening toxicity as fluid and

electrolyte loss associated with persistent and/or severe diarrhoea can result in electrolyte imbalances, renal insufficiency, malnutrition, and extreme dehydration, all of which can lead to cardiovascular compromise and death [53]. Furthermore, these often necessitate dose reductions and treatment breaks, compromising clinical outcomes [54, 55]. The need for prevention of cancer therapy-induced diarrhoea is critical. Identification of the pathogenesis may lead to a more accurate management to help reduce severe complications that may be irreversible [56, 57].

Cancer therapy-induced diarrhoea is also associated with considerable economic costs with recent reports suggesting that additional costs of up to $25,000 (USD) per chemotherapy cycle are incurred [58]. These costs are attributed to patients with cancer therapy-induced diarrhoea having an increased risk of infection, increased hospital stays and increased resource utilisation for supportive care measures [59, 60]. Consequently, prevention, minimisation, and/or prediction of cancer therapy-induced diarrhoea may significantly reduce health system costs over the total course of cancer treatment.

Small molecule ErbB receptor tyrosine kinase inhibitors (TKIs) are used for the treatment of a variety of cancers that overexpress ErbB receptors. These cancers include, but are not limited to breast, non-small cell lung cancer (NSCLC) and head and neck cancers. Small molecule ErbB TKIs act by competitively binding to the intracellular ATP domain of the tyrosine kinase, effectively inhibiting phosphorylation of the receptor and therefore downstream signalling [61, 62]. To date, the mechanism(s) of action of ErbB TKI-induced diarrhoea has yet to be elucidated. This is in contrast to diarrhoea induced by traditional chemotherapy agents including fluropyrimidines, topotecans, platinum analogues, folate inhibitors and taxanes [12]. Recent research has suggested

that chemotherapy-induced diarrhoea is a result of severe intestinal damage caused by mucositis. Mucositis is a multi-factorial process whereby acute damage to the intestinal mucosa (including, increased apoptosis, villous atrophy, crypt hypoplasia and dilation, loss of epithelium, excessive mucous secretion, necrosis and inflammation) causes an imbalance between absorption and secretion, ultimately resulting in an anatomic derangement diarrhoea phenotype [12, 63, 64]. Numerous preclinical and clinical studies have documented the pathobiology of chemotherapy-induced diarrhoea and have reported that it is largely based on indirect biological signalling, rather than direct tissue damage [65-70]. The mechanisms of chemotherapy-induced diarrhoea are becoming better characterised, this is not the case for TKI-induced diarrhoea; this critical review will outline potential mechanisms of ErbB receptor TKI-induced diarrhoea.

ErbB receptors

Many tumours including but not limited to breast, NSCLC, and squamous cell cancers of the head and neck, have been identified as overexpressing ErbB receptors. This has meant that many targeted therapies have been developed to act on the ErbB family of receptors [14]. The ErbB family (interchangeably known as HER/EGFR), is comprised of four membrane receptor tyrosine kinases: ErbB1 (HER1 or EGFR), ErbB2 (HER2), ErbB3 (HER3), and ErbB4 (HER4) [39]. The activity of the ErbB receptors is dictated by the expression of their ligands [6], which can be classified into three groups: Group 1) those binding specifically to ErbB1; Group 2) ligands which exhibit dual specificity binding to both ErbB1 and ErbB4; and Group 3) neuregulins, which can be further sub-classified based upon their ability to bind only ErbB4 or both ErbB3 and ErbB4 (Table 1) [7]. To date, no ligand has been identified as being specific for ErbB2, although this receptor does form heterodimers with the other ErbB receptors.

Table 1: ErbB receptors and their ligands

Receptor	Ligands
ErbB1	EGF, Areg, TGFα
ErbB1 and ErbB4	Btc, HBEGF and Ereg
ErbB3 and ErbB4	Nrg1 and Nrg2
ErbB4	Nrg3 and Nrg4

EGF: Epidermal Growth Factor; Areg: Amphiregulin; TGF: transforming growth factor; Btc: Betacellulin; HBEGF: Heparin-binding EGF-like growth factor; Ereg: Epiregulin; Nrg: Neuregulins.

When ligands bind to the extracellular domain of the ErbB receptors, receptor dimerisation and phosphorylation of intracellular tyrosine kinase domains occur. This leads to activation of a cascade of signalling pathways including the mitogen activated protein kinases/ extracellular signal regulated kinases (MAPK/ERK), and phosphatidylinositol-3'-kinase (PI3K/Akt) pathways [8]. Once activated, these pathways lead to changes in both protein functions and activation of gene transcription [8-10], leading to interactions with apoptotic signalling, cell proliferation, differentiation, migration and survival. These can all promote tumorigenesis [9, 11].

In addition to being expressed on cancer cells, ErbB receptors are also found on healthy cells throughout the body. Of specific interest to this review are the receptors expressed in the gastrointestinal tract. Specifically, they are abundantly expressed on the basolateral membranes of healthy intestinal epithelial cells and are crucial for essential normal functions and development in the gut [41, 71]. For example, ErbB receptors activated on intestinal epithelial cells cause a cascade of complex signalling pathways resulting in maintenance of mucosal integrity via induction of mucus and prostaglandin synthesis, promotion of enterocyte migration, prevention of intestinal epithelial cell apoptosis, decreasing bacterial translocation and preservation of gut barrier function after injury [40, 72].

The first anti-cancer agents targeting ErbB receptors were developed in the 1980's. This led to the development of the first generation of two overarching subtypes of ErbB receptor inhibitors: monoclonal antibodies, and small molecule tyrosine kinase inhibitors [73-76]. Monoclonal antibodies are directed against the extracellular domain of ErbB receptors, whereas small molecule TKIs act directly on cytoplasmic domains of ErbB

TKI activity. The overexpression of ErbB receptors in many solid tumours is correlated with advanced stages and often a worse prognosis of the cancer [77]. In many different cancer cell types, the ErbB pathway becomes hyper-activated by a range of mechanisms, including overproduction of ligands, overproduction of receptors, or constitutive activation of receptors [71]. This hyper-activity and hence key role of the ErbB network has made it an attractive target for therapies. After an initial response however, patients being treated with first generation ErbB TKIs often develop secondary mutations such as T790M, MET or HER2 amplifications, resulting in acquired resistance [78]. Ultimately, this limits the effectiveness of these first-generation agents over time. Pan-ErbB TKIs are now considered second-generation and are resistant to acquired mutations. As a result, these TKIs are now commonly used. However, they are associated with clinical toxicities which are important to recognise and manage.

ErbB TKIs and diarrhoea

Toxicities are common in patients receiving first generation ErbB TKIs, including, but not limited to erlotinib, gefitinib, and lapatinib. In particular, up to 69% of patients experience diarrhoea [61]. Large randomised trials have shown that erlotinib and lapatinib induce diarrhoea in 40-60% of patients, with approximately 10% of these presenting with grade 3-4 symptoms (National Cancer Institute Common Toxicity Criteria) [79, 80]. One of the most frequent toxicities associated with second-generation pan-ErbB TKIs is also diarrhoea. Recent clinical data suggests that all grades of diarrhoea are more frequently seen with pan-ErbB TKIs than first generation ErbB TKIs (e.g. dacomitinib vs. eroltinib). Up to 96% of patients receiving second generation pan-ErbB TKI's develop diarrhoea, and perhaps more importantly, the incidence of grade 3 (severe) diarrhoea is significantly higher [81]. Further exacerbating this diarrhoea is that

many TKIs are given daily for months at a time, and side effects are therefore often chronic, unlike the acute manifestations typically seen following traditional chemotherapy regimens.

Do ErbB TKIs induce diarrhoea via a distinctly different mechanism than chemotherapy-induced diarrhoea?

One common hypothesis for the mechanism of action of diarrhoea following TKI treatment is thought to be due to inhibition of ErbB signalling within intestinal epithelia, leading to direct mucosal atrophy and damage [82-84]. Research suggested that this diarrhoea was associated with reduced growth, characterised by reduced growth and healing of the intestinal epithelium leading to mucosal atrophy due to the stimulatory effect of ErbB pathway on enterocyte proliferation [85], nutrient and electrolyte transport [86], brush border enzyme expression [87] and epithelial restitution being impeded [88]. Increased frequency of diarrhoea in patients using oral compounds (e.g. small molecule TKI's) compared to monoclonal antibodies supports this theory. This direct mucosal damage hypothesis mimics chemotherapy-induced diarrhoea, bought about by the manifestation of mucositis (Figure 1).

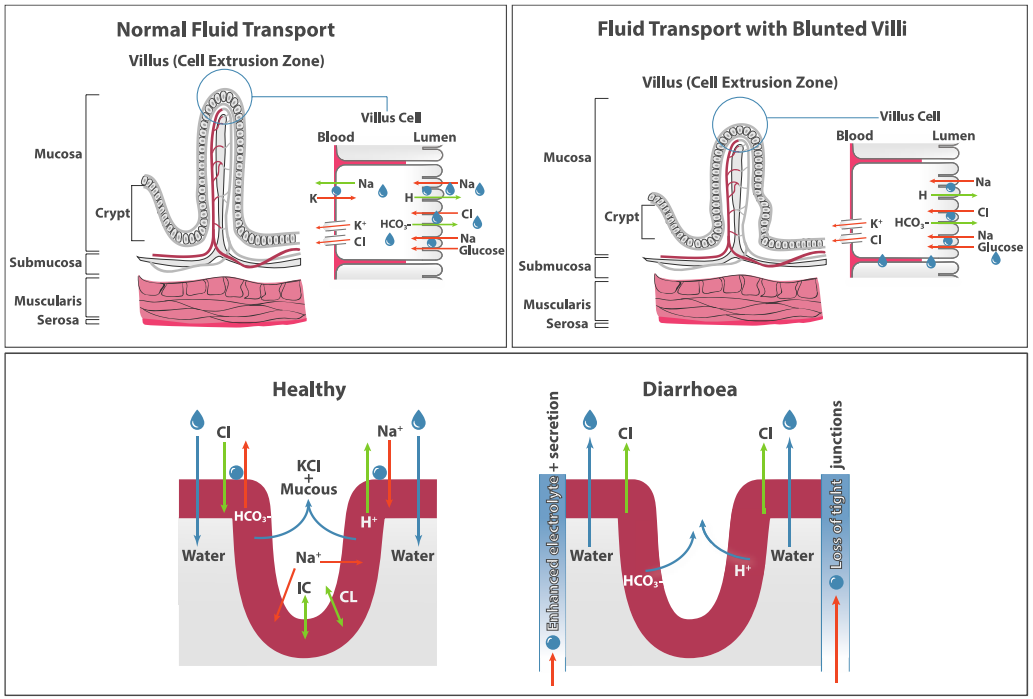

Figure 1: (A) In a normal villus fluid transport is tightly controlled and there is a net absorption of fluid. **(B)** In chemotherapy induced gut toxicity, the villus is blunted and there is less area for absorption of fluid. The manifestation of chemotherapy-induced diarrhoea is largely driven by small intestinal changes. **(C)** Small molecule ErbB TKI induced diarrhoea is likely due to secretory mechanisms within the colon. The tight control of chloride secretion is lost, resulting in an accumulation of fluid in the lumen.

A more recent hypothesis suggests that despite a similar clinical manifestation as is seen in traditional chemotherapy induced diarrhoea, ErbB TKI-induced diarrhoea is due to a distinctly different pathological mechanism [14, 89]. This followed the recent development of a preclinical model to study the gastrointestinal toxicity associated with ErbB inhibitors [15]. Using lapatinib, an oral small molecule ErbB1 and ErbB2 TKI for 7-28 days, this large (n=128) study showed no significant pathology in the intestines of rats, despite rats displaying a dose-dependent diarrhoea profile consistent with that observed clinically [15]. No significant changes were noted in intestinal weights and no significant histopathology was noted in the jejunum or colon, indicating that no significant pathology in the intestines occurred as a result of lapatinib treatment [15]. In fact, it was found that jejunum crypts were significantly longer, and contained increased mitotic cells in rats treated with lapatinib [90]. This is in stark contrast to what is noted in mucositis models of rats treated with chemotherapeutic agents such as irinotecan causing severe intestinal damage and atrophy [63, 91]. This is therefore highly suggestive that the mechanism of ErbB TKI-induced diarrhoea is profoundly different from chemotherapy-induced diarrhoea. Further investigation found that serum biochemistry levels of chloride were decreased in rats treated with high dose lapatinib, correlating with diarrhoea incidence, suggesting that chloride loss via the intestinal lumen may be involved in the manifestation of small molecule ErbB TKI induced diarrhoea [90]. However, this was inconclusive. Furthermore, studies using another kinase inhibitor, flavopiridol, showed no intestinal damage, despite clinical manifestation of diarrhoea [92, 93]. Additional investigation showed treatment with flavopiridol directly stimulated chloride secretion across monolayers of human colonocytes in modified Ussing chambers [94].

Paradoxically, a study by Hoda et al. (2010), showed in a chemotherapy model of gut toxicity, that chloride secretion was increased in rats treated with methotrexate [95]. While the severity and incidence of diarrhoea was not reported, it was suggested by the authors that increased chloride secretion may be part of the mechanism responsible for chemotherapy induced diarrhoea. However, given the limited evidence of this in the wider literature, it requires further investigation.

Other research has also established that ErbB receptors have a limited role in the development of mucositis induced diarrhoea [96]. Transgenic mice that overexpress EGF (a ligand for ErbB1) in the small intestine, showed no improvements in weight recovery, mucosal architecture, apoptosis or proliferation compared to controls following fluorouracil, a chemotherapeutic known to induce mucositis [96]. This was also the case in mice treated with exogenous EGF following fluorouracil. These findings are highly suggestive that the ErbB family of receptors does not play a significant role in the development of mucositis associated diarrhoea. Given that ErbB TKIs target these receptors, it is likely that their physiological function is critically involved in the development of the associated diarrhoea. This supports the indication that ErbB TKIs induce diarrhoea via a distinct mechanism to chemotherapy-induced diarrhoea. Together, this suggests that the pathogenic mechanisms of ErbB TKI-induced diarrhoea are not necessarily the same as for other cancer treatments, and there remains a vast gap in the knowledge regarding the biological mechanisms responsible.

Chloride secretion and diarrhoea

Chloride secretion occurs throughout the length of the gastrointestinal tract and is critical for normal physiological functioning of the gut [97]. The chloride secretory mechanism

has several transmembrane transport pathways. In the colon, chloride is taken into the cell via the basolateral membrane through the sodium potassium chloride co-transporter in an electro-neutral manner. This process is driven largely by the sodium potassium ATPase pump [97]. Potassium channels are also located on the basolateral membranes, and allow for potassium recycling and prevention of cellular depolarisation. This preserves the electrical driving force for chloride secretion from the apical membrane of the cell. Chloride then accumulates in the lumen via the cAMP dependent cystic fibrosis transmembrane conductance regulator (CFTR) chloride channels, and the calcium activated chloride channels (CaCC). The presence of chloride in the lumen provides the electrochemical driving force for paracellular movement of sodium. The resulting accumulation of sodium chloride in the lumen provides the osmotic gradient for water to flow to the lumen [97]. The normal chloride secretory process is outlined in Figure 2. The secretion of chloride ions is important in controlling fluid flow across various epithelial surfaces, including the intestine, helping to keep it moist.

There are two key mechanisms whereby chloride secretion is initiated. (1) a cAMP-dependent pathway; which elicits a delayed and prolonged response and (2) a calcium ion-dependent pathway; which elicits a rapid and transient response [98]. The transient nature of the calcium ion-dependent response, even in the face of sustained increases in intracellular calcium suggests calcium dependent agonists generate an inhibitory signal. This inhibitory signal then serves to limit the extent of the chloride secretory response [99]. Under normal homeostasis, this process is tightly regulated. However, any homeostatic breakdown can lead to various complications, such as diarrhoea where secretion is exaggerated [100].

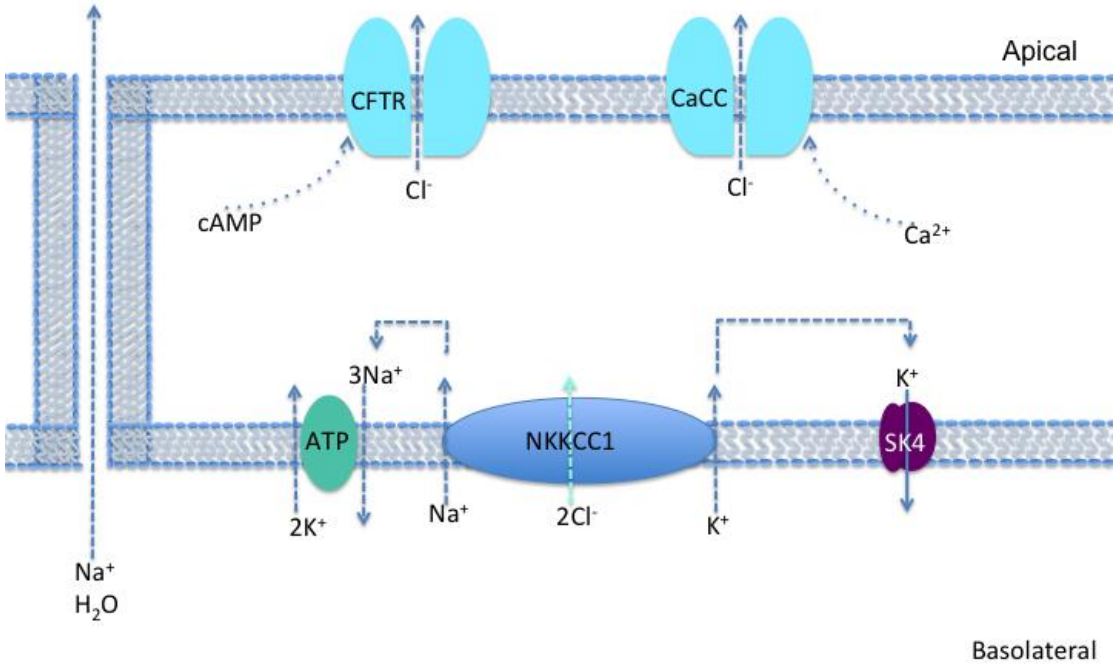

Figure 2: Chloride secretory mechanism in normal intestinal epithelium. cAMP, cyclic adenosine monophosphate; CFTR, cystic fibrosis transmembrane conductance regulator; CaCC, calcium activated chloride channel; ATP, adenosine triphosphate

ErbB receptors are abundantly expressed on the basolateral membrane of intestinal epithelial cells and are critical regulators of intestinal ion transport via multiple downstream pathways [10]. The intricate pathways that result from binding and dimerisation lead to negative regulation of both chloride secretion and sodium absorption [10]. ErbB receptors have been shown to exert both an inhibitory effect on chloride secretion (Figure 3) [8]. Binding of EGF to ErbB1 leads to homodimerisation and heterodimerisation with ErbB2 exerting an inhibitory effect on chloride secretion signalling via PI3K/Akt and PKC pathways; these distinct pathways inhibit the basolateral potassium channels (Figure 3) [101, 102].

Based on the negative regulatory roles ErbB receptors play in chloride secretion, it is reasonable to suggest that when receptors are inhibited from phosphorylating (as is the case with TKIs), they are no longer able to negatively regulate chloride secretion. This results in excessive movement of chloride into the lumen, providing the driving force for paracellular movement of sodium and subsequently water leading to a secretory diarrhoea phenotype. This hypothesis is supported by research with genistein, an isoflaovone that acts as an ErbB1 TKI, which has shown to reverse the inhibitory effect of EGF on chloride secretion [100, 103]. In contrast however, some TKIs including erbstatin analogue, tryphostin A23, tryrphostin A51 and herbimycin A are not associated with an increase in epithelial chloride secretion [104]. This is contradictory to the increased chloride secretion seen following tyrosine kinase inhibition with other agents [104]. This may be explained due to the differing mechanisms of action of each drug, and strongly suggests that different TKIs may need to be considered independently.

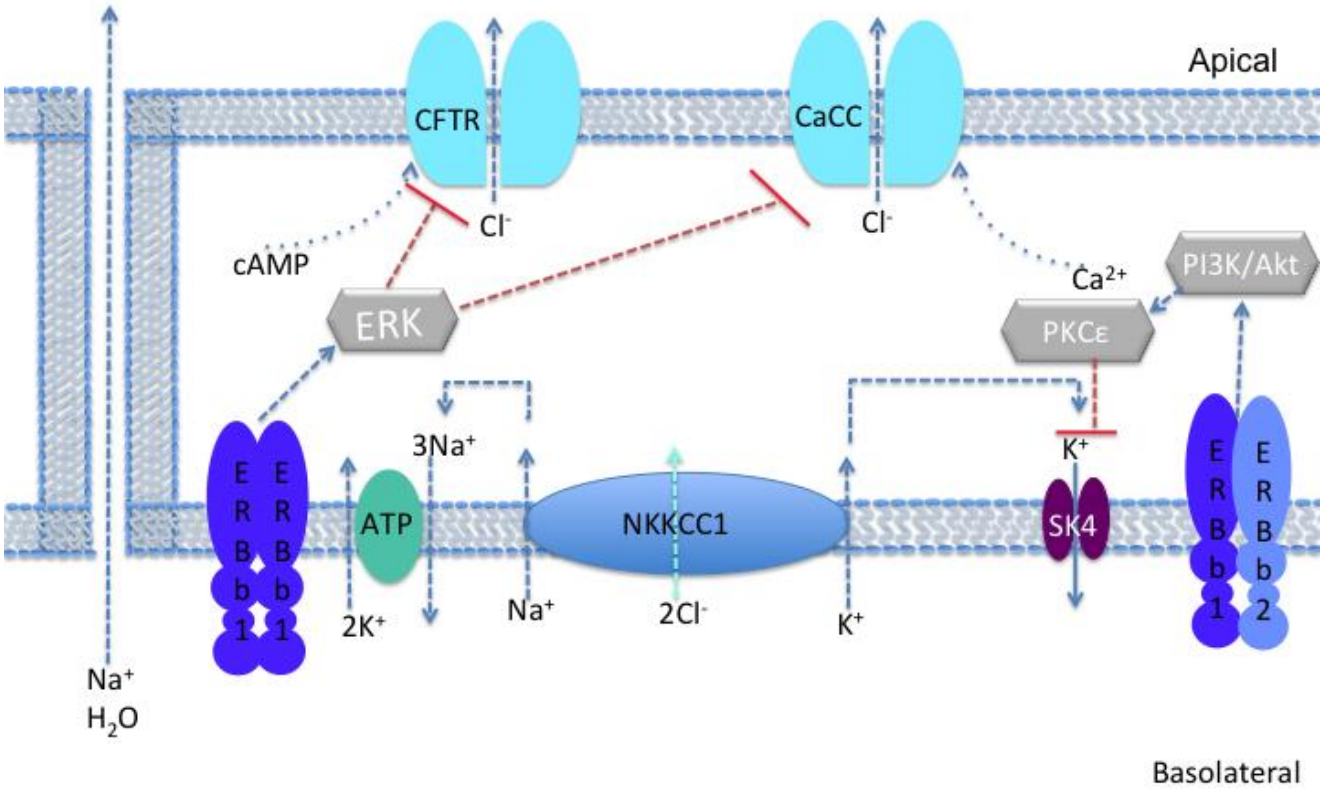

Figure 3: Negative regulation of chloride secretion by ErbB receptors

TKI and chemotherapy concomitant therapy

Concomitant chemotherapy and TKIs has increased due to a greater therapeutic effectiveness [62]. However, this has meant toxicities increase. A meta-analysis including 3918 patients from six trials of erlotinib, gefitinib, and vandetanib found that the addition of an ErbB1 inhibitor to a variety of different chemotherapeutics significantly increased the severity of diarrhoea [105]. Furthermore, concomitant lapatinib with capecitabine increased diarrhoea from 30% (when capecitabine is given alone) to 65% in combination. Likewise, the addition of lapatinib with paclitaxel increased diarrhoea incidence from 28% to 48% [106]. These combination therapies not only result in more severe diarrhoea, but also complicate identifying and treating the causes and underlying mechanisms, which are likely to be multifactorial. Understanding the mechanisms is important as attributing all mucosal toxicity on the concomitant chemotherapy, without considering the TKIs may lead to the wrong intervention [107]. Diarrhoea is not always the same and a distinction needs to be made between secretory and anatomic derangement diarrhoea in these cases. Diarrhoea seen in patients undergoing concomitant TKI/chemotherapy treatment may be due to either the direct mechanisms caused by the agents themselves, or amplification of injury mechanisms in combination [89]. There are known shared metabolic and drug efflux pathways of various TKIs and chemotherapeutic agents, which may explain the more severe diarrhoea associated with concomitant therapy. For example, concomitant treatment can down-regulate CYP3A4 and UGT1A1, increasing exposure to both TKI and chemotherapeutic agents sharing common metabolic pathways which may increase toxicity [108, 109]. Additionally, both TKIs and chemotherapeutics are substrates for drug efflux transporters of the ATP binding cassette family. This means that they may

impede drug clearance of the other drug, subsequently drug accumulation can result with potentially increased toxicity [110].

While the use of concomitant treatment no doubt contributes to the toxicity profile, patients prescribed ErbB TKI monotherapy also demonstrate systemic treatment complications. Given the drugs different mechanisms of action, this supports a hypothesis suggesting that ErbB TKIs trigger deregulation of chloride channels, driving water into the lumen, resulting in a secretory diarrhoea phenotype, as opposed to the mucositis driven anatomical derangement diarrhoea phenotype typically seen in chemotherapy induced diarrhoea. Given the reduced quality of life associated with diarrhoea is further exacerbated in concomitant treatment, further research is crucial.

Pharmacogenetic studies have shown a link between TKI-induced diarrhoea and allelic variants of *ABCG2*, a polymorphic efflux transporter protein (also known as breast cancer resistance gene *BCRP*), highly expressed in the intestines. A common functional single-nucleotide polymorphism (SNP) in the *ABCG2* gene was associated with diarrhoea in patients treated with gefitinib, an ErbB1 small molecule TKI [111]. This suggests that patients with reduced *ABCG2* activity due to a common genetic variation are at increased risk for substrate drug-induced diarrhoea, with implications for optimising treatment with small molecule ErbB TKIs. However, further research is required before meaningful conclusions can be made.

Current treatment approaches for TKI-induced diarrhoea

Currently, management of TKI-induced diarrhoea is very similar to management of chemotherapy-induced diarrhoea and includes patient education and both non-

pharmacologic and pharmacologic management strategies. This ignores the probability of a differing mechanism of diarrhoea development.

Patient education includes advice on dietary changes for the management of ErbB TKI-induced diarrhoea, based on dietary changes recommended for chemotherapy induced-diarrhoea. These dietary modifications include incorporating bananas, rice, apple sauce and toast (BRAT diet), as well as increasing water consumption and avoiding foods/drinks that contain lactose/caffeine; however, these dietary changes are not recommended in anticipation of diarrhoea development [61]. Patients should also avoid foods that exacerbate symptoms, such as greasy, spicy and fried items; and foods that are difficult to digest. Increasing fluid intake to 2 litres/ per day is recommended to avoid dehydration; some fluids should contain sugar or salt to avoid hyponatremia and hypokalaemia caused by electrolyte loss associated with diarrhoea [61].

Pharmacologic management of ErbB TKI-induced diarrhoea is largely limited to loperamide, with the dose based on the grade of diarrhoea experienced by the patient [61]. Loperamide, a synthetic oral opioid drug, works by a number of different mechanisms of action that decrease peristalsis and fluid secretion, resulting in longer gastrointestinal transit time and increased absorption of fluids and electrolytes from the gastrointestinal tract [112]. Alternatives to loperamide are also available for managing diarrhoea, however their use and effectiveness can differ by geographic location and the diarrhoea severity. Some of these include diphenoxylate–atropine and codeine, either of which can be used with loperamide [61]. Dose reductions are not recommended for grade 1 diarrhoea. At grade 2, if the patient does not respond to loperamide after 48 hours, it is recommended the ErbB TKI is temporarily discontinued until the diarrhoea

returns to grade 1, at which time the ErbB TKI is resumed, often at a lower dose [61]. It is recommended that the ErbB TKI should be permanently discontinued if diarrhoea does not reach grade 1 within 14 days despite best supportive care and withholding of the ErbB TKI [61]. Patients presenting with grade 3-4 diarrhoea should be admitted to hospital for the administration of intravenous fluids and electrolyte replacement.

Potential treatment approaches for TKI-induced diarrhoea

If the hypothesis of increased chloride secretion being responsible for TKI-induced diarrhoea is correct, there may be more effective treatment strategies. If TKI-induced diarrhoea is induced by increased chloride secretion, the two major apical channels for chloride secretion in enterocytes, CFTR and CaCC, present as promising targets. Ideally, these treatment approaches would have minimal systemic absorption, and act on the external pore of the chloride channels, to limit systemic effects. While this is appealing in terms of reducing systemic absorption, and therefore potential drug interactions and toxicities, concerns have been raised in regards to the potential barrier of the inhibitor reaching the deep intestinal crypts given the strong convective washout force observed during secretory diarrhoeas [113]. CFTR inhibitors include CFTRinh-172, which binds to the cytoplasmic side of the channel and stabilises the channel closed state [114], and the glycine hydrazides, which target the extracellular CFTR surface in the channel pore [113]. CaCC inhibitors are less common and include $CaCC_{inh}$-A01, a red wine extract that has been shown to prevent watery diarrhoea in a mouse model of rotavirus [115]. Recently, crofelemer, a natural product extract, was approved for the treatment of diarrhoea induced by antiretroviral medication for HIV patients. Crofelemer is extracted from the stem bark latex of the croton lechleri tree. It has been shown to dose-dependently reduce intestinal fluid secretion in cell culture and mouse models [116,

117]. It has been used for many years in Peru and Ecuador to treat diarrhoea, and has been investigated for the treatment of traveller's diarrhoea, infectious diarrhoea and diarrhoea predominant irritable bowel syndrome [116, 117]. While the precise mechanism of crofelemer is unclear, it is known that the antisecretory activity of crofelemer is due to its dual inhibitory action on the two principle Cl^- channels in the apical membrane of intestinal epithelial cells, CFTR and CaCC [118]. As crofelemer effectively inhibits *both* of the principle Cl- channels, it is an attractive agent to reduce secretory diarrhoea. Clinical studies have demonstrated that crofelemer is a safe and tolerable drug, with no adverse effects being reported [119-121].

Conclusion

With the increasing incidence of malignancy, coupled with the advent of more aggressive treatment modalities, ErbB TKI induced diarrhoea remains a significant clinical burden and a fuller understanding of the basic biological mechanisms is therefore required. The pathogenesis of ErbB TKI induced diarrhoea remains unknown, and understanding this is ultimately integral to developing interventions, leading to safer and more optimised cancer treatment. The negative regulation of chloride secretion by ErbB receptors being disrupted by tyrosine kinase inhibition provides a strong rationale for a secretory diarrhoea phenotype hypothesis. Considering the increased utilisation and therapeutic efficacy of ErbB TKIs, further research to gain the ability to prevent diarrhoea is urgently warranted [122].

Statement of Authorship

Title of Paper	Dacomitinib-induced diarrhoea is associated with altered gastrointestinal permeability and disruption in ileal histology in rats
Publication Status	☒ Published ☐ Accepted for Publication ☐ Submitted for Publication ☐ Unpublished and Unsubmitted w ork w ritten in manuscript style
Publication Details	Primary research paper International Journal of Cancer (2017) 140: 2820-2829

Principal Author

Name of Principal Author (Candidate)	Ysabella Van Sebille		
Contribution to the Paper	First author and main contributor. I developed the concept, did the data curation, formal analysis, investigation, methodology, project administration, validation, visualisation, writing the original draft, and reviewing and editing.		
Overall percentage (%)	90%		
Certification:	This paper reports on original research I conducted during the period of my Higher Degree by Research candidature and is not subject to any obligations or contractual agreements with a third party that would constrain its inclusion in this thesis. I am the primary author of this paper.		
Signature		Date	September, 2017

Co-Author Contributions

By signing the Statement of Authorship, each author certifies that:

i. the candidate's stated contribution to the publication is accurate (as detailed above);

ii. permission is granted for the candidate in include the publication in the thesis; and

iii. the sum of all co-author contributions is equal to 100% less the candidate's stated contribution.

Name of Co-Author	Rachel Gibson		
Contribution to the Paper	Rachel was involved in conceptualisation, supervision, and reviewing manuscript drafts		
Signature		Date	September, 2017

Name of Co-Author	Hannah Wardill		
Contribution to the Paper	Hannah was involved in investigation, methodology, and reviewing manuscript drafts		
Signature		Date	September, 2017

Name of Co-Author	Kate Secombe		
Contribution to the Paper	Kate was involved in investigation, and methodology		
Signature		Date	September, 2017

Name of Co-Author	Imogen Ball		
Contribution to the Paper	Imogen was involved in investigation, and methodology		
Signature		Date	September, 2017

Name of Co-Author	Dorothy Keefe		
Contribution to the Paper	Dorothy was involved in funding acquisition		
Signature		Date	September, 2017

Name of Co-Author	John Finnie		
Contribution to the Paper	John was involved in investigation and methodology		
Signature	Not Available. Signed on behalf.	Date	September, 2017

Name of Co-Author	Joanne Bowen		
Contribution to the Paper	Joanne was involved in conceptualisation, funding acquisition, investigation, methodology, project administration, supervision, and reviewing manuscript drafts		
Signature		Date	September, 2017

Chapter 3 Dacomitinib-induced diarrhoea is associated with altered gastrointestinal permeability and disruption in ileal histology in rats

This chapter was published in The International Journal of Cancer (**Van Sebille, Y.Z.,** Gibson, R. J., Wardill, H.R., Secombe, K.R., Ball, I.A., Keefe, D.M., Finnie, J.W., Bowen, J.M. 2017. Dacomitinib-induced diarrhoea is associated with altered gastrointestinal permeability and disruption in ileal histology in rats. *International Journal of Cancer,* 140, 2820-2829.)

Abstract

Dacomitinib – an irreversible pan-ErbB tyrosine kinase inhibitor (TKI) – causes diarrhoea in 75% of patients. Dacomitinib-induced diarrhoea has not previously been investigated and the mechanisms remain poorly understood. The present study aimed to develop an *in-vitro* and *in-vivo* model of dacomitinib-induced diarrhoea to investigate underlying mechanisms. T84 cells were treated with 1-4 μM dacomitinib and resistance and viability were measured using transepithelial electrical resistance (TEER) and XTT assays. Rats were treated with 7.5 mg/kg dacomitinib daily *via* oral gavage for 7 or 21 days (n = 6/group). Weights, and diarrhoea incidence were recorded daily. Rats were administered FITC-dextran 2 hours before cull, and serum levels of FITC-dextran were measured and serum biochemistry analysis was conducted. Detailed histopathological analysis was conducted throughout the gastrointestinal tract. Gastrointestinal expression of ErbB1, ErbB2, and ErbB4 was analysed using RT-PCR. The ileum and the colon were analysed using multiplex for expression of various cytokines. T84 cells treated with dacomitinib showed no alteration in TEER or cell viability. Rats treated with

dacomitinib developed severe diarrhoea, and had significantly lower weight gain. Further, dacomitinib treatment led to severe histopathological injury localised to the ileum. This damage coincided with increased levels of MCP1 in the ileum, and preferential expression of ErbB1 in this region compared to all other regions.
This study showed dacomitinib induces severe ileal damage accompanied by increased MCP1 expression, and gastrointestinal permeability in rats. The histological changes were most pronounced in the ileum, which was also the region with the highest relative expression of ErbB1.

Introduction

Dacomitinib (PF-00299804) is an orally administered, highly selective irreversible small-molecule pan-ErbB receptor tyrosine kinase inhibitor (TKI) under development for treatment of recurrent or metastatic non-small cell lung cancer (NSCLC) [42]. It acts by covalently binding to the intracellular adenosine triphosphate domain of each of the three kinase-active members of the ErbB family (ErbB1, ErbB2 and ErbB4). This effectively inhibits phosphorylation of the receptors and therefore downstream signalling [40]. In addition to being expressed on cancer cells, the ErbB family are also abundantly expressed on the basolateral membrane of healthy gastrointestinal epithelial cells, and are crucial for essential functions including maintenance of mucosal integrity *via* induction of mucus and prostaglandin synthesis, promotion of enterocyte migration, prevention of intestinal epithelial cell apoptosis, decreasing bacterial translocation and preservation of gut barrier function after injury [41, 71, 72].

Dacomitinib is currently in phase III clinical trials for NSCLC and has shown significant therapeutic effects, specifically to tumours which have not previously responded to

conventional single receptor inhibitors [48]. Furthermore, dacomitinib has shown to be effective against tumours with mutations developed for acquired resistance of targeted therapies [123]. However a commonly reported adverse event among all trials has been diarrhoea, with up to 78% of patients developing some degree of diarrhoea [124]. Severe diarrhoea commonly results in dose reductions and patient withdrawal from clinical trials [124]. Of particular clinical importance is dacomitinib is delivered in a continuous manner over many months; therefore, to optimise dacomitinib therapy, adequate management or prevention of chronic diarrhoea is essential to minimise the impact on the patient's quality of life, increase safety and the ability to complete the course of therapy. Currently management for dacomitinib-induced diarrhoea follows that used in conventional chemotherapy (daily loperamide), however the mechanisms underlying this diarrhoea are likely different [16]. Recent phase II research has investigated both antibiotic and probiotic prophylactic treatment for dacomitinib-induced diarrhoea, with no change in diarrhoea reported [125]. It is hypothesised that the development of dacomitinib-induced diarrhoea differs from conventional chemotherapy-induced diarrhoea and does not result due to direct cytotoxicity but rather occurs through alternative mechanisms [16, 82]. As such, traditional diarrhoea management may be not targeting the underlying changes for optimal management. Therefore, this study assessed direct cytotoxicity in an *in vitro* model, and then aimed to develop an *in vivo* rat model of dacomitinib-induced diarrhoea, characterising the changes that dacomitinib causes through the gastrointestinal tract.

Materials and Methods

Chemicals

Dacomitinib (PF-00299804) was kindly provided by Pfizer Pharmaceuticals. For all *in vivo* experiments dacomitinib was suspended in 0.5% (w/w) hydroxypropyl-methylcellulose to a final concentration of 2 mg/ml. For all *in vitro* experiments dacomitinib was suspended in DMSO. SN38 and TX100 were used as positive controls *in vitro,* both suspended in DMSO. Exposure of DMSO to cells did not exceed 0.01%.

In vitro Model

The model utilised T84 cells (passage 5-15) derived from a human colorectal carcinoma (Culture Collections, Porton Down, UK). Cells were authenticated by Culture Collections by DNA profiling and were used within 6 months of receipt. Cells were maintained at 37°C in 5% CO_2/95% air in Dulbecco's Modified Eagle Medium (DMEM)/Ham's F-12 Nutrient Mixture containing 15mM HEPES, L-glutamine and 10% foetal bovine serum (FBS) and were routinely screened for mycoplasma infection. Cells were seeded at a density of 100,000 cells/cm^2 on 1.12 cm^2, 0.4 μm pore polyester transwell inserts (Corning Life Sciences, MA, USA) or at 10,000 cells in 96 well microtiter flat-bottom plates (Becton Dickinson, USA) for transepithelial electrical resistance (TEER) measurements and cell proliferation (XTT) assays (Roche, Australia) respectively. Dacomitinib was diluted to a series of concentrations (1 - 4 μM) and exposed to cells *via* the apical side for 24 - 48 hours. An equivalent dilution of DMSO was used as vehicle control treatment. SN-38 (5 μM), an inhibitor of topoisomerase 1, was used as the positive control as it is recognised for its cytotoxicity [126]. Triton X-100 was used as the positive control for TEER measurements as it is known to

permeabilse T84 cells [127]. All experiments were performed in triplicate and repeated twice.

Polyester transwell inserts support a polarised T84 phenotype with functional tight junctions; TEER is a measure to assess the integrity of this monolayer [127]. Once cells had reached 1000 Ω/cm^2, indicating monolayer formation, cells were exposed to varying doses of dacomitinib for 24 or 48 hours. Transepithelial electrical resistance (TEER) was measured using an EVOM2 epithelial volt-ohm-meter with chopstick electrodes, STX2 (World Precision Instruments, Sarasota, FL, USA) and area adjusted for analysis using the following formula;

TEER monolayer (Ω/cm^2) = [raw TEER (Ω) – TEER blank (Ω)/area of membrane (1.12 cm^2)].

XTT assays were conducted on cells exposed to 1 - 4 μM dacomitinib in total media for 24 hours. Following 24 hours exposure, media and dacomitinib were removed and replaced with 100 μl fresh media and 50 μl of XTT solution; composed of 5 ml XTT labelling reagent and 100 μl of electron coupling reagent (Roche cell proliferation kit, Germany). The microtitre plate was incubated again for 6 hours at 37°C in 5% CO_2/95% air. Absorbance was read at 490 nm using Bio Tek Synergy™ Mx Microplate Reader (Bio Tek, Vermont, USA) and Gen5 version 2.00.18 software to assess the cleavage of tetrazolium salt XTT in the presence of an electron-coupling reagent, producing a soluble formazan salt, only occurring in viable cells.

In vivo Model and Ethics

The study was approved by the Animal Ethics Committee of The University of Adelaide, and complied with the National Health and Medical Research Council (Australia) Code of Practice for Animal Care in Research and Training (2014). Rats were group housed in ventilated cages with three to six animals per cage and were on a 12 h light/dark cycle. Food and water were provided *ad libitum.*

Experimental Design

All experiments were conducted on male Albino Wistar rats (initial age 6 weeks) obtained from The University of Adelaide Laboratory Animal Service (SA, Australia). Rats were treated with dacomitinib at a dose of 7.5 mg/kg administered daily for 7 or 21 days, *via* oral gavage using a soft plastic feeding tube. This treatment schedule mimics the clinical oral administration over many weeks and allows assessment of acute damage (7 days) and prolonged damage (21 days). Control animals received daily gavage with dacomitinib vehicle (0.5% (w/w) hydroxypropyl-methylcellulose. Rats were randomly assigned to treatment groups and culled at 7 and 21 days (n = 6/group). Rats were anaesthetised using isoflurane inhalation, and were culled *via* cardiac exsanguination and cervical dislocation.

Clinical Assessment of Gastrointestinal Toxicity

All rats were monitored two times daily for the presence of diarrhoea. Two independent assessors quantified diarrhoea using a validated grading system where 0 = no diarrhoea, 1 = mild diarrhoea with soft stools and perianal staining, 2 = moderate diarrhoea with loose stools and perianal staining of fur, 3 = severe diarrhoea with watery stools +/- mucous and fur staining incorporating hind legs [15]. Rats were weighed daily to track

weight loss/gain. Rats were culled if they displayed > 15 % weight loss or significant distress and deterioration, in compliance with animal ethical requirements. One animal was removed from the study due to > 15 % weight loss from the dacomitinib group. This animal was not included in any further analysis.

Tissue Preparation

At necropsy, the entire gastrointestinal tract from pyloric sphincter to rectum was dissected and flushed with saline to remove intestinal contents. Samples of jejunum, ileum and colon were collected and either (1) fixed in 10 % formalin for embedding in paraffin, (2) had the mucosal surface scraped and stored in RNA-later at -20 °C for molecular analyses, or (3) had the mucosal surface scraped and snap frozen in liquid nitrogen and stored in -80 °C for immunological analysis. Other organs were collected as routine and fixed in formalin and embed in paraffin. All histopathological analysis was conducted on 5 μm sections tissue cut on a rotary microtome and mounted onto glass Superfrost® microscope slides (Menzel-Gläser, Braunschweig, Germany). Slides were scanned using a NanoZoomer™ (Hamamatsu Photonics, Japan) and assessed with NanoZoomer Digital Pathology software view.2 (Histalim, Montpellier, France).

Blood Biochemistry

Blood samples were collected by cardiac puncture. Serum was separated by centrifugation at 3,000 g for 5 min before being analysed by the Department of Clinical Pathology, SA Pathology, Adelaide, South Australia. A multiple blood analysis (MBA-20) was conducted.

Gastrointestinal Histopathological Analysis

Haematoxylin and eosin (H&E) staining was performed and a well described total tissue injury score was generated based on the occurrences of eight histological criteria in the jejunum and ileum, and six criteria in the colon [128, 129]. These criteria were villous fusion and villous atrophy (jejunum and ileum only), disruption of brush border and surface enterocytes, crypt loss/architectural disruption, disruption of crypts cells, infiltration of polymorphonuclear cells and lymphocytes, dilation of lymphatic's and capillaries, and oedema. Each parameter was scored as present = 1, or absent = 0, in a blinded fashion.

Goblet Cell Analysis

Alcian Blue (1 % Alcian Blue 8GX (CI 74240) in 3 % glacial acetic)/ Periodic acid Schiff staining was performed on jejunum, ileum and colon. Sections were oxidised in 1 % periodic acid before washing then treated in Schiff's reagent. Goblet cells and cavitated cells in crypts and villi that were deemed to be greater than 80% complete were counted, and a total of at least 15 villi/crypts per section analysed. Data presented as average per crypt or villous. All analysis was done in a blinded fashion.

Immunohistochemistry

Immunohistochemical analysis was performed for apoptosis (caspase 3; Abcam, Vic, Australia; #ab4051), and proliferation (Ki67; Abcam, Vic, Australia #ab16667). Changes in these parameters are validated markers for altered tissue kinetics in previous models of cancer therapy induced-gastrointestinal toxicities [63, 69, 70, 90].
Immunohistochemical analysis was performed using Dako reagents on an automated machine (AutostainerPlus™, Dako, Denmark) following standard protocols supplied by

the manufacturer. Briefly, sections were deparaffinised in histolene and rehydrated through graded ethanol before undergoing heat mediated antigen retrieval using an EDTA/Tris buffer (0.37 g/L EDTA, 1.21 g/L Tris; pH 9.0). Retrieval buffer was preheated to 65°C using the Dako PT LINK (pre-treatment module). Slides were immersed in the buffer and the temperature raised to 97°C for 20 minutes. After returning to 65°C, slides were removed and placed in the Dako AutostainerPlus and stained following manufactures guidelines. Negative controls had the primary antibody omitted. Caspase 3 and Ki67 were quantified by counting the number of positively stained cells for 15 crypts. Data presented as average positively stained cells per crypt. All analysis was done in a blinded fashion.

Real Time PCR

To assess the expression of ErbB1, ErbB2 and ErbB4 receptors along the gastrointestinal tract, total RNA was isolated from duodenal, jejunal, ileal and colonic mucosal scrapings. Purification of mRNA was done using the Nucleospin mRNA purification RNA II kit (Macherey-Nagel) following the manufacturer's protocol. 1 µg of RNA was reverse transcribed using iScriptTM cDNA synthesis kit (Bio-Rad) according to the manufacturer's protocol. cDNA was quantified and diluted to a working concentration of 100 ng/µl. Primers for genes of interest were either designed using web-based primer design program Primer 3, version 4 (http://bioinfo.ut.ee/primer3-0.4.0/), or in the case of ErbB4 purchased from BioRad (Gladesville, Australia). Genes of interest were ErbB1 (Forward: 5'-CCCACAGCAAGCCTTCTTCA; Reverse: R: 5'-CACGGCAGCTCCCATTTCTA), ErbB2 (Forward: 5'-GCTCCTCCTTGAGTTGAGTGT; Reverse: 5'-TAGCCTTGGAATGAGTGCGT) and ErbB4 (PrimePCR™ SYBR® Green Assay: ErbB4, rat). ErbB1 and ErbB2 were

denatured at 95°C for 10 seconds, annealed at 52°C for 15 seconds, and extended at 72°C for 20 seconds (40-45 cycles). ErbB4 was following manufactures instructions. Amplified transcripts were detected by SYBR Green (Quantitect, Qiagen) in a Rotor-Gene Q (Qiagen). All reactions were completed in triplicate, with two housekeeping normaliser primers, UBC (Forward: 5'-TCGTACCTTTCTCACCACAGTATCTAG; Reverse: 5'-GAAAACTAAGACACCTCCCCATCA) and B2M (Forward: 5'-TGACCGTGATCTTTCTGGTG; Reverse: 5'-ATCTGAGGTGGGTGGAACTG). Amplification was followed by a melt curve analysis to confirm product specificity. Relative gene expression was determined by delta Ct method [130].

Tissue Cytokine Quantification

Proinflammatory cytokine expression was assessed using 30 mg of ileal and colonic mucosal scraping samples. Mucosa samples were homogenised at room temperature using the QIAGEN TissueLyser LT (Qiagen) for 5 minutes at 50 Hz in 500 μL of the Radioimmunoprecipitation Assay (RIPA) buffer (150 mmol/L NaCl, 1.0% IGEPAL CA-630, 0.5% sodium deoxycholate, 0.1% SDS, and 50 mmol/L Tris, pH 8.0; Sigma Aldrich; #04693116001). Homogenates were centrifuged at 11,000 x g for 15 minutes at 4°C and the supernatant isolated, aliquoted, and stored at -80 °C. Total protein concentration was quantified using the Pierce BCA Protein Assay Kit (ThermoFisher Scientific; #23225). A working concentration of 1 mg/ml was used for cytokine analysis. Levels of 7 different cytokines, including interleukin-1β (IL-1β), interleukin-6 (IL-6), interleukin-17 (IL-17), tumour necrosis factor alpha (TNFα), monocyte chemoattractant protein-1 (MCP-1), interleukin-4 (IL-4) and interleukin-10 (IL-10), were measured in individual ileal and colonic homogenates using Luminex xMAP technology (Milliplex Rat Cytokine Kit, Merck Millipore; #RECYTMAG-65K) as per the manufacturer's

instructions. Each 96 well plate included a 6-point standard curve and two quality controls provided by Merck Millipore.

FITC-dextran Assay

Two hours prior to culling, rats received a 600 mg/kg dose (120 mg/ml) of 4 kDa fluorescein isothiocyanate (FITC)-dextran (Sigma-Aldrich, NSW, Australia, Cat# FD4) *via* oral gavage. Blood was collected *via* cardiac puncture at necropsy into serum-gel clotting activator tubes and protected from light. Samples were centrifuged at 3,000 g for 5 minutes and serum isolated. Serum samples were diluted 1:3 with 1 X PBS and quantified using the Bio Tek Synergy™ Mx Microplate Reader (Bio Tek, Vermont, USA) and Gen5 version 2.00.18 software relative to a standard curve (range 0.0001-10 μg/ml).

Statistical Analysis

Data were compared using Prism version 7.0 (GraphPad® Software, San Diego USA). A D'Agostino Pearson omnibus test was used to assess normality. When normality was confirmed, a two-way analysis of variance (ANOVA) with appropriate post hoc testing was performed to identify statistical significance between groups. In other cases, a Kruskal-Wallis test with Dunn's multiple comparisons test and Bonferroni correction was performed. For diarrhoea data, a Chi^2 test was used.

Results

Dacomitinib Does Not Cause Direct Cytotoxicity to T84 Epithelial Cells

T84 monolayers exhibited comparable TEER between controls and monolayers treated with dacomitinib (1 - 4 μM), with no significant differences detected ($p > 0.05$). TEER readings for cells treated with all doses of dacomitinib were significantly higher than SN38, the positive control ($p < 0.05$) (Figure 1A). Cells treated with varying doses of dacomitinib (1 - 4 μM) had no alterations in cell viability, as measured by XTT absorbance, with no significant differences seen between controls (Figure 1B). Compared to the positive control (SN38), cells treated with dacomitinib had significantly increased viability ($p < 0.05$) (Figure 1B). Combined these results demonstrate that dacomitinib does not cause direct cytotoxicity to T84 cells.

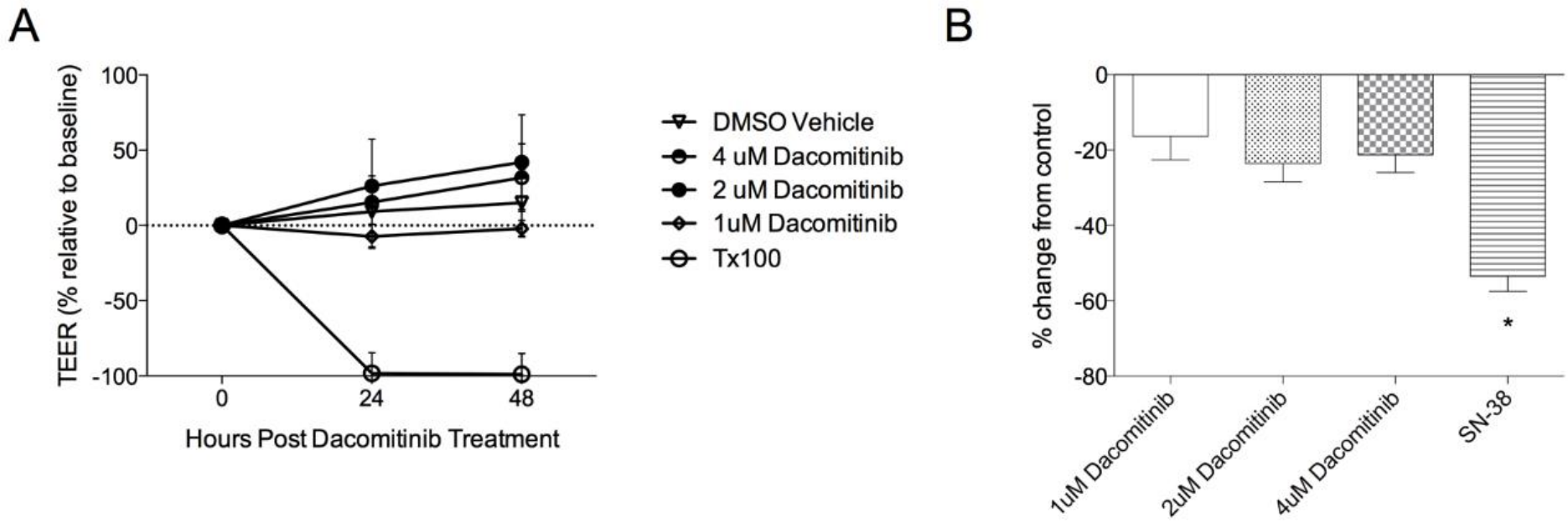

Figure 1 A: Transepithelial electrical resistance (TEER) following dacomitinib exposure (1 – 4 μM) for 24 - 48 hours did not decrease ($p > 0.05$). Data presented as mean ± SEM. Data analysed using two-way ANOVA. B: Absorbance of XTT assay did not decrease following 24 hours of dacomitinib exposure (1 - 4 μM) compared to controls, but was significantly higher than SN-38 ($p < 0.05$). Data presented as mean ± SEM. Data analysed using one-way ANOVA.

Dacomitinib Causes Reproducible, Severe Diarrhoea

Rats treated with vehicle control did not develop diarrhoea at any time point (data not shown). Dacomitinib treatment induced diarrhoea in 100% of rats (Figure 2A), comparable to the incidence seen in clinical trials [124]. Mild diarrhoea developed in a small number of animals from as early as day 2 of treatment, with severe diarrhoea manifesting as early as day 3. Diarrhoea incidence peaked from day 7 onward. The average number of days with diarrhoea was 14 days. Rats treated with dacomitinib had significantly worse diarrhoea than control rats ($p < 0.0001$).

Growth rates of dacomitinib treated rats were significantly lower than control rats from day 10 ($p < 0.0001$) (Figure 2B). At day 21, the control group had gained 46.38 ± 2.459 % body weight compared to day 1, and the dacomitinib group had gained 18.99 ± 5.602 % body weight compared to day 1.

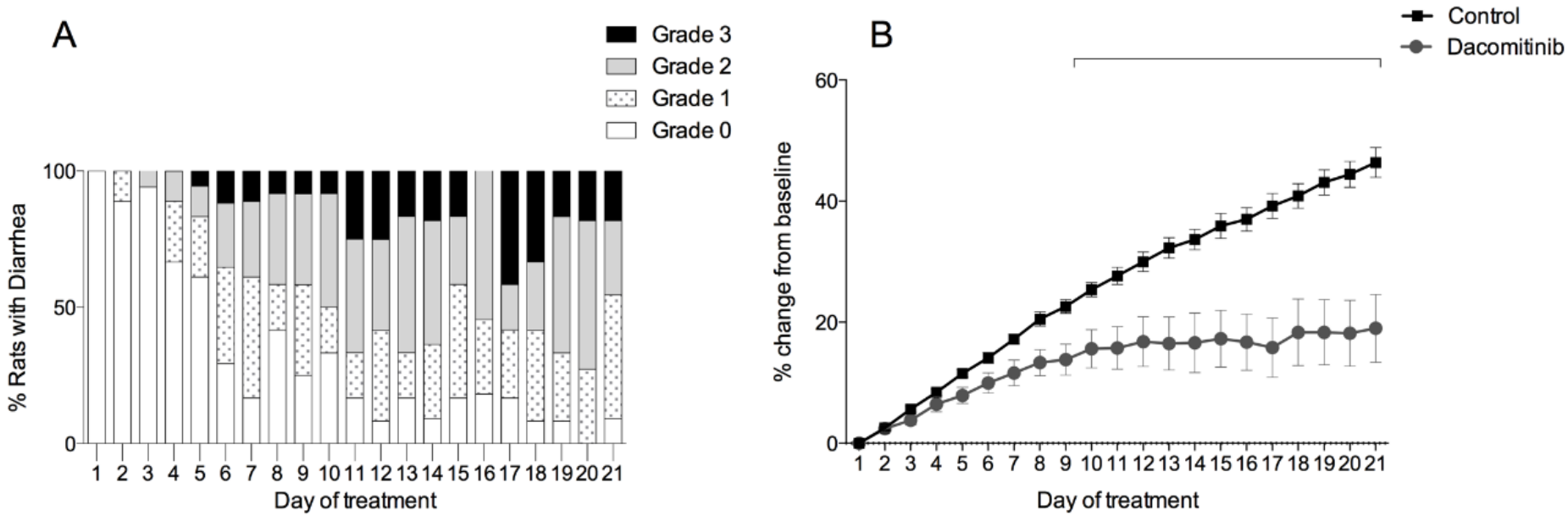

Figure 2 A: Rats treated with vehicle control did not develop diarrhoea. 100% of rats treated with 7.5 mg/kg dacomitinib developed diarrhoea. Diarrhoea data are expressed as a percentage of total animals (per day) with a particular grade of diarrhoea. B: Rats treated with 7.5 mg/kg dacomitinib had significantly lower weight gain than controls from day 10 onward ($p < 0.0001$). Data displayed as a percentage of weight change from baseline (day 1). A Kruskal-Wallis with *post hoc* testing was performed to identify statistical significance.

Dacomitinib Alters Biochemistry and Histology

In rats treated with dacomitinib, serum biochemistry revealed mildly elevated alanine aminotransferase (ALT) which, in the absence of histological changes in the liver, suggested increased permeability of hepatocyte cell membranes with leakage of this cytosolic enzyme into the blood (Supplementary Table 1). There was also a modest increase in blood urea nitrogen (BUN) and creatinine, particularly at 21 days, indicating mild renal dysfunction (Supplementary Table 1). A mild hypoalbuminemia was probably attributable to a combination of malabsorption due to villous atrophy, protein-losing enteropathy associated with severe diarrhoea, and renal proteinuria. All other MBA-20 analytes were within the normal range (Supplementary Table 1). Kidneys of all rats, except one, treated with dacomitinib for 21 days showed acute papillary necrosis with severe coagulation necrosis of medullary tubules and collecting duct epithelium, either complete or with intraluminal, desquamated, necrotic epithelial cells and few, usually degenerating, lining epithelial cells with marked interstitial congestion. One rat treated with dacomitinib for 21 days showed mild hydronephrosis, with dilation of renal pelvis and patchy distension of tubules and collecting ducts. Rats treated with dacomitinib for 7 days exhibited mild glomerulopathy with thickening of the glomerular basement membranes.

Dacomitinib Causes Significant ileal Damage

Rats treated with dacomitinib had significant ileal injury compared to controls at both time points ($p < 0.0001$). This was predominantly characterised by severe villus atrophy with stunting and fusion of villi, which was also attended by enterocyte metaplasia to a low columnar or cuboidal phenotype and mild compensatory expansion of the basal proliferative compartment of crypts. In the congested lamina propria, there was an

increased inflammatory infiltrate comprised of lymphocytes, macrophages, plasma cells and neutrophils, and dilation of lacteals (villous lymphatics) (Figure 3). There were no significant differences in tissue injury at any time point in the jejunum and colon (data not shown). Across both treatment groups no significant differences for both total number of goblet cells or percentage cavitated goblet cells in the jejunum, ileum or colon as assessed *via* AB-PAS staining were seen (data not shown).

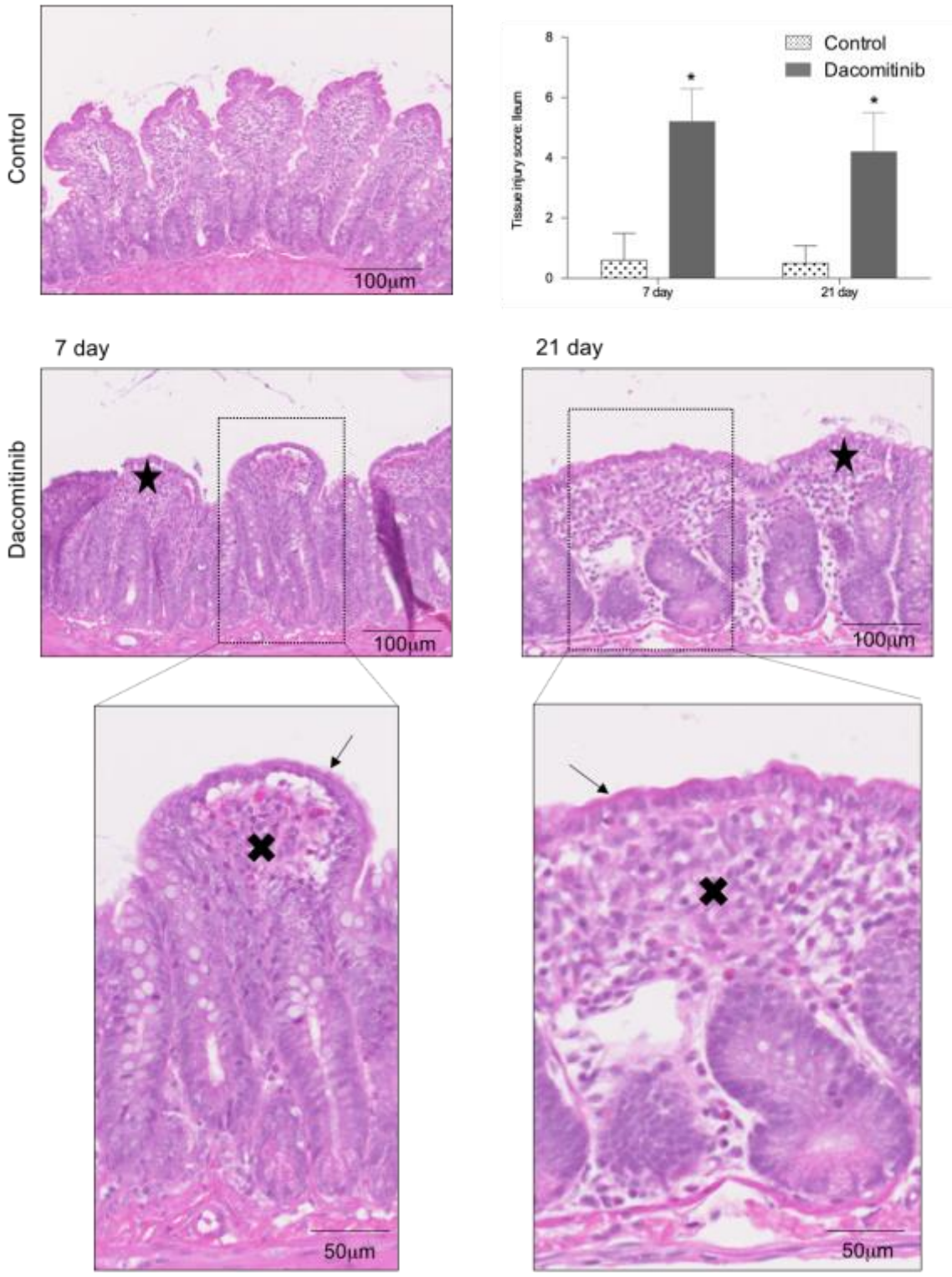

Figure 3 Histological injury was significantly increased in the ileum in rats treated with dacomitinib at both day 7 ($p < 0.0001$) and day 21 ($p < 0.0001$). Histological injury was characterised by villus atrophy/blunting and fusion (indicated by black stars), enterocyte

metaplasia to a low columnar or cuboidal epithelium (indicated by black arrows), and increased inflammatory component in the lamina propria (indicated by black cross). There was no significant change in histological injury in the jejunum or colon. Tissue injury score presented as mean ± SD.

Dacomitinib Did Not Alter Gastrointestinal Apoptosis or Proliferation

To assess gastrointestinal epithelial apoptosis, the number of caspase-3 positively stained crypt cells were counted and means calculated. Gastrointestinal apoptosis was not changed following dacomitinib treatment in the crypts of the jejunum at day 7 (dacomitinib 0.11 ± 0.053 vs control 0.04 ± 0.02) or day 21 (dacomitinib 0.24 ± 0.05 vs control 0.10 ± 0.03). Gastrointestinal apoptosis was not changed following dacomitinib treatment in the crypts of the ileum at day 7 (dacomitinib 0.03 ± 0.02 vs control 0.03 ± 0.01) or day 21 (dacomitinib 0.03 ± 0.01 vs control 0.02 ± 0.02). Gastrointestinal apoptosis was not changed following dacomitinib treatment in the crypts of the colon at day 7 (dacomitinib 1.27 ± 0.37 vs control 1.20 ± 0.27) or day 21 (dacomitinib 0.94 ± 0.17 vs control 0.82 ± 0.18). To assess proliferation within crypts, the number of Ki-67 positively stained cells were counted and means calculated. Gastrointestinal proliferation was not changed following dacomitinib treatment in the crypts of the jejunum at day 7 (dacomitinib 21.72 ± 0.53 vs control 21.07 ± 0.07) or day 21 (dacomitinib 18.82 ± 1.31 vs control 22.70 ± 0.68). Gastrointestinal proliferation was not changed following dacomitinib treatment in the crypts of the ileum at day 7 (dacomitinib 33.71 ± 3.60 vs control 38.81 ± 2.63) or day 21 (dacomitinib 39.02 ± 1.66 vs control 40.57± 1.84). Gastrointestinal proliferation was not changed following dacomitinib treatment in the crypts of the colon at day 7 (dacomitinib 12.85 ± 0.87 vs control 14.56 ± 3.74) or day 21 (dacomitinib 11.91 ± 2.30 vs control 16.22 ± 1.88).

ErbB1 Receptor is Highly Expressed in the Ileum

The mRNA expression of ErbB1 was significantly higher in the ileum compared to the other regions of the gastrointestinal tract in untreated control rats ($p = 0.0336$) (Figure 4).

The expression of ErbB2 and ErbB4 was unchanged throughout the gastrointestinal tract ($p > 0.05$). Treatment with dacomitinib did not change the expression of the ErbB receptors ($p > 0.05$) (data not shown).

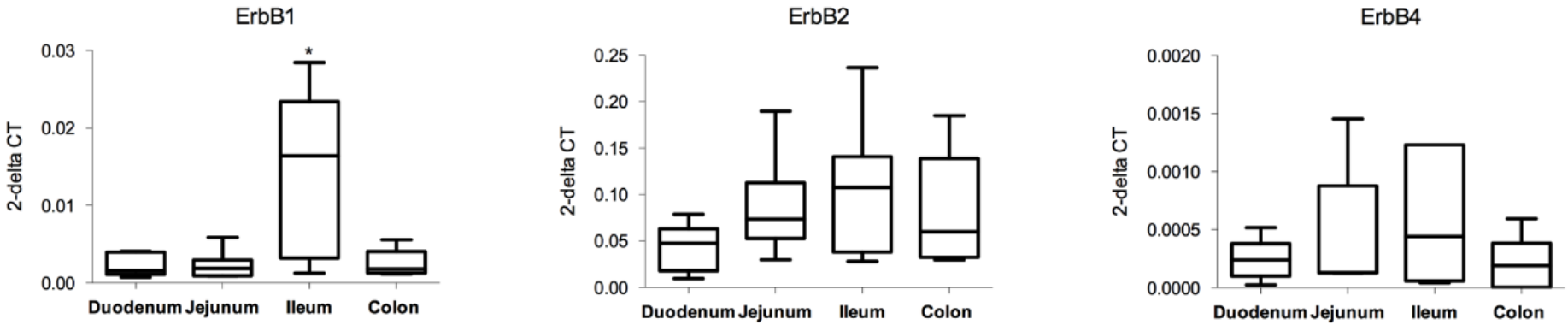

Figure 4 ErbB1 expression is significantly higher in the ileum compared to other areas of the gastrointestinal tract (p = 0.0336). Relative mRNA expression of ErbB receptors to UBC and B2M. Data presented as min-max. Data analysed using one-way ANOVA.

Dacomitinib Treatment Increases Levels of monocyte chemoattractant protein-1 (MCP-1) in the ileum

There were significant increases in the expression of MCP-1 in the ileum of rats treated with dacomitinib compared to controls ($p = 0.001$). No changes were seen in the colon. Rats treated with dacomitinib showed no statistically significant change in IL-1β, IL-6, IL-17, TNFα, IL-4, and IL-10 expression in the ileum or colon when compared to vehicle controls (Figure 5).

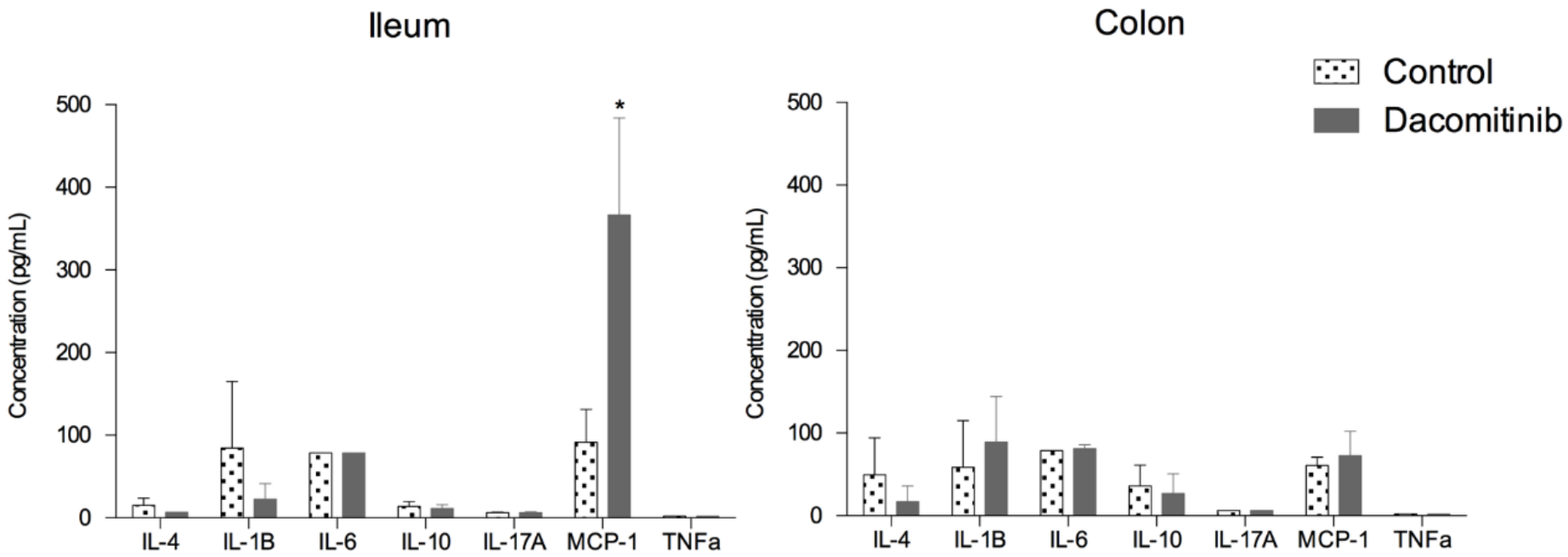

Figure 5 Cytokine expression in the mucosa of the ileum and colon. MCP-1 was significantly increased in the ileum of rats treated with dacomitinib ($p = 0.001$) compared to controls. Data presented as mean with SD (pg/mL). Multiple t-tests were performed to identify statistical significance. MCP-1 expression was increased in the mucosa of the ileum in animals treated with dacomitinib compared to control ($p = 0.001$).

Dacomitinib Caused Increased Gastrointestinal Permeability

Serum FITC-dextran levels were elevated in rats treated with dacomitinib compared to vehicle controls, ($p = 0.0018$) (Figure 6).

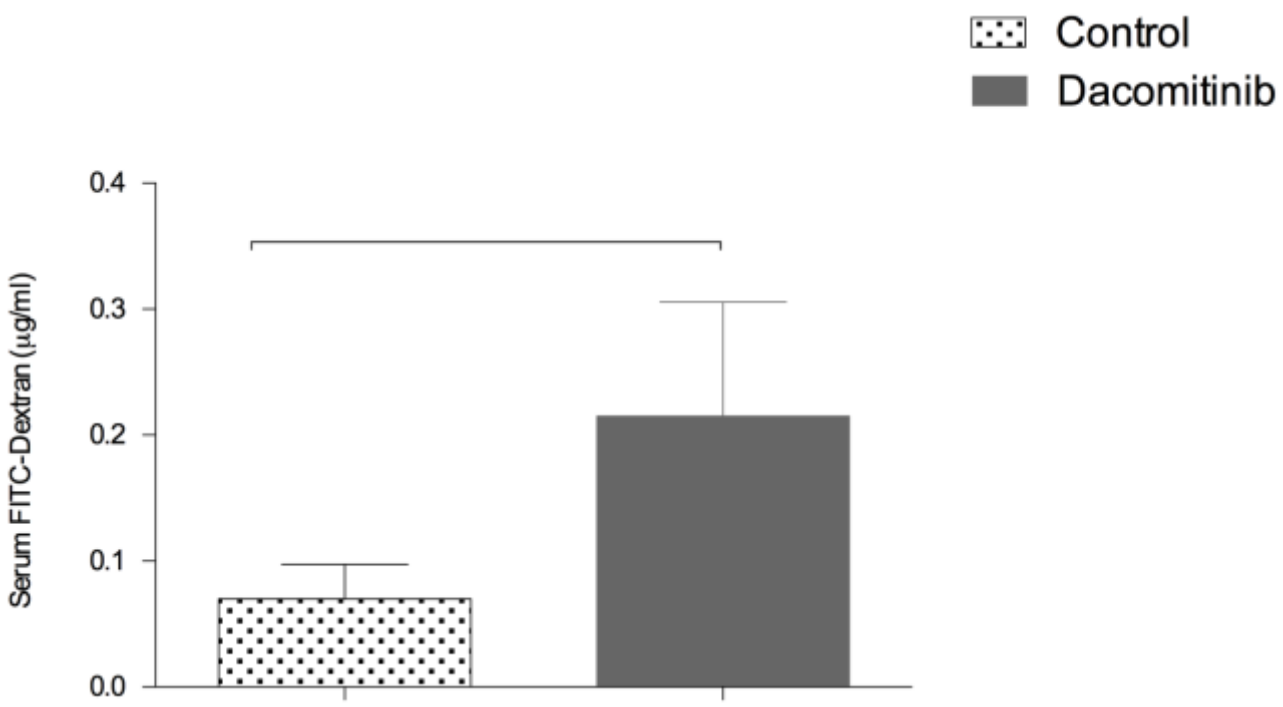

Figure 6 Serum FITC-dextran levels were significantly increased in rats treated with dacomitinib (p = 0.0018) indicating intestinal barrier dysfunction. Data presented as mean with SD. Data analysed using one-way ANOVA.

Discussion

Dacomitinib is an emerging small molecule TKI for the treatment of NSCLC, with clinical trials showing diarrhoea as an adverse event in over 75% of patients [124]. The mechanisms of ErbB TKI-induced diarrhoea are unclear with conflicting hypotheses presented in the literature [16]. The present study found dacomitinib does not cause direct cytotoxicity to T84 epithelial cells, supporting the study hypothesis, and previous literature suggesting that ErbB TKI induced-diarrhoea is not due to direct cell death [14, 89]. However, this may be explained because of the colorectal origin of T84 cells, as in rats dacomitinib causes diarrhoea that appears associated with histopathological alterations in the ileum and intestinal barrier disruption. This is the first time gastrointestinal morphometry and function have been characterised following dacomitinib, demonstrating dacomitinib causes histopathological damage confined to the ileum in rats. In murine models of ErbB TKI-induced gastrointestinal side effects, there has previously been evidence of histological changes characterised by villous atrophy [82-85, 87].

TKI's have previously been associated with diarrhoea, and this has been largely hypothesised to be of a secretory phenotype [16, 82]. In a previous rat model of lapatinib-induced diarrhoea, blood biochemistry showed a significant decrease in serum chloride. This decrease coincided with diarrhoea in rats treated with high-dose lapatinib, suggesting a possible secretory diarrhoea phenotype [90]. However, in the current study we saw no changes in serum chloride suggesting negligible secretory processes. Although not the primary focus of the study, the findings from blood biochemistry indicate rats treated with dacomitinib had significant changes in renal biochemistry, with supplementary histological investigation supporting this. These findings are despite renal

clearance of dacomitinib being only minimal [131]. As such, the renal pathology seen in this model is likely to be a species-specific response to high dose dacomitinib. The increased level of liver enzymes seen in the present study is consistent with elevations noted clinically [131], and are unsurprising given that dacomitinib is largely metabolised by the liver through oxidative and conjugative metabolism [131].

Traditional chemotherapeutic agents are known to cause severe gastrointestinal cytotoxicity, resulting in histological damage manifesting as anatomic derangement diarrhoea [63, 129]. However, throughout the literature there are conflicting findings regarding the histopathological changes in the gastrointestinal tract associated with ErbB TKI-induced diarrhoea [16]. For example, a recent study by Bowen et al, (2012) showed lapatinib-induced diarrhoea was not associated with gastrointestinal histopathological changes, typically associated with anatomic derangement diarrhoea [15]. Hare et al (2007) showed treatment with gefitinib in a murine model was associated with villous atrophy, confined to the duodenum only [132]. However, Rasmussen et al (2010) suggested that inhibition of the ErbB receptors with erlotinib causes direct mucosal atrophy and damage, which, similar to this study, was most pronounced in the ileum of mice [83]. The present study showed largely negative results, with marginal changes noted in the jejunum or colon. However, significant histopathological changes were noted in the ileum, characterised by significant villus atrophy. Unlike traditional chemotherapy-induced diarrhoea, villus shortening and blunting was localised to the ileum, with terminally differentiated enterocytes being the most affected. There were only mild compensatory changes in the deep crypt progenitor compartment and no associated goblet cell hyperplasia or apoptosis. This supports the hypothesis suggesting

an alternative mechanism may be responsible for the changes seen following dacomitinib treatment.

While small intestinal damage has previously been attributed to greater exposure of the unabsorbed drug to the mucosal surface compared to the colon [133], this is not a plausible explanation in the current study, as the jejunum showed minimal histopathological damage. The differential expression or ErbB receptors through regions of the gastrointestinal tract has not been previously characterised. Data from the present study indicates ErbB1 is preferentially expressed in the ileum compared to other regions of the gastrointestinal tract. It is therefore possible that the high degree of histopathology observed in the ileum may be linked to the high expression of ErbB1. Unlike first generation ErbB TKIs that are susceptible to mutations that affect binding affinity, second generation ErbB TKIs (such as dacomitinib) are irreversible and resistant to mutations, they have therefore demonstrated a higher binding affinity [134]. This may account for the more severe ileal damage seen in our model, and the associated diarrhoea.

Elevated MCP-1 was evident in the ileum, suggesting an inflammatory response characterised, in part, by monocyte infiltration, which may contribute to the ileal tissue injury. This is of particular significance as inflammation has been associated with the induction of a ‘leaky’ gut [135, 136]. Mucosal enterocyte barrier disruption has been associated with a number of gastrointestinal pathologies characterised by diarrhoea [137]. It has been suggested that altered intestinal permeability worsens clinical outcomes, as it allows for translocation of endotoxin and bacteria [136]. Additionally, it has been proposed that breakdown of the intestinal mucosal barrier contributes to

diarrhoea through leak-flux mechanisms allowing passive movement of water into the lumen [138]. Our findings partially support this with increased serum FITC-dextran seen following dacomitinib treatment. The increased gastrointestinal permeability noted in this study is most likely indicative of tight junction disruption, the main regulators of paracellular permeability. Tight junctions join the apical margins of adjacent enterocytes and, while permeable to small molecules and water, form a barrier to transepithelial macromolecular movement; the basolateral aspect of enterocytes is the site of Na-K-dependent ATPase that drives the sodium pump. Further studies are required to examine the impact of dacomitinib on specific tight junction proteins. Although barrier dysfunction is emerging as a key driver of chemotherapy induced diarrhoea, this is the first study to implicate barrier dysfunction in the development of TKI induced diarrhoea, and will form the basis of further investigation.

Conclusion

In summary, this study has shown that dacomitinib induces severe ileal damage and gastrointestinal permeability in this model. The high expression of ErbB1 in the ileum, was also accompanied by the localised damage seen only in this region. This is the first study to provide a detailed interrogation of the intestinal changes associated with dacomitinib treatment and advances our understanding of diarrhoea processes induced by not only this agent, but assists in further characterising the poorly understood mechanisms of ErbB TKI- induced diarrhoea.

Supplementary Table

	7 day		21 day	
	Control	Dacomitinib	Control	Dacomitinib
Sodium (mmol/L)	137.50	138.50	139.50	140.00
Potassium (mmol/L)	7.88	7.98	6.80	6.95
Chloride (mmol/L)	99.33	102.00*	100.00	99.33
Bicarb (mmol/L)	31.17	29.83	29.33	27.50
Anion gap (mmol/L)	14.83	14.50	17.00	19.17*
Glucose (mmol/L)	8.82	8.55	9.15	7.12
Urea (mmol/L)	6.77	5.83	6.40	12.38
Creatinine (umol/L)	9.167	12.17	21.33	39.33*
Cholesterol (mmol/L)	2.40	2.48	1.75	1.75
Urate (mmol/L)	0.12	0.13	0.14	0.09
Phosphate (mmol/L)	2.89	3.14	2.73	2.74
Total Ca (mmol/L)	2.62	2.51	2.54	2.42
Albumin (g/L)	11.83	10.50	13.33	10.67*
Globulin (g/L)	36.50	35.55	40.33	43.67
Protein (g/L)	48.33	45.83	53.67	54.33
ALP (U/L)	395.80	268.70	238.80	205.80*
ALT (U/L)	77.00	90.00	67.17	89.50
AST (U/L)	107.80	148.70	153.00	218.70
LD (U/L)	680.20	1269.00	1658.00	2208.00

Supplementary table 1 Serum biochemistry data presented as mean. Ca: calcium, ALP:

alkaline phosphatase, ALT: alanine aminotransferase, AST: aspartate aminotransferase, LD: lactate dehydrogenase. *indicates significantly different from control at same time point. Data analysed using one-way ANOVA.

Statement of Authorship

Title of Paper	Dacomitinib-induced diarrhoea: targeting chloride secretion with crofelemer
Publication Status Accepted for Publication	☒ Published ☐ Accepted for Publication ☐ Submitted for Publication ☐ Unpublished and Unsubmitted work written in manuscript style
Publication Details	Primary research paper accepted for publication in the International Journal of Cancer (2017) In press

Principal Author

Name of Principal Author (Candidate)	Ysabella Van Sebille		
Contribution to the Paper	First author and main contributor. I developed the concept, did the data curation, formal analysis, investigation, methodology, project administration, validation, visualisation, writing the original draft, and reviewing and editing.		
Overall percentage (%)	90%		
Certification:	This paper reports on original research I conducted during the period of my Higher Degree by Research candidature and is not subject to any obligations or contractual agreements with a third party that would constrain its inclusion in this thesis. I am the primary author of this paper.		
Signature		Date	September, 2017

Co-Author Contributions

By signing the Statement of Authorship, each author certifies that:

i. the candidate's stated contribution to the publication is accurate (as detailed above);

ii. permission is granted for the candidate in include the publication in the thesis; and

iii. the sum of all co-author contributions is equal to 100% less the candidate's stated contribution.

Name of Co-Author	Rachel Gibson		
Contribution to the Paper	Rachel was involved in conceptualisation, supervision, and reviewing manuscript drafts		
Signature		Date	September, 2017

Name of Co-Author	Hannah Wardill		
Contribution to the Paper	Hannah was involved in investigation, methodology, and reviewing manuscript drafts		
Signature		Date	September, 2017

Name of Co-Author	Imogen Ball		
Contribution to the Paper	Imogen was involved in investigation, and methodology		
Signature		Date	September, 2017

Name of Co-Author	Dorothy Keefe		
Contribution to the Paper	Dorothy was involved in funding acquisition.		
Signature		Date	September, 2017

Name of Co-Author	Joanne Bowen		
Contribution to the Paper	Joanne was involved in conceptualisation, funding acquisition, investigation, methodology, project administration, supervision, and reviewing manuscript drafts		
Signature		Date	September, 2017

Chapter 4 Dacomitinib-induced diarrhoea: targeting chloride secretion with crofelemer

This chapter was accepted for publication in The International Journal of Cancer, and was in press at the time of thesis submission (**Van Sebille, Y.Z.,** Gibson, R. J., Wardill, H.R., Ball, I.A., Keefe, D.M., Bowen, J.M. 2017. Dacomitinib-induced diarrhoea: targeting chloride secretion with crofelemer. *International Journal of Cancer,* Accepted, in press.

Abstract

Dacomitinib, an irreversible small-molecule pan-ErbB TKI, has a high incidence of diarrhoea which has been suggested to be due to chloride secretory mechanisms. Based on this hypothesis, crofelemer, an anti-secretory agent may be an effective intervention. T84 monolayers were treated with 1μM dacomitinib and 10μM crofelemer, and mounted into Ussing chambers for electrogenic ion analysis. Crofelemer attenuated increases in chloride secretion in cells treated with dacomitinib. Albino Wistar rats (n=48) were treated with 7.5 mg/kg dacomitinib and/or 25 mg/kg crofelemer via oral gavage for 21 days. Crofelemer significantly worsened dacomitinib-induced diarrhoea ($p=0.0003$), and did not attenuate weight loss ($p<0.0001$). Sections of the ileum and colon were mounted into Ussing chambers, and secretory processes analysed. This indicated that crofelemer lost its anti-secretory action in the presence of dacomitinib in this model. Mass spectrometry revealed that crofelemer did not change serum concentration of dacomitinib. Serum FITC dextran levels indicated that crofelemer was unable to attenuate dacomitinib-induced barrier dysfunction. Tight junction proteins were visualised with immunofluorescence. Qualitative analysis showed dacomitinib induced proteolysis of ZO-1 and occludin, and internalisation of claudin-1, which was not

attenuated by crofelemer. Detailed histopathological analysis showed that crofelemer was unable to attenuate dacomitinib-induced ileal damage. Crofelemer worsened dacomitinib-induced diarrhoea, suggesting that antisecretory drug therapy may be ineffective in this setting.

Introduction

Dacomitinib (PF-00299804) is an orally administered, irreversible small-molecule pan-ErbB receptor tyrosine kinase inhibitor (TKI) under development for the treatment of recurrent or metastatic non-small cell lung cancer (NSCLC) [42]. Dacomitinib acts by covalently binding to the intracellular adenosine triphosphate domain of each of the three kinase-active members of the ErbB family (ErbB1, ErbB2 and ErbB4). This effectively inhibits phosphorylation of the receptor and therefore inhibits downstream signalling [40]. The most commonly reported adverse event associated with dacomitinib therapy has been diarrhoea, with an incidence of around 73% [124]. Although less common, severe diarrhoea can result in dose reductions (28%), treatment interruptions (12%) and treatment discontinuation (8%) from clinical trials [139]. Of particular clinical importance, dacomitinib is delivered in a continuous manner over many months, meaning diarrhoea is often prolonged, and as such, impacts significantly on quality of life. Currently the treatment for TKI-induced diarrhoea is loperamide or octreotide, however very few studies have looked at antidiarrhoeal agents in a targeted approach [61, 140-142].

Research in our laboratory has recently indicated that ErbB TKIs induce diarrhoea due to chloride secretory mechanisms [16]. ErbB receptors are abundantly expressed on the basolateral membrane of healthy intestinal epithelial cells, and are crucial for normal functions and development of the gut. Of particular importance to this study, ErbB

receptors in healthy settings are negative regulators of chloride secretion [41, 71]. This study therefore hypothesised that inhibition of these receptors through the action of dacomitinib would result in a loss of the negative regulation of chloride, thus resulting in a secretory diarrhoea phenotype.

Crofelemer is an antisecretory antidiarrhoeal proanthocyanidin oligomer extracted from *Croton lechleri.* It is approved by the U.S Federal Drug Administration (FDA) for the treatment of diarrhoea induced by antiretroviral medication for HIV patients and has been proposed as an intervention for pertuzumab-induced diarrhoea [143]. Crofelemer inhibits the two principal apical channels for chloride secretion in enterocytes, with partial inhibition of the cAMP –dependent cystic fibrosis transmembrane conductance regulator (CFTR) and complete inhibition of the calcium activated chloride channel (CaCC) [118]. Clinical studies have demonstrated that crofelemer is a safe and tolerable drug, with no adverse effects being reported [119-121]. Crofelemer is also appealing because it is too large and polarised to be systemically absorbed, limiting any systemic effects including drug interactions and toxicities [16]. Therefore, this study investigated the effect of dacomitinib and crofelemer on chloride secretion *in vitro,* and then translated the study to a preclinical rat model of dacomitinib-induced diarrhoea.

Materials and Methods

Chemicals

Dacomitinib (PF-00299804) was kindly provided by Pfizer. Dacomitinib is soluble in dimethyl sulfoxide (DMSO) at 19 mg/ml. Aliquots of dacomitinib in DMSO (Sigma Aldrich) were added to Ringer's solution (composition in mmol/L: NaCl 115.4; KCl 5; $MgCl_2$ 1.2; NaH_2PO_4 0.6; $NaHCO_3$ 25; $CaCl_2$ 1.2 and glucose 10) to create a 50 μM

concentration. Appropriate volumes were added to Ussing chambers to reach a final concentration of 1 μM with previous studies demonstrating doses above this result in off-target or non-specific effects [144]. Secretory effects below 1 μM are therefore more likely to be due to the specific effect of the drug on its designed molecular target. Crofelemer (Salix Pharmaceuticals) was diluted with DMSO to 21 mg/ml (10 mM) and was diluted in ringer solution and administered at 10 μM. This dose has previously been shown to inhibit secretagogue activated chloride secretion in T84 cells [118]. Exposure of DMSO to cells did not exceed 0.01%. The same concentration of DMSO was used as a vehicle control. For all *in vivo* experiments, dacomitinib was suspended in 0.5% (w/w) hydroxypropyl-methylcellulose (Sigma Aldrich) in sterile distilled water to a final concentration of 2 mg/ml. Crofelemer was suspended to a final concentration of 5 mg/ml in sterile distilled water.

In vitro Model

Cell Preparation and Maintenance

This study utilised T84 cells (passage 5-15) derived from a human colorectal carcinoma (Culture Collections, Porton Down, UK). Cells were certified mycoplasma-free and authenticated by Culture Collections by DNA profiling and used within 6 months of receipt. Cells were maintained at 37°C in 5% CO_2/95% air in Dulbecco's Modified Eagle Medium (DMEM)/Ham's F-12 Nutrient Mixture containing 15mM HEPES, L-glutamine and 10% foetal bovine serum (FBS) supplemented with 1 % penicillin/gentamicin+fungizone and were grown in sterile, multi-well tissue culture plates under identical growth conditions. The T84 cell line retained its original morphology and growth characteristics over the range of passages used. Cells were seeded at a density of 100,000 cells/cm^2 on 1.12 cm^2, 0.4 μm pore polyester transwell

inserts (Corning Life Sciences, MA, USA). Cell culture media in both the apical and basolateral chambers was changed every 48 hours. Transepithelial electrical resistance (TEER) was monitored daily using an EVOM2 epithelial volt-ohm-meter with chopstick electrodes (World Precision Instruments, Sarasota, FL, USA) for 1 week during the growth period and area adjusted for analysis using the following formula; TEER monolayer (Ω/cm2) = [raw TEER (Ω) – TEER blank (Ω)]/area of membrane (cm2).

In vitro Electrophysiological Studies using Ussing Chambers

To test whether dacomitinib increased intestinal epithelial cell Cl^- secretion, short-circuit current (I_{sc}) was measured in T84 cells in symmetrical physiological solutions in Ussing chambers. Once adequate resistance was reached (determined by TEER of > 1000 Ω cm^2)[127], T84 monolayers were then placed onto 1.12 cm^2 aperture sliders (Physiologic Instruments; P2302) and mounted into Ussing chambers and continuously bathed in an oxygenated, glucose-fortified Ringer's solution at 37°C. Cells were voltage clamped to zero potential difference by the application of short-circuit current (I_{sc}) and baseline established. Cells were allowed to equilibrate for 20 minutes and before dacomitinib and crofelemer were administered. Dacomitinib was administered at a range of time points, with 15 minutes showing peak intestinal secretion, this time point was used for all further analyses. Both dacomitinib and crofelemer were administered in the Ussing chamber to the apical side. Crofelemer was added first, followed by dacomitinib after 10 minutes. Once cells had been exposed to dacomitinib for 15 minutes, the baseline I_{sc} (μA/cm^2) was determined as the mean over a 5-min period (5 values) immediately prior to administration of secretagogues. Cells were pretreated via the apical chamber with amiloride (20 μmol/L), to inhibit the apical epithelial sodium channel before being treated with carbachol (Ca^{2+} agonist; 100 μmol/L) applied to the basolateral chamber.

The I_{sc} response was then measured and determined as the change in I_{sc} following agonist administration ($\Delta\mu A/cm^2$), representing stimulated chloride secretion using Acquire and Analyze software 2.3 (Physiologic Instruments).

In vivo Model

Ethics

The study was approved by the Animal Ethics Committee of The University of Adelaide (approval number: M215-13), and complied with the National Health and Medical Research Council (Australia) Code of Practice for Animal Care in Research and Training (2014). All experiments were conducted in male Albino Wistar rats (initial age approximately 6 weeks) obtained from The University of Adelaide Laboratory Animal Service (SA, Australia). Rats were group housed in ventilated cages with three to six animals per cage. They were housed in approved conditions on a 12-hour light/dark cycle. Food and water were provided *ad libitum*.

Experimental Design

Rats were treated with crofelemer (25 mg/kg) and dacomitinib (7.5 mg/kg) administered daily for 21 days, both via oral gavage using a soft plastic feeding tube. Control animals received daily gavage with dacomitinib vehicle (0.5% (w/w) hydroxypropyl-methylcellulose) and crofelemer vehicle (sterile distilled water). The dose volume for oral gavage was approximately 5 ml/kg. Rats were randomly assigned to treatment groups and killed at 21 days (n = 6/group). Rats were anaesthetised using isoflurane inhalation, and were killed via cardiac exsanguination and cervical dislocation.

Clinical Assessment of Gastrointestinal Toxicity

All rats were monitored twice daily for the presence of diarrhoea for the duration of the study. Diarrhoea was quantified by two independent assessors using a well-established grading system where 0 = no diarrhoea, 1 = mild diarrhoea with soft stools and perianal staining, 2 = moderate diarrhoea with loose stools and perianal staining of fur, 3 = severe diarrhoea with watery stools +/- mucous and fur staining incorporating hind legs [15]. Rats were weighed daily to track weight loss/gain. Rats were killed if they displayed > 15 % weight loss from baseline or significant distress and clinical deterioration, in compliance with animal ethical requirements.

Tissue Preparation

At necropsy, the entire gastrointestinal tract from pyloric sphincter to rectum was dissected and flushed with saline to remove intestinal contents. Both the small and large intestines were weighed immediately after resection. Samples of jejunum, ileum and colon were collected and (1) fixed in 10 % formalin for embedding in paraffin, or (2) were placed in Ringer's solution with 10 μM indomethacin for Ussing chamber experiments.

In vivo Electrophysiological Studies using Ussing Chambers

Distal colon and ileum tissue was cut longitudinally along the mesentery and external muscle layers were carefully dissected and removed under micro-dissection microscopes in a Ringer's/indomethacin solution. Tissue was then immediately placed onto 0.5 cm^2 aperture sliders (Physiologic Instruments; P2305), mounted into Ussing chambers (Physiologic Instruments; #EM-CSYS-8) and continuously bathed in an oxygenated, glucose-fortified ringer solution at 37°C for electrophysiological analysis. The epithelium was voltage clamped to zero potential difference by the application of short-

circuit current (I_{sc}) and baseline established. Throughout the experiment, the epithelium was continuously short-circuited by the automatic voltage clamp device with correction for solution resistance. In 1 min intervals, a voltage step of ±2 mV (U) was applied to the tissue and the change in short-circuit current (I_{sc}) measured. Tissue was allowed to equilibrate for 20 minutes and baseline I_{sc} ($\mu A/cm^2$) was determined as the mean over a 5-min period (5 values) immediately prior to administration of secretagogues. Tissue was pretreated via the apical chamber with amiloride (20 μmol/L), to inhibit the apical epithelial sodium channel before being treated with carbachol (Ca^{2+} agonist; 100 μmol/L) applied to the basolateral chamber. The I_{sc} response was then measured and determined as the change in I_{sc} following agonist administration ($\Delta\mu A/cm^2$), representing stimulated chloride secretion using Acquire and Analyze software 2.3 (Physiologic Instruments).

Serum Drug Analysis

Determination of serum dacomitinib concentration (range 3-10000 ng/ml) by liquid chromatography/ mass spectrometry (LC/MS/MS) was conducted at the Pharmaceutical Science Sector Laboratory, School of Pharmacy and Medical Sciences, University of South Australia under GLP conditions. Blood samples were collected by cardiac puncture and serum separated. Dacomitinib and the internal standard was extracted from serum using a protein precipitation clean up, before separation by HPLC on a Phenomenex Luna C18 reverse phase column. Elutes were monitored by an API 3000 MS/MS detector operated in positive MRN mode. Samples with dacomitinib concentrations above the linear range were diluted 1:10 with blank rat serum.

FITC-dextran Assay

Two hours prior to culling, rats received a 600 mg/kg dose (120 mg/ml) of 4 kDa fluorescein isothiocyanate (FITC)-dextran (Sigma-Aldrich, NSW, Australia, Cat# FD4) via oral gavage. Blood was collected via cardiac puncture at necropsy into serum-gel clotting activator tubes and protected from light. Samples were centrifuged at 3,000 g for 5 minutes and serum isolated. Serum samples were diluted 1:3 with 1 X phosphate buffer solution (PBS) and quantified using the Bio Tek Synergy™ Mx Microplate Reader (Bio Tek, Vermont, USA) and Gen5 version 2.00.18 software relative to a standard curve (range 0.0001-10 μg/ml).

Histopathological Analysis

Hematoxylin and eosin (H&E) staining was performed on 5 μm sections of jejunum, ileum, and colon cut on a rotary microtome and mounted onto glass Superfrost® microscope slides (Menzel-Gläser, Braunschweig, Germany). Slides were scanned using a NanoZoomer™ (Hamamatsu Photonics, Japan) and assessed with NanoZoomer Digital Pathology software view.2 (Histalim, Montpellier, France). The occurrences of eight histological criteria in the jejunum and ileum were examined to generate a total tissue injury score [136]. These criteria were villous fusion, villous atrophy, disruption of brush border and surface enterocytes, crypt loss/architectural disruption, disruption of crypts cells, infiltration of polymorphonuclear cells and lymphocytes, dilation of lymphatics and capillaries, and oedema. In the colon, the latter six criteria were examined. Each parameter was scored as present = 1, or absent = 0, in a blinded fashion.

Immunohistochemistry

Immunohistochemical analysis was performed for apoptosis (caspase 3; Abcam, Vic, Australia; #ab4051), and proliferation (Ki67; Abcam, Vic, Australia #ab16667. Immunohistochemical analysis was performed using Dako reagents on an automated machine (AutostainerPlus™, Dako, Denmark) following standard protocols supplied by the manufacturer. Briefly, sections were deparaffinised in histolene and rehydrated through graded ethanol before undergoing heat mediated antigen retrieval using an EDTA/Tris buffer (0.37 g/L EDTA, 1.21 g/L Tris; pH 9.0). Retrieval buffer was preheated to 65°C using the Dako PT LINK (pre-treatment module). Slides were immersed in the buffer and the temperature raised to 97°C for 20 minutes. After returning to 65°C, slides were removed and placed in the Dako AutostainerPlus and stained following the manufacture's guidelines. Negative controls had the primary antibody omitted. Caspase 3 and Ki67 were quantified by counting the number of positively stained cells for 15 crypts. Data presented as average positively stained cells per crypt. All analysis was done in a blinded fashion.

Tight Junction Analysis

Immunofluorescence was carried out on 5 μm sections of ileum and colon, cut on a rotary microtome, and mounted onto FLEX IHC microscope slides (Flex Plus Detection System, Dako; #K8020). Immunofluorescence analysis was performed for key tight junction proteins: claudin-1 (Abcam Ab15098; 2 μg/ml; 1:100; Alexa Fluor anti-rabbit 568 nm), ZO-1 (Invitrogen 61-7300; 2.5 μg/ml; 1:100; Alexa Fluor anti-rabbit 568 nm), and occludin (Invitrogen 33-1500; 5 μg/ml; 1:100; Alexa Fluor anti-rabbit 568 nm). Immunofluorescence was performed using Dako reagents on an automated machine

(AutostainerPlus, Dako; #AS480) following standard protocols supplied by the manufacturer. Briefly, sections were deparaffinised in histolene and rehydrated through graded ethanol before undergoing heat-mediated antigen retrieval using an EDTA-NaOH buffer (0.37 g/L EDTA, pH 8.0). Retrieval buffer was preheated to 65°C using Dako PT LINK (pretreatment module; Dako; #PT101). Slides were immersed in the buffer and the temperature raised to 97°C for 20 minutes. After returning to 65°C, slides were placed in the Dako AutostainerPlus, and returned to room temperature with the buffer applied. Tissue was blocked using 10% normal horse serum in 1 X PBS. The primary antibodies were applied for 1 hour using 5% normal horse serum as a diluent. A fluorescently labeled secondary antibody (donkey anti-rabbit or mouse IgG [H+L] secondary antibody, Alexa Fluor 568 conjugate, Invitrogen; #A10042) was applied at 0.8 μg/ml for a further 1 hour, using 1 X PBS + 1% BSA (Sigma-Aldrich; #A2058) and 2% FBS (Sigma-Aldrich; #F2442) as a diluent. Slides were washed using 1 X PBS; counterstained using 1 μg/ml 4',6-diamidino-2-phenylidole (DAPI; Life Sciences; #D1306), and cover slipped using an aqueous mounting medium (Fluorshield, Sigma-Aldrich; #F6182). Negative controls had the primary antibody omitted. Slides were visualised using the SP5 Spectral Scanning Confocal Microscope (Leica). Four areas from each tissue were imaged (40 X magnification) providing a range of areas for both qualitative and quantitative analysis. Immunofluorescence was assessed qualitatively for staining distribution in a blinded fashion. Quantitative analysis was conducted using ImageJ software. Briefly, channels were separated and RGB images converted to 8-bit. Automated thresholding was performed using the MaxEntropy algorithm, chosen based on qualitative assessment of its ability to identify tight junctions, and exclude non-specific staining [145, 146]. Epithelium only was selected, and total stained area was calculated and expressed as a percentage of the total area selected.

Statistical Analysis

Data were compared using Prism version 7.0 (GraphPad® Software, San Diego USA). A D'Agostino Pearson omnibus test was used to assess normality. When normality was confirmed, a two-way analysis of variance (ANOVA) with appropriate post hoc testing was performed to identify statistical significance between groups. In other cases, a Kruskal-Wallis test with Dunn's multiple comparisons test and Bonferroni correction was performed. Diarrhoea was assessed using a Chi-square test. A p-value of < 0.05 was considered significant.

Results

Crofelemer Inhibits Dacomitinib-Induced Chloride Secretion *in vitro*

To test the hypothesis of dacomitinib inducing diarrhoea via a secretory mechanism, short-circuit current (I_{sc}) was measured to assess intestinal cell Cl^- secretion in T84 colonic cells in symmetrical physiological solutions. Previous studies have shown that I_{sc} is reflective of changes in transepithelial chloride secretion in T84 cells [147, 148]. Figure 1A shows baseline I_{sc}, after cells have been exposed to dacomitinib and/or crofelemer, but with no agonist administration. Baseline I_{sc} significantly increased following dacomitinib treatment ($p < 0.0001$; figure 1A) and crofelemer inhibited this dacomitinib-induced increase in I_{sc} ($p < 0.0001$; figure 1A). Administration of CaCC agonist – carbachol – increased I_{sc} in cells treated with dacomitinib (figure 1B). Crofelemer inhibited this increase ($p <0.0001$; figure 1B).

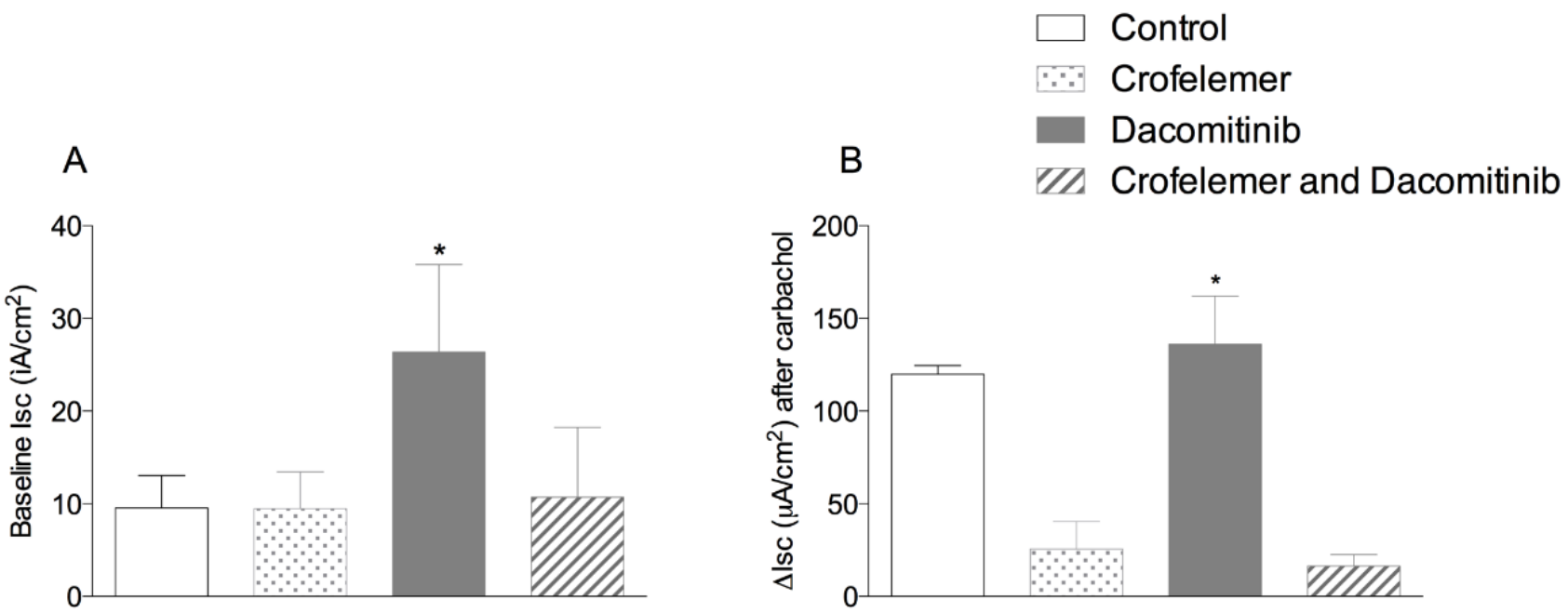

Figure 1 Baseline short-circuit current (Isc) and change in Isc following CaCC agonist carbachol. T84 monolayers were mounted into Ussing chambers and treated with dacomitinib (1 μM) and crofelemer (10 μM) via the apical chamber. **A**: Increased baseline Isc was seen in cells treated with dacomitinib ($p < 0.0001$) which was attenuated with crofelemer ($p < 0.0001$). **B**: Increased delta Isc was also seen in cells treated with dacomitinib following the administration of carbachol, a CaCC agonist, this was also attenuated with crofelemer ($p < 0.0001$). Data presented as mean ± SEM. A one-way ANOVA with Tukey post-hoc was performed to identify statistical significance ($p < 0.05$).

Crofelemer is ineffective at reducing dacomitinib-induced diarrhoea

Following the results seen *in vitro*, which showed dacomitinib increased chloride secretion and crofelemer inhibited it, treatment was then translated into an animal model. Our previous publication presents data of control and dacomitinib alone treated rats [149]. Rats treated with vehicle control did not develop diarrhoea at any time point [149]. Diarrhoea (grade1 - 3) occurred in 100 % of dacomitinib alone rats, which is comparable to the incidence seen in clinical trials [149]. Two rats treated with crofelemer alone developed mild grade 1 diarrhoea on the 3rd and 11th treatment day, likely due to stress (figure 2A). Diarrhoea developed in 100% of rats treated with dacomitinib/crofelemer combination (figure 2B). Approximately 50 % of rats treated with combination crofelemer and dacomitinib had severe diarrhoea (grade 3: severe diarrhoea as watery stools +/- mucous with fur staining incorporating hind legs). Approximately 30 % of rats treated with dacomitinib alone had severe diarrhoea [149]. Rats treated with dacomitinib/crofelemer combination had significantly worse diarrhoea than rats treated with dacomitinib alone ($p = 0.0003$).

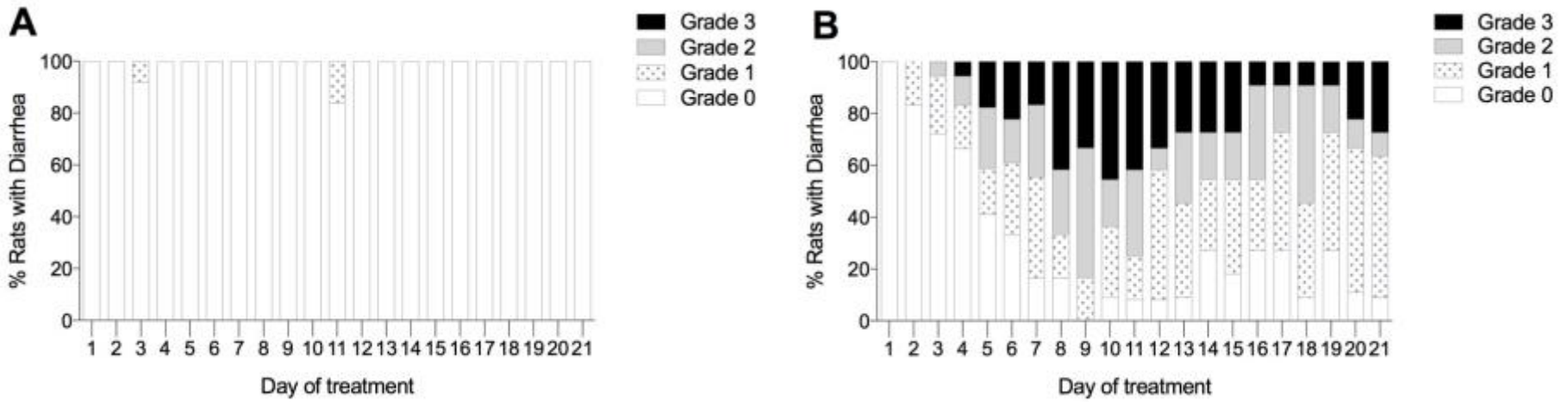

Figure 2 Diarrhoea profiles shown for rats treated with A: crofelemer alone, and B: crofelemer and dacomitinib. To see data of rats treated with control and dacomitinib alone, see Van Sebille et al., 2017 [150]. **A**: Two rats treated with 25 mg/kg crofelemer developed mild, grade 1 diarrhoea on the 3rd and 11th day. **B**: In 100% of rats treated with 7.5 mg/kg dacomitinib and 25 mg/kg crofelemer developed any grade diarrhoea. Rats treated with dacomitinb and crofelemer combination had significantly worse diarrhoea than rats treated with dacomitinib alone ($p = 0.0003$). Data expressed as percentage of total animals per day with a particular grade of diarrhoea. A Chi^2 test was performed to identify statistical significance.

Weight loss

In the crofelemer/dacomitinib combination group, two animals were killed due > 15% weight loss. These animals were not included in downstream analysis. Rats treated with crofelemer/dacomitinib combination had significantly less weight gain than controls from day 10-21 ($p < 0.0001$) (Figure 3). At day 21, the control group had on average gained 46.38 ± 2.459 % [149], the crofelemer group gained 39.27 ± 8.298 %, the dacomitinib group gained 18.99 ± 5.602 % [149], and the crofelemer/dacomitinib combination group gained 13.36 ± 6.846 % body weight compared with day 1 of treatment.

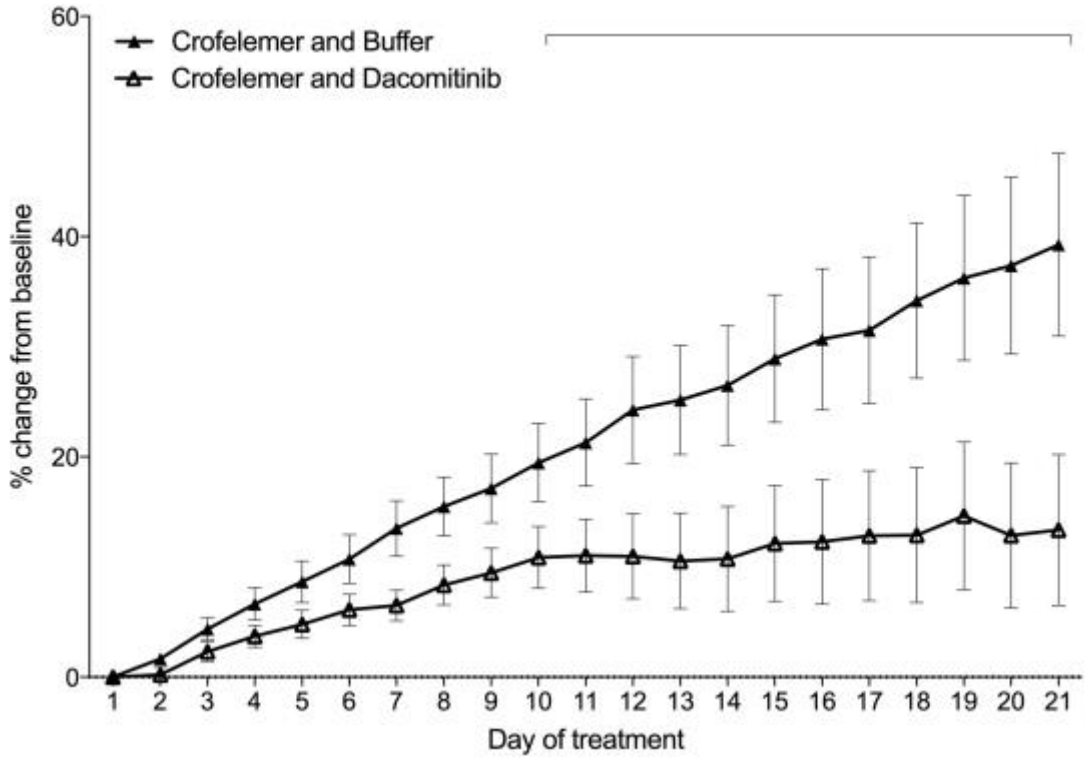

Figure 3 Body weight over the 21-day time course. Data presented as a percentage of weight change from baseline (day 1). A Kruskal-Wallis with post-hoc testing was performed to identify statistical significance. Rats treated with dacomitinib/crofelemer combination (7.5 mg/kg and 25 mg/kg respectively) had significantly less weight gain than the controls from day 10-21 ($p < 0.0001$). To see data of rats treated with control and dacomitinib alone, see Van Sebille et al., 2017 [150]. Rats treated with dacomitinib alone were not significantly different to crofelemer/dacomitinb combination.

Crofelemer did not inhibit chloride secretion in the presence of dacomitinib in this model

Samples of colon and ileum from each animal in the study were mounted in Ussing chambers to record electrogenic ion transport. Baseline readings were recorded to assess baseline differences in transepithelial short circuit current (I_{sc}). Baseline I_{sc} in the ileum was significantly higher in rats treated with combination crofelemer and dacomitinib compared to controls ($p = 0.0408$) (figure 4A). Baseline I_{sc} in the colon was significantly higher in rats treated with combination crofelemer and dacomitinib compared to crofelemer alone ($p = 0.0122$) (figure 4B). Carbachol was administered to elevate levels of intracellular calcium to assess the role of the calcium-activated chloride channels, and indirectly, basolateral potassium channels. No differences were noted between groups in ileum samples following carbachol administration (figure 4C). The response to carbachol in colon samples of rats treated with combination crofelemer and dacomitinib was significantly higher compared to controls, crofelemer alone, and dacomitinib alone ($p < 0.0001$) (figure 4D).

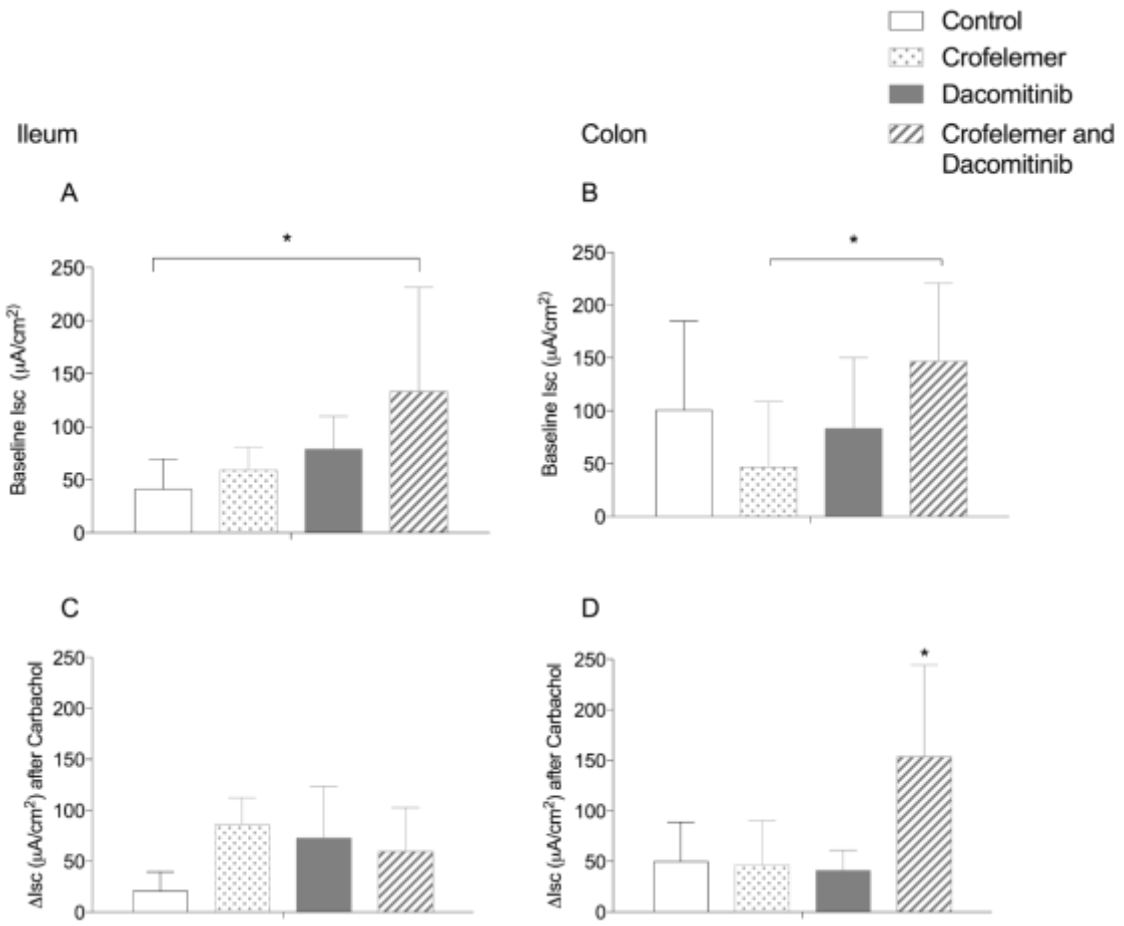

Figure 4 Baseline short circuit current (I_{sc}) of the distal ileum and colon. Segments of the distal colon and ileum were dissected, opened longitudinally and had the external muscle layers removed, before being mounted into Ussing chambers. Increased baseline I_{sc} was seen in rats treated with dacomitinib/crofelemer combination (7.5 mg/kg and 25 mg/kg respectively) compared to controls in the ileum (**A**: $p = 0.0408$) and compared to dacomitinib alone (7.5 mg/kg) in the colon (**B**: $p = 0.0122$). Following the administration of calcium agonist – carbachol – the colon of rats treated with dacomitinib/crofelemer combination had a significantly increased response compared to all other treatment groups (**D**: $p < 0.0001$). No significant changes were noted in the ileum (**C**). Data presented as mean ± SEM. A one-way ANOVA with Tukey post-hoc was performed to identify statistical significance ($p < 0.05$).

Crofelemer does not increase serum absorption of dacomitinib

To assess if crofelemer was increasing the serum absorption of dacomitinib circulating dacomitinib levels were analysed by mass spectrometry in serum samples collected at death, after 21 days of treatment. The average blood concentration of dacomitinib in rats treated with dacomitinib alone was 258.2 ± 51.76 ng/mL and 260.8 ± 36.63 ng/mL in rats treated with dacomitinib and crofelemer combination ($p > 0.05$) (Supplementary Figure 1).

.

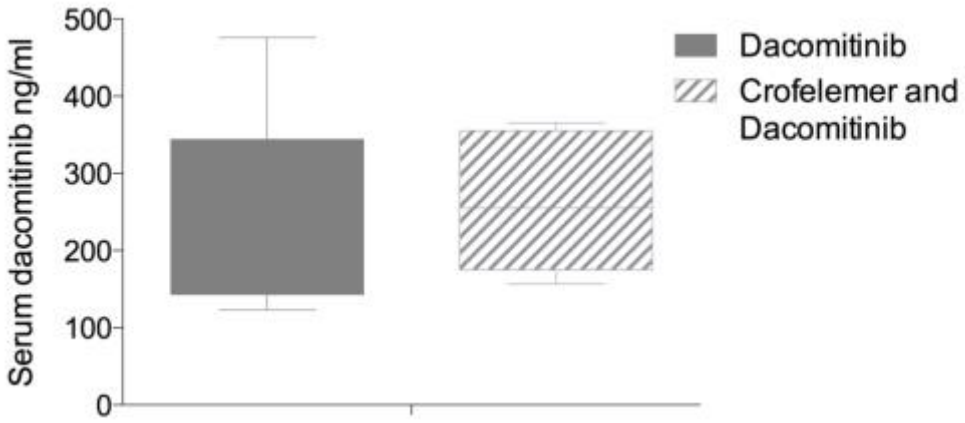

Supplementary Figure 1 Serum dacomitinib concentration. Group mean serum dacomitinib concentration was not changed when given in combination with crofelemer ($p > 0.05$). Data presented as mean, ± min/max. An unpaired t test was performed to identify statistical significance ($p < 0.05$).

Dacomitinib induces gastrointestinal permeability

FITC dextran was administered orally to measure gastrointestinal permeability. Serum FITC dextran levels were significantly elevated in rats of either treatment arm involving dacomitinib [149]. Rats treated with dacomitinib alone had significantly elevated levels of serum FITC dextran compared to controls ($p = 0.0018$) [149], and crofelemer alone ($p = 0.0043$). This was not attenuated with combination crofelemer/dacomitinib treatment, which had significantly elevated levels of serum FITC dextran compared to controls ($p < 0.0001$) and crofelemer alone ($p = 0.0002$) (figure 5).

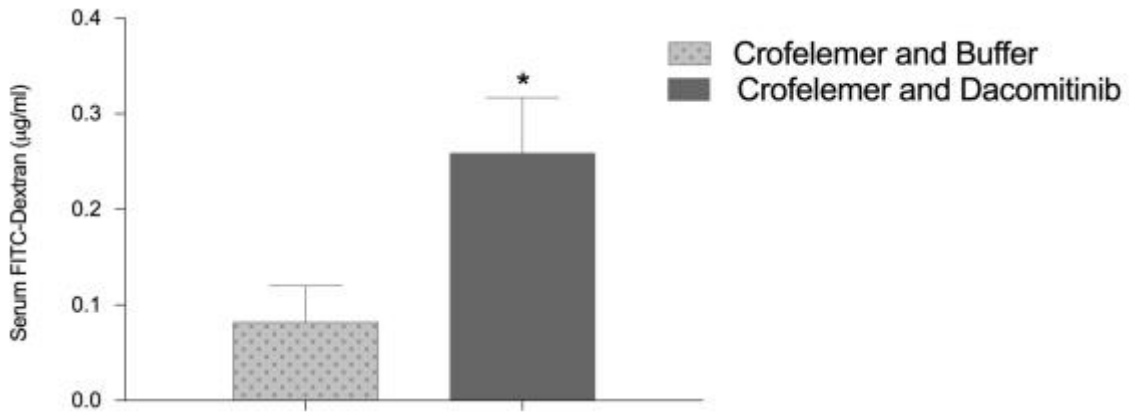

Figure 5 Serum 4kDa FITC-dextran was administered as a 600 mg/kg dose, via oral gavage, 2 hours prior to kill time point. Data expressed as mean ± SEM and were analysed using a one-way ANOVA. To see data of rats treated with control and dacomitinib alone, see Van Sebille et al., 2017 [150]. Both treatment arms involving dacomitinib had significantly elevated levels of serum FITC-dextran, indicating gastrointestinal barrier dysfunction, with no significant differences between these groups. Rats treated with 25 mg/kg crofelemer and 7.5 mg/kg dacomitinib alone had significantly elevated levels of serum FITC dextran compared to crofelemer alone ($p = 0.0002$).

Cytoplasmic redistribution of tight junction proteins contributes to dacomitinib-induced barrier dysfunction

To evaluate if dacomitinib alters permeability through tight junction disruption we investigated tight junction proteins in the intestine. Qualitative analysis of immunofluorescence for tight junction proteins showed membranous staining for all tight junction proteins in vehicle controls, and crofelemer alone controls (figure 6A, C, E, G, I, K, M, O, Q, S, U, W). Immunofluorescence staining for ZO-1 showed focal areas of proteolysis in the ileum (figure 6B, D) and colon (figure 6F, H) of rats treated with dacomitinib and dacomitinib/crofelemer combined. These focal areas of protein disruption were particularly evident in areas of epithelial injury, often occurring alongside phenotypically normal tight junction staining (indicated by arrows). Similar changes in occludin expression were also seen in the ileum (figure 6J, L) and colon (figure 6N, P), with focal areas of proteolysis corresponding with frank epithelial damage in rats treated with dacomitinib and dacomitinib/crofelemer combination. Claudin-1 staining presented with sharp apical intensities and membranous staining down the apicolateral border of the enterocyte in vehicle and crofelemer alone controls in both the ileum (figure 6Q, S) and colon (figure 6U, W). Marked caludin-1 internalisation was evident in rats treated with dacomitinib and dacomitinib/crofelemer combination, particularly in the ileum (figure 6R, T), with complete loss of membranous staining specificity in some areas, and to a lesser extent in the colon (figure 6V, X). There were no apparent differences noted between the two dacomitinib treatment arms. To complement the observation of morphological changes in tight junction proteins, quantitative analysis was conducted on epithelium only, to assess mean percentage area stained. Vehicle control had a mean percentage area staining of 5.23% for claudin-1, 4.27% for ZO-1, and 1.00% for occludin. Crofelemer alone had a mean percentage area

staining of 6.8% for claudin-1, 2.5% for ZO-1, and 0.93% for occludin. Dacomitinib alone had a mean percentage area staining of 4.23% for claudin-1, 3.53% for ZO-1, and 1.87% for occludin. Dacomitinib and crofelemer had a mean percentage area staining of 2.8% for caludin-1, 3.23% for ZO-1, and 1.45% for occludin. No significant differences were noted between groups (data not shown).

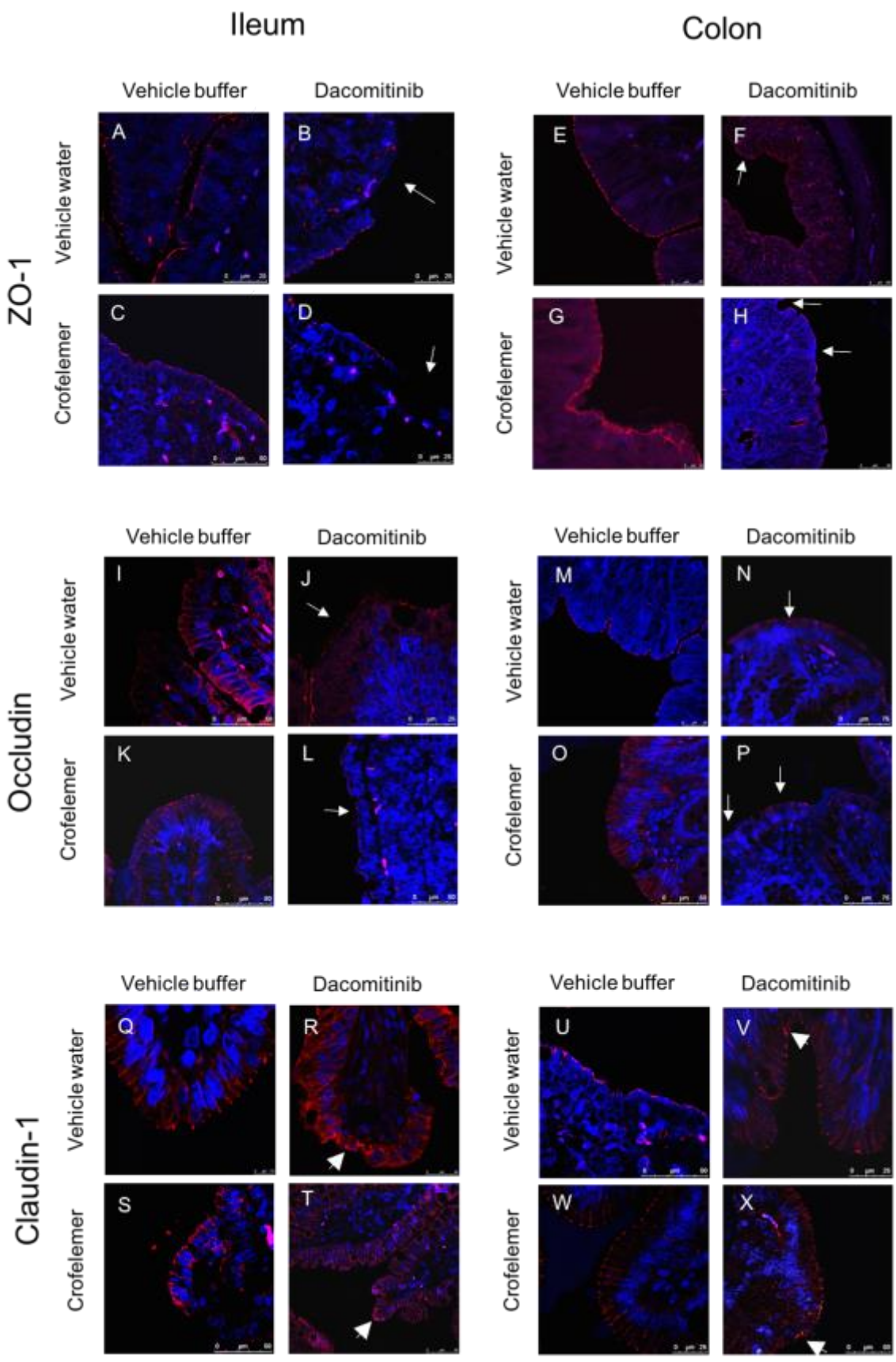
Ileum
Colon
Vehicle buffer
Dacomitinib
Vehicle buffer
Dacomitinib
ZO-1
Vehicle water
Crofelemer
A
B
C
D
E
F
G
H
Occludin
Vehicle water
Crofelemer
I
J
K
L
M
N
O
P
Claudin-1
Vehicle water
Crofelemer
Q
R
S
T
U
V
W
X

Figure 6 Representative images of claudin-1, occludin, and ZO-1 immunofluorescence in the ileum and colon of vehicle- crofelemer- dacomitinib- and dacomitinib/crofelemer combination- treated rats. Vehicle treated, and crofelemer alone treated rats showed phenotypically normal tight junction proteins, with apical staining intensities (A, C, E, G, I, K, M, O, Q, S, U, W). Rats treated with dacomitinib and dacomitinib/crofelemer combination showed no differences, with both displaying focal areas of ZO-1 and occludin disruption, particularly in areas of epithelial injury (B, D, F, H, J, L, N, P, arrows). Rats treated with dacomitinib and dacomitinib/crofelemer combination displayed claudin-1 internalisation, found alongside areas of phenotypically normal tight junctions (R, T, V, X, arrows). Sections of ileum and colon were stained with a primary antibody for claudin-1, occluding and ZO-1 and visualised using an AlexaFluor anti-rabbit 568. Blue counterstaining (DAPI, 405 nm) shows nuclei. Original magnification 20x.

Crofelemer does not attenuate dacomitinib induced histopathological injury

Rats treated with dacomitinib [149], or dacomitinib/crofelemer combination had significant tissue injury in the ileum compared to controls ($p < 0.0001$) (figure 7). This was predominantly characterised by severe villous atrophy with stunting and fusion of villi, which was also attended by enterocyte metaplasia to a low columnar or cuboidal phenotype and mild compensatory expansion of the basal proliferative compartment of crypts. In the congested lamina propria, there was an increased inflammatory infiltrate comprised of lymphocytes, macrophages, plasma cells and neutrophils, and dilation of lacteals (villous lymphatics). There were no significant differences in tissue injury in the jejunum and colon between any groups (data not shown). Dacomitinib did not cause increased apoptosis or proliferation in the gastrointestinal tract compared to controls [149]. When Dacomitinib and crofelemer were given in combination, there was no difference seen in apoptosis or proliferation between any group (data not shown).

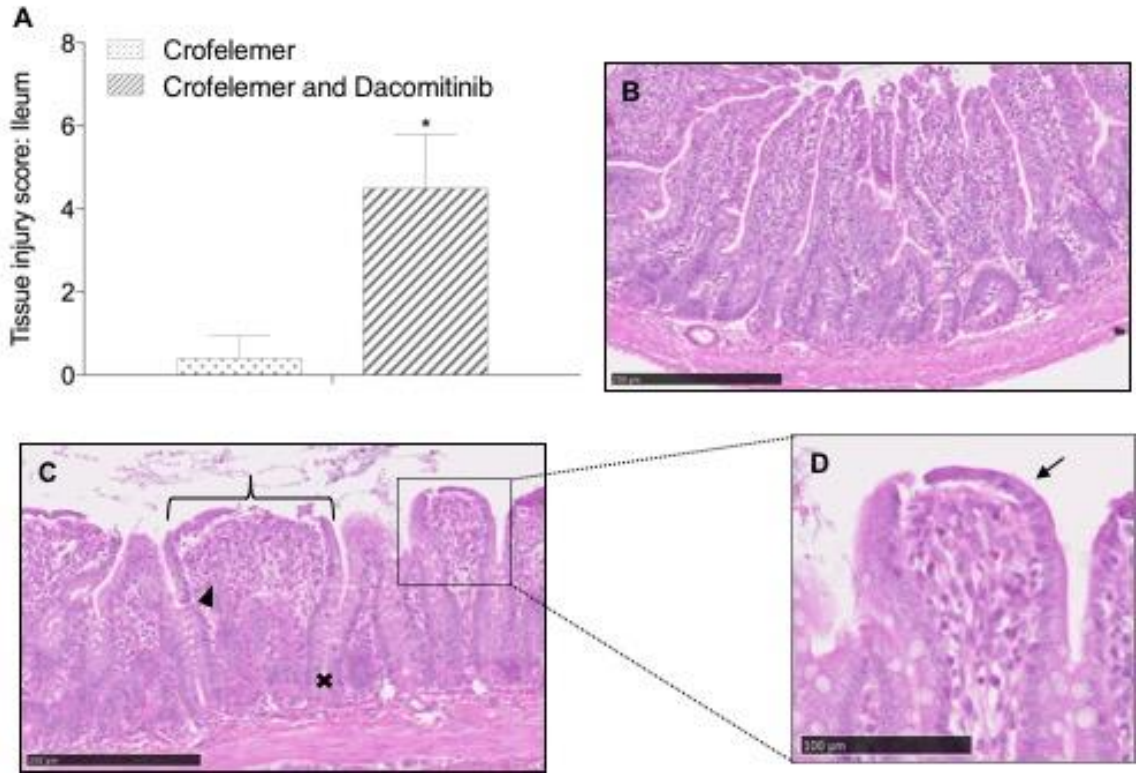

Figure 7 Histopathological parameters in H&E stained ileum. **A:** There were significant increases in tissue injury scores in rats treated with 7.5 mg/kg dacomitinib and 25 mg/kg crofelemer combination ($p < 0.0001$) compared crofelemer control. To see data of rats treated with control and dacomitinib alone, see Van Sebille et al., 2017 [150]. There were no significant differences between crofelemer dacomitinib combination and dacomitinib alone treated rats. **B:** Rats treated with crofelemer alone showed no histopathological damage. Scale bar indicates 250 µM. **C:** Villous atrophy and stunting is evident in the ileum of rats treated with dacomitinib and crofelemer combination. Fusion of villi is indicated by brackets. Compensatory expansion of crypts is indicated by crosses. Increased inflammatory infiltrate is indicated by arrow heads. Scale bar indicates 250 µM. **D:** Enterocyte metaplasia is indicated by arrows. Scale bar indicates 100 µM. Original magnification 40x.

Discussion

Whilst dacomitinib - a second-generation small molecule pan-HER TKI - shows promise for the treatment of NSCLC, its' most commonly reported adverse event is diarrhoea, which significantly impacts on clinical outcomes [124]. Currently no anti-diarrhoeal medication used for the treatment of TKI-induced diarrhoea offers a targeted approach due to the lack of understanding of the underlying mechanisms. HER TKI-induced diarrhoea has recently been hypothesised to be caused by ErbB down-regulation, where blockade leads to excess chloride secretion and thus secretory diarrhoea [16]. Therefore, this study first investigated this hypothesis in an *in vitro* model. We demonstrated that dacomitinib caused increased chloride secretion across polarised epithelia, and that crofelemer, an antisecretory antidiarrhoeal agent, was able to attenuate this increase. Given this positive finding we then aimed to determine if crofelemer was an effective prophylactic for dacomitinib-induced diarrhoea in a rat model.

Despite the results seen *in vitro*, rats treated with dacomitinib/crofelemer combination had significantly worse diarrhoea than rats treated with dacomitinib alone [149]. Previous investigations of the antisecretory mechanism of crofelemer have demonstrated weak and partial inhibition of CFTR, and complete inhibition of CaCC [118]. Electrophysiological analysis in the present study conducted on T84 cells supported this, with crofelemer inhibiting chloride secretion at baseline, as well as following CaCC agonist administration. However, the electrophysiological analysis in the *in vivo* arm of this study demonstrated that the inhibitory effect of crofelemer on chloride secretion is lost when given in combination with dacomitinib over 21 days. This is the first time crofelemer has been used in a preclinical study of this duration, therefore the lack of effect seen in Ussing experiments *in vivo* may be due to the timing of the *ex vivo*

experiments occurring 24 hours after the last dose of drugs. Furthermore, the tissue was significantly damaged, potentially altering the normal function of transporters. Nevertheless, crofelemer was unable to attenuate dacomitinib-induced diarrhoea. This may be explained by convective drug washout, a concern for drugs with an extracellular target in intestinal crypts, such as crofelemer [151]. Convective washout reduces the efficacy of enterocyte surface targeted Cl^- channel inhibitors, which can be of concern in diarrhoea, due to the potential of washout forces impeding the inhibitor to reach the deep intestinal crypts. However, convective drug washout does not explain why crofelemer was not only ineffective, but also significantly worsened dacomitinib-induced diarrhoea.

Chloride channel blockers have previously been suggested for the investigation of TKI-induced diarrhoea [16], including CFTRinh-172, which binds to the cytoplasmic side of the CFTR channel and stabilises the channel closed state [114]; glycine hydrazides, which target the extracellular CFTR surface in the channel pore [113]; and $CaCC_{inh}$-A01, a red wine extract that has been shown to prevent watery diarrhoea in a mouse model of rotavirus [115]. Crofelemer was selected as an intervention in this study because (a) it was reported as a safe and tolerable drug with no adverse events and was approved for clinical use, (b) its dual inhibitory action on the two principle Cl^- channels in the apical membrane of intestinal epithelial cells, and (c) its lack of systemic absorption due to its size and polarity [118], suggesting that it would not interact with dacomitinib systemically. Given the worsened effects seen in the present study, this might suggest that crofelemer can be systemically absorbed if administered in conjunction with drugs that cause barrier disruption and small intestinal damage such as dacomitinib. Serum mass spectrometry did not indicate that crofelemer altered the absorption of dacomitinib when looking at serum nadir levels only. A more detailed pharmacokinetic study would

be required to assess if the combination drug protocol altered maximum concentrations or time to peak. There are currently no reported contraindications for crofelemer and this is the first study to show that crofelemer may worsen diarrhoea in certain situations. The results from this study suggest that crofelemer should be investigated for contraindications before being used in combination with other drugs.

Although the *in vitro* electrophysiological analysis indicated that dacomitinib induced excess chloride secretion, the *ex vivo* electrophysiological analysis did not suggest that dacomitinib causes excess chloride secretion in intestinal tissue following 21 days of treatment. This may be due to not only the timing of the Ussing experiments as previously mentioned, but additionally, the *in vivo* model was a chronic dosing schedule, whereas Ussing experiments in the *in vitro* model were conducted after only one treatment, 15 minutes after exposure. The disadvantage of cell line work should also be considered. T84 monolayer cell lines lack other mucosal cell interactions, and of particular importance in this study, the impact that inflammation has on tight junctions. Clinical studies have also indicated that neratinib, a pan-HER ErbB TKI has a fecal osmotic gap that is consistent with the values for secretory diarrhoea [152]. Previous work investigating lapatinib, an ErbB1 and ErbB2 TKI, suggested that diarrhoea was associated with chloride secretion, indicated by decreased serum chloride levels, which the authors proposed may be due to loss of chloride via the intestinal lumen [15]. However, this was the only measure of secretory mechanisms and is therefore inconclusive. Another kinase inhibitor, flavopiridol, has been reported to stimulate chloride secretion across monolayers of human colonocytes in modified Ussing chambers [94]. Nevertheless, given this was conducted *in vitro* the results need to be translated to an *in vivo* model for more in-depth understanding. This is especially

important considering the differing results of the *in vitro* and *in vivo* arms of the present study. Despite the growing support in the literature for the hypothesis of TKI-induced diarrhoea being due to excess chloride secretion, this is the first study to assess secretory diarrhoea *ex vivo* using Ussing chamber analysis. The results of this study do not support the hypothesis that diarrhoea second to TKI treatment is due to excess chloride secretion. The potential flaw in the hypothesis (EGFR in normal settings are negative regulators of chloride secretion, and so when inhibited there is a loss of negative regulation, and thus increased chloride secretion), is that the hypothesis does not consider that the tissue may be inflamed, and hence behave differently. The assumption that inflamed tissue would behave in a similar manner to normal tissue is a fundamental caveat of the hypothesis. This is highlighted by McCole et al., who showed in a model of DSS-induced colitis, that EGF behaves in a contradictory way in inflamed tissue (i.e. enhances chloride secretion instead of inhibiting it) [153]. Therefore, future research could administer dacomitinib and crofelemer to healthy gastrointestinal tissue in Ussing chambers, instead of using ex vivo treated tissue, in order to dissect whether the inflammatory changes in the present model overshadow the effects of the drugs themselves.

This is the first study to compare functional *in vivo* permeability, and morphological assessment of tight junction proteins in the setting of dacomitinib-induced gut toxicity. Our previous research has indicated that dacomitinib induces severe ileal damage and barrier dysfunction [149]. This study further characterised this barrier dysfunction; showing increases in barrier permeability to 4kDa FITC-dextran, and clear changes to tight junction proteins. Tight junctions are critical in maintaining gastrointestinal health and homeostasis. Despite this, they are highly plastic structures vulnerable to post-

transcriptional and -translational modification by a variety of pathological cues [154, 155]. Tight junction disruption has been identified following treatment with a number of chemotherapeutic agents, both preclinically [137, 156] and clinically [157-159]. To date, many studies have shown architectural abnormalities, and functional alteration, of key tight junction proteins such as claudin-1, ZO-1, and occludin. As such, the current study focused on these three proteins, despite the numerous other proteins present within the junctional complex. Given the complexity of tight junction physiology, further investigation could be directed towards the behaviour of junctional adhesion molecule-A (JAM-A), following dacomitinib given its involvement in inflammatory settings [160]. Despite increased research in this area, assessment of barrier function, and in particular tight junction analysis has never been conducted in TKI models. The present study identified derangement of claudin-1, ZO-1, and occludin, characterised by severe cytoplasmic redistribution and disassembly of the tight junction unit. However quantitative analysis showed no significant differences in percentage area stained. This method of quantification may not have sufficient power to detect the subtle changes that occur upon protein translocation, thus explaining the disparity between qualitative and quantitative analyses. Internalisation of tight junction proteins is well recognised to contribute to poor barrier function, and loss of tight junction apposition [136, 155]. In the current study, cytoplasmic redistribution of claudin-1 was seen in the ileum, where peak histopathological damage was also seen. However, the mechanisms causing this tight junction dysfunction remain to be elucidated. Previous research has suggested that tight junction dysfunction can be pro-inflammatory cytokine mediated [136, 155, 161]. Given the increased inflammatory infiltrate noted in the lamina propria of the ileum in this study, this might suggest that this may be a contributive factor to tight junction dysfunction in this study. While the mechanisms remain unclear, intestinal barrier

dysfunction second to cancer treatment is becoming more evident in both preclinical [136] and clinical models [157]. Clinically, this is highly important as barrier dysfunction permits LPS translocation [129], systemic toxicity [157], bacterial translocation and colonisation in mesenteric lymph nodes and the spleen, increasing the risk of infection, graft-versus-host disease [162], and sepsis [163]. Intestinal barrier dysfunction has also been suggested to exacerbate direct gastrointestinal damage from the cancer therapy, worsening quality of life and clinical outcomes for patients [136]. It is therefore imperative that the mechanisms that lead to barrier dysfunction second to cancer treatment are further investigated, so that therapeutic targets may be identified and interventions developed to prevent local toxicity transitioning to systemic toxicity, to reduce associated risks.

Conclusion

In summary, this study showed that crofelemer was unable to attenuate dacomitinib-induced diarrhoea, and in fact, worsened it in the current model. Despite the growing support for secretory diarrhoea as the mechanism of TKI-induced diarrhoea, this study provided little support for this hypothesis, suggesting that antisecretory drug therapy may be ineffective in this setting. This is the first study to provide a detailed interrogation of the barrier changes associated with dacomitinib treatment. Tight junction disruption is a hallmark trait of many pathological states. A wealth of research now implicates poor tight junction integrity following treatment with various chemotherapeutic agents, however, this is the first study to implicate these changes in a TKI model. This study advances our understanding of diarrhoea processes induced by not only this agent, but assists in further characterising the poorly understood mechanisms of ErbB TKI- induced diarrhoea.

Statement of Authorship

Title of Paper	Use of zebrafish to model chemotherapy and targeted therapy gastrointestinal toxicity
Publication Status Submitted for Publication	☐ Published ☐ Accepted for Publication ☒ Submitted for Publication ☐ Unpublished and Unsubmitted work written in manuscript style
Publication Details	Primary research paper submitted for publication in Supportive Care in Cancer (2017) Under review

Principal Author

Name of Principal Author (Candidate)	Ysabella Van Sebille		
Contribution to the Paper	First author and main contributor. I developed the concept, was involved in funding acquisition, did the data curation, formal analysis, investigation, methodology, project administration, validation, visualisation, writing the original draft, and reviewing and editing.		
Overall percentage (%)	90%		
Certification:	This paper reports on original research I conducted during the period of my Higher Degree by Research candidature and is not subject to any obligations or contractual agreements with a third party that would constrain its inclusion in this thesis. I am the primary author of this paper.		
Signature		Date	September, 2017

Co-Author Contributions

By signing the Statement of Authorship, each author certifies that:

i. the candidate's stated contribution to the publication is accurate (as detailed above);

ii. permission is granted for the candidate in include the publication in the thesis; and

iii. the sum of all co-author contributions is equal to 100% less the candidate's stated contribution.

Name of Co-Author	Joanne Bowen		
Contribution to the Paper	Joanne was involved in conceptualisation, funding acquisition, project administration, supervision, and reviewing manuscript drafts		
Signature		Date	September, 2017

Name of Co-Author	Rachel Gibson		
Contribution to the Paper	Rachel was involved in supervision, and reviewing manuscript drafts.		
Signature		Date	September, 2017

Name of Co-Author	Hannah Wardill		
Contribution to the Paper	Hannah was involved in reviewing manuscript drafts.		
Signature		Date	September, 2017

Name of Co-Author	Tom Carney		
Contribution to the Paper	Tom was involved in conceptualisation, funding acquisition, investigation, methodology, project administration, supervision, validation, and reviewing manuscript drafts.		
Signature		Date	September, 2017

Chapter 5 Use of zebrafish to model chemotherapy and targeted therapy gastrointestinal toxicity

This chapter has been submitted to Supportive Care in Cancer. (**Van Sebille, Y.Z.,** Gibson, R. J., Wardill, H.R., Carney, T.J., Bowen, J.M., 2017. Use of zebrafish to model chemotherapy and targeted therapy gastrointestinal toxicity. *Supportive Care in Cancer*, Under review.

Abstract

Gastrointestinal toxicity arising from cancer treatment remains a key reason for treatment discontinuation, significantly compromising remission. There are drawbacks to the currently used in vitro and rodent models, and a lack of translatability from in vitro to in vivo work. A screening-amenable alternative in vivo model such as zebrafish would, therefore, find immediate application. This study utilised a transgenic reporter line of zebrafish to investigate its utility as an alternative vertebrate model to bridge the gap between simple *in vitro* cellular studies and complex *in vivo* models for understanding gastrointestinal toxicity induced by chemotherapy and targeted therapy. Transgenic zebrafish larvae were administered afatinib or SN38 in water, and assessed for viability and eGFP induction. Adult zebrafish were administered afatinib via oral gavage, and SN38 via intraperitoneal injection. Fish were killed after 24 hours, and had gastrointestinal tracts removed and assessed for histopathological damage, goblet cell changes and apoptosis. Whilst treatment with either compound did not induce eGFP in the gastrointestinal tract of larvae, SN38 caused histopathological damage to adult intestines. The lack of eGFP induction may be due to poor solubility of the drugs. Chemotherapy agents with high solubility and permeability would be more amenable to

these models. Further progress in this area would be greatly facilitated by the generation of robust and reproducible genetic models of zebrafish intestinal toxicity that mimic the known pathobiological pathways in rodents and humans, and can be readily induced in a short time-frame.

Introduction

Gastrointestinal toxicity arising from systemic cancer treatment such as chemotherapy and targeted therapies remains a key reason for treatment cessation, significantly compromising chances of remission. These side effects are frequently associated with traditional chemotherapy drugs, and now are increasingly recognised to be associated with targeted therapies [124]. Patients commonly report gastrointestinal toxicity as being the most impactful on quality of life, influencing their willingness and ability to comply with treatment [51]. This results in dose reductions, interruptions and discontinuation, reducing remission rates [51].

Currently, the animal models used to study gastrointestinal toxicity arising from cancer treatment are primarily rodent models[164]. These models have provided extensive information on mechanisms, and prompted specific hypotheses about the effect of cancer treatment on any regions of the gastrointestinal tract [164]. However, there are challenges associated with rodent models including being prohibitively expensive, time consuming, and the relative difficulty of genetic manipulation. *In vitro* models are also utilised to study gastrointestinal toxicity. Epithelial cell lines derived from the intestine are cultured as monolayers, in attempt to mimic the intestinal epithelium [127]. However, there are many limitations to *in vitro* work, and while they can be useful to understand simple mechanisms, they lack stromal, neural and immune signalling which

is of key importance for modelling gastrointestinal toxicity. Further, they cannot recapitulate the complex systemic metabolism of compounds and thus do not assay the full spectrum of compound derivatives found *in vivo*. Considering the constraints of *in vivo* and *in vitro* models currently used, an alternative model to study cancer treatment-induced gastrointestinal toxicity that allows rapid, miniaturised, multi-organ toxicity, screening-amenable testing is warranted.

Recently, a new zebrafish transgenic eGFP reporter, *Tg(cyp2k18:egfp),* was developed by identifying highly upregulated genes as biomarkers of liver toxicity [165]. Although this transgenic zebrafish reporter line was initially developed for liver toxicity, upon further testing, it was identified that the line also induced eGFP in the gastrointestinal tract following drug treatment, highlighting this organ as a major detoxification site. Detailed investigations have also reported the intestinal morphology and genetic expression of the zebrafish, demonstrating it as a useful model for gastrointestinal disease models [166-168]. Transcriptome profiling has demonstrated that the large anterior portion (58%) of the zebrafish intestine has a similar RNA profile to the human small intestine, followed by a small transitional zone (14%), a tissue resembling the caecum (14%) and lastly a profile resembling the rectum (14%) [168]. Zebrafish do not have separated stomach or colon sections, and instead have a continuous tube with segments expressing some genes characteristic of human colon and rectum [168].

Here we exploit this newly developed transgenic zebrafish reporter line to investigate its utility as an alternative vertebrate model to bridge the gap between simple *in vitro* cellular studies and complex *in vivo* models for understanding gastrointestinal toxicity induced by SN38 and afatinib. These agents are associated with high levels of

gastrointestinal toxicity, manifesting as diarrhoea, and represent two classes of anti-cancer agents; classical cytotoxic chemotherapy (SN38, a topoisomerase 1 inhibitor) and targeted agents (afatinib, a pan-HER tyrosine kinase inhibitor) [91, 169-172]. Thus, this study aimed to assess the efficacy of zebrafish as a platform to study gastrointestinal toxicity second to anticancer chemotherapy and targeted therapy.

Methods

Fish Husbandry

Experiments were conducted under the authority of the Institutional Animal Care and Use Committee (IAUCUC) of the Biological Resource Centre, A*STAR (Protocol number 120751), mandated by National Advisory Committee for Laboratory Animal Research Guidelines of the Agri-Food and Veterinary Authority, Singapore.
Zebrafish (*Danio rerio*) were housed in the zebrafish facility of the Institute of Molecular and Cell Biology, a division of A*STAR, Singapore. Larvae were obtained through natural crosses and staged as previously described by Kimmel et al., 1995 [173]. Embryos and larvae were raised and treated in water containing 60 µg/ml sea salt (Red Sea Aquatics, UK), and 1% methylene blue.

Zebrafish used included wildtype (AB strain), Tg(*cyp2k18:egfp)* reporter line and Tg(*BACmpx:gfp*) reporter line. The development of both the Tg(*cyp2k18:egfp)* reporter line and Tg(*BACmpx:gfp)* line have been described previously [165, 174].

Drug Treatment

For treatment of both larvae and adults, SN38 (Tocris bioscience, 2684) was used as the chemotherapeutic agent, and afatinib (AdooQ, A10141) was used as the HER-TKI agent.

Both were administered to mimic clinical administration (afatinib orally, and SN38 via intraperitoneal injection). Diclofenac (Sigma D6899) was used as the positive control to cause hepatic and gastrointestinal toxicity reported by Tg(*cyp2k18:egfp*) zebrafish line (larvae only). Larvae were treated at 3 days post fertilisation (dpf). Drug compounds were dissolved in DMSO, and added to the egg water in a 12 well plate (volume 2 ml/well), with 10 larvae/well. All treatments were conducted in duplicate. Compounds were dissolved in DMSO, and diluted in egg water for larvae treatment. DMSO exposure to larvae or adult fish did not exceed 0.01%. SN38 and afatinib were administered to larvae at a range of concentrations from 0.5-900 µM for 24 hours, and optimal dose for treatment was determined as 300 µM. Positive controls (Tg:*cyp2k18* line only) were administered diclofenac at a concentration of 13 µM for 24 hours as this is known to induce eGFP in this line [165]. Controls were administered the corresponding solvent concentration (DMSO, 0.01%).

Adult zebrafish were weighed and administered 100 µg/g afatinib via oral gavage, with the maximum volume administered not exceeding 1% of the fish bodyweight. Afatinib was dissolved in DMSO, and diluted in PBS. DMSO exposure did not exceed 0.01%. Controls were administered the corresponding solvent concentrations (DMSO, 0.01%). The oral gavage technique was modified from Collymore and colleagues [175]. A soft, flexible 20 µl ultra-micro tip (Eppendorf) was trimmed to 5cm in total length, and the cut edge was assessed under a dissection microscope to ensure cut edges were blunt, with no bevelled or sharp edges. A sponge was cut with a groove and soaked in facility system water to hold zebrafish during gavage procedure. The ultra-micro tip was attached to a pipette and appropriate volume drawn up, ensuring no bubbles were present, and gently inserted into mouth, below the gills. To ensure procedure was effective, Casper

transparent zebrafish [176], were gavaged with phenol red (1:10 dilution with a 0.5% phenol red solution in Dulbecco's PBS). This indicated that the solution was entering the intestinal bulb and not exiting via the gills, and that fish did not expel the solution through their mouth (Supplementary Figure 1). Fish were killed 24 hours following gavage.

Adult zebrafish were weighed and administered 100 µg/g SN38 via intraperitoneal injection, with the maximum volume administered not exceeding 1% of the fish bodyweight. SN38 was dissolved in DMSO, and diluted in PBS. DMSO exposure did not exceed 0.01%. Controls were administered the corresponding solvent concentrations (DMSO, 0.01%). Using a 10 µl micro syringe (Hamilton) the correct volume was injected into the fish on the ventral body wall, posterior to the pelvic girdle and anterior to the anus, roughly midway along the length of a pelvic fin. The tip of the needle was pointing rostrally, and was inserted shallowly. Fish were killed 24 hours following injection.

Supplementary Figure 1: Casper zebrafish gavaged with phenol red. Arrow indicates phenol red in intestinal bulb of transparent Casper fish following gavage.

Imaging and tissue preparation

For imaging, larvae were anaesthetised with 0.02% Tricane (buffered to pH 7.0) and placed on a petri dish under a Leica MZ16FA. Only larvae were imaged for eGFP induction as they are transparent.

Adult fish were culled by placing in 0.02% Tricane. A shallow longitudinal incision on the ventral side, from the gills to the anus, was made to remove the intestines which were uncoiled and the anterior 60% of the intestines were fixed in 4% PFA overnight before processing and embedding in paraffin.

Histopathological analysis

Hematoxylin and eosin (H&E) staining was performed on 4 μm sections of intestine, cut on a rotary microtome and mounted onto glass Superfrost® microscope slides (Menzel-Gläser, Braunschweig, Germany). Slides were scanned using a NanoZoomer™ (Hamamatsu Photonics, Japan) and assessed with NanoZoomer Digital Pathology software view.2 (Histalim, Montpellier, France). The occurrences of six histological criteria in the intestine were examined to generate a total tissue injury score [136]. These criteria were villous fusion, villous atrophy, disruption of brush border and surface enterocytes, infiltration of polymorphonuclear cells and lymphocytes, dilation of lymphatics and capillaries, and oedema. Each parameter was scored as present = 1, or absent = 0, in a blinded fashion (YZVS).

Goblet Cell Analysis

Alcian Blue (1 % Alcian Blue 8GX (CI 74240) in 3 % glacial acetic)/ Periodic acid Schiff staining was performed on 4 μm sections the intestine. Sections were oxidised in 1 % periodic acid before washing then treated in Schiff's reagent. Slides were scanned

using a NanoZoomer™ (Hamamatsu Photonics, Japan) and assessed with NanoZoomer Digital Pathology software view.2 (Histalim, Montpellier, France). Data presented as average per villus. All analysis was done in a blinded fashion (YZVS).

Immunohistochemistry

Immunohistochemical analysis was performed for apoptosis analysis (caspase 3; BD Pharmingen #559565). Change in caspase-3 is a validated marker for altered tissue kinetics in previous models of cancer therapy induced-gastrointestinal toxicities [63, 69, 70, 90]. Immunohistochemical analysis was performed using Dako reagents on an automated machine (AutostainerPlus™, Dako, Denmark) following standard protocols supplied by the manufacturer. Briefly, sections were deparaffinised in histolene and rehydrated through graded ethanol before undergoing heat mediated antigen retrieval using an EDTA/Tris buffer (0.37 g/L EDTA, 1.21 g/L Tris; pH 9.0). Retrieval buffer was preheated to 65°C using the Dako PT LINK (pre-treatment module). Slides were immersed in the buffer and the temperature raised to 97°C for 20 minutes. After returning to 65°C, slides were removed and placed in the Dako AutostainerPlus and stained following manufactures guidelines. Negative controls had the primary antibody omitted. Caspase 3 was quantified by counting the number of positively stained cells. Data presented as average positively stained cells per villus. All analysis was done in a blinded fashion (YZVS).

Statistics

Data were compared using Prism version 7.0 (GraphPad® Software, San Diego USA). A D'Agostino Pearson omnibus test was used to assess normality. When normality was confirmed, a one-way analysis of variance (ANOVA) with appropriate post hoc testing

was performed to identify statistical significance between groups. In other cases, a Kruskal-Wallis test with Dunn's multiple comparisons test and Bonferroni correction was performed. Differences were considered significant when $p < 0.05$.

Results

Dose titration

Larvae Zebrafish

Zebrafish larvae (n = 10/group) were treated with varying doses of afatinib and SN38, ranging from 100 µM to 1 mM to determine optimal treatment dose. SN-38 did not cause mortality in larvae at any concentration tested. In contrast, afatinib induced dose-dependent mortality (Figure 1). The optimal dose of afatinib for larvae was determined as LC25 (300 µM).

Adult Zebrafish

Adult zebrafish (n = 6/group) were treated with SN38 (by intra peritoneal injection) or afatinib (by oral gavage) at 10, 20, 30 and 40 µg/g based on previous publications [177]. SN-38 and afatinib did not cause mortality or noticeable morbidity in adult fish, and hence 40 µg/g was dosed for the remainder of the study.

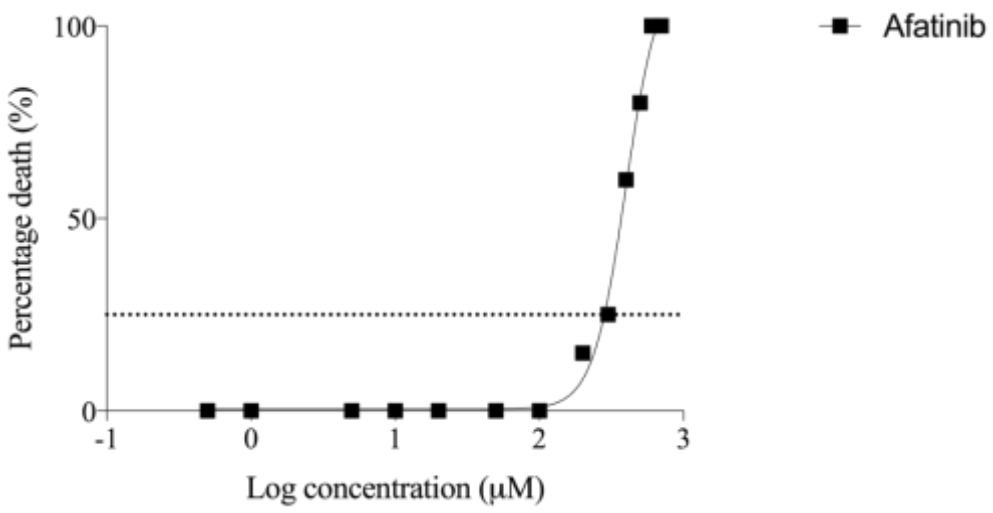

Figure 1: Percent death of larvae Administration of varying concentrations of afatinib caused lethality in zebrafish larvae. At does below 100 µM, no larvae died. Doses above 600 µM caused lethality in 100% of larvae. LC25 (dotted line) was 300 µM, and this was determined as the optimal dose for further treatment. SN38 did not cause death at any concentration.

Transgenic zebrafish larvae fluorescence imaging

To assess the effectiveness of zebrafish Tg(*cyp2k18:egfp*) reporter line as a high-throughput screening for gastrointestinal toxicity of cancer treatment, larvae were treated with SN38 and afatinib, anti-cancer compounds with known gastrointestinal toxicity profiles; and positive control, diclofenac [165]. Larvae were imaged for induction of eGFP in the gastrointestinal tract of Tg(*cyp2k18:egfp*) reporter line. To assess gut inflammation, the neutrophil reporter line, Tg(*BACmpx:gfp*) was also exposed to both compounds. As expected, diclofenac induced eGFP in the gastrointestinal tract of the Tg(*cyp2k18*:egfp) zebrafish larvae (figure 2a); SN38 and afatinib did not elicit a response (Figure 2c, d). SN38 and afatinib induced neutrophil translocation from the vasculature (indicated by white arrow in untreated control, figure 2e) to surrounding tissues, however, this was not specific to the gastrointestinal tract (Figure 2f, g). Visual inspection indicated a relative decrease in translocation of neutrophils in larvae treated with SN38 (Figure 2f) compared to afatinib treated larvae (Figure 2g).

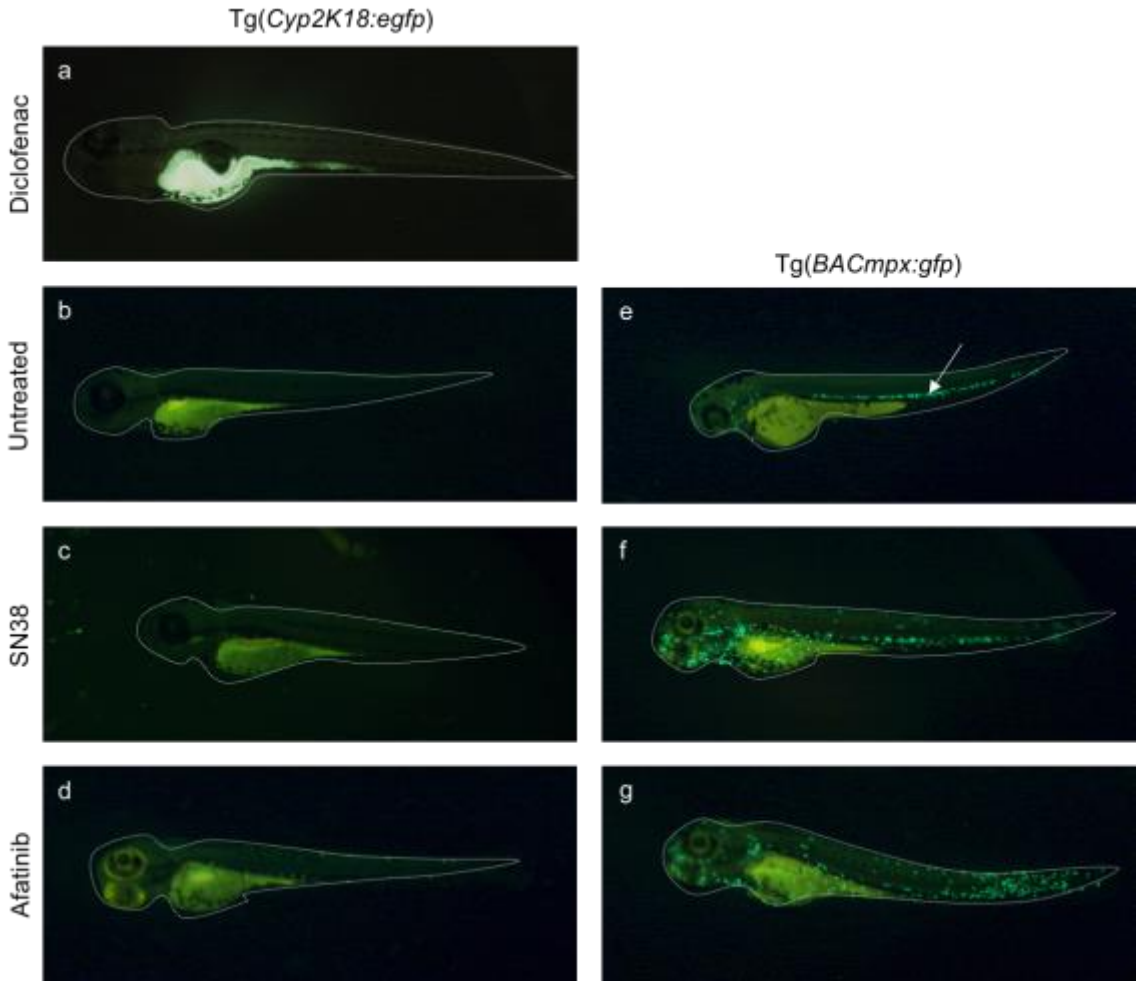

Figure 2: Fluorescent microscope still images of Tg(cyp2k18:egfp) and Tg(BACmpx:gfp) larvae zebrafish at 4dpf. 2a: Diclofenac (positive control) induced eGFP in gastrointestinal tract of Tg(cyp2k18:egfp). 2b: Untreated larvae did not display eGFP in gastrointestinal tract Tg(cyp2k18:egfp). 2c: SN38 treatment did not induce eGFP in gastrointestinal tract Tg(cyp2k18:egfp). 2d: Afatinib treatment did not induce eGFP in gastrointestinal tract Tg(cyp2k18:egfp). 2e, white arrow: Untreated Tg(BACmpx:gfp) displayed neutrophils contained to the vasculature. 2f: SN38 treated Tg(BACmpx:gfp) displayed some neutrophil translocation from the vasculature. 2g: Afatinib treated Tg(BACmpx:gfp) displayed neutrophil translocation from the vasculature.

Histopathological intestinal analysis in adult zebrafish

To assess the effect of cancer drugs on the histopathology of the gastrointestinal tract, six key markers of damage were assessed in adult zebrafish: disruption of brush border and surface enterocytes, infiltration of polymorphonuclear cells and lymphocytes, dilation of lymphatics and capillaries, oedema, villus fusion and villus atrophy. Both Tg(*cyp2k18:egfp)* (n=6) and wildtype AB (n=6) adult zebrafish treated with afatinib did not display histopathological damage to the intestines ($p > 0.05$) (figure 3a, b, c). Both Tg(*cyp2k18:egfp*) (n=6) ($p = 0.0076$) and wildtype AB (n=6) ($p = 0.0407$) zebrafish treated with SN38 had significantly increased histopathological scores compared to controls (n=6 Tg(*cyp2k18:egfp);* n=6 AB wildtype) (figure 3a, d). The adult Tg(*cyp2k18:efp*) zebrafish were not different from the wild type (AB) at baseline ($p > 0.05$), or in response to treatment ($p > 0.05$). To assess the effect of cancer drugs on goblet cells in the gastrointestinal tract, AB-PAS staining was analysed. There was no significant difference between either the transgenic (5.736 +/- 1.49 cells per villus in DMSO IP; 7.446 +/- 1.092 cell per villus in DMSO gavage) or AB controls (5.923 +/- 2.06 cells per villus in DMSO IP; 7.625 +/- 1.205 cells per villus DMSO gavage). There was no significant difference in fish treated with either SN38 (8.454 +/- 1.229 per villus in AB fish; 6.528 +/- 2.135 per villus in Tg(*cyp2k18:egfp*) fish), or afatinib (5.508 +/- 1.482 cells per villus in AB fish; 6.392 +/- 1.957 cells per villus in Tg(*cyp2k18:egfp*) fish), ($p > 0.05$). Caspase 3 staining to identify apoptotic cells in the intestine showed no significant difference between either the transgenic or wildtype line in controls and fish treated with either SN38 or afatinib ($p > 0.05$; data not shown).

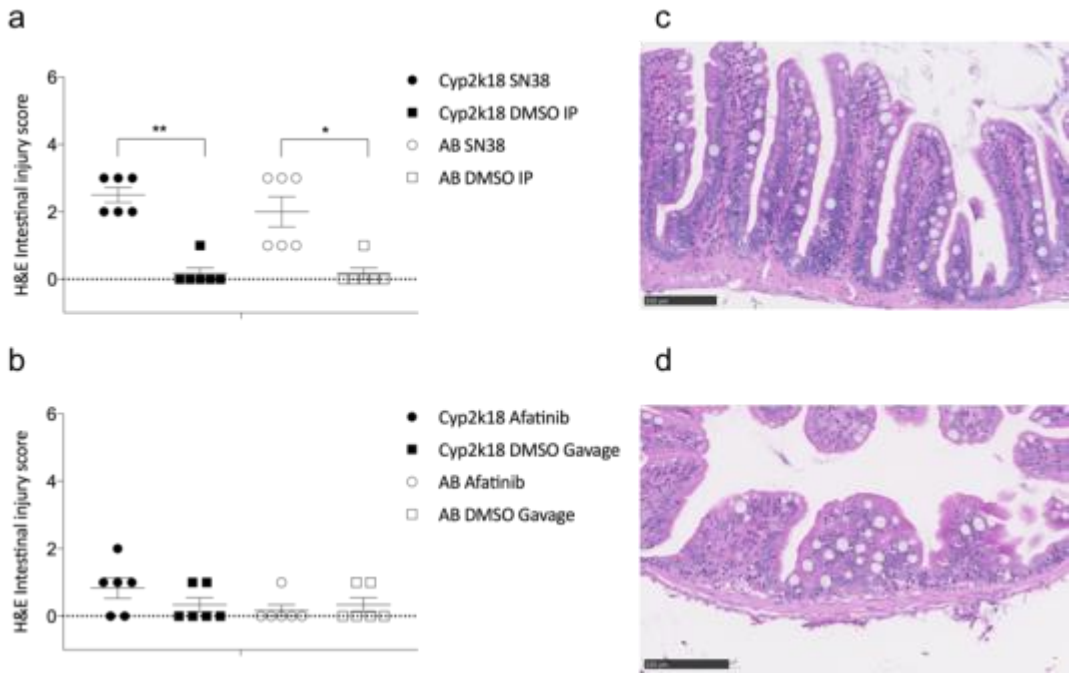

Figure 3: Histopathological injury in zebrafish. 3a: Adult Tg(cyp2k18:egfp) and adult AB zebrafish treated with SN38 had significant histopathological intestinal injury compared to controls (**p=0.0076 and *p = 0.0407 respectively). **3b**: Adult zebrafish treated with afatinib did not develop histopathological intestinal injury (p>0.05). **3c**: Representative image of adult Tg(cyp2k18:egfp) zebrafish treated with DMSO control. **3d**: Representative image of adult Tg(cyp2k18:egfp) zebrafish treated with SN38.

Discussion

Gastrointestinal toxicity is a common side effect of cancer therapies, and can restrict administration dose, and thus treatment efficacy. There is a pressing need for diverse models and assays to better understand the mechanisms, and identify toxicity early in drug development. The zebrafish model has been recognized as a powerful tool for human disease modelling, toxicology and drug screening assays, based largely on its ease of handling, fecundity, low cost, rapid external development, amenability to genetic manipulation as well as its genetic similarity to higher vertebrates [178]. There has been minimal use of the zebrafish model to study gastrointestinal toxicity; with one model reporting mucositis findings when developing a hand-foot disease model with PEGylated doxorubicin [177]. Here, we aimed to utilise a newly developed transgenic reporter line as a novel model to screen anti-cancer drugs that induce gastrointestinal toxicity.

The Tg(*cyp2k18:egfp*) reporter line was developed to screen liver toxicity drugs, however, on testing it was noted that eGFP was also induced in the gastrointestinal tract if toxicity was induced [165]. Non-steroidal anti-inflammatory agents such as diclofenac have long been reported to induce gastrointestinal injury [179]. It was therefore logical to test the ability of this line as a reporter line for cancer treatments that induce both hepatotoxicity and gastrointestinal toxicity. In this model, two agents known to induce severe gastrointestinal-toxicity were used to assess the viability of the Tg(*cyp2k18:egfp*) line as a high throughput, low cost screening tool. However, upon testing it was noted that following treatment with both chosen drugs, SN38 and afatinib, no induction of eGFP was seen in larvae. It is now becoming appreciated that each toxicant is likely to induce a unique set of transcriptional responses and that a global toxic reporter is unlikely to exist. It was noted previously that diverse toxicity reporter lines each

responded differently to hepatotoxicants [165]. Ideally any toxicity assay would involve a number of independent reporter lines. Unbiased transcriptional profiling of the toxic response to afatinib and SN38 in the zebrafish might yield novel markers for transgenic reporter development.

A key drawback in using zebrafish for the study of toxicity, is that larvae must receive the compound in water. Drug solubility is therefore a major factor to be considered when utilising this model. While this study overcame this limitation in adult fish by administering drugs via oral gavage or intraperitoneal injection, such approaches are not feasible in larvae nor are adults readily screenable for reporter eGFP induction due to inherent opacity. Whilst understood that SN38 and afatinib engage a different pathway for metabolism than Cyp2K18, these agents have been shown to induce hepatotoxicity in other models, the precise mechanisms of which are unknown [180, 181]. Therefore, the potential confounding issue in this model may be that sufficient concentrations were not achieved to induce liver or gastrointestinal toxicity due to the low solubility, and thus lack of absorption. The solubility of SN38 has previously been identified as problematic, and hence development of soluble SN38 is now being investigated, and may be useful in this model in the future [182]. Nevertheless, afatinib was soluble, and indeed, caused some lethality at doses above 200 μM, however it is unclear if the lethality was of gastrointestinal origin.

Adult zebrafish treated with afatinib did not show histopathological damage. There are a number of reasons to potentially explain this: (1) histopathological damage is only occasionally reported as a feature of targeted-therapy induced gastrointestinal toxicity; (2) when histopathology is reported; it is most commonly only in the ileum, and it is

possible that given the differences in zebrafish gastrointestinal anatomy this was not seen. The zebrafish lacks a stomach, with the regionalisation of the adult zebrafish being more gradual. The morphology of the zebrafish intestine is analogous to the villus structure of mammalian intestines, with capacious folds of the epithelium that protrude into the lumen, increasing the surface area with the finger-like projections, however do not contain crypts [168]; (3) afatinib is typically administered daily over many weeks, and so a single dose may not cause gastrointestinal toxicity. Further studies are therefore needed to further investigate this model with a time-course, however the tolerance of daily gavage to zebrafish is unclear.

While a robust and tractable genetic model of gastrointestinal toxicity is not available yet, the identification of genes required for the rapid proliferation of zebrafish intestinal epithelial cells during development has highlighted a number of essential genes that could be targeted to disable gastrointestinal toxicity [183]. Moreover, appreciation of the utility of zebrafish to study intestinal inflammation is gaining momentum. In particular, zebrafish provide opportunities to investigate the integrity of intestinal epithelial barrier function, a key emerging marker of gastrointestinal toxicity second to cancer treatment, with FITC-dextran gavage. With currently available tools, the interplay between epigenetic regulators, intestinal injury, microbiota composition and innate immune cell mobilisation can be analysed in exquisite detail [183]. This provides excellent opportunities to define critical events that could be targeted therapeutically. Furthermore, the use of zebrafish larvae as hosts for xenografts of human tissue, while still in its infancy, holds great promise that zebrafish could provide a practical, preclinical personalised medicine platform for the rapid assessment of the drug sensitivity of the patient. Furthermore, there are nascent, yet encouraging, efforts to generate humanised

transgenic zebrafish lines for more accurate reconstitution of human drug metabolism [184].

Conclusion

Zebrafish are providing several productive avenues for toxicology research, however a timely screening model for gastrointestinal toxicity second to cancer treatment is yet to be developed. Here, we aimed to utilise a newly developed transgenic reporter line to address this need, however, the transgenic line did not report gastrointestinal toxicity using the compounds tested. This may be explained due to poor solubility, providing an unclear picture of whether these larvae were induced for any type of injury. We therefore had to concentrate our attention on the adult fish in the direct delivery of the compounds. Chemotherapy agents with high solubility and permeability would be more amenable to these models. In addition, different drugs may invoke highly unique genomic responses, and hence we did not see induction of eGFP in larvae in response to these compounds. Further progress in this area would be greatly facilitated by the generation of robust and reproducible genetic models of zebrafish intestinal toxicity that mimic the known pathobiological pathways in rodents and humans, and can be readily induced in a short time-frame. This would include identification of more gastrointestinal toxicity reporter genes in zebrafish from these and other drugs. Suitably apt models will have the potential to deliver novel cancer drugs by providing a platform for high throughput chemical screens.

Chapter 6 General Discussion

Introduction

The use of TKIs is increasing, and despite intentions of reduced toxicity, the prevalence of diarrhoea, one of the most troublesome and prevalent symptom of toxicity, has increased [124]. This has been further exacerbated with the advent of second generation pan-HER TKIs [124]. Initial research suggested the mechanisms causing diarrhoea were consistent with chemotherapy-induced mucositis, characterised by direct mucosal atrophy [16]. However, as more research emerged, conflicting findings made it unclear if there was indeed a uniform pattern to characterise toxicity of tyrosine kinase inhibitors as previously hypothesised.

This thesis aimed to address the knowledge gap and provide a detailed interrogation of mechanisms underpinning gastrointestinal toxicity second to pan-HER TKI treatment (Chapter 3). I selected, dacomitinib as an ideal agent, as it (a) was associated with high levels of diarrhoea (Chapter 1), (b) is a second generation TKI characterised by irreversible receptor binding [37] and (c) inhibits all active members of the HER family [37]. Given the growing body of evidence in support for a chloride secretory mechanism of HER TKI-induced diarrhoea (Chapter 2), this thesis also investigated crofelemer as an intervention for dacomitinib-induced diarrhoea (Chapter 4). I chose crofelemer as it (a) dose-dependently inhibits the two major apical chloride channels found in the intestines [118], and (b) has previously been approved for the treatment of diarrhoea [185]. Utilising gold standard Ussing chambers, electrogenic ion movement across the epithelium was investigated. There is increasing acceptance for the hypothesis of TKI-

induced diarrhoea being attributable to chloride secretion, now resulting in crofelemer being proposed in clinical trials for the treatment of cancer therapy induced diarrhoea [143]. The body of work described in this thesis:

- Characterised dacomitinib-induced diarrhoea, with strong evidence provided of barrier dysfunction and mucosal atrophy.
- Showed that damage was confined to the ileum following dacomitinib treatment. This was also the area with highest relative expression of ErbB1.
- Suggested that crofelemer is not useful in this particular setting, as not only was it unable to attenuate diarrhoea, it also made it worse.
- Did not support the initial hypothesis of chloride secretion being a mechanism of dacomitinib-induced diarrhoea in this model.

Given the stark contrast seen between the *in vitro* and *in vivo* studies of Chapter 4, where the *in vitro* proof of concept was not translated to the whole-organism model, Chapter 5 aimed to bridge the gap between *in vitro* and rodent models, with a zebrafish model of gastrointestinal toxicity. Zebrafish are providing several productive avenues for toxicology research and Chapter 5 aimed to harness this to develop a timely screening model for gastrointestinal toxicity second to cancer treatment. The transgenic reporter line utilised in this model did not report gastrointestinal toxicity as predicted. However, it did highlight that the generation of robust and reproducible genetic models of zebrafish intestinal toxicity is warranted. A model that can be readily induced in a short time-frame will have the potential to provide a novel platform for high throughput gastrointestinal toxicity screens.

Histopathological damage to the ileum, barrier dysfunction, and inflammation: traits of dacomitinib-induced gastrointestinal toxicity

With the advent of targeted therapies, it was anticipated that side effects would be few, however this has not come to fruition [14, 122]. In fact, the incidence of gastrointestinal toxicity is increasing with their use, which is exacerbated by the chronic oral administration and concomitant treatment [16]. Despite this increasing incidence, there is still limited understanding of mechanisms underpinning the toxicity, with literature reporting varying findings ranging from no histopathological damage seen, to significant damage. It is therefore imperative to provide a detailed investigation of mechanisms underpinning TKI-induced gastrointestinal toxicity. Dacomitinib was an attractive agent to use to interrogate mechanisms as it is associated with high levels of diarrhoea, and irreversibly targets all active members of the HER family.

There have been contradictions throughout the literature about whether TKI-induced diarrhoea is associated with histopathological damage (as is this case with traditional chemotherapy-induced diarrhoea) [16]. The study presented in Chapter 3 demonstrated for the first time that dacomitinib was associated with significant histopathological damage. This was characterised by a number of validated features of mucosal injury, with terminally differentiated enterocytes being the most affected. Importantly, this damage was isolated to the ileum, with no other areas of the gastrointestinal tract identified as displaying histopathological damage.

Furthermore, an analysis of 7 cytokines common to mucosal injury following cytotoxic treatment, were analysed, and only MCP-1 was found to be upregulated, and again this was confined to the ileum. MCP-1 is a monocyte chemoattractant which is also highly

upregulated in patients with inflammatory bowel disease (IBD) [186]. IBD is characterised by increased permeability and an influx of granulocytes and monocytes which exacerbate inflammation and tissue injury. The parallels could open the avenue for future therapeutic interventions such as granulocyte and monocyte adsorptive apheresis (GMA), which has been successful in the IBD field [187]. However, when considering systemic interventions such as this, careful considerations must be made about their safety in regards to tumour growth.

The localisation of injury to the ileum may begin to explain why there has been such variation in the literature around histopathology of TKI-induced gastrointestinal toxicity, as if the ileum specifically was not assessed, no damage would be noted. The publication arising from Chapter 3 was also the first to characterise ErbB receptor expression along the gastrointestinal tract of rats, revealing that ErbB1 is expressed at a relatively higher rate in the ileum compared to other regions of the tract. This correlates with the site of histopathological damage, which may suggest why peak damage was seen at this site.

Mucosal enterocyte barrier disruption has been associated with a number of gastrointestinal disorders characterised by diarrhoea, and is suggested to worsen clinical outcomes, as it allows for translocation of endotoxin and bacteria [136]. Additionally, previous research has shown alterations in intestinal barrier function following various cytotoxic treatments, with tight junction dysfunction gaining momentum as a key feature of chemotherapy-induced gastrointestinal toxicity [137, 188]. However, the role barrier function has in TKI-induced gastrointestinal toxicity has been largely ignored. The study described in Chapter 3 utilised FITC-dextran to show barrier dysfunction following dacomitinib treatment. This barrier dysfunction was then further characterised in the

study described in Chapter 4, with tight junction defects characterised in the ileum and colon. Three important tight junction proteins were investigated given their established role in maintaining barrier function [188]. Notably, these changes also coincided in the ileum, the region where peak histopathological damage and inflammation was seen. This is of particular importance, as inflammation has been associated with the induction of a 'leaky' gut [135, 136]. Furthermore, although not presented, I found that colon tissue mounted into Ussing chambers from rats treated with dacomitinib in either treatment schedule, showed no difference in conductance, a measure of permeability ($p > 0.05$). Conversely, rats treated with crofelemer and dacomitinib combination showed significantly increased conductance in the ileum compared to all other treatment groups ($p < 0.003$), indicating increased barrier dysfunction in this group. Characterising intestinal barrier dysfunction is central to understanding the development of gastrointestinal toxicity, as it is proposed that breakdown of the intestinal mucosal barrier contributes to diarrhoea through leak-flux mechanisms allowing passive movement of water into the lumen [138]. In addition, inflammation in the gastrointestinal tract is also reported to decrease sodium absorption, thereby further contributing to fluid loss in diarrhoea [189]. Furthermore, given the histopathological damage is pronounced at the ileum, it is likely to lead to decreased bile acid uptake, further contributing to diarrhoea [190].

Highlighting limitations to the hypothesis of chloride secretory mechanisms for TKI-induced diarrhoea with crofelemer

The gold standard in management of cancer-therapy induced diarrhoea are the MASCC/ISOO clinical practice guidelines for the management of mucositis second to cancer treatment [60]. Although no recommendations are made by these guidelines on how to treat diarrhoea second to TKIs, there is a call for more research of TKI-induced diarrhoea [191]. Currently, pharmacologic management of ErbB TKI-induced diarrhoea is largely limited to loperamide, a synthetic oral opioid drug that decreases peristalsis and fluid secretion [61]. However, no anti-diarrhoeal medication used for the management of TKI-induced diarrhoea offers a targeted approach, primarily due to the lack of understanding of the underlying mechanisms. This thesis (Chapter 2) described the emerging anecdotal evidence for chloride secretion as a mechanistic hypothesis for TKI-induced diarrhoea, and offered crofelemer, an anti-secretory, anti-diarrhoeal as a targeted treatment. This publication was provided as the rationale for a phase II evaluation of crofelemer for the prevention and prophylaxis of diarrhoea in patients administered pertuzumab-based regimens by Gao and colleagues, who are currently recruiting patients [143].

The research presented in Chapter 4 demonstrated that *in vitro* experiments supported the hypothesis of chloride secretion as the underlying mechanism of dacomitinib-induced diarrhoea. However, when these findings were translated into a whole organism, and *ex vivo* model, there was minimal evidence supporting chloride secretion as a mechanism for dacomitinib-induced diarrhoea. Although my study utilised the gold standard of assessing electrogenic ion movement across an epithelium, the Ussing chamber (Physiologic Instruments), there come limitations with the method. Ussing chambers

measure electrogenic secretion, however are unable to measure electroneutral sodium chloride transport [192]. In the context of other inflammatory bowel diseases, sodium transport is considered important in measuring changes in bowel function. In fact, the predominant mechanism of IBD associated diarrhoea involves impairment of electroneutral sodium chloride absorption, with very little role, if any played by anion secretion [193]. However, as this was not the primary outcome of interest given the prevailing chloride secretion hypothesis, this was not assessed in this thesis. Although the *ex vivo* Ussing chamber investigations did not return evidence for a secretory diarrhoea phenotype following dacomitinib treatment, blood biochemistry results may indicate otherwise. There was a significant increase in the anion gap, a marker of metabolic acidosis. Acidosis occurs when bicarbonate is lost, however, our results showed no significant loss in bicarbonate, thus making the interpretation quite difficult in this context. Given the decreased albumin results, which can be related to kidney damage, this further exacerbates complications in interpretation. Nevertheless, the blatant differences and lack of translatability from the *in vitro* and *in vivo* components of this thesis should be considered. T84 monolayers lack other neuro-immune mucosal cell interactions, and of particular importance to this thesis, the impact that inflammation has on tight junctions, which can influence chloride secretion via leak flux mechanisms. The *ex vivo* analysis of this study utilised tissue from animals exposed to dacomitinib for 21 days, and was therefore inflamed. This is in stark contrast to the *in vitro* component, in which dacomitinib was administered to healthy cells. While future studies could consider administering dacomitinib in the Ussing chamber to 'healthy' animal tissue to see acute changes; there are clear limitations to this.

When a drug is added to healthy tissue to model response, it does not take into account that clinically the gut would be in an inflamed state. The tissue hence reacts very differently than in the healthy state due to altered expression of proteins and transporters [153]. Therefore, this method of analysis does not adequately represent the true changes in function and signalling. In fact, the state of gastrointestinal inflammation may point to potential flaws in the hypothesis of TKI-induced diarrhoea being due to secretory mechanisms. The hypothesis is based on ErbB being a negative regulator of chloride secretion in normal settings, and so when inhibited there is a loss of negative regulation, and thus increased chloride secretion. This hypothesis was supported by previous research with HER-1 TKI, lapatinib, which was not associated with inflammation [90]. However, the hypothesis does not consider that the tissue may be inflamed, and hence behave differently, a fundamental caveat. This is primarily demonstrated with DSS-induced colitis models, that have shown that when tissue is in an inflamed state, ErbB1 phosphorylation actually enhances chloride secretion, instead of inhibiting it [153].

Crofelemer has previously been shown to exert its antisecretory effect via partial inhibition of CFTR, and complete inhibition of CaCC (TMEM16A) [118]. Current literature suggests it has no contraindications. It was chosen for use in this thesis based on its lack of systemic absorption and its reported selectivity in acting only on the apical side of the CaCC and CFTR chloride channels of the gastrointestinal tract [118]. The *in vitro* arm presented in Chapter 4 clearly demonstrated that crofelemer inhibited chloride secretion, supported by the current literature. Conversely, when I translated crofelemer to the *in vivo* arm, the electrophysiological analysis demonstrated that crofelemer had no inhibitory effect on chloride secretion. Additionally, crofelemer was unable to attenuate dacomitinib-induced diarrhoea in this model, and in fact, worsened it. Convective drug

washout may explain the lack of effect seen with crofelemer, but does not explain the significantly worse clinical presentation. It was unlikely that this was associated with increased dacomitinib exposure given the cMin was unaffected with crofelemer co-treatment, however without doing a more in-depth pharmacokinetic analysis, conclusions cannot be confidently drawn. Regardless, this is the first study to suggest that crofelemer may have paradoxical effects, and warrants further investigation before crofelemer is used in conjunction with other pharmaceuticals. Research with crofelemer has previously been focused on non-infectious diarrhoea, driven by chloride secretory mechanisms [117], with only one study suggesting that crofelemer may be effective in an infectious diarrhoea context [194].

Bridging the gap between *in vitro* and whole-organism models with zebrafish

The study presented in Chapter 5 aimed to harness zebrafish as a model to overcome the prohibitive expense and time constraints of currently used rodent models. While *in vitro* models have helped for high throughput screening, the lack of surrounding cells and tissues limits their usefulness. Often this results in a lack of translatability, as was clearly seen in Chapter 4. Zebrafish allow for rapid, miniaturised, whole-organism toxicity testing due to their ease of handling, fecundity, low cost, rapid external development, amenability to genetic manipulation and the genetic similarity to higher vertebrates [183]. To date, there has been minimal use of zebrafish for the study of gastrointestinal toxicity, however their use in other gastrointestinal diseases is gaining momentum [178].

Zebrafish express ErbB receptors [195], and chloride channels [196, 197]. As such, I decided to further exploit zebrafish and investigate their feasibility in this field. Chapter 5 utilised the Tg(*cyp2k18:egfp*) transgenic reporter line with the hypothesis that the eGFP would be induced in the gastrointestinal tract if toxicity was induced in larvae, allowing for rapid screening of gastrointestinal toxicity. Unfortunately, due to the material transfer agreement (MTA) with Pfizer Pharmaceuticals, dacomitinib was unable to be used in this model. Afatinib was therefore selected as the pan-HER TKI, as it is readily available and is the same class as dacomitinib (characterised in Chapters 3 and 4). The active metabolite of irinotecan, SN38, was selected as the cytotoxic as it has been well characterised in the literature as causing severe gastrointestinal toxicity and diarrhoea [127]. Together, they represent two different classes of cancer drugs known to cause gastrointestinal toxicity. Upon testing with SN38 and afatinib, I found that the Tg(*cyp2k18:egfp*) reporter line was unable to screen for gastrointestinal toxicity

following either of these two drugs, as eGFP was not induced in the gastrointestinal tracts of the larvae. One of the key limitations of using aquatic animals, is that all drugs must be administered in water, making drug solubility a major contributing factor in the success of the model. Therefore, the potential confounding issue in this model may be that sufficient concentrations were not achieved to induce liver or gastrointestinal toxicity due to low solubility and/or poor permeability, and thus lack of gastrointestinal absorption. This may offer an explanation as to why no fluorescence was seen. While this study overcame this limitation in adult fish by administering drugs via oral gavage or intraperitoneal injection, such approaches are not feasible in larvae nor are adults readily screenable for reporter eGFP induction due to inherent opacity. Nevertheless, the use of zebrafish to screen new compounds is gaining momentum [198-201]. Their use is not just attractive to toxicity, but also molecular oncology, with the opportunity to investigate multiple genetic alterations associated with the development of human cancers and validation of novel anticancer drug targets [198]. Particularly, the transparent zebrafish models can be used as a xenotransplantation system to rapidly assess tumorigenesis and metastatic behaviour of cancer stem or progenitor cells [198]. Given the success of zebrafish reporter lines for toxicity screening others have yielded, it may be worthwhile taking a more targeted approach, such that soluble cancer drugs known to induce gastrointestinal toxicity are administered to zebrafish. In this way, highly upregulated genes in the gastrointestinal tract can be identified as biomarkers of toxic response, and tagged with eGFP. Creating such a model could subsequently be used for high throughput screening of new cancer drugs, however the heterogeneity of the many classes of cancer drugs would need to be considered.

Despite overcoming treatment difficulties in adults, afatinib still did not induce gastrointestinal histopathological damage, potentially due to regionalisation of the zebrafish intestine not representing the ileum closely enough. As outlined in Chapters 3 and 4, the ileum is the key region damaged following pan-HER TKI administration. Additionally, this model used a single dose administration, as opposed to the typical protracted administration of pan-HER TKIs, where 7 days is needed to see histopathological damage, which may explain the lack of damage seen in zebrafish. Given this, it is possible that afatinib exposure may not have been sufficient, and future studies would need to test for retention and absorption of any drug used.

Although the transgenic reporter line was unable to screen for gastrointestinal toxicity, the adult zebrafish administered SN38 did show histopathological damage to the intestines reminiscent of changes seen in clinical samples. This is the first time SN38 has been administered in adult zebrafish, and given the positive result, could be expanded on to other drugs, particularly the growing area of oral formulations of SN38. Given the many advantages of utilising zebrafish, and the evidence that zebrafish can indeed develop gastrointestinal injury from cytotoxic agents, further investigation is warranted. While a robust and tractable genetic model of gastrointestinal toxicity is not available yet, the identification of genes required for the rapid proliferation of zebrafish intestinal epithelial cells during development has highlighted a number of essential genes that could be targeted to disable gastrointestinal toxicity [202]. Moreover, zebrafish are being exploited for other gastrointestinal inflammatory pathologies, and intestinal epithelial barrier function has been identified as a characteristic in these models [166]. Given the increasing acknowledgement of barrier dysfunction as a key factor in the development of gastrointestinal toxicity (as outlined in Chapter 4), zebrafish may provide a unique

platform to investigate this. With currently available tools, the interplay between epigenetic regulators, intestinal injury, microbiota composition and innate immune cell mobilisation can be analysed in exquisite detail [183]. This provides excellent opportunities to define critical events that could be targeted therapeutically.

Conclusion

It is clear that second generation, pan-HER TKIs induce diarrhoea in a high proportion of patients. With the increasing use of these agents, understanding the mechanisms of HER TKI-induced diarrhoea are crucial. This will enable researchers to investigate potentially effective interventions to help prevent adverse event aggravation, dose reductions or therapy discontinuation.

The studies presented in this thesis have shown that pan-HER TKI-induced gastrointestinal toxicity is associated with histopathological damage, inflammation, and intestinal barrier dysfunction in the ileum, the region where ErbB1 is preferentially expressed. It is likely that this injury seen following HER TKI treatment, is the cause of diarrhoea. Through a number of investigations, this thesis highlighted limitations to the mechanistic hypothesis of HER TKI-induced diarrhoea being of secretory phenotype. Furthermore, the publications airing from this thesis are the first to suggest that crofelemer may have contraindications, emphasising the importance of preclinical trials, and that crofelemer should be used with caution when prescribed with other medications. This thesis has also brought light to the potential future use of zebrafish as a high throughput screening tool for gastrointestinal toxicity. Further progress in this area would be greatly facilitated by the generation of robust and reproducible genetic models of zebrafish intestinal toxicity that can be readily induced in a short time-frame, allowing opportunities to define critical events that can be therapeutically targeted.

Chapter 7 References

1. Siegel, R., J. Ma, Z. Zou, *et al.*, *Cancer statistics, 2014.* CA Cancer J Clin, 2014. **64**(1): p. 9-29.
2. Peters, S., A.A. Adjei, C. Gridelli, *et al.*, *Metastatic non-small-cell lung cancer (NSCLC): ESMO Clinical Practice Guidelines for diagnosis, treatment and follow-up.* Ann Oncol, 2012. **23 Suppl 7**: p. vii56-64.
3. Ettinger, D.S., W. Akerley, H. Borghaei, *et al.*, *Non-small cell lung cancer.* J Natl Compr Canc Netw, 2012. **10**(10): p. 1236-71.
4. Chan, B.A. and B.G. Hughes, *Targeted therapy for non-small cell lung cancer: current standards and the promise of the future.* Transl Lung Cancer Res, 2015. **4**(1): p. 36-54.
5. Yaish, P., A. Gazit, C. Gilon, *et al.*, *Blocking of EGF-dependent cell proliferation by EGF receptor kinase inhibitors.* Science, 1988. **242**(4880): p. 933-5.
6. Pinkas-Kramarski, R., I. Alroy, and Y. Yarden, *ErbB receptors and EGF-like ligands: cell lineage determination and oncogenesis through combinatorial signaling.* Journal of mammary gland biology and neoplasia, 1997. **2**(2): p. 97-107.
7. Dent, P., A. Yacoub, J. Contessa, *et al.*, *Stress and radiation-induced activation of multiple intracellular signaling pathways.* Radiation research, 2003. **159**(3): p. 283-300.
8. McCole, D.F. and K.E. Barrett, *Decoding epithelial signals: critical role for the epidermal growth factor receptor in controlling intestinal transport function.* Acta physiologica, 2009. **195**(1): p. 149-59.
9. Henson, E.S. and S.B. Gibson, *Surviving cell death through epidermal growth factor (EGF) signal transduction pathways: implications for cancer therapy.* Cellular signalling, 2006. **18**(12): p. 2089-97.
10. Paul, G., R.R. Marchelletta, D.F. McCole, *et al.*, *Interferon-gamma alters downstream signaling originating from epidermal growth factor receptor in intestinal epithelial cells: functional consequences for ion transport.* The Journal of biological chemistry, 2012. **287**(3): p. 2144-55.
11. Ayyappan, S., D. Prabhakar, and N. Sharma, *Epidermal growth factor receptor (EGFR)-targeted therapies in esophagogastric cancer.* Anticancer research, 2013. **33**(10): p. 4139-55.
12. Gibson, R.J. and A.M. Stringer, *Chemotherapy-induced diarrhoea.* Current opinion in supportive and palliative care, 2009. **3**(1): p. 31-5.
13. Burstein, H.J., Y. Sun, L.Y. Dirix, *et al.*, *Neratinib, an irreversible ErbB receptor tyrosine kinase inhibitor, in patients with advanced ErbB2-positive breast cancer.* J Clin Oncol, 2010. **28**(8): p. 1301-7.
14. Keefe, D.M. and E.H. Bateman, *Tumor control versus adverse events with targeted anticancer therapies.* Nature reviews. Clinical oncology, 2012. **9**(2): p. 98-109.
15. Bowen, J.M., B.J. Mayo, E. Plews, *et al.*, *Development of a rat model of oral small molecule receptor tyrosine kinase inhibitor-induced diarrhoea.* Cancer biology & therapy, 2012. **13**(13): p. 1269-75.
16. Van Sebille, Y.Z., R.J. Gibson, H.R. Wardill, *et al.*, *ErbB small molecule tyrosine kinase inhibitor (TKI) induced diarrhoea: Chloride secretion as a mechanistic hypothesis.* Cancer Treat Rev, 2015. **41**(7): p. 646-52.

17. Iivanainen, E. and K. Elenius, *ErbB targeted drugs and angiogenesis.* Curr Vasc Pharmacol, 2010. **8**(3): p. 421-31.
18. Wakeling, A.E., S.P. Guy, J.R. Woodburn, *et al., ZD1839 (Iressa): an orally active inhibitor of epidermal growth factor signaling with potential for cancer therapy.* Cancer Res, 2002. **62**(20): p. 5749-54.
19. Moyer, J.D., E.G. Barbacci, K.K. Iwata, *et al., Induction of apoptosis and cell cycle arrest by CP-358,774, an inhibitor of epidermal growth factor receptor tyrosine kinase.* Cancer Res, 1997. **57**(21): p. 4838-48.
20. Mok, T.S., Y.L. Wu, S. Thongprasert, *et al., Gefitinib or carboplatin-paclitaxel in pulmonary adenocarcinoma.* N Engl J Med, 2009. **361**(10): p. 947-57.
21. Zhou, C., Y.L. Wu, G. Chen, *et al., Erlotinib versus chemotherapy as first-line treatment for patients with advanced EGFR mutation-positive non-small-cell lung cancer (OPTIMAL, CTONG-0802): a multicentre, open-label, randomised, phase 3 study.* Lancet Oncol, 2011. **12**(8): p. 735-42.
22. Rosell, R., E. Carcereny, R. Gervais, *et al., Erlotinib versus standard chemotherapy as first-line treatment for European patients with advanced EGFR mutation-positive non-small-cell lung cancer (EURTAC): a multicentre, open-label, randomised phase 3 trial.* Lancet Oncol, 2012. **13**(3): p. 239-46.
23. Thatcher, N., A. Chang, P. Parikh, *et al., Gefitinib plus best supportive care in previously treated patients with refractory advanced non-small-cell lung cancer: results from a randomised, placebo-controlled, multicentre study (Iressa Survival Evaluation in Lung Cancer).* Lancet, 2005. **366**(9496): p. 1527-37.
24. Sun, J.M., K.H. Lee, S.W. Kim, *et al., Gefitinib versus pemetrexed as second-line treatment in patients with nonsmall cell lung cancer previously treated with platinum-based chemotherapy (KCSG-LU08-01): an open-label, phase 3 trial.* Cancer, 2012. **118**(24): p. 6234-42.
25. Cufer, T., E. Vrdoljak, R. Gaafar, *et al., Phase II, open-label, randomized study (SIGN) of single-agent gefitinib (IRESSA) or docetaxel as second-line therapy in patients with advanced (stage IIIb or IV) non-small-cell lung cancer.* Anticancer Drugs, 2006. **17**(4): p. 401-9.
26. Kim, E.S., V. Hirsh, T. Mok, *et al., Gefitinib versus docetaxel in previously treated non-small-cell lung cancer (INTEREST): a randomised phase III trial.* Lancet, 2008. **372**(9652): p. 1809-18.
27. Lee, D.H., K. Park, J.H. Kim, *et al., Randomized Phase III trial of gefitinib versus docetaxel in non-small cell lung cancer patients who have previously received platinum-based chemotherapy.* Clin Cancer Res, 2010. **16**(4): p. 1307-14.
28. Mok, T.S., Y.L. Wu, S. Thongprasert, *et al., Gefitinib or carboplatin-paclitaxel in pulmonary adenocarcinoma.* The New England journal of medicine, 2009. **361**(10): p. 947-57.
29. Maemondo, M., A. Inoue, K. Kobayashi, *et al., Gefitinib or chemotherapy for non-small-cell lung cancer with mutated EGFR.* N Engl J Med, 2010. **362**(25): p. 2380-8.
30. Goss, G., D. Ferry, R. Wierzbicki, *et al., Randomized phase II study of gefitinib compared with placebo in chemotherapy-naive patients with advanced non-small-cell lung cancer and poor performance status.* J Clin Oncol, 2009. **27**(13): p. 2253-60.
31. Morere, J.F., J.M. Brechot, V. Westeel, *et al., Randomized phase II trial of gefitinib or gemcitabine or docetaxel chemotherapy in patients with advanced*

non-small-cell lung cancer and a performance status of 2 or 3 (IFCT-0301 study). Lung Cancer, 2010. **70**(3): p. 301-7.
32. Mitsudomi, T., S. Morita, Y. Yatabe, *et al., Gefitinib versus cisplatin plus docetaxel in patients with non-small-cell lung cancer harbouring mutations of the epidermal growth factor receptor (WJTOG3405): an open label, randomised phase 3 trial.* Lancet Oncol, 2010. **11**(2): p. 121-8.
33. Zhang, L., S. Ma, X. Song, *et al., Gefitinib versus placebo as maintenance therapy in patients with locally advanced or metastatic non-small-cell lung cancer (INFORM; C-TONG 0804): a multicentre, double-blind randomised phase 3 trial.* Lancet Oncol, 2012. **13**(5): p. 466-75.
34. Crino, L., F. Cappuzzo, P. Zatloukal, *et al., Gefitinib versus vinorelbine in chemotherapy-naive elderly patients with advanced non-small-cell lung cancer (INVITE): a randomized, phase II study.* J Clin Oncol, 2008. **26**(26): p. 4253-60.
35. Xu, Y., H. Liu, J. Chen, *et al., Acquired resistance of lung adenocarcinoma to EGFR-tyrosine kinase inhibitors gefitinib and erlotinib.* Cancer Biol Ther, 2010. **9**(8): p. 572-82.
36. Gotoh, N., *Somatic mutations of the EGF receptor and their signal transducers affect the efficacy of EGF receptor-specific tyrosine kinase inhibitors.* Int J Clin Exp Pathol, 2011. **4**(4): p. 403-9.
37. Carpenter, R.L. and H.W. Lo, *Dacomitinib, an emerging HER-targeted therapy for non-small cell lung cancer.* Journal of thoracic disease, 2012. **4**(6): p. 639-42.
38. Ramalingam, S.S., F. Blackhall, M. Krzakowski, *et al., Randomized phase II study of dacomitinib (PF-00299804), an irreversible pan-human epidermal growth factor receptor inhibitor, versus erlotinib in patients with advanced non-small-cell lung cancer.* Journal of clinical oncology : official journal of the American Society of Clinical Oncology, 2012. **30**(27): p. 3337-44.
39. Takahashi, T., N. Boku, H. Murakami, *et al., Phase I and pharmacokinetic study of dacomitinib (PF-00299804), an oral irreversible, small molecule inhibitor of human epidermal growth factor receptor-1, -2, and -4 tyrosine kinases, in Japanese patients with advanced solid tumors.* Investigational new drugs, 2012. **30**(6): p. 2352-63.
40. Dietrich, E. and K. Antoniades, *Molecularly targeted drugs for the treatment of cancer: oral complications and pathophysiology.* Hippokratia, 2012. **16**(3): p. 196-9.
41. Hare, K.J., B. Hartmann, H. Kissow, *et al., The intestinotrophic peptide, glp-2, counteracts intestinal atrophy in mice induced by the epidermal growth factor receptor inhibitor, gefitinib.* Clinical cancer research : an official journal of the American Association for Cancer Research, 2007. **13**(17): p. 5170-5.
42. Abdul Razak, A.R., D. Soulieres, S.A. Laurie, *et al., A phase II trial of dacomitinib, an oral pan-human EGF receptor (HER) inhibitor, as first-line treatment in recurrent and/or metastatic squamous-cell carcinoma of the head and neck.* Annals of oncology : official journal of the European Society for Medical Oncology / ESMO, 2013. **24**(3): p. 761-9.
43. Campbell, A., K. Reckamp, D. Camidge, *et al., PF-00299804 (PF299) patient (pt)-reported outcomes (PROs) and efficacy in adenocarcinoma (adeno) and nonadeno non-small cell lung cancer (NSCLC): a phase (P) II trial in advanced NSCLC after failure of chemotherapy (CT) and erlotinib (E).* Journal of clinical oncology : official journal of the American Society of Clinical Oncology, 2010. **28**(5).

44. Reckamp, K.L., G. Giaccone, D.R. Camidge, *et al., A phase 2 trial of dacomitinib (PF-00299804), an oral, irreversible pan-HER (human epidermal growth factor receptor) inhibitor, in patients with advanced non-small cell lung cancer after failure of prior chemotherapy and erlotinib.* Cancer, 2014. **120**(8): p. 1145-1154.
45. Janne, P.A., D.S. Boss, D.R. Camidge, *et al., Phase I dose-escalation study of the pan-HER inhibitor, PF299804, in patients with advanced malignant solid tumors.* Clinical cancer research : an official journal of the American Association for Cancer Research, 2011. **17**(5): p. 1131-9.
46. Ramalingam, S.S., F. Blackhall, M. Krzakowski, *et al., Randomized phase II study of dacomitinib (PF-00299804), an irreversible pan-human epidermal growth factor receptor inhibitor, versus erlotinib in patients with advanced non-small-cell lung cancer.* J Clin Oncol, 2012. **30**(27): p. 3337-44.
47. Ruiz-Garcia, A., N. Giri, R.R. Labadie, *et al., A phase I open-label study to investigate the potential drug-drug interaction between single-dose dacomitinib and steady-state paroxetine in healthy volunteers.* J Clin Pharmacol, 2013.
48. Ramalingam, S.S., P.A. Janne, T. Mok, *et al., Dacomitinib versus erlotinib in patients with advanced-stage, previously treated non-small-cell lung cancer (ARCHER 1009): a randomised, double-blind, phase 3 trial.* Lancet Oncol, 2014. **15**(12): p. 1369-78.
49. Janne, P.A., A.T. Shaw, D.R. Camidge, *et al., Combined Pan-HER and ALK/ROS1/MET Inhibition with Dacomitinib and Crizotinib in Advanced Non-small Cell Lung Cancer: Results of a Phase I Study.* J Thorac Oncol, 2016.
50. Ellis, P.M., F.A. Shepherd, M. Millward, *et al., Dacomitinib compared with placebo in pretreated patients with advanced or metastatic non-small-cell lung cancer (NCIC CTG BR.26): a double-blind, randomised, phase 3 trial.* Lancet Oncol, 2014. **15**(12): p. 1379-88.
51. Lalla, R.V., J. Bowen, A. Barasch, *et al., MASCC/ISOO clinical practice guidelines for the management of mucositis secondary to cancer therapy.* Cancer, 2014. **120**(10): p. 1453-61.
52. Benson, A.B., 3rd, J.A. Ajani, R.B. Catalano, *et al., Recommended guidelines for the treatment of cancer treatment-induced diarrhoea.* Journal of clinical oncology : official journal of the American Society of Clinical Oncology, 2004. **22**(14): p. 2918-26.
53. Stein, A., W. Voigt, and K. Jordan, *Chemotherapy-induced diarrhoea: pathophysiology, frequency and guideline-based management.* Therapeutic advances in medical oncology, 2010. **2**(1): p. 51-63.
54. Foote, M., *The Importance of Planned Dose of Chemotherapy on Time: Do We Need to Change Our Clinical Practice?* The oncologist, 1998. **3**(5): p. 365-368.
55. Di Fiore, F. and E. Van Cutsem, *Acute and long-term gastrointestinal consequences of chemotherapy.* Best practice & research. Clinical gastroenterology, 2009. **23**(1): p. 113-24.
56. Davila, M. and R.S. Bresalier, *Gastrointestinal complications of oncologic therapy.* Nature clinical practice. Gastroenterology & hepatology, 2008. **5**(12): p. 682-96.
57. Vincenzi, B., G. Schiavon, F. Pantano, *et al., Predictive factors for chemotherapy-related toxic effects in patients with colorectal cancer.* Nature clinical practice. Oncology, 2008. **5**(8): p. 455-65.
58. Carlotto, A., V.L. Hogsett, E.M. Maiorini, *et al., The economic burden of toxicities associated with cancer treatment: review of the literature and analysis*

of nausea and vomiting, diarrhoea, oral mucositis and fatigue. PharmacoEconomics, 2013. **31**(9): p. 753-66.
59. Elting, L.S., C. Cooksley, M. Chambers, *et al., The burdens of cancer therapy. Clinical and economic outcomes of chemotherapy-induced mucositis.* Cancer, 2003. **98**(7): p. 1531-9.
60. Lalla, R.V., J. Bowen, A. Barasch, *et al., MASCC/ISOO clinical practice guidelines for the management of mucositis secondary to cancer therapy.* Cancer, 2014.
61. Hirsh, V., N. Blais, R. Burkes, *et al., Management of diarrhoea induced by epidermal growth factor receptor tyrosine kinase inhibitors.* Curr Oncol, 2014. **21**(6): p. 329-36.
62. Belani, C.P., *The role of irreversible EGFR inhibitors in the treatment of non-small cell lung cancer: overcoming resistance to reversible EGFR inhibitors.* Cancer Invest, 2010. **28**(4): p. 413-23.
63. Gibson, R.J., J.M. Bowen, M.R. Inglis, *et al., Irinotecan causes severe small intestinal damage, as well as colonic damage, in the rat with implanted breast cancer.* Journal of gastroenterology and hepatology, 2003. **18**(9): p. 1095-100.
64. Gibson, R.J. and D.M. Keefe, *Cancer chemotherapy-induced diarrhoea and constipation: mechanisms of damage and prevention strategies.* Supportive care in cancer : official journal of the Multinational Association of Supportive Care in Cancer, 2006. **14**(9): p. 890-900.
65. Sonis, S.T., *The pathobiology of mucositis.* Nature reviews. Cancer, 2004. **4**(4): p. 277-84.
66. Lin, C.C., C.Y. Liu, M.J. Chen, *et al., Profiles of circulating endothelial cells and serum cytokines during adjuvant chemoradiation in rectal cancer patients.* Clinical & translational oncology : official publication of the Federation of Spanish Oncology Societies and of the National Cancer Institute of Mexico, 2013. **15**(10): p. 855-60.
67. Sonis, S., L. Elting, D. Keefe, *et al., Unanticipated frequency and consequences of regimen-related diarrhoea in patients being treated with radiation or chemoradiation regimens for cancers of the head and neck or lung.* Supportive care in cancer : official journal of the Multinational Association of Supportive Care in Cancer, 2014.
68. Logan, R.M., A.M. Stringer, J.M. Bowen, *et al., The role of pro-inflammatory cytokines in cancer treatment-induced alimentary tract mucositis: pathobiology, animal models and cytotoxic drugs.* Cancer treatment reviews, 2007. **33**(5): p. 448-60.
69. Logan, R.M., R.J. Gibson, J.M. Bowen, *et al., Characterisation of mucosal changes in the alimentary tract following administration of irinotecan: implications for the pathobiology of mucositis.* Cancer chemotherapy and pharmacology, 2008. **62**(1): p. 33-41.
70. Keefe, D.M., J. Brealey, G.J. Goland, *et al., Chemotherapy for cancer causes apoptosis that precedes hypoplasia in crypts of the small intestine in humans.* Gut, 2000. **47**(5): p. 632-7.
71. Yarden, Y. and M.X. Sliwkowski, *Untangling the ErbB signalling network.* Nature reviews. Molecular cell biology, 2001. **2**(2): p. 127-37.
72. Chen, C.L., X. Yu, I.O. James, *et al., Heparin-binding EGF-like growth factor protects intestinal stem cells from injury in a rat model of necrotizing enterocolitis.* Laboratory investigation; a journal of technical methods and pathology, 2012. **92**(3): p. 331-44.

73. Masui, H., T. Kawamoto, J.D. Sato, *et al., Growth inhibition of human tumor cells in athymic mice by anti-epidermal growth factor receptor monoclonal antibodies.* Cancer research, 1984. **44**(3): p. 1002-7.
74. Normanno, N., C. Bianco, A. De Luca, *et al., Target-based agents against ErbB receptors and their ligands: a novel approach to cancer treatment.* Endocrine-related cancer, 2003. **10**(1): p. 1-21.
75. Sharma, S.V., D.W. Bell, J. Settleman, *et al., Epidermal growth factor receptor mutations in lung cancer.* Nature reviews. Cancer, 2007. **7**(3): p. 169-81.
76. Zandi, R., A.B. Larsen, P. Andersen, *et al., Mechanisms for oncogenic activation of the epidermal growth factor receptor.* Cellular signalling, 2007. **19**(10): p. 2013-23.
77. Mendelsohn, J., *Targeting the epidermal growth factor receptor for cancer therapy.* Journal of clinical oncology : official journal of the American Society of Clinical Oncology, 2002. **20**(18 Suppl): p. 1S-13S.
78. Liao, B.C., C.C. Lin, and J.C. Yang, *Second and third-generation epidermal growth factor receptor tyrosine kinase inhibitors in advanced nonsmall cell lung cancer.* Curr Opin Oncol, 2015. **27**(2): p. 94-101.
79. Herbst, R.S., D. Prager, R. Hermann, *et al., TRIBUTE: a phase III trial of erlotinib hydrochloride (OSI-774) combined with carboplatin and paclitaxel chemotherapy in advanced non-small-cell lung cancer.* Journal of clinical oncology : official journal of the American Society of Clinical Oncology, 2005. **23**(25): p. 5892-9.
80. Shepherd, F.A., J. Rodrigues Pereira, T. Ciuleanu, *et al., Erlotinib in previously treated non-small-cell lung cancer.* The New England journal of medicine, 2005. **353**(2): p. 123-32.
81. Takeda, M., I. Okamoto, and K. Nakagawa, *Pooled safety analysis of EGFR-TKI treatment for EGFR mutation-positive non-small cell lung cancer.* Lung Cancer, 2015. **88**(1): p. 74-9.
82. Loriot, Y., G. Perlemuter, D. Malka, *et al., Drug insight: gastrointestinal and hepatic adverse effects of molecular-targeted agents in cancer therapy.* Nature clinical practice. Oncology, 2008. **5**(5): p. 268-78.
83. Rasmussen, A.R., N.E. Viby, K.J. Hare, *et al., The intestinotrophic peptide, GLP-2, counteracts the gastrointestinal atrophy in mice induced by the epidermal growth factor receptor inhibitor, erlotinib, and cisplatin.* Dig Dis Sci, 2010. **55**(10): p. 2785-96.
84. Yusta, B., D. Holland, J.A. Koehler, *et al., ErbB signaling is required for the proliferative actions of GLP-2 in the murine gut.* Gastroenterology, 2009. **137**(3): p. 986-96.
85. Berlanga-Acosta, J., R.J. Playford, N. Mandir, *et al., Gastrointestinal cell proliferation and crypt fission are separate but complementary means of increasing tissue mass following infusion of epidermal growth factor in rats.* Gut, 2001. **48**(6): p. 803-7.
86. Opleta-Madsen, K., J. Hardin, and D.G. Gall, *Epidermal growth factor upregulates intestinal electrolyte and nutrient transport.* The American journal of physiology, 1991. **260**(6 Pt 1): p. G807-14.
87. Goodlad, R.A., K.B. Raja, T.J. Peters, *et al., Effects of urogastrone-epidermal growth factor on intestinal brush border enzymes and mitotic activity.* Gut, 1991. **32**(9): p. 994-8.

88. Dignass, A.U. and D.K. Podolsky, *Cytokine modulation of intestinal epithelial cell restitution: central role of transforming growth factor beta.* Gastroenterology, 1993. **105**(5): p. 1323-32.
89. Bowen, J.M., *Mechanisms of TKI-induced diarrhoea in cancer patients.* Current opinion in supportive and palliative care, 2013. **7**(2): p. 162-7.
90. Bowen, J.M., B.J. Mayo, E. Plews, *et al.*, *Determining the mechanisms of lapatinib-induced diarrhoea using a rat model.* Cancer Chemother Pharmacol, 2014. **74**(3): p. 617-27.
91. Gibson, R.J., J.M. Bowen, E. Alvarez, *et al.*, *Establishment of a single-dose irinotecan model of gastrointestinal mucositis.* Chemotherapy, 2007. **53**(5): p. 360-9.
92. Senderowicz, A.M., D. Headlee, S.F. Stinson, *et al.*, *Phase I trial of continuous infusion flavopiridol, a novel cyclin-dependent kinase inhibitor, in patients with refractory neoplasms.* J Clin Oncol, 1998. **16**(9): p. 2986-99.
93. Senderowicz, A.M., *Flavopiridol: the first cyclin-dependent kinase inhibitor in human clinical trials.* Invest New Drugs, 1999. **17**(3): p. 313-20.
94. Kahn, M.E., A. Senderowicz, E.A. Sausville, *et al.*, *Possible mechanisms of diarrhoeal side effects associated with the use of a novel chemotherapeutic agent, flavopiridol.* Clin Cancer Res, 2001. **7**(2): p. 343-9.
95. Hoda, M.R., M. Scharl, S.J. Keely, *et al.*, *Apical leptin induces chloride secretion by intestinal epithelial cells and in a rat model of acute chemotherapy-induced colitis.* Am J Physiol Gastrointest Liver Physiol, 2010. **298**(5): p. G714-21.
96. Huang, F.S., C.J. Kemp, J.L. Williams, *et al.*, *Role of epidermal growth factor and its receptor in chemotherapy-induced intestinal injury.* American journal of physiology. Gastrointestinal and liver physiology, 2002. **282**(3): p. G432-42.
97. Barrett, K.E. and S.J. Keely, *Chloride secretion by the intestinal epithelium: molecular basis and regulatory aspects.* Annual review of physiology, 2000. **62**: p. 535-72.
98. Dharmsathaphorn, K. and S.J. Pandol, *Mechanism of chloride secretion induced by carbachol in a colonic epithelial cell line.* The Journal of clinical investigation, 1986. **77**(2): p. 348-54.
99. Dharmsathaphorn, K., J. Cohn, and G. Beuerlein, *Multiple calcium-mediated effector mechanisms regulate chloride secretory responses in T84-cells.* The American journal of physiology, 1989. **256**(6 Pt 1): p. C1224-30.
100. Uribe, J.M., C.M. Gelbmann, A.E. Traynor-Kaplan, *et al.*, *Epidermal growth factor inhibits Ca(2+)-dependent Cl- transport in T84 human colonic epithelial cells.* The American journal of physiology, 1996. **271**(3 Pt 1): p. C914-22.
101. Keely, S.J. and K.E. Barrett, *ErbB2 and ErbB3 receptors mediate inhibition of calcium-dependent chloride secretion in colonic epithelial cells.* The Journal of biological chemistry, 1999. **274**(47): p. 33449-54.
102. Chow, J.Y., J.M. Uribe, and K.E. Barrett, *A role for protein kinase cepsilon in the inhibitory effect of epidermal growth factor on calcium-stimulated chloride secretion in human colonic epithelial cells.* The Journal of biological chemistry, 2000. **275**(28): p. 21169-76.
103. Deachapunya, C. and S. Poonyachoti, *Activation of chloride secretion by isoflavone genistein in endometrial epithelial cells.* Cellular physiology and biochemistry : international journal of experimental cellular physiology, biochemistry, and pharmacology, 2013. **32**(5): p. 1473-86.

104. Illek, B., H. Fischer, and T.E. Machen, *Alternate stimulation of apical CFTR by genistein in epithelia.* The American journal of physiology, 1996. **270**(1 Pt 1): p. C265-75.
105. Chen, P., L. Wang, B. Liu, *et al.*, *EGFR-targeted therapies combined with chemotherapy for treating advanced non-small-cell lung cancer: a meta-analysis.* European journal of clinical pharmacology, 2011. **67**(3): p. 235-43.
106. Crown, J.P., H.A. Burris, 3rd, F. Boyle, *et al.*, *Pooled analysis of diarrhoea events in patients with cancer treated with lapatinib.* Breast cancer research and treatment, 2008. **112**(2): p. 317-25.
107. Keefe, D.M. and R.J. Gibson, *Mucosal injury from targeted anti-cancer therapy.* Supportive care in cancer : official journal of the Multinational Association of Supportive Care in Cancer, 2007. **15**(5): p. 483-90.
108. Medina, P.J. and S. Goodin, *Lapatinib: a dual inhibitor of human epidermal growth factor receptor tyrosine kinases.* Clinical therapeutics, 2008. **30**(8): p. 1426-47.
109. Keisner, S.V. and S.R. Shah, *Pazopanib: the newest tyrosine kinase inhibitor for the treatment of advanced or metastatic renal cell carcinoma.* Drugs, 2011. **71**(4): p. 443-54.
110. van Erp, N.P., H. Gelderblom, and H.J. Guchelaar, *Clinical pharmacokinetics of tyrosine kinase inhibitors.* Cancer treatment reviews, 2009. **35**(8): p. 692-706.
111. Cusatis, G., V. Gregorc, J. Li, *et al.*, *Pharmacogenetics of ABCG2 and adverse reactions to gefitinib.* J Natl Cancer Inst, 2006. **98**(23): p. 1739-42.
112. Baker, D.E., *Loperamide: a pharmacological review.* Rev Gastroenterol Disord, 2007. **7 Suppl 3**: p. S11-8.
113. Thiagarajah, J.R., E.A. Ko, L. Tradtrantip, *et al.*, *Discovery and development of antisecretory drugs for treating diarrhoeal diseases.* Clin Gastroenterol Hepatol, 2014. **12**(2): p. 204-9.
114. Caci, E., A. Caputo, A. Hinzpeter, *et al.*, *Evidence for direct CFTR inhibition by CFTR(inh)-172 based on Arg347 mutagenesis.* Biochem J, 2008. **413**(1): p. 135-42.
115. Ko, E.A., B.J. Jin, W. Namkung, *et al.*, *Chloride channel inhibition by a red wine extract and a synthetic small molecule prevents rotaviral secretory diarrhoea in neonatal mice.* Gut, 2014. **63**(7): p. 1120-9.
116. Crutchley, R.D., J. Miller, and K.W. Garey, *Crofelemer, a novel agent for treatment of secretory diarrhoea.* The Annals of pharmacotherapy, 2010. **44**(5): p. 878-84.
117. Cottreau, J., A. Tucker, R. Crutchley, *et al.*, *Crofelemer for the treatment of secretory diarrhoea.* Expert review of gastroenterology & hepatology, 2012. **6**(1): p. 17-23.
118. Tradtrantip, L., W. Namkung, and A.S. Verkman, *Crofelemer, an antisecretory antidiarrhoeal proanthocyanidin oligomer extracted from Croton lechleri, targets two distinct intestinal chloride channels.* Molecular pharmacology, 2010. **77**(1): p. 69-78.
119. Holodniy, M., J. Koch, M. Mistal, *et al.*, *A double blind, randomized, placebo-controlled phase II study to assess the safety and efficacy of orally administered SP-303 for the symptomatic treatment of diarrhoea in patients with AIDS.* The American journal of gastroenterology, 1999. **94**(11): p. 3267-73.
120. DiCesare, D., H.L. DuPont, J.J. Mathewson, *et al.*, *A double blind, randomized, placebo-controlled study of SP-303 (Provir) in the symptomatic treatment of*

acute diarrhoea among travelers to Jamaica and Mexico. The American journal of gastroenterology, 2002. **97**(10): p. 2585-8.
121. Mangel, A.W. and P. Chaturvedi, *Evaluation of crofelemer in the treatment of diarrhoea-predominant irritable bowel syndrome patients.* Digestion, 2008. **78**(4): p. 180-6.
122. Keefe, D. and L. Anthony, *Tyrosine kinase inhibitors and gut toxicity: a new era in supportive care.* Current opinion in supportive and palliative care, 2008. **2**(1): p. 19-21.
123. Engelman, J.A., K. Zejnullahu, C.M. Gale, *et al., PF00299804, an irreversible pan-ERBB inhibitor, is effective in lung cancer models with EGFR and ERBB2 mutations that are resistant to gefitinib.* Cancer research, 2007. **67**(24): p. 11924-32.
124. Van Sebille, Y.Z., R.J. Gibson, H.R. Wardill, *et al., Gastrointestinal toxicities of first and second-generation small molecule human epidermal growth factor receptor tyrosine kinase inhibitors in advanced nonsmall cell lung cancer.* Curr Opin Support Palliat Care, 2016.
125. Lacouture, M.E., D.M. Keefe, S. Sonis, *et al., A phase II study (ARCHER 1042) to evaluate prophylactic treatment of dacomitinib-induced dermatologic and gastrointestinal adverse events in advanced non-small-cell lung cancer.* Ann Oncol, 2016. **27**(9): p. 1712-8.
126. Bowen, J.M., R.J. Gibson, A.G. Cummins, *et al., Intestinal mucositis: the role of the Bcl-2 family, p53 and caspases in chemotherapy-induced damage.* Supportive care in cancer : official journal of the Multinational Association of Supportive Care in Cancer, 2006. **14**(7): p. 713-31.
127. Wardill, H.R., R.J. Gibson, Y.Z. Van Sebille, *et al., A novel in vitro platform for the study of SN38-induced mucosal damage and the development of Toll-like receptor 4-targeted therapeutic options.* Exp Biol Med (Maywood), 2016.
128. Howarth, G.S., G.L. Francis, J.C. Cool, *et al., Milk growth factors enriched from cheese whey ameliorate intestinal damage by methotrexate when administered orally to rats.* J Nutr, 1996. **126**(10): p. 2519-30.
129. Wardill, H.R., R.J. Gibson, Y.Z. Van Sebille, *et al., Irinotecan-Induced Gastrointestinal Dysfunction and Pain Are Mediated by Common TLR4-Dependent Mechanisms.* Mol Cancer Ther, 2016. **15**(6): p. 1376-86.
130. Livak, F. and D.G. Schatz, *Alternative splicing of rearranged T cell receptor delta sequences to the constant region of the alpha locus.* Proc Natl Acad Sci U S A, 1998. **95**(10): p. 5694-9.
131. Giri, N., J.C. Masters, A. Plotka, *et al., Investigation of the impact of hepatic impairment on the pharmacokinetics of dacomitinib.* Invest New Drugs, 2015. **33**(4): p. 931-41.
132. Hare, K.J., B. Hartmann, H. Kissow, *et al., The intestinotrophic peptide, glp-2, counteracts intestinal atrophy in mice induced by the epidermal growth factor receptor inhibitor, gefitinib.* Clin Cancer Res, 2007. **13**(17): p. 5170-5.
133. Bowen, J.M., *Development of the rat model of lapatinib-induced diarrhoea.* Scientifica (Cairo), 2014. **2014**: p. 194185.
134. Peters, S., S. Zimmermann, and A.A. Adjei, *Oral epidermal growth factor receptor tyrosine kinase inhibitors for the treatment of non-small cell lung cancer: comparative pharmacokinetics and drug-drug interactions.* Cancer Treat Rev, 2014. **40**(8): p. 917-26.

135. Velandia-Romero, M.L., M.A. Calderon-Pelaez, and J.E. Castellanos, *In Vitro Infection with Dengue Virus Induces Changes in the Structure and Function of the Mouse Brain Endothelium.* PLoS One, 2016. **11**(6): p. e0157786.
136. Wardill, H.R., J.M. Bowen, Y.Z. Van Sebille, *et al.*, *TLR4-dependent claudin-1 internalization and secretagogue-mediated chloride secretion regulate irinotecan-induced diarrhoea.* Mol Cancer Ther, 2016.
137. Nakao, T., N. Kurita, M. Komatsu, *et al.*, *Irinotecan injures tight junction and causes bacterial translocation in rat.* J Surg Res, 2012. **173**(2): p. 341-7.
138. Schmitz, H., M. Fromm, C.J. Bentzel, *et al.*, *Tumor necrosis factor-alpha (TNFalpha) regulates the epithelial barrier in the human intestinal cell line HT-29/B6.* J Cell Sci, 1999. **112 (Pt 1)**: p. 137-46.
139. Kim, D.W., E.B. Garon, A. Jatoi, *et al.*, *Impact of a planned dose interruption of dacomitinib in the treatment of advanced non-small-cell lung cancer (ARCHER 1042).* Lung Cancer, 2017. **106**: p. 76-82.
140. Jankowitz, R.C., J. Abraham, A.R. Tan, *et al.*, *Safety and efficacy of neratinib in combination with weekly paclitaxel and trastuzumab in women with metastatic HER2positive breast cancer: an NSABP Foundation Research Program phase I study.* Cancer Chemother Pharmacol, 2013. **72**(6): p. 1205-12.
141. Pessi, M.A., N. Zilembo, E.R. Haspinger, *et al.*, *Targeted therapy-induced diarrhoea: A review of the literature.* Crit Rev Oncol Hematol, 2014. **90**(2): p. 165-79.
142. Andreyev, J., P. Ross, C. Donnellan, *et al.*, *Guidance on the management of diarrhoea during cancer chemotherapy.* Lancet Oncol, 2014. **15**(10): p. e447-60.
143. Gao, J.J., M. Tan, P.R. Pohlmann, *et al.*, *HALT-D: A Phase II Evaluation of Crofelemer for the Prevention and Prophylaxis of Diarrhoea in Patients With Breast Cancer on Pertuzumab-Based Regimens.* Clin Breast Cancer, 2016.
144. Ather, F., H. Hamidi, M.S. Fejzo, *et al.*, *Dacomitinib, an irreversible Pan-ErbB inhibitor significantly abrogates growth in head and neck cancer models that exhibit low response to cetuximab.* PloS one, 2013. **8**(2): p. e56112.
145. Sahoo, P.K., S. Soltani, A.K.C. Wong, *et al.*, *A Survey of Thresholding Techniques.* Computer Vision Graphics and Image Processing, 1988. **41**(2): p. 233-260.
146. Mahmoudi, L. and A. El Zaart, *A Survey of Entropy Image Thresholding Techniques.* 2012 2nd International Conference on Advances in Computational Tools for Engineering Applications (Actea), 2012: p. 204-209.
147. Dharmsathaphorn, K. and S.J. Pandol, *Mechanism of chloride secretion induced by carbachol in a colonic epithelial cell line.* J Clin Invest, 1986. **77**(2): p. 348-54.
148. Kachintorn, U., M. Vajanaphanich, A.E. Traynor-Kaplan, *et al.*, *Activation by calcium alone of chloride secretion in T84 epithelial cells.* Br J Pharmacol, 1993. **109**(2): p. 510-7.
149. Van Sebille, Y.Z., R.J. Gibson, H.R. Wardill, *et al.*, *Dacomitinib-induced diarrhoea is associated with altered gastrointestinal permeability and disruption in ileal histology in rats.* Int J Cancer, 2017.
150. Van Sebille, Y.Z.A., R.J. Gibson, H.R. Wardill, *et al.*, *Dacomitinib-induced diarrhoea is associated with altered gastrointestinal permeability and disruption in ileal histology in rats.* Int J Cancer, 2017. **140**(12): p. 2820-2829.
151. Jin, B.J., J.R. Thiagarajah, and A.S. Verkman, *Convective washout reduces the antidiarrhoeal efficacy of enterocyte surface-targeted antisecretory drugs.* J Gen Physiol, 2013. **141**(2): p. 261-72.

152. Abbas, R., B.A. Hug, C. Leister, *et al., A double-blind, randomized, multiple-dose, parallel-group study to characterize the occurrence of diarrhoea following two different dosing regimens of neratinib, an irreversible pan-ErbB receptor tyrosine kinase inhibitor.* Cancer Chemother Pharmacol, 2012. **70**(1): p. 191-9.
153. McCole, D.F., G. Rogler, N. Varki, *et al., Epidermal growth factor partially restores colonic ion transport responses in mouse models of chronic colitis.* Gastroenterology, 2005. **129**(2): p. 591-608.
154. Khan, N. and A.R. Asif, *Transcriptional regulators of claudins in epithelial tight junctions.* Mediators Inflamm, 2015. **2015**: p. 219843.
155. Gonzalez-Mariscal, L., R. Tapia, and D. Chamorro, *Crosstalk of tight junction components with signaling pathways.* Biochim Biophys Acta, 2008. **1778**(3): p. 729-56.
156. Wardill, H.R., J.M. Bowen, N. Al-Dasooqi, *et al., Irinotecan disrupts tight junction proteins within the gut : implications for chemotherapy-induced gut toxicity.* Cancer Biol Ther, 2014. **15**(2): p. 236-44.
157. Blijlevens, N.M., J.P. Donnelly, and B.E. de Pauw, *Prospective evaluation of gut mucosal barrier injury following various myeloablative regimens for haematopoietic stem cell transplant.* Bone Marrow Transplant, 2005. **35**(7): p. 707-11.
158. Keefe, D.M., A.G. Cummins, B.M. Dale, *et al., Effect of high-dose chemotherapy on intestinal permeability in humans.* Clin Sci (Lond), 1997. **92**(4): p. 385-9.
159. Wardill, H.R., R.M. Logan, J.M. Bowen, *et al., Tight junction defects are seen in the buccal mucosa of patients receiving standard dose chemotherapy for cancer.* Support Care Cancer, 2016. **24**(4): p. 1779-88.
160. Monteiro, A.C. and C.A. Parkos, *Intracellular mediators of JAM-A-dependent epithelial barrier function.* Ann N Y Acad Sci, 2012. **1257**: p. 115-24.
161. Schulzke, J.D., S. Ploeger, M. Amasheh, *et al., Epithelial tight junctions in intestinal inflammation.* Ann N Y Acad Sci, 2009. **1165**: p. 294-300.
162. Blijlevens, N.M., J.P. Donnelly, and B.E. De Pauw, *Mucosal barrier injury: biology, pathology, clinical counterparts and consequences of intensive treatment for haematological malignancy: an overview.* Bone Marrow Transplant, 2000. **25**(12): p. 1269-78.
163. van der Velden, W.J., A.H. Herbers, T. Feuth, *et al., Intestinal damage determines the inflammatory response and early complications in patients receiving conditioning for a stem cell transplantation.* PLoS One, 2010. **5**(12): p. e15156.
164. Al-Dasooqi, N., S.T. Sonis, J.M. Bowen, *et al., Emerging evidence on the pathobiology of mucositis.* Supportive care in cancer : official journal of the Multinational Association of Supportive Care in Cancer, 2013. **21**(7): p. 2075-83.
165. Poon, K.L., X. Wang, S.G. Lee, *et al., Editor's Highlight: Transgenic Zebrafish Reporter Lines as Alternative In Vivo Organ Toxicity Models.* Toxicol Sci, 2017. **156**(1): p. 133-148.
166. Wallace, K.N., S. Akhter, E.M. Smith, *et al., Intestinal growth and differentiation in zebrafish.* Mech Dev, 2005. **122**(2): p. 157-73.
167. Noaillac-Depeyre, J. and N. Gas, *Electron microscopic study on gut epithelium of the tench (Tinca tinca L.) with respect to its absorptive functions.* Tissue Cell, 1976. **8**(3): p. 511-30.
168. Wang, Z., J. Du, S.H. Lam, *et al., Morphological and molecular evidence for functional organization along the rostrocaudal axis of the adult zebrafish intestine.* BMC Genomics, 2010. **11**: p. 392.

169. Umezawa, T., T. Kiba, K. Numata, *et al.*, *Comparisons of the pharmacokinetics and the leukopenia and thrombocytopenia grade after administration of irinotecan and 5-fluorouracil in combination to rats.* Anticancer Res, 2000. **20**(6B): p. 4235-42.
170. Araki, E., M. Ishikawa, M. Iigo, *et al.*, *Relationship between development of diarrhoea and the concentration of SN-38, an active metabolite of CPT-11, in the intestine and the blood plasma of athymic mice following intraperitoneal administration of CPT-11.* Jpn J Cancer Res, 1993. **84**(6): p. 697-702.
171. Pedroso, S.H., A.T. Vieira, R.W. Bastos, *et al.*, *Evaluation of mucositis induced by irinotecan after microbial colonization in germ-free mice.* Microbiology, 2015. **161**(10): p. 1950-60.
172. Wind, S., D. Schnell, T. Ebner, *et al.*, *Clinical Pharmacokinetics and Pharmacodynamics of Afatinib.* Clin Pharmacokinet, 2017. **56**(3): p. 235-250.
173. Kimmel, C.B., W.W. Ballard, S.R. Kimmel, *et al.*, *Stages of embryonic development of the zebrafish.* Dev Dyn, 1995. **203**(3): p. 253-310.
174. Renshaw, S.A., C.A. Loynes, D.M. Trushell, *et al.*, *A transgenic zebrafish model of neutrophilic inflammation.* Blood, 2006. **108**(13): p. 3976-8.
175. Collymore, C., S. Rasmussen, and R.J. Tolwani, *Gavaging adult zebrafish.* J Vis Exp, 2013(78).
176. White, R.M., A. Sessa, C. Burke, *et al.*, *Transparent adult zebrafish as a tool for in vivo transplantation analysis.* Cell Stem Cell, 2008. **2**(2): p. 183-9.
177. Chen, Y.H., Y.T. Lee, C.C. Wen, *et al.*, *Modeling pegylated liposomal doxorubicin-induced hand-foot syndrome and intestinal mucositis in zebrafish.* Onco Targets Ther, 2014. **7**: p. 1169-75.
178. Santoriello, C. and L.I. Zon, *Hooked! Modeling human disease in zebrafish.* J Clin Invest, 2012. **122**(7): p. 2337-43.
179. Matsui, H., O. Shimokawa, T. Kaneko, *et al.*, *The pathophysiology of non-steroidal anti-inflammatory drug (NSAID)-induced mucosal injuries in stomach and small intestine.* J Clin Biochem Nutr, 2011. **48**(2): p. 107-11.
180. Takeda, M. and K. Nakagawa, *Toxicity profile of epidermal growth factor receptor tyrosine kinase inhibitors in patients with epidermal growth factor receptor gene mutation-positive lung cancer.* Mol Clin Oncol, 2017. **6**(1): p. 3-6.
181. Cai, Z., J. Yang, X. Shu, *et al.*, *Chemotherapy-associated hepatotoxicity in colorectal cancer.* J BUON, 2014. **19**(2): p. 350-6.
182. Bala, V., S. Rao, and C.A. Prestidge, *Facilitating gastrointestinal solubilisation and enhanced oral absorption of SN38 using a molecularly complexed silica-lipid hybrid delivery system.* Eur J Pharm Biopharm, 2016. **105**: p. 32-9.
183. Lobert, V.H., D. Mouradov, and J.K. Heath, *Focusing the Spotlight on the Zebrafish Intestine to Illuminate Mechanisms of Colorectal Cancer.* Adv Exp Med Biol, 2016. **916**: p. 411-37.
184. Poon, K.L., X. Wang, A.S. Ng, *et al.*, *Humanizing the zebrafish liver shifts drug metabolic profiles and improves pharmacokinetics of CYP3A4 substrates.* Arch Toxicol, 2017. **91**(3): p. 1187-1197.
185. Patel, T.S., R.D. Crutchley, A.M. Tucker, *et al.*, *Crofelemer for the treatment of chronic diarrhoea in patients living with HIV/AIDS.* HIV/AIDS, 2013. **5**: p. 153-62.
186. Xavier, R.J. and D.K. Podolsky, *Unravelling the pathogenesis of inflammatory bowel disease.* Nature, 2007. **448**(7152): p. 427-34.
187. Sakuraba, A., S. Motoya, K. Watanabe, *et al.*, *An open-label prospective randomized multicenter study shows very rapid remission of ulcerative colitis by*

intensive granulocyte and monocyte adsorptive apheresis as compared with routine weekly treatment. Am J Gastroenterol, 2009. **104**(12): p. 2990-5.
188. Wardill, H.R. and J.M. Bowen, *Chemotherapy-induced mucosal barrier dysfunction: an updated review on the role of intestinal tight junctions.* Current opinion in supportive and palliative care, 2013. **7**(2): p. 155-61.
189. Eisenhut, M., *Changes in ion transport in inflammatory disease.* J Inflamm (Lond), 2006. **3**: p. 5.
190. Stelzner, M., S. Somasundaram, and T. Khakberdiev, *Systemic effects of acute terminal ileitis on uninflamed gut aggravate bile acid malabsorption.* J Surg Res, 2001. **99**(2): p. 359-64.
191. Elting, L.S., Y.C. Chang, P. Parelkar, *et al.*, *Risk of oral and gastrointestinal mucosal injury among patients receiving selected targeted agents: a meta-analysis.* Support Care Cancer, 2013. **21**(11): p. 3243-54.
192. Clarke, L.L., *A guide to Ussing chamber studies of mouse intestine.* Am J Physiol Gastrointest Liver Physiol, 2009. **296**(6): p. G1151-66.
193. Priyamvada, S., R. Gomes, R.K. Gill, *et al.*, *Mechanisms Underlying Dysregulation of Electrolyte Absorption in Inflammatory Bowel Disease-Associated Diarrhoea.* Inflamm Bowel Dis, 2015. **21**(12): p. 2926-35.
194. Teixeira, A.G., L. Stephens, T.J. Divers, *et al.*, *Effect of crofelemer extract on severity and consistency of experimentally induced enterotoxigenic Escherichia coli diarrhoea in newborn Holstein calves.* J Dairy Sci, 2015. **98**(11): p. 8035-43.
195. Miguel, J.C., A.A. Maxwell, J.J. Hsieh, *et al.*, *Epidermal growth factor suppresses intestinal epithelial cell shedding through a MAPK-dependent pathway.* J Cell Sci, 2017. **130**(1): p. 90-96.
196. Navis, A., L. Marjoram, and M. Bagnat, *Cftr controls lumen expansion and function of Kupffer's vesicle in zebrafish.* Development, 2013. **140**(8): p. 1703-12.
197. Vocke, K., K. Dauner, A. Hahn, *et al.*, *Calmodulin-dependent activation and inactivation of anoctamin calcium-gated chloride channels.* J Gen Physiol, 2013. **142**(4): p. 381-404.
198. Mimeault, M. and S.K. Batra, *Emergence of zebrafish models in oncology for validating novel anticancer drug targets and nanomaterials.* Drug Discov Today, 2013. **18**(3-4): p. 128-40.
199. Lin, S., Y. Zhao, T. Xia, *et al.*, *High content screening in zebrafish speeds up hazard ranking of transition metal oxide nanoparticles.* ACS Nano, 2011. **5**(9): p. 7284-95.
200. Mathias, J.R., M.T. Saxena, and J.S. Mumm, *Advances in zebrafish chemical screening technologies.* Future Med Chem, 2012. **4**(14): p. 1811-22.
201. Wiley, D.S., S.E. Redfield, and L.I. Zon, *Chemical screening in zebrafish for novel biological and therapeutic discovery.* Methods Cell Biol, 2017. **138**: p. 651-679.
202. Cheesman, S.E., J.T. Neal, E. Mittge, *et al.*, *Epithelial cell proliferation in the developing zebrafish intestine is regulated by the Wnt pathway and microbial signaling via Myd88.* Proc Natl Acad Sci U S A, 2011. **108 Suppl 1**: p. 4570-7.

Appendix 1: Publications arising from this thesis

This thesis was written by publication. All chapters are in their **original** format, with the exception of spelling changes to ensure consistent English spelling, and references. Here, pdf files of published papers are included.

EDITORIAL

Gastrointestinal toxicities of first and second-generation small molecule human epidermal growth factor receptor tyrosine kinase inhibitors in advanced nonsmall cell lung cancer

Ysabella Z.A. Van Sebille[a], Rachel J. Gibson[b], Hannah R. Wardill[a], and Joanne M. Bowen[a]

INTRODUCTION

Lung cancer remains the leading cause of cancer-related death worldwide, with nonsmall cell lung cancer (NSCLC) representing 85% of all lung cancer diagnoses [1,2]. Platinum-based chemotherapy is recommended as standard first-line treatment, however, the objective response rate is modest and recurrence eventually occurs for most patients [3]. The landscape of NSCLC therapeutics has changed over the past decade in response to discovery that many tumours overexpress the human epidermal growth factor receptor (HER) family. This has resulted in the introduction of small molecule HER tyrosine kinase inhibitors (TKIs) for the treatment of NSCLC [4]. Many new HER TKIs have since emerged, moving from single HER targets (primarily HER1), such as gefitinib and erlotinib to pan-HER targets such as dacomitinib and afatinib. Additionally, these small molecule therapeutics have moved from first to second-generation agents; now resistant to the acquired mutations of the first-generation class of drugs, such as the T790 mutation. It was originally anticipated with the advent of these targeted therapies that patients would experience less toxicity than traditional cytotoxic therapies. Although undoubtedly these new agents have improved therapy significantly, they also have downsides, namely, causing unexpected adverse event profiles. This editorial will focus on the predominant HER TKI-related side-effect, namely diarrhoea, addressing the change in the gastrointestinal toxicity profiles seen from the single HER-targeted drugs to the second-generation pan HER-targeted drugs using gefitinib and dacomitinib as examples.

HUMAN EPIDERMAL GROWTH FACTOR RECEPTOR TYROSINE KINASE INHIBITORS

TKIs were first described in 1988, and specifically inhibited the HER1 [5]. The activity of the HER receptors is dictated by the expression of their ligands, which can be classified into three groups: those binding specifically to HER1; those exhibiting dual specificity binding to HER1 and HER4; and neuregulins subclassified upon their capacity to bind HER3 and HER4 or only HER4 [6,7]. Currently, no ligand has been identified to be specific for HER2, however, it is understood that this receptor forms heterodimers with the other HER receptors. Upon ligand binding to the HER receptor, heterodimerization or homodimerization of receptors occurs, leading to a cascade of signalling pathways [8]. Among the pathways activated are ERK, and PI3K/Akt. Pathway activation leads to changes in protein functions and activation of gene transcription [8–10]. Briefly, these complex signalling pathways result in interactions with apoptotic signalling, cell proliferation, differentiation, migration, and survival, which can promote tumourigenesis [9,11].

DIARRHOEA

For oral agents administered daily, toxicities of any grade are extremely important as they can determine compliance. Despite this, adverse events remain largely ignored, with the emphasis placed on efficacy. Diarrhoea is a severe, dose-limiting, and the most common adverse event of small molecule HER TKI treatment [12]. HER TKI-induced diarrhoea can become evident as early as 2–3 days after initiation of treatment, and given the daily and

[a]School of Medicine, University of Adelaide and [b]Division of Health Sciences, University of South Australia, Adelaide, Australia

Correspondence to Ysabella Z.A. Van Sebille, School of Medicine, University of Adelaide, North Terrace, Adelaide 5005, Australia.
Tel: +61 8 83133787; e-mail: ysabella.vansebille@adelaide.edu.au

Curr Opin Support Palliat Care 2016, 10:152–156
DOI:10.1097/SPC.0000000000000210

Table 1. Diarrhoea grading scale

Grade 1	Grade 2	Grade 3	Grade 4	Grade 5
Increase of less than four stools over baseline	Increase of four to six stools over baseline; i.v. fluids <24 h	Increase of at least seven stools over baseline; incontinence; i.v. fluids ≥24 h; hospitalization indicated; limits activities of daily living	Life-threatening consequences; urgent; intervention indicated	Death

i.v., intravenous.

continuous manner of HER TKI treatment, can persist for substantial periods of time, significantly impacting on patients' quality of life, resulting in poor compliance and therapy interruption [13]. The severity of diarrhoea is most commonly graded using the National Cancer Institute's Common Terminology Criteria for Adverse Events (Table 1). Grade 3 (severe) diarrhoea can result in fluid and electrolyte loss, which then can lead to dehydration, electrolyte imbalances, and renal insufficiency. Additionally, alterations in gastrointestinal transit and digestion can lead to nutritional deficiencies that can negatively impact the quality of life of patients. Furthermore, given that therapy with HER TKIs tends to continue for more than 10 months, grade 1–2 toxicities should be considered equally important, and appropriate management of diarrhoea is essential.

MECHANISMS

The underlying mechanism(s) of HER TKI-induced diarrhoea remain poorly understood. Despite a similar clinical manifestation to traditional chemotherapy treatment-induced diarrhoea, toxicities associated with targeted therapies are hypothesized to have different pathogenic mechanisms [14]. Preclinical studies using targeted therapies have shown diarrhoea is not correlative with intestinal mucosal damage [15], suggestive of pathogenic mechanisms that differs to traditional cytotoxic cancer treatments. Gaining significant momentum is the hypothesis that HER TKI-induced diarrhoea is a result of excess chloride secretion based on the established role of HERs in regulating ion conductance channels in the colon [16]. Currently, treatment for cancer therapy-induced diarrhoea is limited; coupled with increasing cancer prevalence, it is clear that the need for a fuller understanding of the mechanism(s), and subsequently therapeutic targets will not abate. Ultimately, such an understanding should eventually point to safer, more targeted and more effective therapies for cancer sufferers.

FIRST-GENERATION HUMAN EPIDERMAL GROWTH FACTOR RECEPTOR TYROSINE KINASE INHIBITOR: GEFITINIB

Gefitinib (Iressa; AstraZeneca, London, UK, http://www.astrazeneca.com) was the first oral HER TKI approved in the United States. Gefitinib reversibly binds to the ATP-binding pocket of the tyrosine kinase domain of HER1 subsequently inhibiting kinase-dependent signal transduction [17–19]. Gefitinib has demonstrated benefit in terms of response rate and time to progression in adults with metastatic NSCLC who have activating HER1 mutations [20–22]. However, results from multiple clinical trials have demonstrated that between 25 and 55% of patients, receiving gefitinib monotherapy, develop diarrhoea (Table 2).

SECOND-GENERATION HUMAN EPIDERMAL GROWTH FACTOR RECEPTOR TYROSINE KINASE INHIBITOR: DACOMITINIB

Resistance to reversible HER1 TKIs such as gefitinib has increased, leading to the development of novel target-based therapies such as dacomitinib for the treatment of NSCLC harbouring exon 19 deletions or exon 21 (L858R) mutations [35–37]. Conventional HER TKIs such as gefitinib are reversible: they competitively bind to the HER1 tyrosine kinase domain [38]. However, the simultaneous activation of different HER family members through dynamic hetero and homodimerization can compromise the therapeutic efficacy by inhibition of a single receptor [39]. Dacomitinib (PF- 00299804, Pfizer) was developed to irreversibly (covalently) bind to the ATP domain of each of the three kinase-active members of the HER family (HER1, HER2, and HER4) effectively inactivating them [40]. Subsequently, signal transduction pathways implicated in the proliferation and survival of cancer cells are blocked [41]. Dacomitinib has shown significant therapeutic efficacy in NSCLC, specifically to tumours that have not previously responded to conventional single receptor inhibitors, and also against tumours with

Table 2. Clinical trials of gefitinib

Study	Experimental design	Diarrhoea (all grades, %)	Diarrhoea grades 3–4 (%)
Thatcher *et al.*, 2005 [23]	NSCLC Phase III ($n=1688$)	27	3
Sun *et al.*, 2012 [24]	NSCLC Phase III ($n=135$)	26.5	0
Cufer *et al.*, 2006 [25]	NSCLC Phase II ($n=140$)	26.5	2.9
Kim *et al.*, 2008 [26]	NSCLC Phase III ($n=1466$)	35	2.5
Lee *et al.*, 2010 [27]	NSCLC Phase III ($n=161$)	25.9	1.2
Mok *et al.*, 2009 [28]	NSCLC Phase III ($n=1217$)	46.6	3.8
Maemondo *et al.*, 2010 [29]	NSCLC Phase III ($n=161$)	34.2	0.9
Goss *et al.*, 2009 [30]	NSCLC Phase II ($n=201$)	51	3
Morère *et al.*, 2010 [31]	NSCLC Phase II ($n=128$)	28	5
Mitsudomi *et al.*, 2010 [32]	NSCLC Phase III ($n=117$)	54	1.1
Zhang *et al.*, 2012 [33]	NSCLC Phase III ($n=298$)	25	0
Crinò *et al.*, 2008 [34]	NSCLC Phase II ($n=196$)	25.5	4.3

NSCLC, nonsmall cell lung cancer.

mutations developed for acquired resistance of targeted therapies [37–39]. Dacomitinib is currently in phase III clinical trials, and the most commonly reported adverse event among all trials has been diarrhoea, commonly resulting in dose reductions and patient withdrawal from clinical trials [38,39,42–44] (Table 3).

CONCLUSION

Over the past decade, therapies for advanced NSCLC have significantly changed with the development of small molecule TKIs moving from single to pan-HER targets. The median percentage of patients developing diarrhoea from gefitinib is 27.5%, with a median of 2.5% developing grade 3 or higher diarrhoea; compared to a median of 74% of patients developing diarrhoea from dacomitinib, with a median of 12% developing grade 3 or higher. Using gefitinib and dacomitinib as examples, it is clear that second-generation, pan-HER TKIs induce diarrhoea in a higher proportion of patients, and to a worse degree than first-generation single-HER TKIs. The HER family of receptors are mainly expressed on cells of epithelial origin, including those of the gastrointestinal tract, and inhibitors of the HER pathway are therefore associated with gastrointestinal side-effects, with diarrhoea constituting the most frequent. Perhaps, the increased incidence and worse diarrhoea seen with pan-HER TKIs vs. single-HER TKIs suggests that other members of the HER family, and not only HER1 are important in the mechanism(s) of HER TKI-induced diarrhoea. Although understanding of the role of HER1 in growth and repair of the gastrointestinal tract (GIT) is well understood, little is known of the role of other HER receptors in GIT homeostasis.

Dacomitinib is a novel HER family blocker that has demonstrated anticancer activity in Phase II and III studies in NSCLC patients whose tumours

Table 3. Clinical trials of dacomitinib

Study	Experimental design	Diarrhoea (all grades, %)	Diarrhoea grades 3–4 (%)
Jänne *et al.*, 2011 [45]	NSCLC Phase I ($n=121$)	66.7	11
Reckamp *et al.*, 2014 [44]	NSCLC Phase II ($n=66$)	84.8	12.1
Abdul Razak *et al.*, 2013 [42]	NSCLC Phase II ($n=69$)	84.1	15.9
Ramalingam *et al.*, 2012[46]	NSCLC Phase II ($n=94$)	73.1	11.8
Takahashi *et al.*, 2012 [39]	NSCLC Phase I ($n=13$)	92	0
Ruiz-Garcia *et al.*, 2013 [47]	NSCLC Phase I ($n=14$)	14	0
Ramalingam *et al.*, 2014[48]	NSCLC Phase III ($n=878$)	72	12
Jänne *et al.*, 2016 [49]	NSCLC Phase I ($n=70$)	74	16
Ellis *et al.*, 2014 [50]	NSCLC Phase III ($n=720$)	78	13

NSCLC, nonsmall cell lung cancer.

harbour HER mutations. Gefitinib is currently the standard of care for these patients as first-line treatment. Following positive clinical trial data, dacomitinib may replace gefitinib as the first-line choice of treatment for epidermal growth factor receptor (EGFR) mutation-positive advanced NSCLC patients. Given the aforementioned concerns associated with dacomitinib-induced diarrhoea, education on the frequency of HER TKI-associated diarrhoea, as well as early diagnosis, timely management and reassessment and close patient follow-up, will help to prevent adverse event aggravation, dose reductions, or therapy discontinuation, thus encouraging patient compliance and allowing patients to obtain the maximum therapeutic benefit from this novel agent.

Acknowledgements

None.

Financial support and sponsorship

None.

Conflicts of interest

There are no conflicts of interest.

REFERENCES AND RECOMMENDED READING

Papers of particular interest, published within the annual period of review, have been highlighted as:
- ■ of special interest
- ■■ of outstanding interest

1. Siegel R, Ma J, Zou Z, *et al.* Cancer statistics, 2014. CA Cancer J Clin 2014; 64:9–29.
2. Peters S, Adjei AA, Gridelli C, *et al.* Metastatic nonsmall-cell lung cancer (NSCLC): ESMO Clinical Practice Guidelines for diagnosis, treatment and follow-up. Ann Oncol 2012; (23 Suppl 7):vii56–vii64.
3. Ettinger DS, Akerley W, Borghaei H, *et al.* Nonsmall cell lung cancer. J Natl Compr Canc Netw 2012; 10:1236–1271.
4. Chan BA, Hughes BG. Targeted therapy for nonsmall cell lung cancer: current standards and the promise of the future. Transl Lung Cancer Res 2015; 4:36–54.
5. Yaish P, Gazit A, Gilon C, *et al.* Blocking of EGF-dependent cell proliferation by EGF receptor kinase inhibitors. Science 1988; 242:933–935.
6. Pinkas-Kramarski R, Alroy I, Yarden Y. ErbB receptors and EGF-like ligands: cell lineage determination and oncogenesis through combinatorial signaling. J Mammary Gland Biol Neoplasia 1997; 2:97–107.
7. Dent P, Yacoub A, Contessa J, *et al.* Stress and radiation-induced activation of multiple intracellular signaling pathways. Radiat Res 2003; 159:283–300.
8. McCole DF, Barrett KE. Decoding epithelial signals: critical role for the epidermal growth factor receptor in controlling intestinal transport function. Acta Physiol 2009; 195:149–159.
9. Henson ES, Gibson SB. Surviving cell death through epidermal growth factor (EGF) signal transduction pathways: implications for cancer therapy. Cell Signal 2006; 18:2089–2097.
10. Paul G, Marchelletta RR, McCole DF, *et al.* Interferon-gamma alters downstream signaling originating from epidermal growth factor receptor in intestinal epithelial cells: functional consequences for ion transport. J Biol Chem 2012; 287:2144–2155.
11. Ayyappan S, Prabhakar D, Sharma N. Epidermal growth factor receptor (EGFR)-targeted therapies in esophagogastric cancer. Anticancer Res 2013; 33:4139–4155.
12. Gibson RJ, Stringer AM. Chemotherapy-induced diarrhoea. Curr Opin Support Palliat Care 2009; 3:31–35.
13. Burstein HJ, Sun Y, Dirix LY, *et al.* Neratinib, an irreversible ErbB receptor tyrosine kinase inhibitor, in patients with advanced ErbB2-positive breast cancer. J Clin Oncol 2010; 28:1301–1307.
14. Keefe DM, Bateman EH. Tumor control versus adverse events with targeted anticancer therapies. Nat Rev Clin Oncol 2012; 9:98–109.
15. Bowen JM, Mayo BJ, Plews E, *et al.* Development of a rat model of oral small molecule receptor tyrosine kinase inhibitor-induced diarrhea. Cancer Biol Ther 2012; 13:1269–1275.
16. Van Sebille YZ, Gibson RJ, Wardill HR, *et al.* ErbB small molecule tyrosine kinase inhibitor (TKI) induced diarrhoea: chloride secretion as a mechanistic hypothesis. Cancer Treat Rev 2015; 41:646–652.
17. Ivanisinen E, Elenius K. ErbB targeted drugs and angiogenesis. Curr Vasc Pharmacol 2010; 8:421–431.
18. Wakeling AE, Guy SP, Woodburn JR, *et al.* ZD1839 (Iressa): an orally active inhibitor of epidermal growth factor signaling with potential for cancer therapy. Cancer Res 2002; 62:5749–5754.
19. Moyer JD, Barbacci EG, Iwata KK, *et al.* Induction of apoptosis and cell cycle arrest by CP-358,774, an inhibitor of epidermal growth factor receptor tyrosine kinase. Cancer Res 1997; 57:4838–4848.
20. Mok TS, Barbacci EG, Iwata KK, *et al.* Gefitinib or carboplatin-paclitaxel in pulmonary adenocarcinoma. N Engl J Med 2009; 361:947–957.
21. Zhou C, Wu YL, Chen G, *et al.* Erlotinib versus chemotherapy as first-line treatment for patients with advanced EGFR mutation-positive nonsmall-cell lung cancer (OPTIMAL, CTONG-0802): a multicentre, open-label, randomised, phase 3 study. Lancet Oncol 2011; 12:735–742.
22. Rosell R, Carcereny E, Gervais R, *et al.* Erlotinib versus standard chemotherapy as first-line treatment for European patients with advanced EGFR mutation-positive nonsmall-cell lung cancer (EURTAC): a multicentre, open-label, randomised phase 3 trial. Lancet Oncol 2012; 13:239–246.
23. Thatcher N, Chang A, Parikh P, *et al.* Gefitinib plus best supportive care in previously treated patients with refractory advanced nonsmall-cell lung cancer: results from a randomised, placebo-controlled, multicentre study (Iressa Survival Evaluation in Lung Cancer). Lancet 2005; 366:1527–1537.
24. Sun JM, Lee KH, Kim SW, *et al.* Gefitinib versus pemetrexed as second-line treatment in patients with nonsmall cell lung cancer previously treated with platinum-based chemotherapy (KCSG-LU08-01): an open-label, phase 3 trial. Cancer 2012; 118:6234–6242.
25. Cufer T, Vrdoljak E, Gaafar R, *et al.* Phase II, open-label, randomized study (SIGN) of single-agent gefitinib (IRESSA) or docetaxel as second-line therapy in patients with advanced (stage IIIb or IV) nonsmall-cell lung cancer. Anticancer Drugs 2006; 17:401–409.
26. Kim ES, Hirsh V, Mok T, *et al.* Gefitinib versus docetaxel in previously treated nonsmall-cell lung cancer (INTEREST): a randomised phase III trial. Lancet 2008; 372:1809–1818.
27. Lee DH, Park K, Kim JH, *et al.* Randomized Phase III trial of gefitinib versus docetaxel in nonsmall cell lung cancer patients who have previously received platinum-based chemotherapy. Clin Cancer Res 2010; 16:1307–1314.
28. Mok TS, Wu YL, Thongprasert S, *et al.* Gefitinib or carboplatin-paclitaxel in pulmonary adenocarcinoma. N Engl J Med 2009; 361:947–957.
29. Maemondo M, Inoue A, Kobayashi K, *et al.* Gefitinib or chemotherapy for nonsmall-cell lung cancer with mutated EGFR. N Engl J Med 2010; 362:2380–2388.
30. Goss G, Ferry D, Wierzbicki R, *et al.* Randomized phase II study of gefitinib compared with placebo in chemotherapy-naive patients with advanced nonsmall-cell lung cancer and poor performance status. J Clin Oncol 2009; 27:2253–2260.
31. Morere JF, Brechot JM, Westeel V, *et al.* Randomized phase II trial of gefitinib or gemcitabine or docetaxel chemotherapy in patients with advanced nonsmall-cell lung cancer and a performance status of 2 or 3 (IFCT-0301 study). Lung Cancer 2010; 70:301–307.
32. Mitsudomi T, Morita S, Yatabe Y, *et al.* Gefitinib versus cisplatin plus docetaxel in patients with nonsmall-cell lung cancer harbouring mutations of the epidermal growth factor receptor (WJTOG3405): an open label, randomised phase 3 trial. Lancet Oncol 2010; 11:121–128.
33. Zhang L, Ma S, Song X, *et al.* Gefitinib versus placebo as maintenance therapy in patients with locally advanced or metastatic nonsmall-cell lung cancer (INFORM; C-TONG 0804): a multicentre, double-blind randomised phase 3 trial. Lancet Oncol 2012; 13:466–475.
34. Crino L, Cappuzzo F, Zatloukal P, *et al.* Gefitinib versus vinorelbine in chemotherapy-naive elderly patients with advanced nonsmall-cell lung cancer (INVITE): a randomized, phase II study. J Clin Oncol 2008; 26:4253–4260.
35. Xu Y, Liu H, Chen J, *et al.* Acquired resistance of lung adenocarcinoma to EGFR-tyrosine kinase inhibitors gefitinib and erlotinib. Cancer Biol Ther 2010; 9:572–582.
36. Gotoh N. Somatic mutations of the EGF receptor and their signal transducers affect the efficacy of EGF receptor-specific tyrosine kinase inhibitors. Int J Clin Exp Pathol 2011; 4:403–409.
37. Carpenter RL, Lo HW. Dacomitinib, an emerging HER-targeted therapy for nonsmall cell lung cancer. J Thorac Dis 2012; 4:639–642.
38. Ramalingam SS, Blackhall F, Krzakowski M, *et al.* Randomized phase II study of dacomitinib (PF-00299804), an irreversible pan-human epidermal growth factor receptor inhibitor, versus erlotinib in patients with advanced nonsmall-cell lung cancer. J Clin Oncol 2012; 30:3337–3344.

39. Takahashi T, Boku N, Murakami H, *et al.* Phase I and pharmacokinetic study of dacomitinib (PF-00299804), an oral irreversible, small molecule inhibitor of human epidermal growth factor receptor-1, -2, and -4 tyrosine kinases, in Japanese patients with advanced solid tumors. Invest New Drugs 2012; 30:2352–2363.
40. Dietrich E, Antoniades K. Molecularly targeted drugs for the treatment of cancer: oral complications and pathophysiology. Hippokratia 2012; 16:196–199.
41. Hare KJ, Hartmann B, Kissow H, *et al.* The intestinotrophic peptide, glp-2, counteracts intestinal atrophy in mice induced by the epidermal growth factor receptor inhibitor, gefitinib. Clin Cancer Res 2007; 13:5170–5175.
42. Abdul Razak AR, Soulieres D, Laurie SA, *et al.* A phase II trial of dacomitinib, an oral pan-human EGF receptor (HER) inhibitor, as first-line treatment in recurrent and/or metastatic squamous-cell carcinoma of the head and neck. Ann Oncol 2013; 24:761–769.
43. Campbell A, Reckamp K, Camidge D, *et al.* PF-00299804 (PF299) patient (pt)-reported outcomes (PROs) and efficacy in adenocarcinoma (adeno) and nonadeno nonsmall cell lung cancer (NSCLC): a phase (P) II trial in advanced NSCLC after failure of chemotherapy (CT) and erlotinib (E). J Clin Oncol 2010; 28. (suppl): 15s (suppl; abstr 7596).
44. Reckamp KL, Giaccone G, Camidge DR, *et al.* A phase 2 trial of dacomitinib (PF-00299804), an oral, irreversible pan-HER (human epidermal growth factor receptor) inhibitor, in patients with advanced nonsmall cell lung cancer after failure of prior chemotherapy and erlotinib. Cancer 2014; 120:1145–1154.
45. Janne PA, Boss DS, Camidge DR, *et al.* Phase I dose-escalation study of the pan-HER inhibitor, PF299804, in patients with advanced malignant solid tumors. Clin Cancer Res 2011; 17:1131–1139.
46. Ramalingam SS, Blackhall F, Krzakowski M, *et al.* Randomized phase II study of dacomitinib (PF-00299804), an irreversible pan-human epidermal growth factor receptor inhibitor, versus erlotinib in patients with advanced nonsmall-cell lung cancer. J Clin Oncol 2012; 30:3337–3344.
47. Ruiz-Garcia A, Giri N, Labadie RR, *et al.* A phase I open-label study to investigate the potential drug-drug interaction between single-dose dacomitinib and steady-state paroxetine in healthy volunteers. J Clin Pharmacol 2013; 54:555–562.
48. Ramalingam SS, Janne PA, Mok T, *et al.* Dacomitinib versus erlotinib in patients with advanced-stage, previously treated nonsmall-cell lung cancer (ARCHER 1009): a randomised, double-blind, phase 3 trial. Lancet Oncol 2014; 15:1369–1378.
49. Janne PA, Shaw AT, Camidge DR, *et al.* Combined Pan-HER and ALK/ROS1/MET inhibition with dacomitinib and crizotinib in advanced nonsmall cell lung cancer: results of a phase I study. J Thorac Oncol 2016. [Epub ahead of print]
50. Ellis PM, Shepherd FA, Millward M, *et al.* Dacomitinib compared with placebo in pretreated patients with advanced or metastatic nonsmall-cell lung cancer (NCIC CTG BR.26): a double-blind, randomised, phase 3 trial. Lancet Oncol 2014; 15:1379–1388.

Cancer Treatment Reviews 41 (2015) 646–652

Contents lists available at ScienceDirect

Cancer Treatment Reviews

journal homepage: www.elsevierhealth.com/journals/ctrv

New Drugs

ErbB small molecule tyrosine kinase inhibitor (TKI) induced diarrhoea: Chloride secretion as a mechanistic hypothesis

Ysabella Z.A. Van Sebille [a,b,*], Rachel J. Gibson [b], Hannah R. Wardill [a,b], Joanne M. Bowen [a]

[a] School of Medical Sciences, Discipline of Physiology, University of Adelaide, Australia
[b] School of Medical Sciences, Discipline of Anatomy and Pathology, University of Adelaide, Australia

ARTICLE INFO

Article history:
Received 5 May 2015
Received in revised form 25 May 2015
Accepted 26 May 2015

Keywords:
TKI
Mucositis
Diarrhoea
Chloride secretion
ErbB (EGFR, HER)

ABSTRACT

Diarrhoea is a common, debilitating and potentially life threatening toxicity of many cancer therapies. While the mechanisms of diarrhoea induced by traditional chemotherapy have been the focus of much research, the mechanism(s) of diarrhoea induced by small molecule ErbB TKI, have received relatively little attention. Given the increasing use of small molecule ErbB TKIs, identifying this mechanism is key to optimal cancer care. This paper critically reviews the literature and forms a hypothesis that diarrhoea induced by small molecule ErbB TKIs is driven by intestinal chloride secretion based on the negative regulation of chloride secretion by ErbB receptors being disrupted by tyrosine kinase inhibition.

Introduction

In clinical oncology practice diarrhoea is a very common and severe side effect of cancer treatments including radiotherapy, chemotherapy, and targeted therapies [1]. Diarrhoea occurs in between 50% and 100% of patients depending on their treatment regimen [2,3]. It is a debilitating and potentially life threatening toxicity as fluid and electrolyte loss associated with persistent and/or severe diarrhoea can result in electrolyte imbalances, renal insufficiency, malnutrition, and extreme dehydration, all of which can lead to cardiovascular compromise and death [4]. Furthermore, these often necessitate dose reductions and treatment breaks, compromising clinical outcomes [5,6]. The need for prevention of cancer therapy-induced diarrhoea is critical. Identification of the pathogenesis may lead to a more accurate management to help reduce severe complications that may be irreversible [7,8].

Cancer therapy-induced diarrhoea is also associated with considerable economic costs with recent reports suggesting that additional costs of up to $25,000 (USD) per chemotherapy cycle are incurred [9]. These costs are attributed to patients with cancer therapy-induced diarrhoea having an increased risk of infection, increased hospital stays and increased resource utilisation for supportive care measures [10,11]. Consequently, prevention, minimisation, and/or prediction of cancer therapy-induced diarrhoea may significantly reduce health system costs over the total course of cancer treatment.

Small molecule ErbB receptor tyrosine kinase inhibitors (TKIs) are used for the treatment of a variety of cancers that overexpress ErbB receptors. These cancers include but are not limited to breast, non-small cell lung cancer (NSCLC) and head and neck cancers. Small molecule ErbB TKIs act by competitively binding to the intracellular ATP domain of the tyrosine kinase, effectively inhibiting phosphorylation of the receptor and therefore downstream signalling [12,13]. To date, the mechanism(s) of action of ErbB TKI-induced diarrhoea has yet to be elucidated. This is in contrast to diarrhoea induced by traditional chemotherapy agents including fluropyrimidines, topotecans, platinum analogues, folate inhibitors and taxanes [2]. Recent research has suggested that chemotherapy-induced diarrhoea is a result of severe intestinal damage caused by mucositis. Mucositis is a multi-factorial process whereby acute damage to the intestinal mucosa (including, increased apoptosis, villus atrophy, crypt hypoplasia and dilation, loss of epithelium, excessive mucous secretion, necrosis and inflammation) causes an imbalance between absorption and secretion, ultimately resulting in an anatomic derangement diarrhoea phenotype [2,14,15]. Numerous preclinical and clinical studies have documented the pathobiology of chemotherapy-induced diarrhoea and have reported that it is largely based on indirect biological signalling, rather than direct tissue damage [16–21]. The mechanisms of chemotherapy-induced diarrhoea are becoming

* Corresponding author at: School of Medical Sciences, University of Adelaide, North Terrace, Adelaide 5005, Australia. Tel.: +61 8 83133787.
E-mail address: ysabella.vansebille@adelaide.edu.au (Y.Z.A. Van Sebille).

http://dx.doi.org/10.1016/j.ctrv.2015.05.011
0305-7372/

better characterised, this is not the case for TKI-induced diarrhoea; this critical review will outline potential mechanisms of ErbB receptor TKI-induced diarrhoea.

ErbB receptors

Many tumours including but not limited to breast, NSCLC, squamous cell cancers of the head and neck, have been identified as overexpressing ErbB receptors. This has meant that many targeted therapies have been developed to act on the ErbB family of receptors [22]. The ErbB family (interchangeably known as HER/EGFR), is comprised of four membrane receptor tyrosine kinases: ErbB1 (HER1 or EGFR), ErbB2 (HER2), ErbB3 (HER3), and ErbB4 (HER4) [23]. The activity of the ErbB receptors is dictated by the expression of their ligands [24], which can be classified into three groups: Group (1) those binding specifically to ErbB1; Group (2) ligands which exhibit dual specificity binding to both ErbB1 and ErbB4; and Group (3) neuregulins, which can be further sub-classified based upon their ability to bind only ErbB4 or both ErbB3 and ErbB4 (Table 1) [25]. To date, no ligand has been identified as being specific for ErbB2, although this receptor does form heterodimers with the other ErbB receptors.

When ligands bind to the extracellular domain of the ErbB receptors, receptor dimerisation and phosphorylation of intracellular tyrosine kinase domains occur. This leads to activation of a cascade of signalling pathways including the mitogen activated protein kinases/extracellular signal regulated kinases (MAPK/ERK), and phosphatidylinositol-3'-kinase (PI3K/Akt) pathways [26]. Once activated, these pathways lead to changes in both protein functions and activation of gene transcription [26–28], leading to interactions with apoptotic signalling, cell proliferation, differentiation, migration and survival. These can all promote tumourigenesis [27,29].

In addition to being expressed on cancer cells, ErbB receptors are also found on healthy cells throughout the body, of specific interest to this review are the receptors expressed in the gastrointestinal tract. Specifically, they are abundantly expressed on the basolateral membranes of healthy intestinal epithelial cells and are crucial for essential normal functions and development in the gut [30,31]. For example, ErbB receptors activated on intestinal epithelial cells cause a cascade of complex signalling pathways resulting in maintenance of mucosal integrity via induction of mucus and prostaglandin synthesis, promotion of enterocyte migration, prevention of intestinal epithelial cell apoptosis, decreasing bacterial translocation and preservation of gut barrier function after injury [32,33].

The first anti-cancer agents targeting ErbB receptors were developed in the 1980s. This led to the development of the first generation of two overarching subtypes of ErbB receptor inhibitors: monoclonal antibodies, and small molecule tyrosine kinase inhibitors [34–37]. Monoclonal antibodies are directed against the extracellular domain of ErbB receptors, whereas small molecule TKIs act directly on cytoplasmic domains of ErbB TKI activity. The overexpression of ErbB receptors in many solid tumours is correlated with advanced stages and often a worse prognosis of the cancer [38]. In many different cancer cell types, the ErbB pathway becomes hyper-activated by a range of mechanisms, including overproduction of ligands, overproduction of receptors, or constitutive activation of receptors [31]. This hyper-activity and hence key role of the ErbB network has made it an attractive target for therapies. After an initial response however, patients being treated with first generation ErbB TKIs often develop secondary mutations such as T790M, MET or HER2 amplifications, resulting in acquired resistance [39]. Ultimately, this limits the effectiveness of these first generation agents over time. Pan-ErbB TKIs are now considered second-generation and are resistant to acquired mutations. As a result, these TKIs are now commonly used. However, they are associated with clinical toxicities and which are important to recognise and manage.

Table 1
ErbB receptors and their ligands.

Receptor	Ligands
ErbB1	EGF, Areg, TGFα
ErbB1 and ErbB4	Btc, HBEGF and Ereg
ErbB3 and ErbB4	Nrg1 and Nrg2
ErbB4	Nrg3 and Nrg4

EGF: Epidermal Growth Factor; Areg: Amphiregulin; TGF: transforming growth factor; Btc: Betacellulin; HBEGF: Heparin-binding EGF-like growth factor; Ereg: Epiregulin; Nrg: Neuregulins.

ErbB TKIs and diarrhoea

Toxicities are common in patients receiving first generation ErbB TKIs, including but not limited to erlotinib, gefitinib, and lapatinib. In particular, up to 69% of patients experience diarrhoea [12]. Large randomised trials have shown that erlotinib and lapatinib induce diarrhoea in 40–60% of patients, with approximately 10% of these presenting with grade 3–4 symptoms (National Cancer Institute Common Toxicity Criteria) [40,41]. One of the most frequent toxicity associated with second-generation pan-ErbB TKIs is also diarrhoea. Recent clinical data suggests that all grades of diarrhoea are more frequently seen with pan-ErbB TKIs than first generation ErbB TKIs (e.g. dacomitinib vs. erolitinib). Up to 96% of patients receiving second generation pan-ErbB TKI's develop diarrhoea, and perhaps more importantly, the incidence of grade 3 (severe) diarrhoea is significantly higher [42]. Further exacerbating this diarrhoea is that many TKIs are given daily for months at a time, and side effects are therefore often chronic, unlike the acute manifestations typically seen following traditional chemotherapy regimens.

Do ErbB TKIs induce diarrhoea via a distinctly different mechanism than chemotherapy-induced diarrhoea?

One common hypothesis for the mechanism of action of diarrhoea following TKI treatment is thought to be due to inhibition of ErbB signalling within intestinal epithelia, leading to direct mucosal atrophy and damage [43–45]. Research suggested that this diarrhoea was associated with reduced growth, characterised by reduced growth and healing of the intestinal epithelium leading to mucosal atrophy due to the stimulatory effect of ErbB pathway on enterocyte proliferation [46], nutrient and electrolyte transport [47], brush border enzyme expression [48] and epithelial restitution being impeded [49]. Increased frequency of diarrhoea in patients using oral compounds (e.g. small molecule TKI's) compared to monoclonal antibodies supports this theory. This direct mucosal damage hypothesis mimics chemotherapy-induced diarrhoea, bought about by the manifestation of mucositis (Fig. 1).

A more recent hypothesis suggests that despite a similar clinical manifestation as is seen in traditional chemotherapy induced diarrhoea, ErbB TKI-induced diarrhoea is due to a distinctly different pathological mechanism [22,50]. This followed the recent development of a preclinical model to study the gastrointestinal toxicity associated with ErbB inhibitors [51]. Using lapatinib, an oral small molecule ErbB1 and ErbB2 TKI for 7–28 days, this large ($n = 128$) study showed no significant pathology in the intestines of rats, despite rats displaying a dose-dependent diarrhoea profile consistent with that observed clinically [51]. No significant changes were noted in intestinal weights and no significant histopathology was

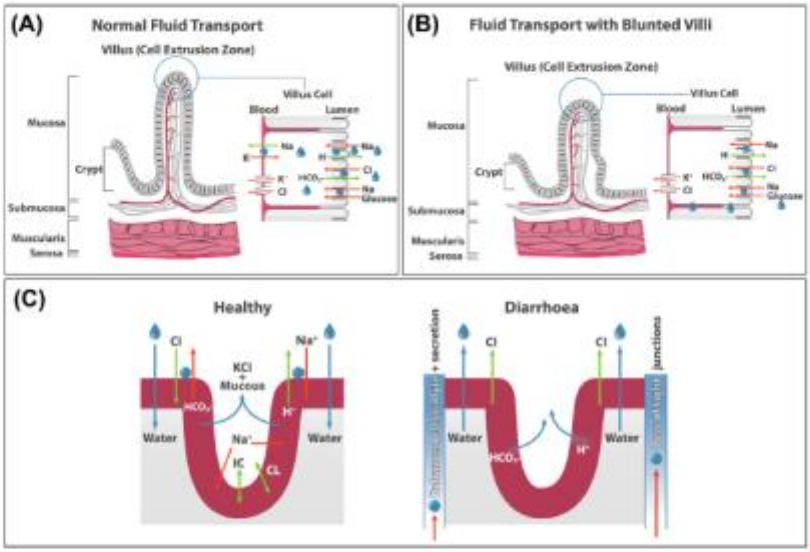

Fig. 1. (A) In a normal villus fluid transport is tightly controlled and there is a net absorption of fluid. (B) In chemotherapy induced gut toxicity, the villus is blunted and there is less area for absorption of fluid. The manifestation of chemotherapy-induced diarrhoea is largely driven by small intestinal changes. (C) Small molecule ErbB TKI induced diarrhoea is likely due to secretory mechanisms within the colon. The tight control of chloride secretion is lost, resulting in an accumulation of fluid in the lumen.

noted in the jejunum or colon, indicating that no significant pathology in the intestines occurred as a result of lapatinib treatment [51]. In fact, it was found that jejunum crypts were significantly longer, and contained increased mitotic cells in rats treated with lapatinib [52]. This is in stark contrast to what is noted in mucositis models of rats treated with chemotherapeutic agents such as irinotecan causing severe intestinal damage and atrophy [14,53]. This is therefore highly suggestive that the mechanism of ErbB TKI-induced diarrhoea is profoundly different from chemotherapy-induced diarrhoea. Further investigation found that serum biochemistry levels of chloride were decreased in rats treated with high dose lapatinib, correlating with diarrhoea incidence, suggesting that chloride loss via the intestinal lumen may be involved in the manifestation of small molecule ErbB TKI induced diarrhoea [52]. However, this was inconclusive. Furthermore, studies using another kinase inhibitor, flavopiridol, showed no intestinal damage, despite clinical manifestation of diarrhoea [54,55]. Additional investigation showed treatment with flavopiridol directly stimulated chloride secretion across monolayers of human colonocytes in modified Ussing chambers [56].

Paradoxically, a study by Hoda et al. (2010), showed in a chemotherapy model of gut toxicity, that chloride secretion was increased in rats treated with methotrexate [57]. While the severity and incidence of diarrhoea was not reported, it was suggested by the authors that increased chloride secretion may be part of the mechanism responsible for chemotherapy induced diarrhoea. However, given the limited evidence of this in the wider literature, it requires further investigation.

Other research has also established that ErbB receptors have a limited role in the development of mucositis induced diarrhoea [58]. Transgenic mice that overexpress EGF (a ligand for ErbB1) in the small intestine, showed no improvements in weight recovery, mucosal architecture, apoptosis or proliferation compared to controls following fluorouracil, a chemotherapeutic known to induce mucositis [58]. This was also the case in mice treated with exogenous EGF following fluorouracil. These findings are highly suggestive that the ErbB family of receptors does not play a significant role in the development of mucositis associated diarrhoea. Given that ErbB TKIs target these receptors, it is likely that their physiological function is critically involved in the development of the associated diarrhoea. This supports the indication that ErbB TKIs induce diarrhoea via a distinct mechanism to chemotherapy-induced diarrhoea. Together, this suggests that the pathogenic mechanisms of ErbB TKI-induced diarrhoea are not necessarily the same as for other cancer treatments, and there remains a vast gap in the knowledge regarding the biological mechanisms responsible.

Chloride secretion and diarrhoea

Chloride secretion occurs throughout the length of the gastrointestinal tract and is critical for normal physiological functioning of the gut [59]. The chloride secretory mechanism has several transmembrane transport pathways. In the colon, chloride is taken into the cell via the basolateral membrane through the sodium potassium chloride co-transporter in an electro-neutral manner. This process is driven largely by the sodium potassium ATPase pump [59]. Potassium channels are also located on the basolateral membranes, and allow for potassium recycling and prevention of cellular depolarisation. This preserves the electrical driving force for chloride secretion from the apical membrane of the cell. Chloride then accumulates in the lumen via the cAMP dependent cystic fibrosis transmembrane conductance regulator (CFTR) chloride channels, and the calcium activated chloride channels (CaCC). The presence of chloride in the lumen provides the electrochemical driving force for paracellular movement of sodium. The resulting accumulation of sodium chloride in the lumen provides the

osmotic gradient for water to flow to the lumen [59]. The normal chloride secretory process is outlined in Fig. 2. The secretion of chloride ions is important in controlling fluid flow across various epithelial surfaces, including the intestine, helping to keep it moist.

There are two key mechanisms whereby chloride secretion is initiated. (1) a cAMP-dependent pathway; which elicits a delayed and prolonged response and (2) a calcium ion-dependent pathway; which elicits a rapid and transient response [60]. The transient nature of the calcium ion-dependent response, even in the face of sustained increases in intracellular calcium suggests calcium dependent agonists generate an inhibitory signal. This inhibitory signal then serves to limit the extent of the chloride secretory response [61]. Under normal homoeostasis, this process is tightly regulated. However, any homoeostatic breakdown can lead to various complications, such as diarrhoea where secretion is exaggerated [62].

ErbB receptors are abundantly expressed on the basolateral membrane of intestinal epithelial cells and are critical regulators of intestinal ion transport via multiple downstream pathways [28]. The intricate pathways that result from binding and dimerisation lead to negative regulation of both chloride secretion and sodium absorption [28]. ErbB receptors have been shown to exert both an inhibitory effect on chloride secretion (Fig. 3) [26]. Binding of EGF to ErbB1 leads to homodimerisation and heterodimerisation with ErbB2 exerting an inhibitory effect on chloride secretion signalling via PI3K/Akt and PKC pathways; these distinct pathways inhibit the basolateral potassium channels (Fig. 3) [63,64].

Based on the negative regulatory roles ErbB receptors play in chloride secretion, it is reasonable to suggest that when receptors are inhibited from phosphorylating (as is the case with TKIs), they are no longer able to negatively regulate chloride secretion. This results in excessive movement of chloride into the lumen, providing the driving force for paracellular movement of sodium and subsequently water leading to a secretory diarrhoea phenotype. This hypothesis is supported by research with genistein, an isoflavone that acts as an ErbB1 TKI, which has shown to reverse the inhibitory effect of EGF on chloride secretion [62,65]. In contrast however, some TKIs including erbstatin analogue, tyrphostin A23, tyrphostin A51 and herbimycin A are not associated with an increase in epithelial chloride secretion [66]. This is contradictory to the increased chloride secretion seen following tyrosine kinase inhibition with other agents [66]. This may be explained due to the differing mechanisms of action of each drug, and strongly suggests that different TKIs may need to be considered independently.

TKI and chemotherapy concomitant therapy

Concomitant chemotherapy and TKIs has increased due to a greater therapeutic effectiveness [13]. However, this has meant toxicities increase. A meta-analysis including 3918 patients from six trials of erlotinib, gefitinib, and vandetanib found that the addition of an ErbB1 inhibitor to a variety of different chemotherapeutics significantly increased the severity of diarrhoea [67]. Furthermore, concomitant lapatinib with capecitabine increased diarrhoea from 30% (when capecitabine is given alone) to 65% in combination. Likewise the addition of lapatinib with paclitaxel increased diarrhoea incidence from 28% to 48% [68]. These combination therapies not only result in more severe diarrhoea but also complicate identifying and treating the causes and underlying mechanisms, which are likely to be multifactorial. Understanding the mechanisms is important as attributing all mucosal toxicity on the concomitant chemotherapy, without considering the TKIs may lead to the wrong intervention [69]. Diarrhoea is not always the same and a distinction needs to be made between secretory and anatomic derangement diarrhoea in these cases. Diarrhoea seen in patients undergoing concomitant TKI/chemotherapy treatment may be due to either the direct mechanisms caused by the agents themselves, or amplification of injury mechanisms in combination [50]. There are known shared metabolic and drug efflux pathways of various TKIs and chemotherapeutic agents, which may explain the more severe diarrhoea associated with concomitant therapy. For example, concomitant treatment can down-regulate CYP3A4 and UGT1A1, increasing exposure to both TKI and chemotherapeutic agents sharing common metabolic pathways which may increase toxicity [70,71]. Additionally, both TKIs and chemotherapeutics are substrates for drug efflux transporters of the ATP binding cassette family. This means that they

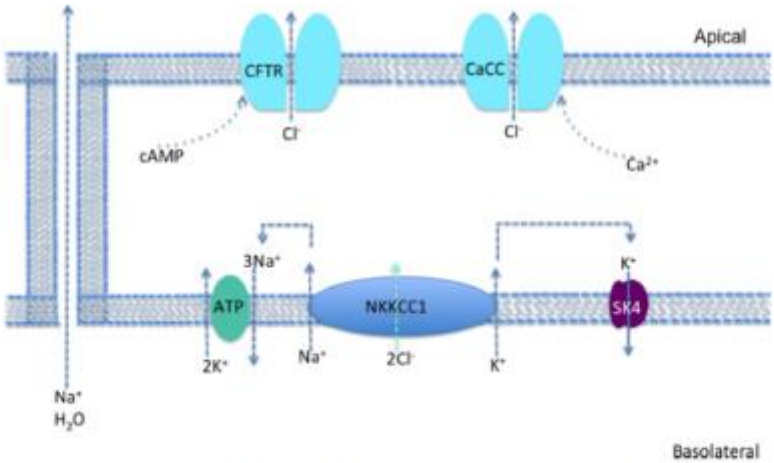

Fig. 2. Chloride secretory mechanism in normal intestinal epithelium. cAMP, cyclic adenosine monophosphate; CFTR, cystic fibrosis transmembrane conductance regulator; CaCC, calcium activated chloride channel; ATP, adenosine triphosphate.

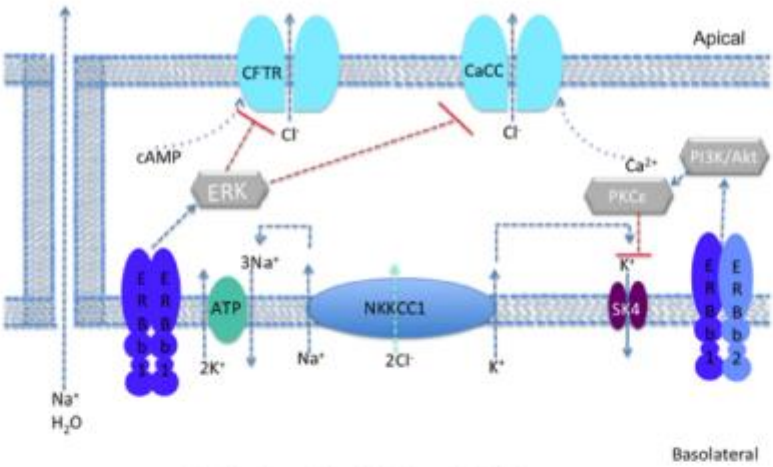

Fig. 3. Negative regulation of chloride secretion by ErbB receptors.

may impede drug clearance of the other drug, subsequently drug accumulation can result with potentially increased toxicity [72].

While the use of concomitant treatment no doubt contributes to the toxicity profile, patients prescribed ErbB TKIs monotherapy also demonstrate systemic treatment complications. Given the drugs different mechanisms of action, this supports a hypothesis suggesting that ErbB TKIs trigger deregulation of chloride channels, driving water into the lumen, resulting in a secretory diarrhoea phenotype, as opposed to the mucositis driven anatomical derangement diarrhoea phenotype typically seen in chemotherapy induced diarrhoea. Given the reduced quality of life associated with diarrhoea is further exacerbated in concomitant treatment, further research is crucial.

Pharmacogenetic studies have shown a link between TKI-induced diarrhoea and allelic variants of *ABCG2*, a polymorphic efflux transporter protein (also known as breast cancer resistance gene *BCRP*), highly expressed in the intestines. A common functional single-nucleotide polymorphism (SNP) in the *ABCG2* gene was associated with diarrhoea in patients treated with gefitinib, an ErbB1 small molecule TKI [73]. This suggests that patients with reduced *ABCG2* activity due to a common genetic variation are at increased risk for substrate drug-induced diarrhoea, with implications for optimising treatment with small molecule ErbB TKIs. However, further research is required before meaningful conclusions can be made.

Current treatment approaches for TKI-induced diarrhoea

Currently, management of TKI-induced diarrhoea is very similar to management of chemotherapy-induced diarrhoea and includes patient education and both non-pharmacologic and pharmacologic management strategies. This ignores the probability of a differing mechanism of diarrhoea development.

Patient education includes advice on dietary changes for the management of ErbB TKI-induced diarrhoea, based on dietary changes recommended for chemotherapy induced-diarrhoea. These dietary modifications include incorporating bananas, rice, apple sauce and toast (BRAT diet), as well as increasing water consumption and avoiding foods/drinks that contain lactose/caffeine; however, these dietary changes are not recommended in anticipation of diarrhoea development [12]. Patients should also avoid foods that exacerbate symptoms, such as greasy, spicy and fried items; and foods that are difficult to digest. Increasing fluid intake to 2 l/per day is recommended to avoid dehydration; some fluids should contain sugar or salt to avoid hyponatremia and hypokalemia caused by electrolyte loss associated with diarrhoea [12].

Pharmacologic management of ErbB TKI-induced diarrhoea is largely limited to loperamide, with the dose based on the grade of diarrhoea experienced by the patient [12]. Loperamide, a synthetic oral opioid drug, works by a number of different mechanisms of action that decrease peristalsis and fluid secretion, resulting in longer gastrointestinal transit time and increased absorption of fluids and electrolytes from the gastrointestinal tract [74]. Alternatives to loperamide are also available for managing diarrhoea, however their use and effectiveness can differ by geographic location and the diarrhoea severity. Some of these include diphenoxylate–atropine and codeine, either of which can be used with loperamide [12]. Dose reductions are not recommended for grade 1 diarrhoea. At grade 2, if the patient does not respond to loperamide after 48 h, it is recommended the ErbB TKI is temporarily discontinued until the diarrhoea returns to grade 1, at which time the ErbB TKI is resumed, often at a lower dose [12]. It is recommended that the ErbB TKI should be permanently discontinued if diarrhoea does not reach grade 1 within 14 days despite best supportive care and withholding of the ErbB TKI [12]. Patients presenting with grade 3–4 diarrhoea should be admitted to hospital for the administration of intravenous fluids and electrolyte replacement.

Potential treatment approaches for TKI-induced diarrhoea

If the hypothesis of increased chloride secretion being responsible for TKI-induced diarrhoea is correct, there may be more effective treatment strategies. If TKI-induced diarrhoea is induced by increased chloride secretion, the two major apical channels for chloride secretion in enterocytes, CFTR and CaCC, present as promising targets. Ideally, these treatment approaches would have minimal systemic absorption, and act on the external pore of the chloride channels, to limit systemic effects. While this is appealing

in terms of reducing systemic absorption, and therefore potential drug interactions and toxicities, concerns have been raised in regards to the potential barrier of the inhibitor reaching the deep intestinal crypts given the strong convective washout force observed during secretory diarrhoeas [75]. CFTR inhibitors include CFTRinh-172, which binds to the cytoplasmic side of the channel and stabalises the channel closed state [76], and the glycine hydrazides, which target the extracellular CFTR surface in the channel pore [75]. CaCC inhibitors are less common and include $CaCC_{inh}$-A01, a red wine extract that has been shown to prevent watery diarrhoea in a mouse model of rotavirus [77]. Recently, crofelemer, a natural product extract, was approved for the treatment of diarrhoea induced by antiretroviral medication for HIV patients. Crofelemer is extracted from the stem bark latex of the croton lechleri tree. It has been shown to dose-dependently reduce intestinal fluid secretion in cell culture and mouse models [78,79]. It has been used for many years in Peru and Ecuador to treat diarrhoea, and has been investigated for the treatment of traveller's diarrhoea, infectious diarrhoea and diarrhoea predominant irritable bowel syndrome [78,79]. While the precise mechanism of crofelemer is unclear, it is known that the antisecretory activity of crofelemer is due to its dual inhibitory action on the two principle Cl^- channels in the apical membrane of intestinal epithelial cells, CFTR and CaCC [80]. As crofelemer effectively inhibits *both* of the principle Cl^- channels, it is an attractive agent to reduce secretory diarrhoea. Clinical studies have demonstrated that crofelemer is a safe and tolerable drug, with no adverse effects being reported [81–83].

Conclusion

With the increasing incidence of malignancy, coupled with the advent of more aggressive treatment modalities, ErbB TKI induced diarrhoea remains a significant clinical burden and a fuller understanding of the basic biological mechanisms is therefore required. The pathogenesis of ErbB TKI induced diarrhoea remains unknown, and understanding this is ultimately integral to developing interventions, leading to safer and more optimised cancer treatment. The negative regulation of chloride secretion by ErbB receptors being disrupted by tyrosine kinase inhibition provides a strong rationale for a secretory diarrhoea phenotype hypothesis. Considering the increased utilisation and therapeutic efficacy of ErbB TKIs, further research to gain the ability to prevent diarrhoea is urgently warranted [84].

Conflict of interest

None.

References

[1] Lalla RV et al. MASCC/ISOO clinical practice guidelines for the management of mucositis secondary to cancer therapy. Cancer 2014;120(10):1453–61.
[2] Gibson RJ, Stringer AM. Chemotherapy-induced diarrhoea. Curr Opin Support Palliat Care 2009;3(1):31–5.
[3] Benson 3rd AB et al. Recommended guidelines for the treatment of cancer treatment-induced diarrhea. J Clin Oncol 2004;22(14):2918–26.
[4] Stein A, Voigt W, Jordan K. Chemotherapy-induced diarrhea: pathophysiology, frequency and guideline-based management. Ther Adv Med Oncol 2010;2(1):51–63.
[5] Foote M. The importance of planned dose of chemotherapy on time: do we need to change our clinical practice? Oncologist 1998;3(5):365–8.
[6] Di Fiore F, Van Cutsem E. Acute and long-term gastrointestinal consequences of chemotherapy. Best Pract Res Clin Gastroenterol 2009;23(1):113–24.
[7] Davila M, Bresalier RS. Gastrointestinal complications of oncologic therapy. Nat Clin Pract Gastroenterol Hepatol 2008;5(12):682–96.
[8] Vincenzi B et al. Predictive factors for chemotherapy-related toxic effects in patients with colorectal cancer. Nat Clin Pract Oncol 2008;5(8):455–65.
[9] Carlotto A et al. The economic burden of toxicities associated with cancer treatment: review of the literature and analysis of nausea and vomiting, diarrhoea, oral mucositis and fatigue. PharmacoEconomics 2013;31(9):753–66.
[10] Elting LS et al. The burdens of cancer therapy. Clinical and economic outcomes of chemotherapy-induced mucositis. Cancer 2003;98(7):1531–9.
[11] Lalla RV et al. MASCC/ISOO clinical practice guidelines for the management of mucositis secondary to cancer therapy. Cancer 2014.
[12] Hirsh V et al. Management of diarrhea induced by epidermal growth factor receptor tyrosine kinase inhibitors. Curr Oncol 2014;21(6):329–36.
[13] Belani CP. The role of irreversible EGFR inhibitors in the treatment of non-small cell lung cancer: overcoming resistance to reversible EGFR inhibitors. Cancer Invest 2010;28(4):413–23.
[14] Gibson RJ et al. Irinotecan causes severe small intestinal damage, as well as colonic damage, in the rat with implanted breast cancer. J Gastroenterol Hepatol 2003;18(9):1095–100.
[15] Gibson RJ, Keefe DM. Cancer chemotherapy-induced diarrhoea and constipation: mechanisms of damage and prevention strategies. Support Care Cancer 2006;14(9):890–900.
[16] Sonis ST. The pathobiology of mucositis. Nat Rev Cancer 2004;4(4):277–84.
[17] Lin CC et al. Profiles of circulating endothelial cells and serum cytokines during adjuvant chemoradiation in rectal cancer patients. Clin Transl Oncol 2013;15(10):855–60.
[18] Sonis S et al. Unanticipated frequency and consequences of regimen-related diarrhea in patients being treated with radiation or chemoradiation regimens for cancers of the head and neck or lung. Support Care Cancer 2014.
[19] Logan RM et al. The role of pro-inflammatory cytokines in cancer treatment-induced alimentary tract mucositis: pathobiology, animal models and cytotoxic drugs. Cancer Treat Rev 2007;33(5):448–60.
[20] Logan RM et al. Characterisation of mucosal changes in the alimentary tract following administration of irinotecan: implications for the pathobiology of mucositis. Cancer Chemother Pharmacol 2008;62(1):33–41.
[21] Keefe DM et al. Chemotherapy for cancer causes apoptosis that precedes hypoplasia in crypts of the small intestine in humans. Gut 2000;47(5):632–7.
[22] Keefe DM, Bateman EH. Tumor control versus adverse events with targeted anticancer therapies. Nat Rev Clin Oncol 2012;9(2):98–109.
[23] Takahashi T et al. Phase I and pharmacokinetic study of dacomitinib (PF-00299804), an oral irreversible, small molecule inhibitor of human epidermal growth factor receptor-1, -2, and -4 tyrosine kinases, in Japanese patients with advanced solid tumors. Invest New Drugs 2012;30(6):2352–63.
[24] Pinkas-Kramarski R, Alroy I, Yarden Y. ErbB receptors and EGF-like ligands: cell lineage determination and oncogenesis through combinatorial signaling. J Mammary Gland Biol Neoplasia 1997;2(2):97–107.
[25] Dent P et al. Stress and radiation-induced activation of multiple intracellular signaling pathways. Radiat Res 2003;159(3):283–300.
[26] McCole DF, Barrett KE. Decoding epithelial signals: critical role for the epidermal growth factor receptor in controlling intestinal transport function. Acta Physiol 2009;195(1):149–59.
[27] Henson ES, Gibson SB. Surviving cell death through epidermal growth factor (EGF) signal transduction pathways: implications for cancer therapy. Cell Signal 2006;18(12):2089–97.
[28] Paul G et al. Interferon-gamma alters downstream signaling originating from epidermal growth factor receptor in intestinal epithelial cells: functional consequences for ion transport. J Biol Chem 2012;287(3):2144–55.
[29] Ayyappan S, Prabhakar D, Sharma N. Epidermal growth factor receptor (EGFR)-targeted therapies in esophagogastric cancer. Anticancer Res 2013;33(10):4139–55.
[30] Hare KJ et al. The intestinotrophic peptide, glp-2, counteracts intestinal atrophy in mice induced by the epidermal growth factor receptor inhibitor, gefitinib. Clin Cancer Res 2007;13(17):5170–5.
[31] Yarden Y, Sliwkowski MX. Untangling the ErbB signalling network. Nat Rev Mol Cell Biol 2001;2(2):127–37.
[32] Chen CL et al. Heparin-binding EGF-like growth factor protects intestinal stem cells from injury in a rat model of necrotizing enterocolitis. Lab Invest 2012;92(3):331–44.
[33] Dietrich E, Antoniades K. Molecularly targeted drugs for the treatment of cancer: oral complications and pathophysiology. Hippokratia 2012;16(3):196–9.
[34] Masui H et al. Growth inhibition of human tumor cells in athymic mice by anti-epidermal growth factor receptor monoclonal antibodies. Cancer Res 1984;44(3):1002–7.
[35] Normanno N et al. Target-based agents against ErbB receptors and their ligands: a novel approach to cancer treatment. Endocr Relat Cancer 2003;10(1):1–21.
[36] Sharma SV et al. Epidermal growth factor receptor mutations in lung cancer. Nat Rev Cancer 2007;7(3):169–81.
[37] Zandi R et al. Mechanisms for oncogenic activation of the epidermal growth factor receptor. Cell Signal 2007;19(10):2013–23.
[38] Mendelsohn J. Targeting the epidermal growth factor receptor for cancer therapy. J Clin Oncol 2002;20(18 Suppl.):1S–13S.
[39] Liao BC, Lin CC, Yang JC. Second and third-generation epidermal growth factor receptor tyrosine kinase inhibitors in advanced nonsmall cell lung cancer. Curr Opin Oncol 2015;27(2):94–101.
[40] Herbst RS et al. TRIBUTE: a phase III trial of erlotinib hydrochloride (OSI-774) combined with carboplatin and paclitaxel chemotherapy in advanced non-small-cell lung cancer. J Clin Oncol 2005;23(25):5892–8.
[41] Shepherd FA et al. Erlotinib in previously treated non-small-cell lung cancer. N Engl J Med 2005;353(2):123–32.

[42] Takeda M, Okamoto I, Nakagawa K. Pooled safety analysis of EGFR-TKI treatment for EGFR mutation-positive non-small cell lung cancer. Lung Cancer 2015;88(1):74–9.
[43] Loriot Y et al. Drug insight: gastrointestinal and hepatic adverse effects of molecular-targeted agents in cancer therapy. Nat Clin Pract Oncol 2008;5(5):268–78.
[44] Rasmussen AR et al. The intestinotrophic peptide, GLP-2, counteracts the gastrointestinal atrophy in mice induced by the epidermal growth factor receptor inhibitor, erlotinib, and cisplatin. Dig Dis Sci 2010;55(10): 2785–96.
[45] Yusta B et al. ErbB signaling is required for the proliferative actions of GLP-2 in the murine gut. Gastroenterology 2009;137(3):986–96.
[46] Berlanga-Acosta J et al. Gastrointestinal cell proliferation and crypt fission are separate but complementary means of increasing tissue mass following infusion of epidermal growth factor in rats. Gut 2001;48(6):803–7.
[47] Opleta-Madsen K, Hardin J, Gall DG. Epidermal growth factor upregulates intestinal electrolyte and nutrient transport. Am J Physiol 1991;260(6 Pt 1):G807–14.
[48] Goodlad RA et al. Effects of urogastrone-epidermal growth factor on intestinal brush border enzymes and mitotic activity. Gut 1991;32(9):994–8.
[49] Dignass AU, Podolsky DK. Cytokine modulation of intestinal epithelial cell restitution: central role of transforming growth factor beta. Gastroenterology 1993;105(5):1323–32.
[50] Bowen JM. Mechanisms of TKI-induced diarrhea in cancer patients. Curr Opin Support Palliat Care 2013;7(2):162–7.
[51] Bowen JM et al. Development of a rat model of oral small molecule receptor tyrosine kinase inhibitor-induced diarrhea. Cancer Biol Ther 2012;13(13): 1269–75.
[52] Bowen JM et al. Determining the mechanisms of lapatinib-induced diarrhoea using a rat model. Cancer Chemother Pharmacol 2014;74(3):617–27.
[53] Gibson RJ et al. Establishment of a single-dose irinotecan model of gastrointestinal mucositis. Chemotherapy 2007;53(5):360–9.
[54] Senderowicz AM et al. Phase I trial of continuous infusion flavopiridol, a novel cyclin-dependent kinase inhibitor, in patients with refractory neoplasms. J Clin Oncol 1998;16(9):2986–99.
[55] Senderowicz AM. Flavopiridol: the first cyclin-dependent kinase inhibitor in human clinical trials. Invest New Drugs 1999;17(3):313–20.
[56] Kahn ME et al. Possible mechanisms of diarrheal side effects associated with the use of a novel chemotherapeutic agent, flavopiridol. Clin Cancer Res 2001;7(2):343–9.
[57] Hoda MR et al. Apical leptin induces chloride secretion by intestinal epithelial cells and in a rat model of acute chemotherapy-induced colitis. Am J Physiol Gastrointest Liver Physiol 2010;298(5):G714–21.
[58] Huang PS et al. Role of epidermal growth factor and its receptor in chemotherapy-induced intestinal injury. Am J Physiol Gastrointest Liver Physiol 2002;282(3):G432–42.
[59] Barrett KE, Keely SJ. Chloride secretion by the intestinal epithelium: molecular basis and regulatory aspects. Annu Rev Physiol 2000;62:535–72.
[60] Dharmsathaphorn K, Pandol SJ. Mechanism of chloride secretion induced by carbachol in a colonic epithelial cell line. J Clin Investig 1986;77(2): 348–54.
[61] Dharmsathaphorn K, Cohn J, Beuerlein G. Multiple calcium-mediated effector mechanisms regulate chloride secretory responses in T84-cells. Am J Physiol 1989;256(6 Pt 1):C1224–30.
[62] Uribe JM et al. Epidermal growth factor inhibits Ca(2+)-dependent Cl- transport in T84 human colonic epithelial cells. Am J Physiol 1996;271(3 Pt 1):C914–22.
[63] Keely SJ, Barrett KE. ErbB2 and ErbB3 receptors mediate inhibition of calcium-dependent chloride secretion in colonic epithelial cells. J Biol Chem 1999;274(47):33448–54.
[64] Chow JY, Uribe JM, Barrett KE. A role for protein kinase cepsilon in the inhibitory effect of epidermal growth factor on calcium-stimulated chloride secretion in human colonic epithelial cells. J Biol Chem 2000;275(28):21169–76.
[65] Deachapunya C, Poonyachoti S. Activation of chloride secretion by isoflavone genistein in endometrial epithelial cells. Cell Physiol Biochem 2013;32(5):1473–86.
[66] Illek B, Fischer H, Machen TE. Alternate stimulation of apical CFTR by genistein in epithelia. Am J Physiol 1996;270(1 Pt 1):C265–75.
[67] Chen P et al. EGFR-targeted therapies combined with chemotherapy for treating advanced non-small-cell lung cancer: a meta-analysis. Eur J Clin Pharmacol 2011;67(3):235–43.
[68] Crown JP et al. Pooled analysis of diarrhea events in patients with cancer treated with lapatinib. Breast Cancer Res Treat 2008;112(2):317–25.
[69] Keefe DM, Gibson RJ. Mucosal injury from targeted anti-cancer therapy. Support Care Cancer 2007;15(5):483–90.
[70] Medina PJ, Goodin S. Lapatinib: a dual inhibitor of human epidermal growth factor receptor tyrosine kinases. Clin Ther 2008;30(8):1426–47.
[71] Keisner SV, Shah SR. Pazopanib: the newest tyrosine kinase inhibitor for the treatment of advanced or metastatic renal cell carcinoma. Drugs 2011;71(4):443–54.
[72] van Erp NP, Gelderblom H, Guchelaar HJ. Clinical pharmacokinetics of tyrosine kinase inhibitors. Cancer Treat Rev 2009;35(8):692–706.
[73] Cusatis G et al. Pharmacogenetics of ABCG2 and adverse reactions to gefitinib. J Natl Cancer Inst 2006;98(23):1739–42.
[74] Baker DE. Loperamide: a pharmacological review. Rev Gastroenterol Disord 2007;7(Suppl. 3):S11–8.
[75] Thiagarajah JR et al. Discovery and development of antisecretory drugs for treating diarrheal diseases. Clin Gastroenterol Hepatol 2014;12(2):204–9.
[76] Caci E et al. Evidence for direct CFTR inhibition by CFTR(inh)-172 based on Arg347 mutagenesis. Biochem J 2008;413(1):135–42.
[77] Ko EA et al. Chloride channel inhibition by a red wine extract and a synthetic small molecule prevents rotaviral secretory diarrhoea in neonatal mice. Gut 2014;63(7):1120–9.
[78] Crutchley RD, Miller J, Garey KW. Crofelemer, a novel agent for treatment of secretory diarrhea. Ann Pharmacother 2010;44(5):878–84.
[79] Cottreau J et al. Crofelemer for the treatment of secretory diarrhea. Expert Rev Gastroenterol Hepatol 2012;6(1):17–23.
[80] Tradtrantip L, Namkung W, Verkman AS. Crofelemer, an antisecretory antidiarrheal proanthocyanidin oligomer extracted from Croton lechleri, targets two distinct intestinal chloride channels. Mol Pharmacol 2010;77(1):69–78.
[81] Holodniy M et al. A double blind, randomized, placebo-controlled phase II study to assess the safety and efficacy of orally administered SP-303 for the symptomatic treatment of diarrhea in patients with AIDS. Am J Gastroenterol 1999;94(11):3267–73.
[82] DiCesare D et al. A double blind, randomized, placebo-controlled study of SP-303 (Provir) in the symptomatic treatment of acute diarrhea among travelers to Jamaica and Mexico. Am J Gastroenterol 2002;97(10):2585–8.
[83] Mangel AW, Chaturvedi P. Evaluation of crofelemer in the treatment of diarrhea-predominant irritable bowel syndrome patients. Digestion 2008;78(4):180–6.
[84] Keefe D, Anthony L. Tyrosine kinase inhibitors and gut toxicity: a new era in supportive care. Curr Opin Support Palliat Care 2008;2(1):19–21.

IJC
International Journal of Cancer

Dacomitinib-induced diarrhoea is associated with altered gastrointestinal permeability and disruption in ileal histology in rats

Ysabella Z.A. Van Sebille[1], Rachel J. Gibson[1,2], Hannah R. Wardill[1], Kate R. Secombe[1], Imogen A. Ball[1], Dorothy M.K. Keefe[1], John W. Finnie[3] and Joanne M. Bowen[1]

[1]Cancer Treatment Toxicities Group, Adelaide Medical School, University of Adelaide, Adelaide, Australia
[2]Division of Health Sciences, University of South Australia, Adelaide, Australia
[3]SA Pathology, Research Division, Adelaide, Australia

Dacomitinib—an irreversible pan-ErbB tyrosine kinase inhibitor (TKI)—causes diarrhoea in 75% of patients. Dacomitinib-induced diarrhoea has not previously been investigated and the mechanisms remain poorly understood. The present study aimed to develop an *in-vitro* and *in-vivo* model of dacomitinib-induced diarrhoea to investigate underlying mechanisms. T84 cells were treated with 1-4 μM dacomitinib and resistance and viability were measured using transepithelial electrical resistance (TEER) and XTT assays. Rats were treated with 7.5 mg/kg dacomitinib daily *via* oral gavage for 7 or 21 days ($n = 6$/group). Weights, and diarrhoea incidence were recorded daily. Rats were administered FITC-dextran 2 hr before cull, and serum levels of FITC-dextran were measured and serum biochemistry analysis was conducted. Detailed histopathological analysis was conducted throughout the gastrointestinal tract. Gastrointestinal expression of ErbB1, ErbB2 and ErbB4 was analysed using RT-PCR. The ileum and the colon were analysed using multiplex for expression of various cytokines. T84 cells treated with dacomitinib showed no alteration in TEER or cell viability. Rats treated with dacomitinib developed severe diarrhoea, and had significantly lower weight gain. Further, dacomitinib treatment led to severe histopathological injury localised to the ileum. This damage coincided with increased levels of MCP1 in the ileum, and preferential expression of ErbB1 in this region compared to all other regions. This study showed dacomitinib induces severe ileal damage accompanied by increased MCP1 expression, and gastrointestinal permeability in rats. The histological changes were most pronounced in the ileum, which was also the region with the highest relative expression of ErbB1.

Cancer Therapy and Prevention

Dacomitinib (PF-00299804) is an orally administered, highly selective irreversible small-molecule pan-ErbB receptor tyrosine kinase inhibitor (TKI) under development for treatment of recurrent or metastatic non-small cell lung cancer (NSCLC).[1] It acts by covalently binding to the intracellular adenosine triphosphate domain of each of the three kinase-active members of the ErbB family (ErbB1, ErbB2 and ErbB4). This effectively inhibits phosphorylation of the receptors and therefore downstream signaling.[2] In addition to being expressed on cancer cells, the ErbB family are also abundantly expressed on the basolateral membrane of healthy gastrointestinal epithelial cells, and are crucial for essential functions including maintenance of mucosal integrity *via* induction of mucus and prostaglandin synthesis, promotion of enterocyte migration, prevention of intestinal epithelial cell apoptosis, decreasing bacterial translocation and preservation of gut barrier function after injury.[3–5]

Dacomitinib is currently in Phase III clinical trials for NSCLC and has shown significant therapeutic effects, specifically to tumours which have not previously responded to conventional single receptor inhibitors.[6] Furthermore, dacomitinib has shown to be effective against tumours with mutations developed for acquired resistance of targeted therapies.[7] However a commonly reported adverse event among all trials has been diarrhoea, with up to 78% of patients developing some degree of diarrhoea.[8] Severe diarrhoea commonly results in dose reductions and patient withdrawal from clinical trials.[8] Of particular clinical importance is dacomitinib is delivered in a continuous manner over many months; therefore, to optimise dacomitinib therapy, adequate management or prevention of chronic diarrhoea is essential to minimise the impact on the patient's quality of life, increase safety and the ability to complete the course of therapy. Currently management for dacomitinib-induced diarrhoea follows that used in conventional chemotherapy (daily loperamide), however

Key words: dacomitinib, mucositis, diarrhoea, TKI, ErbB
Additional Supporting Information may be found in the online version of this article.
Grant sponsor: Pfizer (Unrestricted investigator initiated)
DOI: 10.1002/ijc.30699
History: Received 13 Dec 2016; Accepted 23 Feb 2017; Online 17 Mar 2017
Correspondence to: Ms Ysabella Van Sebille, Cancer Treatment Toxicities Group, Adelaide Medical School, The University of Adelaide, Frome road, Adelaide, 5005, Tel.: +61-8-83133787, E-mail: ysabella.vansebille@adelaide.edu.au

What's new?
Dacomitinib can hunt down and kill tumor cells that resist other chemotherapy drugs. But the same receptor family that dacomitinib seizes in tumor cells—the ErbB family—also adorn healthy gastrointestinal epithelial cells, causing most patients to suffer from dacomitinib-induced diarrhea. These authors sought to understand the mechanism behind this, in hopes of managing it. In rats, they observed that dacomitinib caused severe injury to the ileum, which is the region with the highest ErbB1 expression, and gastrointestinal permeability. Inflammation by monocyte infiltration also seems likely to contribute to the damage, since they observed increased MCP-1 in the ileum.

the mechanisms underlying this diarrhoea are likely different.[9] Recent Phase II research has investigated both antibiotic and probiotic prophylactic treatment for dacomitinib-induced diarrhoea, with no change in diarrhoea reported.[10] It is hypothesised that the development of dacomitinib-induced diarrhoea differs from conventional chemotherapy-induced diarrhoea and does not result due to direct cytotoxicity but rather occurs through alternative mechanisms.[9,11] As such, traditional diarrhoea management may be not targeting the underlying changes for optimal management. Therefore, this study assessed direct cytotoxicity in an *in vitro* model, and then aimed to develop an *in vivo* rat model of dacomitinib-induced diarrhoea, characterising the changes that dacomitinib causes through the gastrointestinal tract.

Material and Methods

Chemicals

Dacomitinib (PF-00299804) was kindly provided by Pfizer Pharmaceuticals. For all *in vivo* experiments dacomitinib was suspended in 0.5% (w/w) hydroxypropyl-methylcellulose to a final concentration of 2 mg/ml. For all *in vitro* experiments dacomitinib was suspended in DMSO. SN38 and TX100 were used as positive controls *in vitro*, both suspended in DMSO. Exposure of DMSO to cells did not exceed 0.01%.

In vitro model

The model utilised T84 cells (passage 5–15) derived from a human colorectal carcinoma (Culture Collections, Porton Down, UK). Cells were authenticated by Culture Collections by DNA profiling and were used within 6 months of receipt. Cells were maintained at 37°C in 5% CO_2/95% air in Dulbecco's Modified Eagle Medium (DMEM)/Ham's F-12 Nutrient Mixture containing 15 mM HEPES, L-glutamine and 10% foetal bovine serum (FBS) and were routinely screened for mycoplasma infection. Cells were seeded at a density of 100,000 cells/cm^2 on 1.12 cm^2, 0.4 μm pore polyester transwell inserts (Corning Life Sciences, MA) or at 10,000 cells in 96 well microtiter flat-bottom plates (Becton Dickinson) for transepithelial electrical resistance (TEER) measurements and cell proliferation (XTT) assays (Roche, Australia) respectively. Dacomitinib was diluted to a series of concentrations (1–4 μM) and exposed to cells *via* the apical side for 24–48 hr. An equivalent dilution of DMSO was used as vehicle control treatment. SN-38 (5 μM), an inhibitor of topoisomerase 1, was used as the positive control as it is recognised for its cytotoxicity.[12] Triton X-100 was used as the positive control for TEER measurements as it is known to permeabilise T84 cells.[13] All experiments were performed in triplicate and repeated twice.

Polyester transwell inserts support a polarised T84 phenotype with functional tight junctions; TEER is a measure to assess the integrity of this monolayer.[13] Once cells had reached 1,000 Ω/cm^2, indicating monolayer formation, cells were exposed to varying doses of dacomitinib for 24 or 48 hr. Transepithelial electrical resistance (TEER) was measured using an EVOM2 epithelial volt-ohm-meter with chopstick electrodes, STX2 (World Precision Instruments, Sarasota, FL) and area adjusted for analysis using the following formula;

$$\text{TEER monolayer } (\Omega/\text{cm}^2) = [\text{raw TEER } (\Omega) - \text{TEER blank } (\Omega)/\text{area of membrane } (1.12\ \text{cm}^2)].$$

XTT assays were conducted on cells exposed to 1–4 μM dacomitinib in total media for 24 hr. Following 24 hr exposure, media and dacomitinib were removed and replaced with 100 μl fresh media and 50 μl of XTT solution; composed of 5 ml XTT labelling reagent and 100 μl of electron coupling reagent (Roche cell proliferation kit, Germany). The microtitre plate was incubated again for 6 hr at 37°C in 5% CO_2/95% air. Absorbance was read at 490 nm using Bio Tek Synergy™ Mx Microplate Reader (Bio Tek, Vermont) and Gen5 version 2.00.18 software to assess the cleavage of tetrazolium salt XTT in the presence of an electron-coupling reagent, producing a soluble formazan salt, only occurring in viable cells.

In vivo model and ethics

The study was approved by the Animal Ethics Committee of The University of Adelaide, and complied with the National Health and Medical Research Council (Australia) Code of Practice for Animal Care in Research and Training (2014). Rats were group housed in ventilated cages with three to six animals per cage and were on a 12 hr light/dark cycle. Food and water were provided *ad libitum*.

Experimental design

All experiments were conducted on male Albino Wistar rats (initial age 6 weeks) obtained from The University of

Adelaide Laboratory Animal Service (SA, Australia). Rats were treated with dacomitinib at a dose of 7.5 mg/kg administered daily for 7 or 21 days, *via* oral gavage using a soft plastic feeding tube. This treatment schedule mimics the clinical oral administration over many weeks and allows assessment of acute damage (7 days) and prolonged damage (21 days). Control animals received daily gavage with dacomitinib vehicle (0.5% [w/w] hydroxypropyl-methylcellulose). Rats were randomly assigned to treatment groups and culled at 7 and 21 days ($n = 6$/group). Rats were anaesthetised using isoflurane inhalation, and were culled *via* cardiac exsanguination and cervical dislocation.

Clinical assessment of gastrointestinal toxicity

All rats were monitored two times daily for the presence of diarrhoea. Two independent assessors quantified diarrhoea using a validated grading system where 0 = no diarrhoea, 1 = mild diarrhoea with soft stools and perianal staining, 2 = moderate diarrhoea with loose stools and perianal staining of fur, 3 = severe diarrhoea with watery stools ± mucous and fur staining incorporating hind legs.[14] Rats were weighed daily to track weight loss/gain. Rats were culled if they displayed > 15% weight loss or significant distress and deterioration, in compliance with animal ethical requirements. One animal was removed from the study due to > 15% weight loss from the dacomitinib group. This animal was not included in any further analysis.

Tissue preparation

At necropsy, the entire gastrointestinal tract from pyloric sphincter to rectum was dissected and flushed with saline to remove intestinal contents. Samples of jejunum, ileum and colon were collected and either (*i*) fixed in 10% formalin for embedding in paraffin, (*ii*) had the mucosal surface scraped and stored in RNA-later at −20°C for molecular analyses, or (*iii*) had the mucosal surface scraped and snap frozen in liquid nitrogen and stored in −80°C for immunological analysis. Other organs were collected as routine and fixed in formalin and embed in paraffin. All histopathological analysis was conducted on 5 µm sections tissue cut on a rotary microtome and mounted onto glass Superfrost® microscope slides (Menzel-Gläser, Braunschweig, Germany). Slides were scanned using a NanoZoomer™ (Hamamatsu Photonics, Japan) and assessed with NanoZoomer Digital Pathology software view.2 (Histalim, Montpellier, France).

Blood biochemistry

Blood samples were collected by cardiac puncture. Serum was separated by centrifugation at 3,000*g* for 5 min before being analysed by the Department of Clinical Pathology, SA Pathology, Adelaide, South Australia. A multiple blood analysis (MBA-20) was conducted.

Gastrointestinal histopathological analysis

Haematoxylin and eosin (H&E) staining was performed and a well described total tissue injury score was generated based on the occurrences of eight histological criteria in the jejunum and ileum, and six criteria in the colon.[15,16] These criteria were villous fusion and villous atrophy (jejunum and ileum only), disruption of brush border and surface enterocytes, crypt loss/architectural disruption, disruption of crypts cells, infiltration of polymorphonuclear cells and lymphocytes, dilation of lymphatic's and capillaries and oedema. Each parameter was scored as present = 1, or absent = 0, in a blinded fashion.

Goblet cell analysis

Alcian Blue (1% Alcian Blue 8GX (CI 74240) in 3% glacial acetic/Periodic acid Schiff staining was performed on jejunum, ileum and colon. Sections were oxidised in 1% periodic acid before washing then treated in Schiff's reagent. Goblet cells and cavitated cells in crypts and villi that were deemed to be >80% complete were counted, and a total of at least 15 villi/crypts per section analysed. Data presented as average per crypt or villous. All analysis was done in a blinded fashion.

Immunohistochemistry

Immunohistochemical analysis was performed for apoptosis (caspase 3; Abcam, Vic, Australia; #ab4051), and proliferation (Ki67; Abcam, Vic, Australia #ab16667). Changes in these parameters are validated markers for altered tissue kinetics in previous models of cancer therapy induced-gastrointestinal toxicities.[17–20] Immunohistochemical analysis was performed using Dako reagents on an automated machine (AutostainerPlus™, Dako, Denmark) following standard protocols supplied by the manufacturer. Briefly, sections were deparaffinised in histolene and rehydrated through graded ethanol before undergoing heat mediated antigen retrieval using an EDTA/Tris buffer (0.37 g/L EDTA, 1.21 g/L Tris; pH 9.0). Retrieval buffer was preheated to 65°C using the Dako PT LINK (pre-treatment module). Slides were immersed in the buffer and the temperature raised to 97°C for 20 min. After returning to 65°C, slides were removed and placed in the Dako AutostainerPlus and stained following manufactures guidelines. Negative controls had the primary antibody omitted. Caspase 3 and Ki67 were quantified by counting the number of positively stained cells for 15 crypts. Data presented as average positively stained cells per crypt. All analysis was done in a blinded fashion.

Real time PCR

To asses the expression of ErbB1, ErbB2 and ErbB4 receptors along the gastrointestinal tract, total RNA was isolated from duodenal, jejunal, ileal and colonic mucosal scrapings. Purification of mRNA was done using the Nucleospin mRNA purification RNA II kit (Macherey-Nagel) following the

manufacturer's protocol. RNA (1 μg) was reverse transcribed using iScript™ cDNA synthesis kit (Bio-Rad) according to the manufacturer's protocol. cDNA was quantified and diluted to a working concentration of 100 ng/μl. Primers for genes of interest were either designed using web-based primer design program Primer 3, version 4 (http://bioinfo.ut.ee/primer3-0.4.0/), or in the case of ErbB4 purchased from Bio-Rad (Gladesville, Australia). Genes of interest were ErbB1 (Forward: 5'-CCCACAGCAAGCCTTCTTCA; Reverse: R: 5'-CACGGCAGCTCCCATTTCTA), ErbB2 (Forward: 5'-GCTCCTCCTTGAGTTGAGTGT; Reverse: 5'-TAGCCTTG-GAATGAGTGCGT) and ErbB4 (PrimePCR™ SYBR® Green Assay: ErbB4, rat). ErbB1 and ErbB2 were denatured at 95°C for 10 sec, annealed at 52°C for 15 sec, and extended at 72°C for 20 sec (40–45 cycles). ErbB4 was following manufactures instructions. Amplified transcripts were detected by SYBR Green (Quantitect, Qiagen) in a Rotor-Gene Q (Qiagen). All reactions were completed in triplicate, with two housekeeping normaliser primers, UBC (Forward: 5'-TCGTACCTTTCTCA CCACAGTATCTAG; Reverse: 5'-GAAAACTAAGACACCT CCCCATCA) and B2M (Forward: 5'-TGACCGTGATCTTT CTGGTG; Reverse: 5'-ATCTGAGGTGGGTGGAACTG). Amplification was followed by a melt curve analysis to confirm product specificity. Relative gene expression was determined by delta Ct method.[21]

Tissue cytokine quantification

Proinflammatory cytokine expression was assessed using 30 mg of ileal and colonic mucosal scraping samples. Mucosa samples were homogenised at room temperature using the QIAGEN TissueLyser LT (Qiagen) for 5 min at 50 Hz in 500 μL of the Radioimmunoprecipitation Assay (RIPA) buffer (150 mmol/L NaCl, 1.0% IGEPAL CA-630, 0.5% sodium deoxycholate, 0.1% SDS and 50 mmol/L Tris, pH 8.0; Sigma Aldrich; #04693116001). Homogenates were centrifuged at 11,000g for 15 min at 4°C and the supernatant isolated, aliquoted, and stored at −80°C. Total protein concentration was quantified using the Pierce BCA Protein Assay Kit (ThermoFisher Scientific; #23225). A working concentration of 1 mg/ml was used for cytokine analysis. Levels of 7 different cytokines, including interleukin-1β (IL-1β), interleukin-6 (IL-6), interleukin-17 (IL-17), tumour necrosis factor alpha (TNFα), monocyte chemoattractant protein-1 (MCP-1), interleukin-4 (IL-4) and interleukin-10 (IL-10), were measured in individual ileal and colonic homogenates using Luminex xMAP technology (Milliplex Rat Cytokine Kit, Merck Millipore; #RECYTMAG-65 K) as per the manufacturer's instructions. Each 96 well plate included a 6-point standard curve and two quality controls provided by Merck Millipore.

FITC-dextran assay

Two hours prior to culling, rats received a 600 mg/kg dose (120 mg/ml) of 4 kDa fluorescein isothiocyanate (FITC)-dextran (Sigma-Aldrich, NSW, Australia, Cat# FD4) *via* oral gavage. Blood was collected *via* cardiac puncture at necropsy into serum-gel clotting activator tubes and protected from light. Samples were centrifuged at 3,000g for 5 min and serum isolated. Serum samples were diluted 1:3 with 1 X PBS and quantified using the Bio Tek Synergy™ Mx Microplate Reader (Bio Tek, Vermont) and Gen5 version 2.00.18 software relative to a standard curve (range 0.0001–10 μg/ml).

Statistical analysis

Data were compared using Prism version 7.0 (GraphPad® Software, San Diego). A D'Agostino Pearson omnibus test was used to assess normality. When normality was confirmed, a two-way analysis of variance (ANOVA) with appropriate *post hoc* testing was performed to identify statistical significance between groups. In other cases, a Kruskal–Wallis test with Dunn's multiple comparisons test and Bonferroni correction was performed. For diarrhoea data, a Chi^2 test was used.

Results

Dacomitinib does not cause direct cytotoxicity to T84 epithelial cells

T84 monolayers exhibited comparable TEER between controls and monolayers treated with dacomitinib (1–4 μM), with no significant differences detected ($p > 0.05$). TEER readings for cells treated with all doses of dacomitinib were significantly higher than SN38, the positive control ($p < 0.05$; Fig. 1*a*). Cells treated with varying doses of dacomitinib (1–4 μM) had no alterations in cell viability, as measured by XTT absorbance, with no significant differences seen between controls (Fig. 1*b*). Compared to the positive control (SN38), cells treated with dacomitinib had significantly increased viability ($p < 0.05$; Fig. 1*b*). Combined, these results demonstrate that dacomitinib does not cause direct cytotoxicity to T84 cells.

Dacomitinib causes reproducible, severe diarrhoea

Rats treated with vehicle control did not develop diarrhoea at any time point (data not shown). Dacomitinib treatment induced diarrhoea in 100% of rats (Fig. 2*a*), comparable to the incidence seen in clinical trials.[8] Mild diarrhoea developed in a small number of animals from as early as Day 2 of treatment, with severe diarrhoea manifesting as early as Day 3. Diarrhoea incidence peaked from Day 7 onward. The average number of days with diarrhoea was 14 days. Rats treated with dacomitinib had significantly worse diarrhoea than control rats ($p < 0.0001$).

Growth rates of dacomitinib treated rats were significantly lower than control rats from Day 10 ($p < 0.0001$; Fig. 2*b*). At Day 21, the control group had gained 46.38 ± 2.459% body weight compared to Day 1, and the dacomitinib group had gained 18.99 ± 5.602% body weight compared to Day 1.

Dacomitinib alters biochemistry and histology

In rats treated with dacomitinib, serum biochemistry revealed mildly elevated alanine aminotransferase (ALT) which, in the

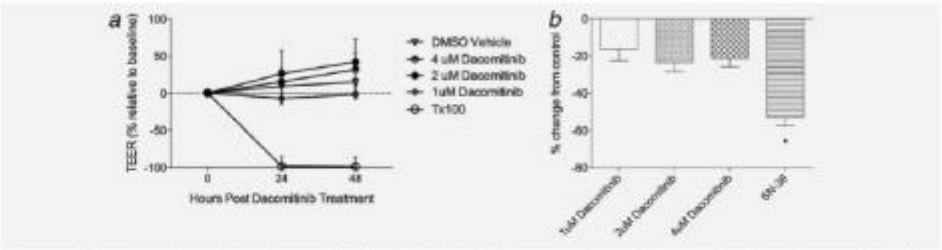

Figure 1. (*a*) Transepithelial electrical resistance (TEER) following dacomitinib exposure (1–4 μM) for 24–48 hr did not decrease ($p > 0.05$). Data presented as mean ± SEM. Data analysed using two-way ANOVA. (*b*) Absorbance of XTT assay did not decrease following 24 hr of dacomitinib exposure (1–4 μM) compared to controls, but was significantly higher than SN-38 ($p < 0.05$). Data presented as mean ± SEM. Data analysed using one-way ANOVA.

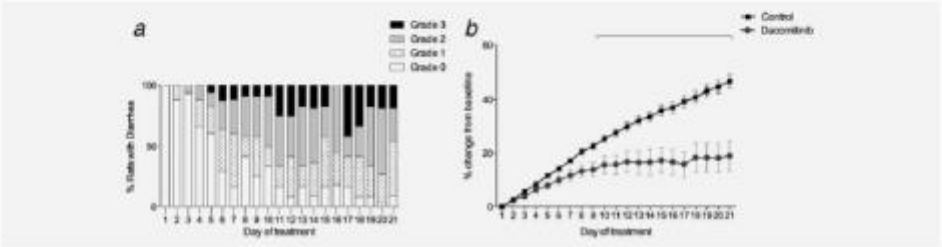

Figure 2. (*a*) Rats treated with vehicle control did not develop diarrhoea. 100% of rats treated with 7.5 mg/kg dacomitinib developed diarrhoea. Diarrhoea data are expressed as a percentage of total animals (per day) with a particular grade of diarrhoea. (*b*) Rats treated with 7.5 mg/kg dacomitinib had significantly lower weight gain than controls from Day 10 onward ($p < 0.0001$). Data displayed as a percentage of weight change from baseline (Day 1). A Kruskal–Wallis with *post hoc* testing was performed to identify statistical significance.

absence of histological changes in the liver, suggested increased permeability of hepatocyte cell membranes with leakage of this cytosolic enzyme into the blood (Supporting Information Table 1). There was also a modest increase in blood urea nitrogen (BUN) and creatinine, particularly at 21 days, indicating mild renal dysfunction (Supporting Information Table 1). A mild hypoalbuminaemia was probably attributable to a combination of malabsorption due to villous atrophy, protein-losing enteropathy associated with severe diarrhoea, and renal proteinuria. All other MBA-20 analytes were within the normal range (Supporting Information Table 1). Kidneys of all rats, except one, treated with dacomitinib for 21 days showed acute papillary necrosis with severe coagulation necrosis of medullary tubules and collecting duct epithelium, either complete or with intraluminal, desquamated, necrotic epithelial cells and few, usually degenerating, lining epithelial cells with marked interstitial congestion. One rat treated with dacomitinib for 21 days showed mild hydronephrosis, with dilation of renal pelvis and patchy distension of tubules and collecting ducts. Rats treated with dacomitinib for 7 days exhibited mild glomerulopathy with thickening of the glomerular basement membranes.

Dacomitinib causes significant ileal damage

Rats treated with dacomitinib had significant ileal injury compared to controls at both time points ($p < 0.0001$). This was predominantly characterised by severe villus atrophy with stunting and fusion of villi, which was also attended by enterocyte metaplasia to a low columnar or cuboidal phenotype and mild compensatory expansion of the basal proliferative compartment of crypts. In the congested lamina propria, there was an increased inflammatory infiltrate comprised of lymphocytes, macrophages, plasma cells and neutrophils and dilation of lacteals (villous lymphatics) (Fig. 3). There were no significant differences in tissue injury at any time point in the jejunum and colon (data not shown). Across both treatment groups no significant differences for both total number of goblet cells or percentage cavitated goblet cells in the jejunum, ileum or colon as assessed *via* AB-PAS staining were seen (data not shown).

Dacomitinib did not alter gastrointestinal apoptosis or proliferation

To assess gastrointestinal epithelial apoptosis, the number of caspase-3 positively stained crypt cells were counted and

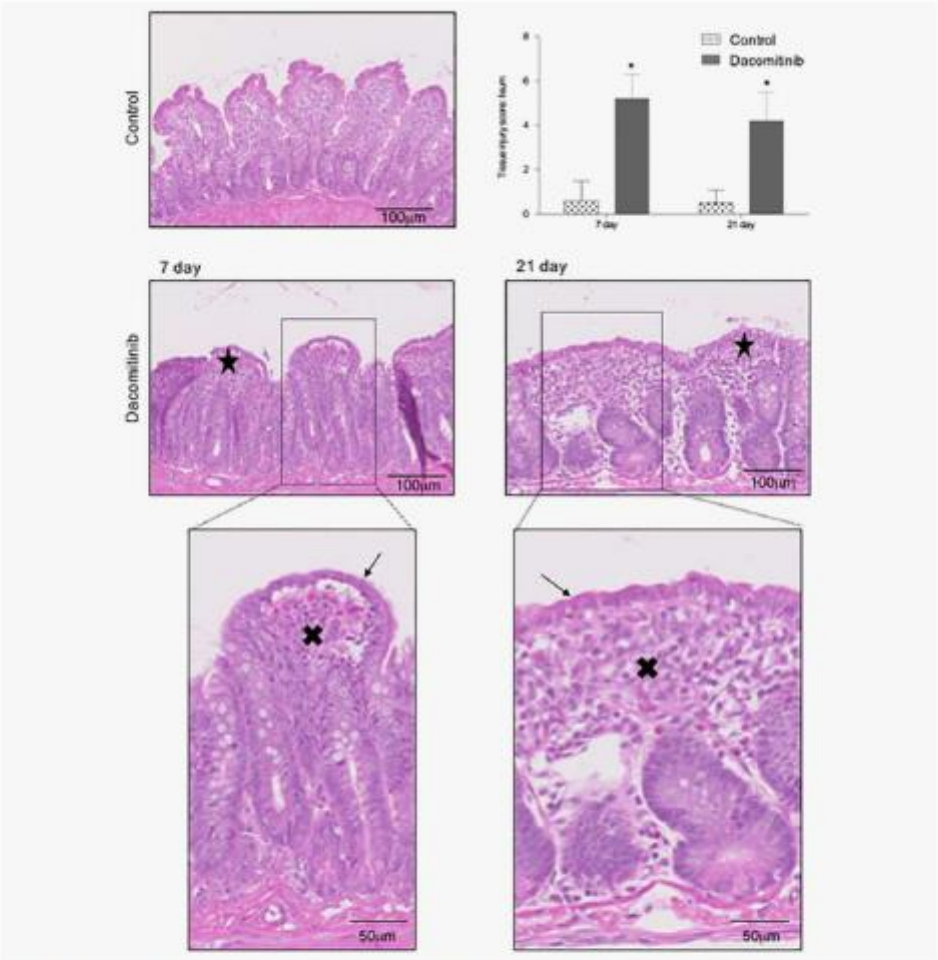

Figure 3. Histological injury was significantly increased in the ileum in rats treated with dacomitinib at both Day 7 ($p < 0.0001$) and Day 21 ($p < 0.0001$). Histological injury was characterised by villus atrophy/blunting and fusion (indicated by black stars), enterocyte metaplasia to a low columnar or cuboidal epithelium (indicated by black arrows), and increased inflammatory component in the lamina propria (indicated by black cross). There was no significant change in histological injury in the jejunum or colon. Tissue injury score presented as mean ± SD. [Color figure can be viewed at wileyonlinelibrary.com]

means calculated. Gastrointestinal apoptosis was not changed following dacomitinib treatment in the crypts of the jejunum at Day 7 (dacomitinib 0.11 ± 0.053 *vs.* control 0.04 ± 0.02) or Day 21 (dacomitinib 0.24 ± 0.05 *vs.* control 0.10 ± 0.03). Gastrointestinal apoptosis was not changed following dacomitinib treatment in the crypts of the ileum at Day 7 (dacomitinib 0.03 ± 0.02 *vs.* control 0.03 ± 0.01) or Day 21 (dacomitinib 0.03 ± 0.01 *vs.* control 0.02 ± 0.02). Gastrointestinal apoptosis was not changed following dacomitinib treatment in the crypts of the colon at Day 7 (dacomitinib 1.27 ± 0.37 *vs.* control 1.20 ± 0.27) or Day 21 (dacomitinib 0.94 ± 0.17 *vs.* control 0.82 ± 0.18). To assess proliferation within crypts, the number of Ki-67 positively stained cells were counted and means calculated. Gastrointestinal

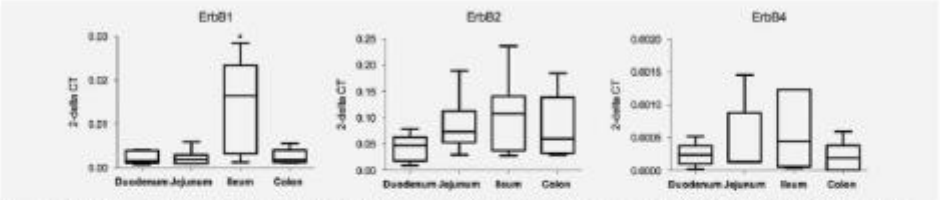

Figure 4. ErbB1 expression is significantly higher in the ileum compared to other areas of the gastrointestinal tract ($p = 0.0336$). Relative mRNA expression of ErbB receptors to UBC and B2M. Data presented as min–max. Data analysed using one-way ANOVA.

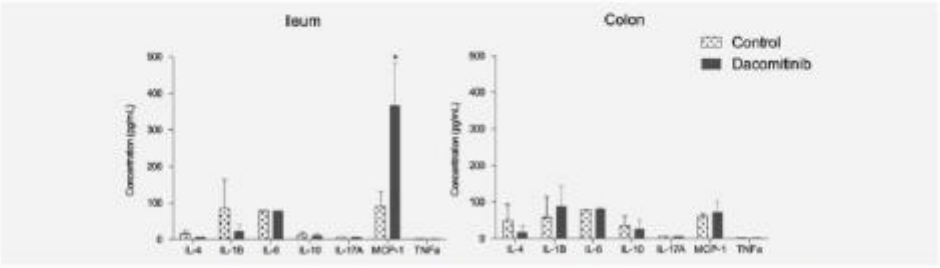

Figure 5. Cytokine expression in the mucosa of the ileum and colon. MCP-1 was significantly increased in the ileum of rats treated with dacomitinib ($p = 0.001$) compared to controls. Data presented as mean with SD (pg/mL). Multiple t-tests were performed to identify statistical significance. MCP-1 expression was increased in the mucosa of the ileum in animals treated with dacomitinib compared to control ($p = 0.001$).

proliferation was not changed following dacomitinib treatment in the crypts of the jejunum at Day 7 (dacomitinib 21.72 ± 0.53 *vs.* control 21.07 ± 0.07) or Day 21 (dacomitinib 18.82 ± 1.31 *vs.* control 22.70 ± 0.68). Gastrointestinal proliferation was not changed following dacomitinib treatment in the crypts of the ileum at Day 7 (dacomitinib 33.71 ± 3.60 *vs.* control 38.81 ± 2.63) or Day 21 (dacomitinib 39.02 ± 1.66 *vs.* control 40.57 ± 1.84). Gastrointestinal proliferation was not changed following dacomitinib treatment in the crypts of the colon at Day 7 (dacomitinib 12.85 ± 0.87 *vs.* control 14.56 ± 3.74) or Day 21 (dacomitinib 11.91 ± 2.30 *vs.* control 16.22 ± 1.88).

ERBb1 receptor is highly expressed in the ileum

The mRNA expression of ErbB1 was significantly higher in the ileum compared to the other regions of the gastrointestinal tract in untreated control rats ($p = 0.0336$; Fig. 4). The expression of ErbB2 and ErbB4 was unchanged throughout the gastrointestinal tract ($p > 0.05$). Treatment with dacomitinib did not change the expression of the ErbB receptors ($p > 0.05$) (data not shown).

Dacomitinib treatment increases levels of monocyte chemoattractant protein-1 (MCP-1) in the ileum

There were significant increases in the expression of MCP-1 in the ileum of rats treated with dacomitinib compared to controls ($p = 0.001$). No changes were seen in the colon. Rats treated with dacomitinib showed no statistically significant change in IL-1β, IL-6, IL-17, TNFα, IL-4 and IL-10 expression in the ileum or colon when compared to vehicle controls (Fig. 5).

Dacomitinib caused increased gastrointestinal permeability

Serum FITC-dextran levels were elevated in rats treated with dacomitinib compared to vehicle controls, ($p = 0.0018$; Fig. 6).

Discussion

Dacomitinib is an emerging small molecule TKI for the treatment of NSCLC, with clinical trials showing diarrhoea as an adverse event in over 78% of patients.[8] The mechanisms of ErbB TKI-induced diarrhoea are unclear with conflicting hypotheses presented in the literature.[9] The present study found dacomitinib does not cause direct cytotoxicity to T84 epithelial cells, supporting the study hypothesis, and previous literature suggesting that ErbB TKI induced-diarrhoea is not due to direct cell death.[22,23] However, this may be explained because of the colorectal origin of T84 cells, as in rats dacomitinib causes diarrhoea that appears associated with histopathological alterations in the ileum and intestinal barrier disruption. This is the first time gastrointestinal morphometry and function have been characterised following dacomitinib, demonstrating dacomitinib causes histopathological

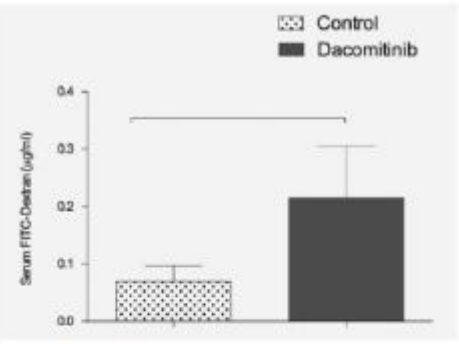

Figure 6. Serum FITC-dextran levels were significantly increased in rats treated with dacomitinib ($p = 0.0018$) indicating intestinal barrier dysfunction. Data presented as mean with SD. Data analysed using one-way ANOVA.

damage confined to the ileum in rats. In murine models of ErbB TKI-induced gastrointestinal side effects, there has previously been evidence of histological changes characterised by villous atrophy.[11,24–27]

TKI's have previously been associated with diarrhoea, and this has been largely hypothesised to be of a secretory phenotype.[9,11] In a previous rat model of lapatinib-induced diarrhoea, blood biochemistry showed a significant decrease in serum chloride. This decrease coincided with diarrhoea in rats treated with high-dose lapatinib, suggesting a possible secretory diarrhoea phenotype.[20] However, in the current study we saw no changes in serum chloride suggesting negligible secretory processes. Although not the primary focus of the study, the findings from blood biochemistry indicate rats treated with dacomitinib had significant changes in renal biochemistry, with supplementary histological investigation supporting this. These findings are despite renal clearance of dacomitinib being only minimal.[28] As such, the renal pathology seen in this model is likely to be a species-specific response to high dose dacomitinib. The increased level of liver enzymes seen in the present study is consistent with elevations noted clinically,[28] and are unsurprising given that dacomitinib is largely metabolised by the liver through oxidative and conjugative metabolism.[28]

Traditional chemotherapeutic agents are known to cause severe gastrointestinal cytotoxicity, resulting in histological damage manifesting as anatomic derangement diarrhoea.[16,17] However, throughout the literature there are conflicting findings regarding the histopathological changes in the gastrointestinal tract associated with ErbB TKI-induced diarrhoea.[9] For example, a recent study by Bowen *et al.* (2012) showed lapatinib-induced diarrhoea was not associated with gastrointestinal histopathological changes, typically associated with anatomic derangement diarrhoea.[14] Hare *et al.* (2007) showed treatment with gefitninib in a murine model was associated with villous atrophy, confined to the duodenum only.[9] However, Rasmussen *et al.* (2010) suggested that inhibition of the ErbB receptors with erlotinib causes direct mucosal atrophy and damage, which, similar to this study, was most pronounced in the ileum of mice.[24] This study showed largely negative results, with marginal changes noted in the jejunum or colon. However, significant histopathological changes were noted in the ileum, characterised by significant villus atrophy. Unlike traditional chemotherapy-induced diarrhoea, villus shortening and blunting was localised to the ileum, with terminally differentiated enterocytes being the most affected. There were only mild compensatory changes in the deep crypt progenitor compartment and no associated goblet cell hyperplasia or apoptosis. This supports the hypothesis suggesting an alternative mechanism may be responsible for the changes seen following dacomitinib treatment.

While small intestinal damage has previously been attributed to greater exposure of the unabsorbed drug to the mucosal surface compared to the colon,[29] this is not a plausible explanation in the current study, as the jejunum showed minimal histopathological damage. The differential expression or ErbB receptors through regions of the gastrointestinal tract has not been previously characterised. Data from the present study indicates ErbB1 is preferentially expressed in the ileum compared to other regions of the gastrointestinal tract. It is therefore possible that the high degree of histopathology observed in the ileum may be linked to the high expression of ErbB1. Unlike first generation ErbB TKIs that are susceptible to mutations that affect binding affinity, second generation ErbB TKIs (such as dacomitinib) are irreversible and resistant to mutations, they have therefore demonstrated a higher binding affinity.[30] This may account for the more severe ileal damage seen in our model, and the associated diarrhoea.

Elevated MCP-1 was evident in the ileum, suggesting an inflammatory response characterised, in part, by monocyte infiltration, which may contribute to the ileal tissue injury. This is of particular significance as inflammation has been associated with the induction of a 'leaky' gut.[31,32] Mucosal enterocyte barrier disruption has been associated with a number of gastrointestinal pathologies characterised by diarrhoea.[33] It has been suggested that altered intestinal permeability worsens clinical outcomes, as it allows for translocation of endotoxin and bacteria.[32] Additionally, it has been proposed that breakdown of the intestinal mucosal barrier contributes to diarrhoea through leak-flux mechanisms allowing passive movement of water into the lumen.[34] Our findings partially support this with increased serum FITC-dextran seen following dacomitinib treatment. The increased gastrointestinal permeability noted in this study is most likely indicative of tight junction disruption, the main regulators of paracellular permeability. Tight junctions join the apical margins of adjacent enterocytes and, while permeable to small molecules and water, form a barrier to transepithelial macromolecular movement; the basolateral aspect of enterocytes is

the site of Na-K-dependent ATPase that drives the sodium pump. Further studies are required to examine the impact of dacomitinib on specific tight junction proteins. Although barrier dysfunction is emerging as a key driver of chemotherapy induced diarrhoea, this is the first study to implicate barrier dysfunction in the development of TKI induced diarrhoea, and will form the basis of further investigation.

Conclusions

In summary, this study has shown that dacomitinib induces severe ileal damage and gastrointestinal permeability in this model. The high expression of ErbB1 in the ileum was also accompanied by the localised damage seen only in this region. This is the first study to provide a detailed interrogation of the intestinal changes associated with dacomitinib treatment and advances our understanding of diarrhoea processes induced by not only this agent, but assists in further characterising the poorly understood mechanisms of ErbB TKI-induced diarrhoea.

ACKNOWLEDGEMENTS

This research was funded by an unrestricted investigator initiated grant with Pfizer.

Ysabella Van Sebille and Hannah Wardill are the recipients of The Doctor Chun Chung Woeg and Madam So Sau Lam Memorial Postgraduate Cancer Research Top Up Scholarship and Australian Postgraduate Awards.

Conflicts of Interest

Professor Gibson is a consultant for Mundipharma and for KaleidoBiosceinces and has received funding for contract research with Onyx Pharmaceuticals. She is also on the Board of Directors for MASCC and the Scientific Chair for the 2017; 2018 Annual Meeting. Professor Keefe has received funding for contract research from Pfizer, Entera and Helsinn and is a consultatnt for Merck, Novartis, Pfizer and Helsinn.

References

1. Abdul Razak AR, Soulieres D, Laurie SA, et al. A phase II trial of dacomitinib, an oral pan-human EGF receptor (HER) inhibitor, as first-line treatment in recurrent and/or metastatic squamous-cell carcinoma of the head and neck. *Ann Oncol* 2013;24:761–9.
2. Dietrich E, Antoniadis K. Molecularly targeted drugs for the treatment of cancer: oral complications and pathophysiology. *Hippokratia* 2012;16:196–9.
3. Hare KJ, Hartmann B, Kissow H, et al. The intestinotrophic peptide, glp-2, counteracts intestinal atrophy in mice induced by the epidermal growth factor receptor inhibitor, gefitinib. *Clin Cancer Res* 2007;13:5170–5.
4. Yarden Y, Sliwkowski MX. Untangling the ErbB signalling network. *Nat Rev Mol Cell Biol* 2001;2:127–37.
5. Chen CL, Yu X, James IO, et al. Heparin-binding EGF-like growth factor protects intestinal stem cells from injury in a rat model of necrotizing enterocolitis. *Lab Invest* 2012;92:331–44.
6. Ramalingam SS, Janne PA, Mok T, et al. Dacomitinib versus erlotinib in patients with advanced-stage, previously treated non-small-cell lung cancer (ARCHER 1009): a randomised, double-blind, phase 3 trial. *Lancet Oncol* 2014;15:1369–78.
7. Engelman JA, Zejnullahu K, Gale CM, et al. PF00299804, an irreversible pan-ERBB inhibitor, is effective in lung cancer models with EGFR and ERBB2 mutations that are resistant to gefitinib. *Cancer Res* 2007;67:11924–32.
8. Van Sebille YZ, Gibson RJ, Wardill HR, et al. Gastrointestinal toxicities of first and second-generation small molecule human epidermal growth factor receptor tyrosine kinase inhibitors in advanced nonsmall cell lung cancer. *Curr Opin Support Palliat Care* 2016;10:152–6.
9. Van Sebille YZ, Gibson RJ, Wardill HR, et al. ErbB small molecule tyrosine kinase inhibitor (TKI) induced diarrhoea: Chloride secretion as a mechanistic hypothesis. *Cancer Treat Rev* 2015;41:646–52.
10. Lacouture ME, Keefe DM, Sonis S, et al. A phase II study (ARCHER 1042) to evaluate prophylactic treatment of dacomitinib-induced dermatologic and gastrointestinal adverse events in advanced non-small-cell lung cancer. *Ann Oncol* 2016;27:1712–8.
11. Loriot Y, Perlemuter G, Malka D, et al. Drug insight: gastrointestinal and hepatic adverse effects of molecular-targeted agents in cancer therapy. *Nat Clin Pract Oncol* 2008;5:268–78.
12. Bowen JM, Gibson RJ, Cummins AG, et al. Intestinal mucositis: the role of the Bcl-2 family, p53 and caspases in chemotherapy-induced damage. *Support Care Cancer* 2006;14:713–31.
13. Wardill HR, Gibson RJ, Van Sebille YZ, et al. A novel in vitro platform for the study of SN38-induced mucosal damage and the development of Toll-like receptor 4-targeted therapeutic options. *Exp Biol Med (Maywood)* 2016;241:1386–94.
14. Bowen JM, Mayo BJ, Plews E, et al. Development of a rat model of oral small molecule receptor tyrosine kinase inhibitor-induced diarrhea. *Cancer Biol Ther* 2012;13:1269–75.
15. Howarth GS, Francis GL, Cool JC, et al. Milk growth factors enriched from cheese whey ameliorate intestinal damage by methotrexate when administered orally to rats. *J Nutr* 1996;126:2519–30.
16. Wardill HR, Gibson RJ, Van Sebille YZ, et al. Irinotecan-Induced Gastrointestinal Dysfunction and Pain Are Mediated by Common TLR4-Dependent Mechanisms. *Mol Cancer Ther* 2016;15:1376–86.
17. Gibson RJ, Bowen JM, Inglis MR, et al. Irinotecan causes severe small intestinal damage, as well as colonic damage, in the rat with implanted breast cancer. *J Gastroenterol Hepatol* 2003;18:1095–100.
18. Keefe DM, Brealey J, Goland GJ, et al. Chemotherapy for cancer causes apoptosis that precedes hypoplasia in crypts of the small intestine in humans. *Gut* 2000;47:632–7.
19. Logan RM, Gibson RJ, Bowen JM, et al. Characterisation of mucosal changes in the alimentary tract following administration of irinotecan: implications for the pathobiology of mucositis. *Cancer Chemother Pharmacol* 2008;62:33–41.
20. Bowen JM, Mayo BJ, Plews E, et al. Determining the mechanisms of lapatinib-induced diarrhoea using a rat model. *Cancer Chemother Pharmacol* 2014;74:617–27.
21. Livak F, Schatz DG. Alternative splicing of rearranged T cell receptor delta sequences to the constant region of the alpha locus. *Proc Natl Acad Sci USA* 1998;95:5694–9.
22. Keefe DM, Bateman EH. Tumor control versus adverse events with targeted anticancer therapies. *Nat Rev Clin Oncol* 2012;9:98–109.
23. Bowen JM. Mechanisms of TKI-induced diarrhea in cancer patients. *Curr Opin Support Palliat Care* 2013;7:162–7.
24. Rasmussen AR, Viby NE, Hare KJ, et al. The intestinotrophic peptide, GLP-2, counteracts the gastrointestinal atrophy in mice induced by the epidermal growth factor receptor inhibitor, erlotinib, and cisplatin. *Dig Dis Sci* 2010;55:2785–96.
25. Yusta B, Holland D, Koehler JA, et al. ErbB signaling is required for the proliferative actions of GLP-2 in the murine gut. *Gastroenterology* 2009;137:986–96.
26. Berlanga-Acosta J, Playford RJ, Mandir N, et al. Gastrointestinal cell proliferation and crypt fission are separate but complementary means of increasing tissue mass following infusion of epidermal growth factor in rats. *Gut* 2001;48:803–7.
27. Goodlad RA, Raja KB, Peters TJ, et al. Effects of urogastrone-epidermal growth factor on intestinal brush border enzymes and mitotic activity. *Gut* 1991;32:994–8.
28. Giri N, Masters JC, Plotka A, et al. Investigation of the impact of hepatic impairment on the pharmacokinetics of dacomitinib. *Invest New Drugs* 2015;33:931–41.
29. Bowen JM. Development of the rat model of lapatinib-induced diarrhoea. *Scientifica (Cairo)* 2014;2014:194185.
30. Peters S, Zimmermann S, Adjei AA. Oral epidermal growth factor receptor tyrosine kinase inhibitors for the treatment of non-small cell lung cancer: comparative pharmacokinetics and drug-drug interactions. *Cancer Treat Rev* 2014;40:917–26.
31. Velandia-Romero ML, Calderon-Pelaez MA, Castellanos JE. In vitro infection with dengue virus induces changes in the structure and

function of the mouse brain endothelium. *PLoS One* 2016;11:e0157786.
32. Wardill HR, Bowen JM, Van Sebille YZ, et al. TLR4-dependent claudin-1 internalisation and secretagogue-mediated chloride secretion regulate irinotecan-induced diarrhea. *Mol Cancer Ther* 2016;15:2767–79.
33. Nakao T, Kurita N, Komatsu M, et al. Irinotecan injures tight junction and causes bacterial translocation in rat. *J Surg Res* 2012;173:341–7.
34. Schmitz H, Fromm M, Bentzel CJ, et al. Tumor necrosis factor-alpha (TNFalpha) regulates the epithelial barrier in the human intest nal cell line HT-29/B6. *J Cell Sci* 1999;112:137–46.

IJC
International Journal of Cancer

Dacomitinib-induced diarrhea: Targeting chloride secretion with crofelemer

Ysabella Z.A. Van Sebille[3], Rachel J. Gibson[2], Hannah R. Wardill[3], Imogen A. Ball[3], Dorothy M.K. Keefe[1] and Joanne M. Bowen[3]

[1]Discipline of Physiology, Adelaide Medical School, University of Adelaide, Australia
[2]Division of Health Sciences, University of South Australia

Dacomitinib, an irreversible small-molecule pan-ErbB TKI, has a high incidence of diarrhea, which has been suggested to be due to chloride secretory mechanisms. Based on this hypothesis, crofelemer, an antisecretory agent may be an effective intervention. T84 monolayers were treated with 1 μM dacomitinib and 10 μM crofelemer, and mounted into Ussing chambers for electrogenic ion analysis. Crofelemer attenuated increases in chloride secretion in cells treated with dacomitinib. Albino Wistar rats ($n = 48$) were treated with 7.5 mg/kg dacomitinib and/or 25 mg/kg crofelemer *via* oral gavage for 21 days. Crofelemer significantly worsened dacomitinib-induced diarrhea ($p = 0.0003$), and did not attenuate weight loss ($p < 0.0001$). Sections of the ileum and colon were mounted into Ussing chambers, and secretory processes analyzed. This indicated that crofelemer lost its anti-secretory action in the presence of dacomitinib in this model. Mass spectrometry revealed that crofelemer did not change serum concentration of dacomitinib. Serum FITC dextran levels indicated that crofelemer was unable to attenuate dacomitinib-induced barrier dysfunction. Tight junction proteins were visualized with immunofluorescence. Qualitative analysis showed dacomitinib induced proteolysis of ZO-1 and occludin, and internalization of claudin-1, which was not attenuated by crofelemer. Detailed histopathological analysis showed that crofelemer was unable to attenuate dacomitinib-induced ileal damage. Crofelemer worsened dacomitinib-induced diarrhea, suggesting that antisecretory drug therapy may be ineffective in this setting.

Dacomitinib (PF-00299804) is an orally administered, irreversible small-molecule pan-ErbB receptor tyrosine kinase inhibitor (TKI) under development for the treatment of recurrent or metastatic non-small cell lung cancer (NSCLC).[1] Dacomitinib acts by covalently binding to the intracellular adenosine triphosphate domain of each of the three kinase-active members of the ErbB family (ErbB1, ErbB2 and ErbB4). This effectively inhibits phosphorylation of the receptor and therefore inhibits downstream signaling.[2] The most commonly reported adverse event associated with dacomitinib therapy has been diarrhea, with an incidence of around 73%.[3] Although less common, severe diarrhea can result in dose reductions (28%), treatment interruptions (12%) and treatment discontinuation (8%) from clinical trials.[4] Of particular clinical importance, dacomitinib is delivered in a continuous manner over many months, meaning diarrhea is often prolonged, and as such, impacts significantly on quality of life. Currently the treatment for TKI-induced diarrhea is loperamide or octreotide, however very few studies have looked at antidiarrheal agents in a targeted approach.[5–8]

Research in our laboratory has recently indicated that ErbB TKIs induce diarrhea due to chloride secretory mechanisms.[9] ErbB receptors are abundantly expressed on the basolateral membrane of healthy intestinal epithelial cells, and are crucial for normal functions and development of the gut. Of particular importance to this study, ErbB receptors in healthy settings are negative regulators of chloride secretion.[10,11] This study therefore hypothesized that inhibition of these receptors through the action of dacomitinib would result in a loss of the negative regulation of chloride, thus resulting in a secretory diarrhea phenotype.

Crofelemer is an antisecretory antidiarrheal proanthocyanidin oligomer extracted from *Croton lechleri*. It is approved by the U.S Federal Drug Administration for the treatment of diarrhea induced by antiretroviral medication for HIV patients and has been proposed as an intervention for pertuzumab-induced diarrhea.[12] Crofelemer inhibits the two principal apical channels for chloride secretion in enterocytes, with partial inhibition of the cAMP –dependent cystic fibrosis transmembrane conductance regulator (CFTR) and complete inhibition of the calcium activated chloride channel (CaCC).[13] Clinical studies have demonstrated that crofelemer

Key words: dacomitinib, mucositis, crofelemer, diarrhea, HER TKI
Additional Supporting Information may be found in the online version of this article.
Grant sponsor: Unrestricted Investigator Initiated Grant with Pfizer, Australia
DOI: 10.1002/ijc.31048
History: Received 26 May 2017; Accepted 31 Aug 2017; Online 16 Sep 2017
Correspondence to: Ms. Ysabella Van Sebille, Adelaide Medical School, University of Adelaide, North Terrace, Adelaide 5005, Australia, Tel.: [61883133787], E-mail: ysabella.vansebille@adelaide.edu.au

What's new?

Dacomitinib, an irreversible inhibitor of the ErbB receptor tyrosine kinase, induces diarrhea in about three-quarters of patients, potentially leading to treatment discontinuation. Diarrhea is suspected to result from effects on chloride secretory mechanisms. The present preclinical study investigated the possibility of using crofelemer, an antisecretory antidiarrheal agent with inhibitory effects on chloride channels, as a prophylactic in patients taking dacomitinib. In cells, crofelemer reduced dacomitinib-induced elevations in chloride secretion. Rats treated with dacomitinib and crofelemer combined, however, experienced severe diarrhea more often than dacomitinib-only treated animals. The findings suggest that crofelemer may have contraindications in dacomitinib-treated patients.

is a safe and tolerable drug, with no adverse effects being reported.[14–16] Crofelemer is also appealing because it is too large and polarized to be systemically absorbed, limiting any systemic effects including drug interactions and toxicities.[9] Therefore, this study investigated the effect of dacomitinib and crofelemer on chloride secretion *in vitro*, and then translated the study to a preclinical rat model of dacomitinib-induced diarrhea.

Material and Methods

Chemicals

Dacomitinib (PF-00299804) was kindly provided by Pfizer. Dacomitinib is soluble in dimethyl sulfoxide (DMSO) at 19 mg/ml. Aliquots of dacomitinib in DMSO (Sigma Aldrich) were added to Ringer's solution (composition in mmol/L: NaCl 115.4; KCl 5; $MgCl_2$ 1.2; NaH_2PO_4 0.6; $NaHCO_3$ 25; $CaCl_2$ 1.2 and glucose 10) to create a 50 μM concentration. Appropriate volumes were added to Ussing chambers to reach a final concentration of 1 μM with previous studies demonstrating doses above this result in off-target or nonspecific effects.[17] Secretory effects below 1 μM are therefore more likely to be due to the specific effect of the drug on its designed molecular target. Crofelemer (Salix Pharmaceuticals) was diluted with DMSO to 21 mg/ml (10 mM) and was diluted in ringer solution and administered at 10 μM. This dose has previously been shown to inhibit secretagogue activated chloride secretion in T84 cells.[13] Exposure of DMSO to cells did not exceed 0.01%. The same concentration of DMSO was used as a vehicle control. For all *in vivo* experiments, dacomitinib was suspended in 0.5% (w/w) hydroxypropylmethylcellulose (Sigma Aldrich) in sterile distilled water to a final concentration of 2 mg/ml. Crofelemer was suspended to a final concentration of 5 mg/ml in sterile distilled water.

In vitro model

Cell preparation and maintenance. This study utsed T84 cells (passage 5–15) derived from a human colorectal carcinoma (Culture Collections, Porton Down, UK). Cells were certified mycoplasma-free and authenticated by Culture Collections by DNA profiling and used within 6 months of receipt. Cells were maintained at 37°C in 5% CO_2/95% air in Dulbecco's Modified Eagle Medium (DMEM)/Ham's F-12 Nutrient Mixture containing 15 mM HEPES, L-glutamine and 10% fetal bovine serum (FBS) supplemented with 1% penicillin/gentamicin + fungizone and were grown in sterile, multiwell tissue culture plates under identical growth conditions. The T84 cell line retained its original morphology and growth characteristics over the range of passages used. Cells were seeded at a density of 100,000 cells/cm^2 on 1.12 cm^2, 0.4 μm pore polyester transwell inserts (Corning Life Sciences, MA). Cell culture media in both the apical and basolateral chambers was changed every 48 hr. Transepithelial electrical resistance (TEER) was monitored daily using an EVOM2 epithelial volt-ohm-meter with chopstick electrodes (World Precision Instruments, Sarasota, FL) for 1 week during the growth period and area adjusted for analysis using the following formula; TEER monolayer (Ω/cm^2) = [raw TEER (Ω) − TEER blank (Ω)]/area of membrane (cm^2).

In vitro electrophysiological studies using Ussing chambers

To test whether dacomitinib increased intestinal epithelial cell Cl^- secretion, short-circuit current (I_{sc}) was measured in T84 cells in symmetrical physiological solutions in Ussing chambers. Once adequate resistance was reached (determined by TEER of > 1000 Ω cm^2),[18] T84 monolayers were then placed onto 1.12 cm^2 aperture sliders (Physiologic Instruments; P2302) and mounted into Ussing chambers and continuously bathed in an oxygenated, glucose-fortified Ringer's solution at 37°C. Cells were voltage clamped to zero potential difference by the application of short-circuit current (I_{sc}) and baseline established. Cells were allowed to equilibrate for 20 min and before dacomitinib and crofelemer were administered. Dacomitinib was administered at a range of time points, with 15 min showing peak intestinal secretion, this time point was used for all further analyses. Both dacomitinib and crofelemer were administered in the Ussing chamber to the apical side. Crofelemer was added first, followed by dacomitinib after 10 min. Once cells had been exposed to dacomitinib for 15 min, the baseline I_{sc} ($\mu A/cm^2$) was determined as the mean over a 5-min period (5 values) immediately prior to administration of secretagogues. Cells were pretreated *via* the apical chamber with amiloride (20 μmol/L), to inhibit the apical epithelial sodium channel before being treated with carbachol (Ca^{2+} agonist; 100 μmol/L) applied to the basolateral chamber. The I_{sc} response was then measured

and determined as the change in I_{sc} following agonist administration ($\Delta\mu A/cm^2$), representing stimulated chloride secretion using Acquire and Analyze software 2.3 (Physiologic Instruments).

In vivo model

Ethics. The study was approved by the Animal Ethics Committee of The University of Adelaide (approval number: M215-13), and complied with the National Health and Medical Research Council (Australia) Code of Practice for Animal Care in Research and Training (2014). All experiments were conducted in male Albino Wistar rats (initial age ~6 weeks) obtained from The University of Adelaide Laboratory Animal Service (SA, Australia). Rats were group housed in ventilated cages with three to six animals per cage. They were housed in approved conditions on a 12-hr light/dark cycle. Food and water were provided *ad libitum*.

Experimental design. Rats were treated with crofelemer (25 mg/kg) and dacomitinib (7.5 mg/kg) administered daily for 21 days, both *via* oral gavage using a soft plastic feeding tube. Control animals received daily gavage with dacomitinib vehicle [0.5% (w/w) hydroxypropyl-methylcellulose] and crofelemer vehicle (sterile distilled water). The dose volume for oral gavage was ~5 mL/kg. Rats were randomly assigned to treatment groups and killed at 21 days ($n = 6$/group). Rats were anaesthetized using isoflurane inhalation, and were killed *via* cardiac exsanguination and cervical dislocation.

Clinical assessment of gastrointestinal toxicity

All rats were monitored twice daily for the presence of diarrhea for the duration of the study. Diarrhea was quantified by two independent assessors using a well-established grading system where 0 = no diarrhea, 1 = mild diarrhea with soft stools and perianal staining, 2 = moderate diarrhea with loose stools and perianal staining of fur, 3 = severe diarrhea with watery stools ± mucous and fur staining incorporating hind legs.[19] Rats were weighed daily to track weight loss/gain. Rats were killed if they displayed > 15% weight loss from baseline or significant distress and clinical deterioration, in compliance with animal ethical requirements.

Tissue preparation

At necropsy, the entire gastrointestinal tract from pyloric sphincter to rectum was dissected and flushed with saline to remove intestinal contents. Both the small and large intestines were weighed immediately after resection. Samples of jejunum, ileum and colon were collected and (*i*) fixed in 10% formalin for embedding in paraffin or (*ii*) were placed in Ringer's solution with 10 μM indomethacin for Ussing chamber experiments.

In vivo electrophysiological studies using Ussing chambers

Distal colon and ileum tissue was cut longitudinally along the mesentery and external muscle layers were carefully dissected and removed under microdissection microscopes in a Ringer's/indomethacin solution. Tissue was then immediately placed onto 0.5 cm^2 aperture sliders (Physiologic Instruments; P2305), mounted into Ussing chambers (Physiologic Instruments; #EM-CSYS-8) and continuously bathed in an oxygenated, glucose-fortified ringer solution at 37°C for electrophysiological analysis. The epithelium was voltage clamped to zero potential difference by the application of short-circuit current (I_{sc}) and baseline established. Throughout the experiment, the epithelium was continuously short-circuited by the automatic voltage clamp device with correction for solution resistance. In 1 min intervals, a voltage step of ±2 mV (U) was applied to the tissue and the change in short-circuit current (I_{sc}) measured. Tissue was allowed to equilibrate for 20 min and baseline I_{sc} ($\mu A/cm^2$) was determined as the mean over a 5-min period (5 values) immediately prior to administration of secretagogues. Tissue was pretreated *via* the apical chamber with amiloride (20 μmol/L), to inhibit the apical epithelial sodium channel before being treated with carbachol (Ca^{2+} agonist; 100 μmol/L) applied to the basolateral chamber. The I_{sc} response was then measured and determined as the change in I_{sc} following agonist administration ($\Delta\mu A/cm^2$), representing stimulated chloride secretion using Acquire and Analyze software 2.3 (Physiologic Instruments).

Serum drug analysis

Determination of serum dacomitinib concentration (range 3–10000 ng/mL) by liquid chromatography/mass spectrometry (LC/MS/MS) was conducted at the Pharmaceutical Science Sector Laboratory, School of Pharmacy and Medical Sciences, University of South Australia under GLP conditions. Blood samples were collected by cardiac puncture and serum separated. Dacomitinib and the internal standard was extracted from serum using a protein precipitation clean up, before separation by HPLC on a Phenomenex Luna C18 reverse phase column. Elutes were monitored by an API 3000 MS/MS detector operated in positive MRN mode. Samples with dacomitinib concentrations above the linear range were diluted 1:10 with blank rat serum.

FITC-dextran assay

Two hours prior to culling, rats received a 600 mg/kg dose (120 mg/mL) of 4 kDa fluorescein isothiocyanate (FITC)-dextran (Sigma-Aldrich, NSW, Australia, Cat# FD4) *via* oral gavage. Blood was collected *via* cardiac puncture at necropsy into serum-gel clotting activator tubes and protected from light. Samples were centrifuged at 3,000*g* for 5 min and serum isolated. Serum samples were diluted 1:3 with 1 × phosphate buffer solution (PBS) and quantified using the Bio Tek Synergy™ Mx Microplate Reader (Bio Tek, Vermont) and Gen5 version 2.00.18 software relative to a standard curve (range 0.0001–10 μg/mL).

Histopathological analysis

Hematoxylin and eosin (H&E) staining was performed on 5 μm sections of jejunum, ileum and colon cut on a rotary

microtome and mounted onto glass Superfrost© microscope slides (Menzel-Gläser, Braunschweig, Germany). Slides were scanned using a NanoZoomer™ (Hamamatsu Photonics, Japan) and assessed with NanoZoomer Digital Pathology software view.2 (Histalim, Montpellier, France). The occurrences of eight histological criteria in the jejunum and ileum were examined to generate a total tissue injury score.[20] These criteria were villous fusion, villous atrophy, disruption of brush border and surface enterocytes, crypt loss/architectural disruption, disruption of crypts cells, infiltration of polymorphonuclear cells and lymphocytes, dilation of lymphatics and capillaries and edema. In the colon, the latter six criteria were examined. Each parameter was scored as present = 1, or absent = 0, in a blinded fashion.

Immunohistochemistry

Immunohistochemical analysis was performed for apoptosis (caspase 3; Abcam, Vic, Australia; #ab4051) and proliferation (Ki67; Abcam, Vic, Australia #ab16667. Immunohistochemical analysis was performed using Dako reagents on an automated machine (AutostainerPlus™, Dako, Denmark) following standard protocols supplied by the manufacturer. Briefly, sections were deparrafinised in histolene and rehydrated through graded ethanol before undergoing heat mediated antigen retrieval using an EDTA/Tris buffer (0.37 g/L EDTA, 1.21 g/L Tris; pH 9.0). Retrieval buffer was preheated to 65°C using the Dako PT LINK (pre-treatment module). Slides were immersed in the buffer and the temperature raised to 97°C for 20 min. After returning to 65°C, slides were removed and placed in the Dako AutostainerPlus and stained following the manufacture's guidelines. Negative controls had the primary antibody omitted. Caspase 3 and Ki67 were quantified by counting the number of positively stained cells for 15 crypts. Data presented as average positively stained cells per crypt. All analysis was done in a blinded fashion.

Tight junction analysis

Immunofluorescence was carried out on 5 μm sections of ileum and colon, cut on a rotary microtome and mounted onto FLEX IHC microscope slides (Flex Plus Detection System, Dako; #K8020). Immunofluorescence analysis was performed for key tight junction proteins: claudin-1 (Abcam Ab15098; 2 μg/mL; 1:100; Alexa Fluor anti-rabbit 568 nm), ZO-1 (Invitrogen 61–7300; 2.5 μg/ml; 1:100; Alexa Fluor anti-rabbit 568 nm) and occludin (Invitrogen 33–1500; 5 μg/mL; 1:100; Alexa Fluor anti-rabbit 568 nm). Immunofluorescence was performed using Dako reagents on an automated machine (AutostainerPlus, Dako; #AS480) following standard protocols supplied by the manufacturer. Briefly, sections were deparaffinzed in histolene and rehydrated through graded ethanol before undergoing heat-mediated antigen retrieval using an EDTA-NaOH buffer (0.37 g/L EDTA, pH 8.0). Retrieval buffer was preheated to 65°C using Dako PT LINK (pretreatment module; Dako; #PT101). Slides were immersed in the buffer and the temperature raised to 97°C for 20 min. After returning to 65°C, slides were placed in the Dako AutostainerPlus, and returned to room temperature with the buffer applied. Tissue was blocked using 10% normal horse serum in 1 × PBS. The primary antibodies were applied for 1 hr using 5% normal horse serum as a diluent. A fluorescently labeled secondary antibody (donkey anti-rabbit or mouse IgG [H + L] secondary antibody, Alexa Fluor 568 conjugate, Invitrogen; #A10042) was applied at 0.8 μg/mL for a further 1 hr, using 1 × PBS + 1% BSA (Sigma-Aldrich; #A2058) and 2% FBS (Sigma-Aldrich; #F2442) as a diluent. Slides were washed using 1 × PBS; counterstained using 1 μg/mL 4′,6-diamidino-2-phenylidole (DAPI; Life Sciences; #D1306) and cover slipped using an aqueous mounting medium (Fluorshield, Sigma-Aldrich; #F6182). Negative controls had the primary antibody omitted. Slides were visualized using the SP5 Spectral Scanning Confocal Microscope (Leica). Four areas from each tissue were imaged (40× magnification) providing a range of areas for both qualitative and quantitative analysis. Immunofluorescence was assessed qualitatively for staining distribution in a blinded fashion. Quantitative analysis was conducted using ImageJ software. Briefly, channels were separated and RGB images converted to 8-bit. Automated thresholding was performed using the MaxEntropy algorithm, chosen based on qualitative assessment of its ability to identify tight junctions and exclude nonspecific staining.[21,22] Epithelium only was selected, and total stained area was calculated and expressed as a percentage of the total area selected.

Statistical analysis

Data were compared using Prism version 7.0 (GraphPad® Software, San Diego). A D'Agostino Pearson omnibus test was used to assess normality. When normality was confirmed, a two-way analysis of variance (ANOVA) with appropriate *post hoc* testing was performed to identify statistical significance between groups. In other cases, a Kruskal-Wallis test with Dunn's multiple comparisons test and Bonferroni correction was performed. Diarrhea was assessed using a χ^2 test. A p values of < 0.05 was considered significant.

Results

Crofelemer inhibits dacomitinib-induced chloride secretion *in vitro*

To test the hypothesis of dacomitinib inducing diarrhea *via* a secretory mechanism, short-circuit current (I_{sc}) was measured to assess intestinal cell Cl^- secretion in T84 colonic cells in symmetrical physiological solutions. Previous studies have shown that I_{sc} is reflective of changes in transepithelial chloride secretion in T84 cells.[23,24] Figure 1*a* shows baseline I_{sc}, after cells have been exposed to dacomitinib and/or crofelemer, but with no agonist administration. Baseline I_{sc} significantly increased following dacomitinib treatment ($p < 0.0001$; Fig. 1*a*) and crofelemer inhibited this dacomitinib-induced increase in I_{sc} ($p < 0.0001$; Fig. 1*a*). Administration of CaCC agonist—carbachol—increased I_{sc} in cells treated with dacomitinib (Fig. 1*b*). Crofelemer inhibited this increase ($p < 0.0001$; Fig. 1*b*).

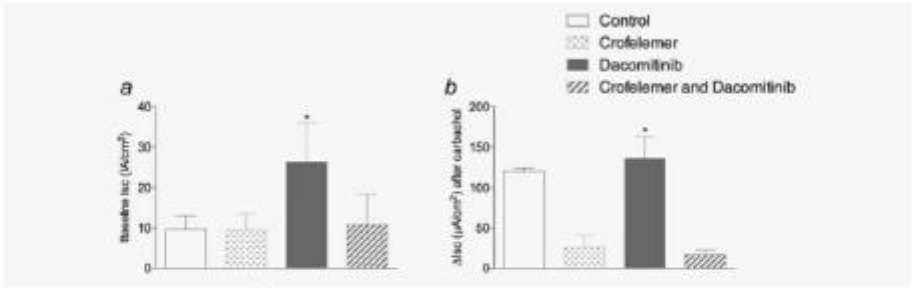

Figure 1. Baseline short-circuit current (I_{sc}) and change in I_{sc} following CaCC agonist carbachol. T84 monolayers were mounted into Ussing chambers and treated with dacomitinib (1 μM) and crofelemer (10 μM) *via* the apical chamber. (*a*) Increased baseline I_{sc} was seen in cells treated with dacomitinib ($p < 0.0001$), which was attenuated with crofelemer ($p < 0.0001$). (*b*) Increased delta I_{sc} was also seen in cells treated with dacomitinib following the administration of carbachol, a CaCC agonist, this was also attenuated with crofelemer ($p < 0.0001$). Data presented as mean ± SEM. A one-way ANOVA with Tukey *post-hoc* was performed to identify statistical significance ($p < 0.05$).

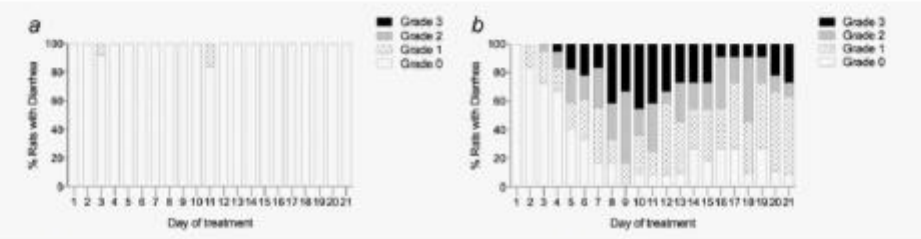

Figure 2. Diarrhea profiles shown for rats treated with vehicle controls (*a*), dacomitinib (*b*), crofelemer control (*c*) and dacomitinib/crofelemer combined (*d*). Rats treated with vehicle control did not develop diarrhea (*a*). One hundred percent of rats treated with 7.5 mg/kg dacomitinib (*b*) and dacomitinib/crofelemer combined (7.5 and 25 mg/kg, respectively) (*d*) developed any grade of diarrhea. Rats treated with dacomitinib/crofelemer combination had significantly worse diarrhea than rats treated with dacomitinib alone ($p = 0.0003$). Data expressed as percentage of total animals per day with a particular grade of diarrhea. A Chi^2 test was performed to identify statistical significance ($p < 0.05$).

Crofelemer is ineffective at reducing dacomitinib-induced diarrhea

Following the results seen *in vitro*, which showed dacomitinib increased chloride secretion and crofelemer inhibited it, treatment was then translated into an animal model. Our previous publication presents data of control and dacomitinib alone treated rats.[25] Rats treated with vehicle control did not develop diarrhea at any time point.[25] Diarrhea (grade 1–3) occurred in 100% of dacomitinib alone rats, which is comparable to the incidence seen in clinical trials.[25] Two rats treated with crofelemer alone developed mild grade 1 diarrhea on the 3rd and 11th treatment day, likely due to stress (Fig. 2*a*). Diarrhea developed in 100% of rats treated with dacomitinib/crofelemer combination (Fig. 2*b*). Approximately 50% of rats treated with combination crofelemer and dacomitinib had severe diarrhea (grade 3: severe diarrhea as watery stools ± mucous with fur staining incorporating hind legs). Approximately 30% of rats treated with dacomitinib alone had severe diarrhea.[25] Rats treated with dacomitinib/crofelemer combination had significantly worse diarrhea than rats treated with dacomitinib alone ($p = 0.0003$).

Weight loss

In the crofelemer/dacomitinib combination group, two animals were killed due > 15% weight loss. These animals were not included in downstream analysis. Rats treated with crofelemer/dacomitinib combination had significantly less weight gain than controls from Day 10 to 21 ($p < 0.0001$; Fig. 3). At Day 21, the control group had on average gained 46.38 ± 2.459%,[25] the crofelemer group gained 39.27 ± 8.298%, the dacomitinib group gained 18.99 ± 5.602%,[25] and the crofelemer/dacomitinib combination group gained 13.36 ± 6.846% body weight compared with Day 1 of treatment.

Crofelemer did not inhibit chloride secretion in the presence of dacomitinib in this model

Samples of colon and ileum from each animal in the study were mounted in Ussing chambers to record electrogenic ion

transport. Baseline readings were recorded to assess baseline differences in transepithelial short circuit current (I_{sc}). Baseline I_{sc} in the ileum was significantly higher in rats treated with combination crofelemer and dacomitinib compared with controls ($p = 0.0408$; Fig. 4*a*). Baseline I_{sc} in the colon was significantly higher in rats treated with combination crofelemer and dacomitinib compared with crofelemer alone ($p = 0.0122$; Fig. 4*b*). Carbachol was administered to elevate levels of intracellular calcium to assess the role of the calcium-activated chloride channels, and indirectly, basolateral potassium channels. No differences were noted between groups in ileum samples following carbachol administration (Fig. 4*c*). The response to carbachol in colon samples of rats treated with combination crofelemer and dacomitinib was significantly higher compared with controls, crofelemer alone and dacomitinib alone ($p < 0.0001$; Fig. 4*d*).

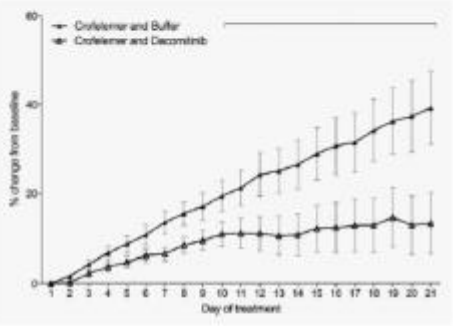

Figure 3. Weight over the 21-day time course. Data presented as a percentage of weight change from baseline (Day 1). A Kruskal-Wallis with *post-hoc* testing was performed to identify statistical significance. Rats treated with dacomitinib (7.5 mg/kg) and dacomitinib/crofelemer combination (7.5 and 25 mg/kg, respectively) had significantly less weight gain than the controls from Day 10–21 ($p < 0.0001$).

Crofelemer does not increase serum absorption of dacomitinib

To assess if crofelemer was increasing the serum absorption of dacomitinib circulating dacomitinib levels were analyzed by mass spectrometry in serum samples collected at death, after 21 days of treatment. The average blood concentration of dacomitinib in rats treated with dacomitinib alone was 258.2 ± 51.76 and 260.8 ± 36.63 ng/mL in rats treated with dacomitinib and crofelemer combination ($p > 0.05$; Supporting Information Figure S1).

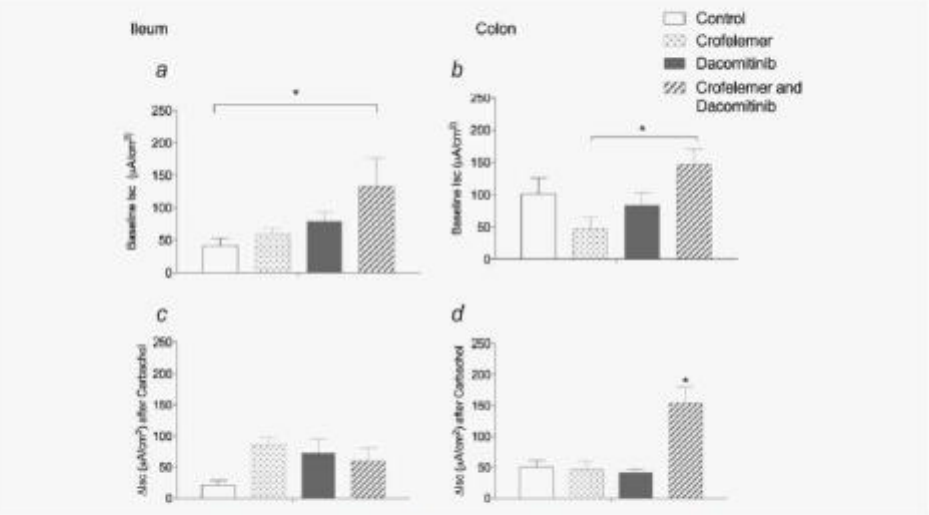

Figure 4. Baseline short circuit current (I_{sc}) of the distal ileum and colon. Segments of the distal colon and ileum were dissected, opened longitudinally and had the external muscle layers removed, before being mounted into Ussing chambers. Increased baseline I_{sc} was seen in rats treated with dacomitinib/crofelemer combination (7.5 and 25 mg/kg, respectively) compared to controls in the ileum (*a*: $p = 0.0408$) and compared with dacomitinib alone (7.5 mg/kg) in the colon (*b*: $p = 0.0122$). Following the administration of calcium agonist—carbachol—the colon of rats treated with dacomitinib/crofelemer combination had a significantly increased response compared with all other treatment groups (*d*: $p < 0.0001$). No significant changes were noted in the ileum (*c*). Data presented as mean ± SEM. A one-way ANOVA with Tukey *post-hoc* was performed to identify statistical significance ($p < 0.05$).

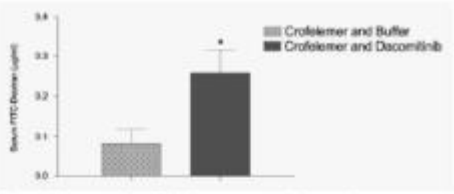

Figure 5. Serum 4 kDa FITC-dextran was administered as a 600 mg/kg dose, *via* oral gavage, 2 hr prior to kill time point. Data expressed as mean ± SEM and were analyzed using a one-way ANOVA. Both treatment arms involving dacomitinib had significantly elevated levels of serum FITC-dextran, indicating gastrointestinal barrier dysfunction. Dacomitinib alone had significantly elevated levels of serum FITC dextran compared to controls ($p = 0.0018$) and crofelemer alone ($p = 0.0043$). This was not attenuated with combination crofelemer/dacomitinib treatment, which had significantly elevated levels of serum FITC dextran compared with controls ($p < 0.0001$) and crofelemer alone ($p = 0.0002$).

Dacomitinib induces gastrointestinal permeability

FITC dextran was administered orally to measure gastrointestinal permeability. Serum FITC dextran levels were significantly elevated in rats of either treatment arm involving dacomitinib.[25] Rats treated with dacomitinib alone had significantly elevated levels of serum FITC dextran compared with controls ($p = 0.0018$),[25] and crofelemer alone ($p = 0.0043$). This was not attenuated with combination crofelemer/dacomitinib treatment, which had significantly elevated levels of serum FITC dextran compared to controls ($p < 0.0001$) and crofelemer alone ($p = 0.0002$; Fig. 5).

Cytoplasmic redistribution of tight junction proteins contributes to dacomitinib-induced barrier dysfunction.

To evaluate if dacomitinib alters permeability through tight junction disruption we investigated tight junction proteins in the intestine. Qualitative analysis of immunofluorescence for tight junction proteins showed membranous staining for all tight junction proteins in vehicle controls, and crofelemer alone controls (Figs. 6*a,c,e,g,i,k*, 6*m*, 6*o*, 6*q*, 6*s*, 6*u* and 6*w*). Immunofluorescence staining for ZO-1 showed focal areas of proteolysis in the ileum (Figs. 6*b* and 6*d*) and colon (Figs. 6*f* and 6*h*) of rats treated with dacomitinib and dacomitinib/crofelemer combined. These focal areas of protein disruption were particularly evident in areas of epithelial injury, often occurring alongside phenotypically normal tight junction staining (indicated by arrows). Similar changes in occludin expression were also seen in the ileum (Figs. 6*j* and 6*l*) and colon (Figs. 6*n* and 6*p*), with focal areas of proteolysis corresponding with frank epithelial damage in rats treated with dacomitinib and dacomitinib/crofelemer combination. Claudin-1 staining presented with sharp apical intensities and membranous staining down the apicolateral border of the enterocyte in vehicle and crofelemer alone controls in both the ileum (Fig. 6*q* and 6*s*) and colon (Figs. 6*u* and 6*w*). Marked caludin-1 internalization was evident in rats treated with dacomitinib and dacomitinib/crofelemer combination, particularly in the ileum (Figs. 6*r* and 6*t*), with complete loss of membranous staining specificity in some areas, and to a lesser extent in the colon (Figs. 6*v* and 6*x*). There were no apparent differences noted between the two dacomitinib treatment arms. To complement the observation of morphological changes in tight junction proteins, quantitative analysis was conducted on epithelium only, to assess mean percentage area stained. Vehicle control had a mean percentage area staining of 5.23% for claudin-1, 4.27% for ZO-1 and 1.00% for occludin. Crofelemer alone had a mean percentage area staining of 6.8% for claudin-1, 2.5% for ZO-1 and 0.93% for occludin. Dacomitinib alone had a mean percentage area staining of 4.23% for claudin-1, 3.53% for ZO-1 and 1.87% for occludin. Dacomitinib and crofelemer had a mean percentage area staining of 2.8% for caludin-1, 3.23% for ZO-1 and 1.45% for occludin. No significant differences were noted between groups (data not shown).

Crofelemer does not attenuate dacomitinib-induced histopathological injury

Rats treated with dacomitinib,[25] or dacomitinib/crofelemer combination had significant tissue injury in the ileum compared with controls ($p < 0.0001$; Fig. 7). This was predominantly characterized by severe villus atrophy with stunting and fusion of villi, which was also attended by enterocyte metaplasia to a low columnar or cuboidal phenotype and mild compensatory expansion of the basal proliferative compartment of crypts. In the congested lamina propria, there was an increased inflammatory infiltrate comprised of lymphocytes, macrophages, plasma cells and neutrophils and dilation of lacteals (villous lymphatics). There were no significant differences in tissue injury in the jejunum and colon between any groups (data not shown). Dacomitinib did not cause increased apoptosis or proliferation in the gastrointestinal tract compared with controls.[25] When Dacomitinib and crofelemer were given in combination, there was no difference seen in apoptosis or proliferation between any group (data not shown).

Discussion

Whilst dacomitinib—a second-generation small molecule pan-HER TKI—shows promise for the treatment of NSCLC, its' most commonly reported adverse event is diarrhea, which significantly impacts on clinical outcomes.[5] Currently, no antidiarrheal medication used for the treatment of TKI-induced diarrhea offers a targeted approach due to the lack of understanding of the underlying mechanisms. HER TKI-induced diarrhea has recently been hypothesized to be caused by ErbB down-regulation, where blockade leads to excess chloride secretion and thus secretory diarrhea.[9] Therefore, this study first investigated this hypothesis in an *in vitro* model. We demonstrated that dacomitinib caused increased chloride secretion across polarized epithelia, and that crofelemer, an antisecretory antidiarrheal agent, was able to attenuate this increase. Given this positive finding, we then aimed

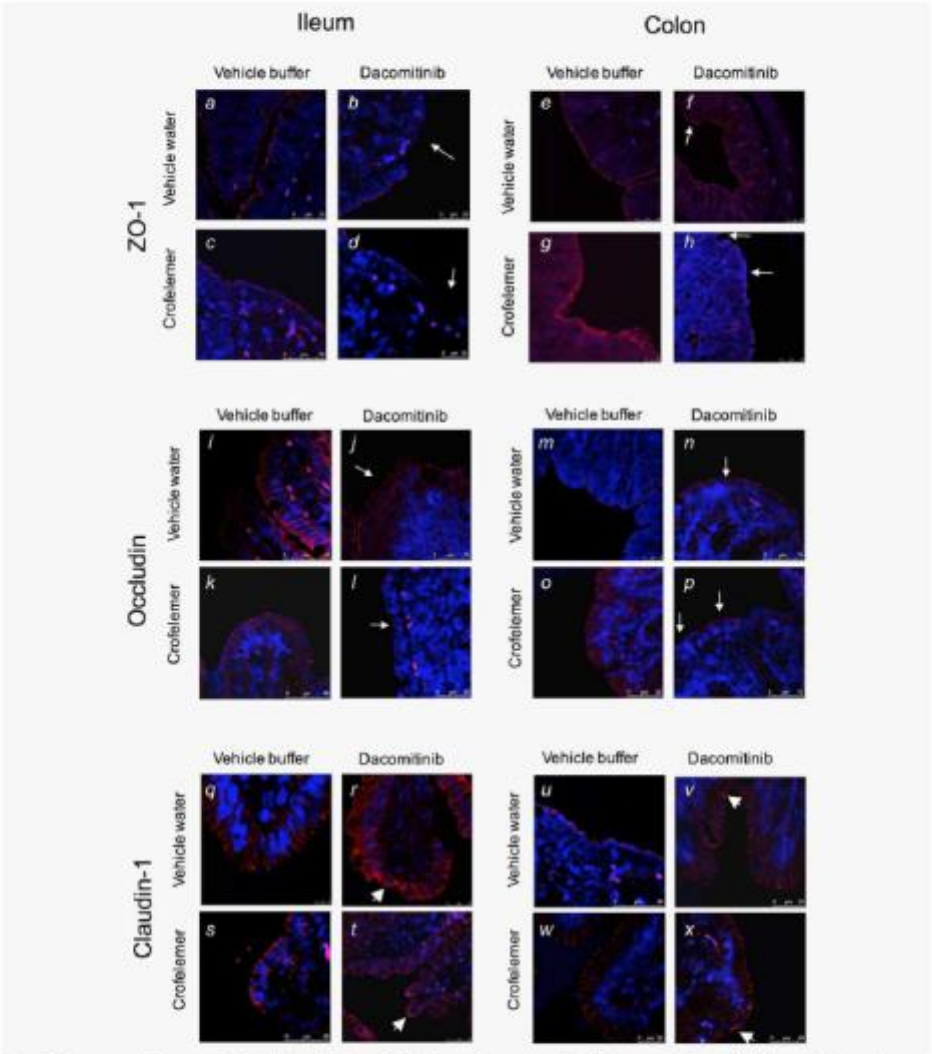

Figure 6. Representative images of claudin-1, occludin and ZO-1 immunofluorescence in the ileum and colon of vehicle- crofelemer- dacomitinib- and dacomitinib/crofelemer combination- treated rats. Vehicle treated, and crofelemer alone treated rats showed phenotypically normal tight junction proteins, with apical staining intensities (*a*, *c*, *e*, *g*, *i*, *k*, *m*, *o*, *q*, *s*, *u* and *w*). Rats treated with dacomitinib and dacomitinib/crofelemer combination showed no differences, with both displaying focal areas of ZO-1 and occludin disruption, particularly in areas of epithelial injury (*b*, *d*, *f*, *h*, *j*, *l*, *n* and *p*, arrows). Rats treated with dacomitinib and dacomitinib/crofelemer combination displayed claudin-1 internalization, found alongside areas of phenotypically normal tight junctions (*r*, *t*, *v* and *x*, arrows). Sections of ileum and colon were stained with a primary antibody for claudin-1, occluding and ZO-1 and visualized using an AlexaFluor anti-rabbit 568. Blue counterstaining (DAPI, 405 nm) shows nuclei. Original magnification 20×. [Color figure can be viewed at wileyonlinelibrary.com]

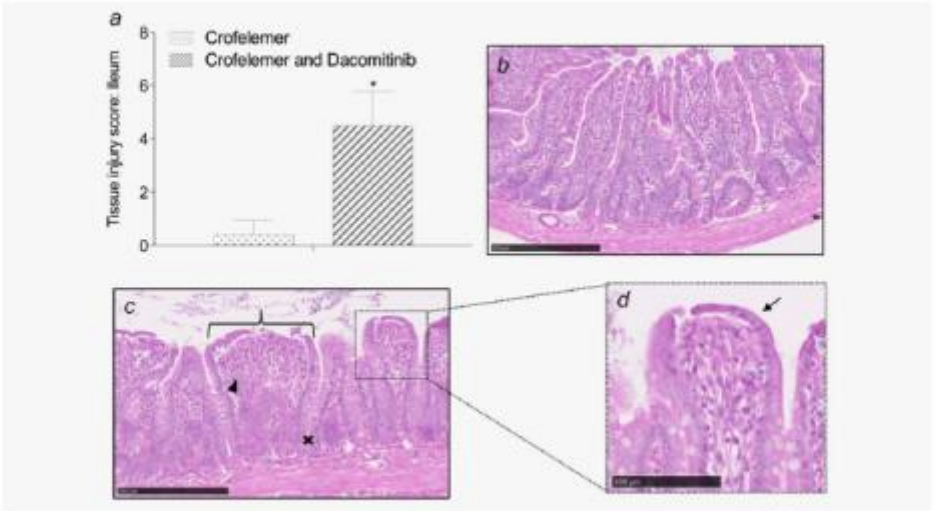

Figure 7. Histopathological parameters in H&E stained ileum. There were significant increases in tissue injury scores (*a*) in rats treated with dacomitinib alone (*c*; $p < 0.0001$), and dacomitinib/crofelemer combination (*d*; $p < 0.0001$) compared to both vehicle control (not shown) and crofelemer control (*b*). Villus atrophy and stunting is evident in all villi in image *c* and *d*. Fusion of villi is indicated by brackets. Enterocyte metaplasia is indicated by arrows. Compensatory expansion of crypts is indicated by crosses. Increased inflammatory infiltrate is indicated by arrow heads. Scale bars indicate 250 μM. Original magnification 40×. [Color figure can be viewed at wileyonlinelibrary.com]

to determine if crofelemer was an effective prophylactic for dacomitinib-induced diarrhea in a rat model.

Despite the results seen *in vitro*, rats treated with dacomitinib/crofelemer combination had significantly worse diarrhea than rats treated with dacomitinib alone.[25] Previous investigations of the antisecretory mechanism of crofelemer have demonstrated weak and partial inhibition of CFTR, and complete inhibition of CaCC.[13] Electrophysiological analysis in this study conducted on T84 cells supported this, with crofelemer inhibiting chloride secretion at baseline, as well as following CaCC agonist administration. However, the electrophysiological analysis in the *in vivo* arm of this study demonstrated that the inhibitory effect of crofelemer on chloride secretion is lost when given in combination with dacomitinib over 21 days. This is the first time crofelemer has been used in a preclinical study of this duration, therefore the lack of effect seen in Ussing experiments *in vivo* may be due to the timing of the *ex vivo* experiments occurring 24 hr after the last dose of drugs. Furthermore, the tissue was significantly damaged, potentially altering the normal function of transporters. Nevertheless, crofelemer was unable to attenuate dacomitinib-induced diarrhea. This may be explained by convective drug washout, a concern for drugs with an extracellular target in intestinal crypts, such as crofelemer.[26] Convective washout reduces the efficacy of enterocyte surface targeted Cl^- channel inhibitors, which can be of concern in diarrhea, due to the potential of washout forces impeding the inhibitor to reach the deep intestinal crypts. However, convective drug washout does not explain why crofelemer was not only ineffective, but also significantly worsened dacomitinib-induced diarrhea.

Chloride channel blockers have previously been suggested for the investigation of TKI-induced diarrhea,[9] including CFTRinh-172, which binds to the cytoplasmic side of the CFTR channel and stabilizes the channel closed state[27]; glycine hydrazides, which target the extracellular CFTR surface in the channel pore[28]; and $CaCC_{inh}$-A01, a red wine extract that has been shown to prevent watery diarrhea in a mouse model of rotavirus.[29] Crofelemer was selected as an intervention in this study because (*i*) it was reported as a safe and tolerable drug with no adverse events and was approved for clinical use, (*ii*) its dual inhibitory action on the two principle Cl^- channels in the apical membrane of intestinal epithelial cells, and (*iii*) its lack of systemic absorption due to its size and polarity,[13] suggesting that it would not interact with dacomitinib systemically. Given the worsened effects seen in the present study, this might suggest that crofelemer can be systemically absorbed if administered in conjunction with drugs that cause barrier disruption and small intestinal damage such as dacomitinib. Serum mass spectrometry did not indicate that crofelemer altered the absorption of dacomitinib when looking at serum nadir levels only. A more detailed pharmacokinetic study would be required to assess if the combination drug protocol altered maximum concentrations or time to peak. There are currently no reported contraindications

for crofelemer and this is the first study to show that crofelemer may worsen diarrhea in certain situations. The results from this study suggest that crofelemer should be investigated for contraindications before being used in combination with other drugs.

Although the *in vitro* electrophysiological analysis indicated that dacomitinib induced excess chloride secretion, the *ex vivo* electrophysiological analysis did not suggest that dacomitinib causes excess chloride secretion in intestinal tissue following 21 days of treatment. This may be due to not only the timing of the Ussing experiments as previously mentioned, but additionally, the *in vivo* model was a chronic dosing schedule, whereas Ussing experiments in the *in vitro* model were conducted after only one treatment, 15 min after exposure. The disadvantage of cell line work should also be considered. T84 monolayer cell lines lack other mucosal cell interactions, and of particular importance in this study, the impact that inflammation has on tight junctions. Clinical studies have also indicated that neratinib, a pan-HER ErbB TKI has a fecal osmotic gap that is consistent with the values for secretory diarrhea.[30] Previous work investigating lapatinib, an ErbB1 and ErbB2 TKI, suggested that diarrhea was associated with chloride secretion, indicated by decreased serum chloride levels, which the authors proposed may be due to loss of chloride *via* the intestinal lumen.[19] However, this was the only measure of secretory mechanisms and is therefore inconclusive. Another kinase inhibitor, flavopiridol, has been reported to stimulate chloride secretion across monolayers of human colonocytes in modified Ussing chambers.[31] Nevertheless, given this was conducted *in vitro* the results need to be translated to an *in vivo* model for more in-depth understanding. This is especially important considering the differing results of the *in vitro* and *in vivo* arms of the present study. Despite the growing support in the literature for the hypothesis of TKI-induced diarrhea being due to excess chloride secretion, this is the first study to assess secretory diarrhea *ex vivo* using Ussing chamber analysis. The results of this study do not support the hypothesis that diarrhea second to TKI treatment is due to excess chloride secretion. The potential flaw in the hypothesis (EGFR in normal settings are negative regulators of chloride secretion, and so when inhibited there is a loss of negative regulation, and thus increased chloride secretion), is that the hypothesis does not consider that the tissue may be inflamed, and hence behave differently. The assumption that inflamed tissue would behave in a similar manner to normal tissue is a fundamental caveat of the hypothesis. This is highlighted by McCole *et al.* who showed in a model of DSS-induced colitis, that EGF behaves in a contradictory way in inflamed tissue (*i.e.*, enhances chloride secretion instead of inhibiting it).[32] Therefore, future research could administer dacomitinib and crofelemer to healthy gastrointestinal tissue in Ussing chambers, instead of using *ex vivo* treated tissue, in order to dissect whether the inflammatory changes in the present model overshadow the effects of the drugs themselves.

This is the first study to compare functional *in vivo* permeability, and morphological assessment of tight junction proteins in the setting of dacomitinib-induced gut toxicity. Our previous research has indicated that dacomitinib induces severe ileal damage and barrier dysfunction.[25] This study further characterized this barrier dysfunction; showing increases in barrier permeability to 4 kDa FITC-dextran, and clear changes to tight junction proteins. Tight junctions are critical in maintaining gastrointestinal health and homeostasis. Despite this, they are highly plastic structures vulnerable to post-transcriptional and -translational modification by a variety of pathological cues.[33,34] Tight junction disruption has been identified following treatment with a number of chemotherapeutic agents, both preclinically[35,36] and clinically.[37–39] To date, many studies have shown architectural abnormalities, and functional alteration, of key tight junction proteins such as claudin-1, ZO-1 and occludin. As such, the current study focused on these three proteins, despite the numerous other proteins present within the junctional complex. Given the complexity of tight junction physiology, further investigation could be directed towards the behavior of junctional adhesion molecule-A, following dacomitinib given its involvement in inflammatory settings.[40] Despite increased research in this area, assessment of barrier function and in particular tight junction analysis has never been conducted in TKI models. The present study identified derangement of claudin-1, ZO-1 and occludin, characterized by severe cytoplasmic redistribution and disassembly of the tight junction unit. However, quantitative analysis showed no significant differences in percentage area stained. This method of quantification may not have sufficient power to detect the subtle changes that occur upon protein translocation, thus explaining the disparity between qualitative and quantitative analyses. Internalisation of tight junction proteins is well recognized to contribute to poor barrier function, and loss of tight junction apposition.[20,34] In the current study, cytoplasmic redistribution of claudin-1 was seen in the ileum, where peak histopathological damage was also seen. However, the mechanisms causing this tight junction dysfunction remain to be elucidated. Previous research has suggested that tight junction dysfunction can be proinflammatory cytokine mediated.[20,34,41] Given the increased inflammatory infiltrate noted in the lamina propria of the ileum in this study, this might suggest that this may be a contributive factor to tight junction dysfunction in this study. While the mechanisms remain unclear, intestinal barrier dysfunction second to cancer treatment is becoming more evident in both preclinical[20] and clinical models.[37] Clinically, this is highly important as barrier dysfunction permits LPS translocation,[42] systemic toxicity,[37] bacterial translocation and colonization in mesenteric lymph nodes and the spleen, increasing the risk of infection, graft-versus-host disease[43] and sepsis.[44] Intestinal barrier dysfunction has also been suggested to exacerbate direct gastrointestinal damage from the cancer therapy, worsening quality of life and clinical outcomes for patients.[20] It is therefore

imperative that the mechanisms that lead to barrier dysfunction second to cancer treatment are further investigated, so that therapeutic targets may be identified and interventions developed to prevent local toxicity transitioning to systemic toxicity, to reduce associated risks.

Conclusion

In summary, this study showed that crofelemer was unable to attenuate dacomitinib-induced diarrhea, and in fact, worsened it in the current model. Despite the growing support for secretory diarrhea as the mechanism of TKI-induced diarrhea, this study provided little support for this hypothesis, suggesting that antisecretory drug therapy may be ineffective in this setting. This is the first study to provide a detailed interrogation of the barrier changes associated with dacomitinib treatment. Tight junction disruption is a hallmark trait of many pathological states. A wealth of research now implicates poor tight junction integrity following treatment with various chemotherapeutic agents; however, this is the first study to implicate these changes in a TKI model. This study advances our understanding of diarrhea processes induced by not only this agent, but assists in further characterizing the poorly understood mechanisms of ErbB TKI-induced diarrhea.

References

1. Abdul Razak AR, Soulieres D, Laurie SA, et al. A phase II trial of dacomitinib, an oral pan-human EGF receptor (HER) inhibitor, as first-line treatment in recurrent and/or metastatic squamous-cell carcinoma of the head and neck. *Ann Oncol* 2013;24:761–9.
2. Dietrich E, Antoniades K. Molecularly targeted drugs for the treatment of cancer: oral complications and pathophysiology. *Hippokratia* 2012;16: 196–9.
3. Van Sebille YZ, Gibson RJ, Wardill HR, et al. Gastrointestinal toxicities of first and second-generation small molecule human epidermal growth factor receptor tyrosine kinase inhibitors in advanced nonsmall cell lung cancer. *Curr Opin Support Palliat Care* 2016;10:152–6.
4. Kim DW, Garon EB, Jatoi A, et al. Impact of a planned dose interruption of dacomitinib in the treatment of advanced non-small-cell lung cancer (ARCHER 1042). *Lung Cancer* 2017;106:76–82.
5. Jankowitz RC, Abraham J, Tan AR, et al. Safety and efficacy of neratinib in combination with weekly paclitaxel and trastuzumab in women with metastatic HER2positive breast cancer: an NSABP Foundation Research Program phase I study. *Cancer Chemother Pharmacol* 2013;72: 1205–12.
6. Prenzi MA, Zilembo N, Haspinger ER, et al. Targeted therapy-induced diarrhea: a review of the literature. *Crit Rev Oncol Hematol* 2014;90:165–79.
7. Andreyev J, Ross P, Donnellan C, et al. Guidance on the management of diarrhoea during cancer chemotherapy. *Lancet Oncol* 2014;15:e447–60.
8. Hirsh V, Blais N, Burkes R, et al. Management of diarrhea induced by epidermal growth factor receptor tyrosine kinase inhibitors. *Curr Oncol* 2014;21:329–36.
9. Van Sebille YZ, Gibson RJ, Wardill HR, et al. ErbB small molecule tyrosine kinase inhibitor (TKI) induced diarrhoea: chloride secretion as a mechanistic hypothesis. *Cancer Treat Rev* 2015; 41:646–52.
10. Hare KJ, Hartmann B, Kissow H, et al. The intestinotrophic peptide, glp-2, counteracts intestinal atrophy in mice induced by the epidermal growth factor receptor inhibitor, gefitinib. *Clin Cancer Res* 2007;13:5170–5.
11. Yarden Y, Sliwkowski MX. *Nat Rev Mol Cell Biol* 2001;2:127–37.
12. Gao JJ, Tan M, Pohlmann PR, et al. HALT-D: a phase II Evaluation of Crofelemer for the Prevention and Prophylaxis of Diarrhea in Patients With Breast Cancer on Pertuzumab-Based Regimens. *Clin Breast Cancer* 2016;17:76–8.
13. Tradtrantip L, Namkung W, Verkman AS. Crofelemer, an antisecretory antidiarrheal proanthocyanidin oligomer extracted from Croton lechleri, targets two distinct intestinal chloride channels. *Mol Pharmacol* 2010;77:69–78.
14. Holodniy M, Koch J, Mistal M, et al. A double blind, randomized, placebo-controlled phase II study to assess the safety and efficacy of orally administered SP-303 for the symptomatic treatment of diarrhea in patients with AIDS. *Am J Gastroenterol* 1999;94:3267–73.
15. DiCesare D, DuPont HL, Matherson JJ, et al. A double blind, randomized, placebo-controlled study of SP-303 (Provir) in the symptomatic treatment of acute diarrhea among travelers to Jamaica and Mexico. *Am J Gastroenterol* 2002;97: 2585–8.
16. Mangel AW, Chaturvedi P. Evaluation of crofelemer in the treatment of diarrhea-predominant irritable bowel syndrome patients. *Digestion* 2008; 78:180–6.
17. Ather F, Hamidi H, Fojzo MS, et al. Dacomitinib, an irreversible Pan-ErbB inhibitor significantly abrogates growth in head and neck cancer models that exhibit low response to cetuximab. *PloS One* 2013;8:e56112.
18. Wardill HR, Gibson RJ, Van Sebille YZ, et al. A novel in vitro platform for the study of SN38-induced mucosal damage and the development of Toll-like receptor 4-targeted therapeutic options. *Exp Biol Med (Maywood)* 2016;241:1386–94.
19. Bowen JM, Mayo BJ, Plews E, et al. Development of a rat model of oral small molecule receptor tyrosine kinase inhibitor-induced diarrhea. *Cancer Biol Ther* 2012;13:1269–75.
20. Wardill HR, Bowen JM, Van Sebille YZ, et al. TLR4-dependent claudin-1 internalization and secretagogue-mediated chloride secretion regulate irinotecan-induced diarrhea. *Mol Cancer Ther* 2016;15:2767–79.
21. Sahoo PK, Sultani S, Wong AKC, et al. A Survey of Thresholding Techniques. *Comput Vis Graphics Image Process* 1988;41:233–60.
22. Mahmoudi L, El Zaart A. *A Survey of Entropy Image Thresholding Techniques*. 2012 2nd International Conference on Advances in Computational Tools for Engineering Applications (Actea), 2012. 204–209.
23. Dharmsathaphorn K, Pandol SJ. Mechanism of chloride secretion induced by carbachol in a colonic epithelial cell line. *J Clin Invest* 1986;77: 348–54.
24. Kachintorn U, Vajaraphanich M, Traynor-Kaplan AE, et al. Activation by calcium alone of chloride secretion in T84 epithelial cells. *Br J Pharmacol* 1993;109:510–7.
25. Van Sebille YZ, Gibson RJ, Wardill HR, et al. Dacomitinib-induced diarrhoea is associated with altered gastrointestinal permeability and disruption in ileal histology in rats. *Int J Cancer* 2017;140: 2820–2829.
26. Jin BJ, Thiagarajah JR, Verkman AS. Convective washout reduces the antidiarrheal efficacy of enterocyte surface-targeted antisecretory drugs. *J Gen Physiol* 2013;141:261–72.
27. Caci E, Caputo A, Hinzpeter A, et al. Evidence for direct CFTR inhibition by CFTR(inh)-172 based on Arg347 mutagenesis. *Biochem J* 2008; 413:135–42.
28. Thiagarajah JR, Ko EA, Tradtrantip L, et al. Discovery and development of antisecretory drugs for treating diarrheal diseases. *Clin Gastroenterol Hepatol* 2014;12:204–9.
29. Ko EA, Jin BJ, Namkung W, et al. Chloride channel inhibition by a red wine extract and a synthetic small molecule prevents rotaviral secretory diarrhoea in neonatal mice. *Gut* 2014;63:1120–9.
30. Abbas R, Hug BA, Leister C, et al. A double-blind, randomized, multiple-dose, parallel-group study to characterize the occurrence of diarrhea following two different dosing regimens of neratinib, an irreversible pan-ErbB receptor tyrosine kinase inhibitor. *Cancer Chemother Pharmacol* 2012;70:191–9.
31. Kahn ME, Senderowicz A, Sausville EA, et al. Possible mechanisms of diarrheal side effects associated with the use of a novel chemotherapeutic agent, flavopiridol. *Clin Cancer Res* 2001;7:343–9.
32. McCole DF, Rogler G, Varki N, et al. Epidermal growth factor partially restores colonic ion transport responses in mouse models of chronic colitis. *Gastroenterology* 2005;129:591–608.
33. Khan N, Asif AR. Transcriptional regulators of claudins in epithelial tight junctions. *Mediators Inflamm* 2015;2015:219843.
34. Gonzalez-Mariscal L, Tapia R, Chamorro D. Crosstalk of tight junction components with signaling pathways. *Biochim Biophys Acta* 2008; 1778:729–56.
35. Wardill HR, Bowen JM, Al-Dasooqi N, et al. Irinotecan disrupts tight junction proteins within the gut: implications for chemotherapy-induced gut toxicity. *Cancer Biol Ther* 2014;15:236–44.

36. Nakao T, Kurita N, Komatsu M, et al. Irinotecan injures tight junction and causes bacterial translocation in rat. *J Surg Res* 2012;173:341–7.
37. Blijlevens NM, Donnelly JP, de Pauw BE. Prospective evaluation of gut mucosal barrier injury following various myeloablative regimens for haematopoietic stem cell transplant. *Bone Marrow Transplant* 2005;35:707–11.
38. Keefe DM, Cummins AG, Dale BM, et al. Effect of high-dose chemotherapy on intestinal permeability in humans. *Clin Sci* 1997;92:385–9.
39. Wardill HR, Logan RM, Bowen JM, et al. Tight junction defects are seen in the buccal mucosa of patients receiving standard dose chemotherapy for cancer. *Support Care Cancer* 2016;24:1779–88.
40. Monteiro AC, Parkos CA. Intracellular mediators of JAM-A-dependent epithelial barrier function. *Ann N Y Acad Sci* 2012;1257:115–24.
41. Schuhke JD, Plooger S, Amasheh M, et al. Epithelial tight junctions in intestinal inflammation. *Ann N Y Acad Sci* 2009;1165:294–300.
42. Wardill HR, Gibson RJ, Van Sebille YZ, et al. Irinotecan-Induced Gastrointestinal Dysfunction and Pain Are Mediated by Common TLR4-Dependent Mechanisms. *Mol Cancer Ther* 2016;15:1376–86.
43. Blijlevens NM, Donnelly JP, De Pauw BE. Mucosal barrier injury: biology, pathology, clinical counterparts and consequences of intensive treatment for haematological malignancy: an overview. *Bone Marrow Transplant* 2000;25:1269–78.
44. van der Velden WJ, Herbers AH, Feuth T, et al. Intestinal damage determines the inflammatory response and early complications in patients receiving conditioning for a stem cell transplantation. *PLoS One* 2010;5:e15156.

Appendix 2: Pfizer Report

Parts of this thesis were funded by an unrestricted investigator initiated grant with Pfizer pharmaceuticals. I developed the report and presented the results to Pfizer's head office in Sydney, Australia. The report is presented here.

TITLE PAGE

Division:	UoA - Physiology	**Compound:**	**Dacomitinib (PF-00299804)**
Information Type:	Part 1, In vivo, repeat dose Part 2, In vitro interrogation study	**Total No. of Pages**	110

Title:	Prevention of dacomitinib-induced diarrhoea by targeting chloride secretion – Final report

Author: Ysabella Van Sebille

26/11/15

STATEMENT BY STUDY DIRECTOR

The current study was conducted in the School of Medical Sciences, The University of Adelaide, South Australia. Whilst all experiments were conducted with the utmost rigor, this laboratory is not GLP certified. With the exception of the blood serum analysis, which was carried out at the IMVS under GLP conditions, all data presented is derived from work not conducted in a GLP laboratory.

Rat experiments were designated in WR (Wistar rat) and were approved by the Animal Ethics Committee of the University of Adelaide and complied with the National Health and Medical Research Council (Australia) Code of Practice for Animal Care in Research and Training (2014). Analyses performed in the School of Medical Sciences, The University of Adelaide were according to the principles of good laboratory practice, following standard operating procedures.

SUMMARY

Study Findings

PART 1

Ethics approved the use of Albino Wistar rats to investigate the mechanisms of dacomitinib-induced diarrhoea and prevention with crofelemer. 34 rats were used in 4 dose-finding pilot studies, 48 rats were used in the main study, 24 rats were used in a follow-up repeat study.

Dose-finding pilot study 1 (n = 8)

Dacomitinib was administered at 7.5 mg/kg/day via oral gavage at 12 pm daily and induced mild to severe diarrhoea without mortality and was deemed appropriate for all further investigations. Crofelemer was administered at 10 mg/kg via oral gavage at 9 am daily. Crofelemer given with control (methyl-cellulose buffer) was safe and showed no clinical signs in rats. When combined with dacomitinib, crofelemer reduced the number of days with diarrhoea compared to dacomitinib alone from 19 to 12. While this dose of crofelemer did decrease the total number of days with diarrhoea, this decrease was not significant.

Dose-finding pilot study 2 (n = 8)

Dacomitinib was administered at 7.5 mg/kg/day via oral gavage at 12 pm daily and induced mild to severe diarrhoea without mortality and was deemed appropriate for all further investigations. Crofelemer was administered at 50 mg/kg via oral gavage at 9 am daily. Crofelemer given with control (methyl-cellulose buffer) was safe and showed no clinical signs in rats. When combined with dacomitinib, crofelemer increased the number of days with diarrhoea compared to dacomitinib alone from 9 to 13. As this dose of crofelemer increased the total number of days with diarrhoea, it was not deemed appropriate.

Dose-finding pilot study 3-4 (n = 16)

Dacomitinib was administered at 7.5 mg/kg/day via oral gavage at 12 pm daily and induced mild to severe diarrhoea without mortality and was deemed appropriate for all further investigations.
(3) Crofelemer was administered at 25 mg/kg via oral gavage at 9 am daily. Crofelemer given with vehicle control (methyl-cellulose buffer) was safe and showed no clinical signs in rats. One rat treated with 25 mg/kg in combination with dacomitinib was removed from the study early due to excessive weight loss (> 15 %). When combined with dacomitinib, crofelemer reduced the number of days with diarrhoea from 19 to 9 and the severity from grade 3 to grade 1, compared to dacomitinib alone.
(4) To assess the best treatment schedule, 25 mg/kg crofelemer was given at 4 pm via oral gavage from the onset of diarrhoea. Crofelemer given in this treatment schedule reduced the total number of days with diarrhoea from 12 to 11. This treatment schedule did not significantly reduce the total number of days with diarrhoea and was not deemed appropriate.
Combination of dacomitinib and crofelemer at 25 mg/kg in the treatment schedule of daily at 9 am (3) was most effective, decreasing the number of days with diarrhoea from 19 to 9. Previous research in mice has shown that 30 mg/kg crofelemer is effective at reducing cholera toxin-induced water accumulation in the intestines. As such, it seems feasible that 25 mg/kg crofelemer in our pilot study reduced diarrhoea by preventing water accumulation in the intestines following dacomitinib treatment. This dose and treatment schedule was continued for the main study.

Main study (n = 48)

Rats were randomly allocated to receive either vehicle controls (water + methyl-cellulose buffer) (n = 12), water + dacomitinib (n = 12), 25 mg/kg crofelemer + methylcellulose buffer (n = 12), or 25 mg/kg crofelemer + dacomitinib (n = 12). All animals completed the study and were killed at either 7 days of treatment (n = 24) or 21 days of treatment (n = 24). There were no significant

differences in the overall incidence (83 % vs. 92 %) or number of days (14 vs. 15) with any grade diarrhoea between groups treated with dacomitinib alone or crofelemer + dacomitinib, respectively. The incidence of severe grade 3 diarrhoea was 50 % and 67 % in dacomitinib alone and crofelemer + dacomitinib groups, respectively.

Animals treated with dacomitinib gained less weight than control animals. Small intestine, stomach, spleen and liver weights were significantly decreased in rats treated with dacomitinib alone compared to water control at 21 days.

In serum biochemistry, anion gap, urea, cholesterol, ALT and LD was significantly increased at day 21 in the groups treated with dacomitinib compared to the water control group. In contrast, albumin was decreased.

Follow up study (n=24)

To further investigate intestinal changes induced by dacomitinib and crofelemer an additional rat study (n = 24) was conducted to assess small intestinal functional changes in Ussing chambers and barrier integrity with FITC dextran. Rats were dosed identically to the previous main study and were killed at 21 days of treatment. A number of rats treated with crofelemer + dacomitinib (n = 2) and water + dacomitinib (n = 2) were removed from the study early due to excessive weight loss (> 15 %) and ethical constraints. Diarrhoea and weight loss trends were consistent with the main study. Ussing camber analysis showed no differences in the ileum. Colon samples were used to increase the n from the main study, results were consistent with the main study. FITC dextran analysis showed that serum concentrations were increased in dacomitinib alone and crofelemer/dacomitinib combination rats.

PART 2

T84 cell culture study

Cell culture was conducted on T84 monolayers grown on polyester Transwell® systems, mounted into Ussing chambers. Dacomitinib (1 μM) and crofelemer (10 μM) were administered via apical routes. Exposure time of T84 monolayers to dacomitinib included 5, 20, 60, and 90 minutes (administration in Ussing chambers), and 3, 6, 24 and 48 hours (administration in Transwell). Dacomitinib administration caused significantly increased baseline chloride secretion following 5 and 20 minutes of exposure, therefore, crofelemer was only assessed at these times. Results showed that dacomitinib induces chloride secretion, and this was inhibited when crofelemer was administered, primarily via the calcium stimulated chloride channel. All experiments were repeated eight times.

PART 1

IN VIVO STUDY		**Compound:**	**Dacomitinib (PF-00299804)**
Information Type:	Repeat Dose Study		

Title:	Part 1: Prevention of dacomitinib-induced diarrhoea by targeting chloride secretion – In vivo study

Table 1. **Repeat dose study - pilot**

Test Article: Dacomitinib and crofelemer

Species/ Strain	**Route (Vehicle/Formulation)**	**Duration of Dosing**	**Doses (mg/kg)**	**Number of Animals/Sex**	**Noteworthy Findings**	**Report No. (Study No.)**
Rat/ Albino Wistar (Harlan)	p.o. dacomitinib (0.5% HPMC) p.o. crofelemer (sterile distilled water)	21 days	0, 7.5 q.d. (12 pm) 0, 10, 25, 50 q.d. (9 am)	24 male		Pf1

Key: p.o. per oral (oral gavage to stomach), q.d. once daily dose (with time indicated in brackets)

Table 1 (Continued).

Report Title: Progress report and results

Test Article: Dacomitinib and crofelemer

Report No.: 1

Study No.: Pf1

Duration of Dosing: 21 days

Duration of Recovery: 0 days

Location: UoA animal holding facility

Species/Strain: Rat /albino Wistar	**Route/Frequency:** Oral gavage, once daily	**Necropsy Dates:** 16/6/14, 17/6/14, 29/07/14
Weight Range on Day 0 (g): Male: 186 – 268	**Test Material:** Dacomitinib, crofelemer **Batch Number:** 0015	**Dosing Period Dates:** **First Dose:** 26/05/14 **Final Dose:** 28/07/14
Initial Weight (g): 219.4 ± 25.2	**Vehicle:** 0.5% HPMC in sterile distilled water	**Testing Facility:** UoA - Physiology
Study in Compliance With GLP: N/A	**Dose Frequency:** Once daily	

Data Collected: Clinical observations, body weight, organ weight, necropsy findings, daily diarrhoea.

Daily Dose dacomitinib (mg/kg)	**0**	**0**	**0**	**0**	**7.5**	**7.5**	**7.5**	**7.5**
Daily Dose crofelemer (mg/kg)	0	10	25	50	0	10	25	50
Numbers of Animals:	6	2	2	2	6	2	2	2
Noteworthy Findings:	No treatment-related adverse events. One rat with chronic renal changes required removal							
Number of Unscheduled Deaths:	0				1			

Clinical Observations: Restraint stress caused urination and defecation during gavage process as expected. Dacomitinib caused persistent diarrhoea without mortality. Crofelemer treatment caused no clinical changes.

Table 1 (Continued). **Report Title:** Pf1 repeat dose study pilot

Clinical Observations								
Daily Dose dacomitinib (D), crofelemer (C) mg/kg	**0D, 0C**	**0D, 10C**	**0D, 25C**	**0D, 50C**	**7.5D, 0C**	**7.5D, 10C**	**7.5D, 25C**	**7.5D, 50C**
	Incidence							
Number of Animals:	**6**	**2**	**2**	**2**	**6**	**2**	**2**	**2**
Any loose feces G1 - 3 (and severe diarrhoea G3 only)	2 (0)	1 (0)	2 (0)	2 (0)	6 (2)	2 (1)	2 (0)	2 (1)
Weight loss (at any time)	0	0	0	0	4	0	1	0
Distended Abdomen	0	0	0	0	0	0	0	0
Decreased activity/Lethargic	0	0	0	0	2	1	1	1
Piloerection	2	2	2	2	4	2	2	2
Hunched posture	0	0	0	0	0	0	0	0

Red discoloration (discharge, material, staining) of fur (around eyes, snout, forelimbs, mouth, penis)	6	2	2	2	6	2	2	2
Swollen extremities (i.e. face, paws)	0	0	0	0	0	0	0	0
Gaunt (stomach sucked in and animal appearing to be in pain)	0	0	0	0	0	0	0	0
Cold	0	0	0	0	0	0	0	0
Hot	0	0	0	0	0	0	0	0
Feet peeling	0	0	0	0	0	0	0	0
Dribbling from mouth	0	0	0	0	0	0	0	0
Touch sensitive	0	0	0	0	0	0	0	0
Eye issues (inflamed and/or blindness)	0	0	0	0	0	0	0	0
Body Weight (g):	**Mean**							
Day 0	232	193	220	220	220	221	213	227
Day 21	341	330	350	3 28	260	265	280	274

Table 1 (Continued). **Report Title:** Pf1 repeat dose study pilot

Daily Dose dacomitinib (D), crofelemer (C) mg/kg		**0D, 0C**	**0D, 10C**	**0D, 25C**	**0D, 50C**	**7.5D, 0C**	**7.5D, 10C**	**7.5D, 25C**	**7.5D, 50C**
Organ Weights		**Mean**							
Spleen	Absolute (g)	0.68	0.75	0.59	0.55	0.48	0.51	0.48	0.72
	Relative (%)	0.2	0.21	0.18	0.17	0.19	0.19	0.19	0.26
Liver	Absolute (g)	13.25	13.25	14.15	14.63	9.69	10.16	9.2	11.31
	Relative (%)	3.84	3.98	4.05	4.46	3.42	3.89	3.82	4.12

Kidney	Absolute (g)	2.53	2.66	2.78	2.44	2.49	2.58	2.61	3.0
	Relative (%)	0.74	0.8	0.79	0.74	0.91	1.0	1.1	1.1
Stomach	Absolute (g)	1.82	1.46	1.88	1.83	1.32	1.07	1.62	1.49
	Relative (%)	0.53	0.43	0.54	0.56	0.6	0.42	0.55	0.54
Small Intestine	Absolute (g)	9.36	10.59	9.86	9.76	7.65	9.53	7.55	9.45
	Relative (%)	2.72	3.20	2.83	2.89	2.74	3.66	3.07	3.55
Large Intestine	Absolute (g)	1.76	2.41	1.89	1.96	1.77	1.87	1.92	1.94
	Relative (%)	0.51	0.72	0.74	0.6	0.69	0.72	0.74	0.72

Table 1 (Continued).	**Report Title:** Pf1 repeat dose study pilot							
Daily Dose dacomitinib (D), crofelemer (C) mg/kg	**0D, 0C**	**0D, 10C**	**0D, 25C**	**0D, 50C**	**7.5D, 0C**	**7.5D, 10C**	**7.5D, 25C**	**7.5D, 50C**
Necropsy Findings	**Incidence**							
No. of Rats Examined:	**6**	**2**	**2**	**2**	**6**	**2**	**2**	**2**
Inflamed Peritoneal Cavity	0	0	0	0	0	0	0	0
Small Intestine	0	0	0	0	1	0	0	1
Large Intestine	0	0	0	0	1	0	0	1
Mesenteric Lymph Nodes	0	0	0	0	1	0	0	0
Peritoneal cavity Fluid Pink/Red	0	0	0	0	0	0	0	0
Clear/Opaque	0	0	0	0	0	0	0	0
Discoloured Spleen	0	0	0	0	0	0	0	0
Liver	0	0	0	0	1	0	0	0
Kidney	0	0	0	0	0	0	0	0
Lesions Small Intestine	0	0	0	0	0	0	0	1
Large Intestine	0	0	0	0	0	1	0	0

	Caecum	0	0	0	0	0	0	0	0
Stomach	Bedding in	0	0	0	0	1	2	1	2
	Bloated	2	1	0	0	6	1	1	1
Liver	Swollen	0	0	0	0	0	0	0	0
Intestines	Blocked	1	0	1	0	0	0	0	1
	Perforated	0	0	0	0	0	0	0	0
	Telescoped	0	0	0	0	1	0	0	0
	Adhered to themselves	0	0	1	0	2	0	0	1
	Watery Contents	0	0	0	0	0	0	0	0
	Yellow contents (includes stomach)	0	0	0	0	0	0	0	0
	Undigested Contents	0	0	0	0	0	0	0	0
Intestines	Vascularised	0	0	0	1	3	0	1	1
	Thin Wall of	0	0	0	0	0	0	0	0
Caecum	Blood in	0	0	0	0	1	0	0	0
Colon	Gaseous/Distended	2	1	2	1	6	1	1	2

Table 1 (Continued)

Percentage of rats per day with diarrhoea (any)

Report title: Pf1 repeat dose study pilot

Daily Dose (D and C) mg/kg	**0D, 0C**	**0D, 10C**	**0D, 25C**	**0D, 50C**	**7.5D, 0C**	**7.5D, 10C**	**7.5D, 25C**	**7.5D, 50C**
	%							
Day 1	0	0	0	0	0	0	0	0
2	33	0	0	0	0	0	0	0
3	0	0	0	0	33	0	0	0
4	0	0	0	0	33	0	50	100
5	0	50	0	0	83	50	50	100
6	0	0	0	0	50	100	100	100
7	0	0	0	0	33	100	50	50
8	0	0	0	0	83	100	100	0

9	0	0	0	0	50	100	50	0
10	0	0	0	0	67	100	50	50
11	0	0	0	0	100	50	50	100
12	0	0	0	0	83	0	100	100
13	0	0	100	0	83	0	0	100
14	0	0	0	100	83	0	0	100
15	0	0	0	0	83	0	0	100
16	0	0	0	50	83	100	0	100
17	0	0	0	0	83	100	0	50
18	17	0	0	0	50	100	0	100
19	0	0	0	50	100	100	0	0
20	0	0	0	0	83	100	0	0
21	0	0	0	0	100	100	0	0

Table 2 Report Title: Pf1 main experiment

Test Article: Dacomitinib and crofelemer

Species/ Strain	Route (Vehicle/Formulation)	Duration of Dosing	Doses (mg/kg)	Number of Animals/Sex	Noteworthy Findings	Report No. (Study No.)
Rat/ Albino Wistar (Harlan)	p.o. dacomitinib in vehicle (0.5% HPMC) p.o. crofelemer in vehicle (sterile distilled water)	7 days 21 days	0, 7.5 q.d. (12 noon) 0, 25 q.d. (9 am)	48 males		PF1 main

Key: p.o. per oral (oral gavage to stomach), q.d. once daily dose (with time indicated in brackets)

Table 2 (Continued).

Report Title: Progress report and results

Test Article: Dacomitinib and crofelemer

Report No.: 1

Duration of Dosing: 21 days

Location: UoA animal holding facility

Study No.: Pf1 main	**Duration of Recovery:** 0 days	
Species/Strain: Rat /albino Wistar	**Route/Frequency:** Oral gavage/Once daily	**Necropsy Dates:** 22/09/14, 23/09/14, 24/09/14, 9/10/14, 10/10/14
Weight Range on Day 0 (g): Male: 147 – 245	**Test Material:** Dacomitinib, crofelemer **Batch Number:** 0015	**Dosing Period Dates:** **First Dose:** 15/09/14 **Final Dose:** 09/10/14
Initial Weight (g): 194.6 ± 30.4	**Vehicle:** 0.5% HPMC in sterile distilled water	**Testing Facility:** UoA - Physiology
Study in Compliance With GLP: N/A	**Dose Frequency:** once daily	

Data Collected: Clinical observations, body weight, clinical biochemistry, organ weights, necropsy findings, daily diarrhoea.

Daily Dose dacomitinib (mg/kg)	0	**0**	7.5	**7.5**
Daily Dose crofelemer (mg/kg)	0	25	0	25
Numbers of Animals:				
Day 7	6	6	6	6
Day 21	6	6	6	6

Noteworthy Findings:	No treatment-related adverse events			
Number of Unscheduled Deaths:	0	0	0	0

Clinical Observations: Restraint stress caused urination and defecation as expected. Dacomitinib caused persistent diarrhoea. Crofelemer did not reduce diarrhoea in rats.

Table 2 (Continued). **Report Title:** Pf1 main study

Clinical Observations

Daily Dose dacomitinib (D), crofelemer (C) mg/kg	**0D, 0C**	**0D, 25C**	**7.5D, 0C**	**7.5D, 25C**
	Incidence			
Number of Animals:	**12**	**12**	**12**	**12**
Any loose faeces G1-3 (and severe diarrhoea G3 only)	4 (0)	2 (0)	10 (6)	11 (8)
Weight loss (at any time)	0	0	4	3
Distended Abdomen	0	0	0	0
Decreased activity/Lethargic	0	0	2	1

Piloerection	2	9	10	12
Hunched posture	0	0	4	6
Red discoloration (discharge, material, staining) of fur (around eyes, snout, forelimbs, mouth, penis)	9	10	9	10
Swollen extremities (i.e. face, paws)	0	0	0	0
Gaunt (stomach sucked in and animal appearing to be in pain)	0	0	0	0
Cold	0	0	0	0
Hot	0	0	0	0
Feet peeling	0	0	0	0
Dribbling from mouth	0	0	0	0
Touch sensitive	0	0	0	0
Eye issues (inflamed and/or blindness)	0	0	0	0
Body Weight (g):	**Mean**			
Day 0	196.8	191.2	192.1	198.3

Day 7	237.8	235.1	220.3	222.3
Day 21	341.2	331.8	258.2	265.8

Daily Dose dacomitinib (D), crofelemer (C) mg/kg		**0D, 0C**	**0D, 25C**	**7.5D, 0C**	**7.5D, 25C**
Organ Weights[1]:		**Mean**			
Spleen - Day 7	Absolute (g)	0.54	0.57	0.49	0.51
- Day 21	Absolute (g)	0.68	0.68	0.51*	0.54*
Liver - Day 7	Absolute (g)	9.33	10.06	8.71	9.71
- Day 21	Absolute (g)	13.25	13.36	9.48*	10.21*
Kidney - Day 7	Absolute (g)	1.87	1.84	1.84	1.84
- Day 21	Absolute (g)	2.54	2.37	2.6	2.42
Stomach - Day 7	Absolute (g)	1.47	1.65	1.42	1.4
- Day 21	Absolute (g)	1.82	1.97	1.32*	1.6

Small Intestine- Day 7	Absolute (g)	8.33	9.18	7.03	7.02
- Day 21	Absolute (g)	9.36	9.99	7.35*	8.38
Large Intestine- Day 7	Absolute (g)	1.63	1.71	1.44	1.57
- Day 21	Absolute (g)	1.76	1.9	1.83	1.66

*Indicates significantly different from water control group (Two-Way ANOVA with Tukey post-hoc test, $p<0.05$)

Table 2 (Continued). **Report Title:** Pf1 main study

Daily Dose dacomitinib (D), crofelemer (C) mg/kg	**0D, 0C**	**0D, 25C**	**7.5D, 0C**	**7.5D, 25C**
Pathology findings	**Incidence**			
No. of Rats Examined:	**12**	**12**	**12**	**12**
Inflamed Peritoneal Cavity	0	0	0	0
Small Intestine	0	0	0	0
Large Intestine	0	0	1	0
Mesenteric Lymph Nodes	0	0	0	0
Infected Mesenteric Lymph Nodes	0	0	0	0
Intestines/Surrounds	0	0	0	0
Peritoneal cavity Fluid Pink/Red	0	0	0	0
Clear/Opaque	0	0	0	0
Discoloured Spleen	0	0	0	0
Liver	0	0	0	0

	Kidney	0	0	0	0
Lesions	Small Intestine	0	0	0	0
	Large Intestine	0	0	0	0
	Caecum	0	0	0	0
	Kidney	0	0	0	0
Stomach	Bedding in	0	0	1	3
	Bloated	0	0	0	0
	Thickened wall	0	0	0	0
Liver	Swollen	0	0	0	0
Intestines	Blocked	1	1	0	1
	Perforated	0	0	0	0
	Telescoped	0	0	0	0
	Adhered to themselves	0	1	0	0
	Watery Contents	0	0	2	0
	Yellow contents (includes stomach)	0	0	2	0
	Undigested contents	0	0	0	0

Caecum	Blood in	0	2	3	5
Intestines	Vascularised	0	0	0	0
	Thin Wall of	0	0	0	0
Colon	Gaseous/Distended	5	7	7	8

Table 2 (Continued). **Report Title:** Pf1 main study

Daily Dose (mg/kg/day)	**0D, 0C**	**0D, 25C**	**7.5D, 0C**	**7.5D, 25C**	**Daily Dose (mg/kg/day)**	**0D, 0C**	**0D, 25C**	**7.5D, 0C**	**7.5D, 25C**
Blood Biochemistry:	**Mean**					**Mean**			
Sodium (mmol/L) Day 7	137.5	138.8	138.5	139	Anion Gap (mmol/L)	14.8	17.0	14.5	17.0
Day 21	139.5	140.5	140.0	140.5	Day 7	14.5	18.0	19.25*	19.2*
					Day 21				

Potassium (mmol/L)	Day 7	7.88	6.92	7.98	6.72	Glucose (mmol/L)	8.82	8.57	8.55	8.22
	Day 21	6.22	6.45	6.73	6.82	Day 7	10.27	7.78	7.12	6.55
						Day 21				
Chloride (mmol/L)	Day 7	99.3	100.2	102.0	101.2	Urea (mmol/L)	6.77	7.30	5.83	5.94
	Day 21	100.0	99.7	99.3	99.8	Day 7	6.63	7.15	12.28*	9.417*
						Day 21				
Bicarb (mmol/L)	Day 7	31.2	28.7	29.3	27.6	Creatinine (umol/L)	9.17	13.7	12.2	19.0
	Day 21	30.3	29.2	27.5	28.5	Day 7	14.1	26.8	39.3*	29.2
						Day 21				

Cholesterol (mmol/L)	Day 7	2.48	2.35	2.08	1.92	Albumin (g/L)	11.8	12.5	10.5	11.0
	Day 21	1.72	1.98	2.35*	2.17	Day 7	13.0	12.7	10.7*	10.5*
						Day 21				
Urate (mmol/L)	Day 7	0.14	0.14	0.13	0.16	Globulin (g/L)	36.5	38.2	35.3	38.8
	Day 21	0.07	0.13	0.09	0.15	Day 7	39.7	41.8	43.7	42.5
						Day 21				
Phosphate (mmol/L)	Day 7	2.89	3.15	3.14	3.03	Protein (g/L)	48.3	50.7	45.8	49.8
	Day 21	2.60	2.85	2.74	2.80	Day 7	52.7	54.5	54.3	53.0
						Day 21				

Total Calcium (mmol/L)	2.62	2.58	2.51	2.49	Tot. Bilirubin (mmol/L)	1	1	1	1
Day 7	2.56	2.56	2.42	2.47	Day 7	1	1	1	1
Day 21					Day 21				
ALP (U/L) Day 7	395.8	399.5	268.7*	286.6*	AST (U/L)	107.8	135.3	148.7	210.8
Day 21	226.3	252.3	205.8	221.7	Day 7	136.7	206.3	217.5	228.0
					Day 21				
ALT (U/L) Day 7	77.0	82.2	90.0	101.2	LD (U/L)	680.2	1281.7	1268.8	1740.5
Day 21	64.0	71.7	77.8	112.0*	Day 7	1111.3	2459.8	2449.3	2895.2 *
					Day 21				

*Indicates significantly different from water control group (Two-Way ANOVA with Tukey post-hoc test, $p < 0.05$)

Table 2 (Continued)

Report Title Pf1 main study

Percentage of rats per day with diarrhoea (any)

Daily Dose dacomitinib (D) & crofelemer (C) mg/kg	**0D, 0C**	**0D, 25C**	**7.5D, 0C**	**7.5D, 25C**
Day	**%**			
1	8.3	0	0	0
2	0	0	8.3	25
3	0	8.3	0	41.7
4	0	0	16.7	41.7
5	0	0	50	91.7
6	0	8.3	66.7	83.3
7	0	0	75	91.7
8	0	0	66.7	83.3
9	0	0	50	100
10	0	0	66.7	83.3

11	0	16.7	100	83.3
12	0	0	83.3	83.3
13	0	0	66.7	66.7
14	0	0	83.3	66.7
15	0	0	66.7	50
16	16.7	0	83.3	66.7
17	0	0	83.3	50
18	0	0	100	66.7
19	0	0	83.3	66.7
20	0	0	83.3	66.7
21	0	0	100	83.3
Average no. days with diarrhoea (only 21 day kill group incl.)	0.17	0.33	14.2	15.0

Table 2 (Continued)

Report Title: Pf1 main study

Gastrointestinal permeability: Fluorescein isothocyanate dextran

	Male			
Daily Dose (mg/kg/day)	**0D, 0C**	**0D, 25C**	**7.5D, 0C**	**7.5D, 25C**
	Group Mean			
Serum FITC-Dextran (µg/ml)				
Day 21	0.1458	0.1337	0.5866	0.6557*

*Indicates significantly different from control group (One-Way ANOVA with Tukey post-hoc test, $p < 0.05$)

Table 2 (Continued)

Report Title: Pf1 main study

Small intestinal and colonic electrogenic ion transport

	Male			
Daily Dose (mg/kg/day)	**0D, 0C**	**0D, 25C**	**7.5D, 0C**	**7.5D, 25C**
	Group Mean			
Baseline Isc colon ($\mu A/cm^2$)				
Day 7	89.52	34.64	51.89	160.6*
Day 21	100.8	47.15	83.40	147.1*
Baseline Isc Ileum ($\mu A/cm^2$)				
Day 21	41.33	59.55	18.66	133.4
Baseline conductance colon (mS/cm^2)				
Day 7	28.99	15.87	23.67	19.03
Day 21	33.28	23.26	28.82	51.91*

Baseline conductance ileum (mS/cm^2)				
Day 21	27.60	34.65	42.56	93.45*
Baseline voltage colon (mV/cm^2)	0.005086	-0.01950	-0.01589	
Day 7	0.001982	0.001549	-0.06716	-0.0004768
Day 21				0.2284
	0.3800	-0.001755		
Baseline voltage ileum (mV/Cm^2)			0.7647	
	39.13	114.2		0.02333
Day 21	391.7	47.5	45.87	
			126.8	52.88
Baseline resistance colon (R_t/cm^2)		28.78		35.45
			63.63	
Day 7	78.10			14.17
Day 21				
Baseline resistance ileum (R_t/cm^2)				
Day 21				

ΔIsc following forskolin colon				
Day 7	137.2	184.8	109.0	105.0
Day 21	90.05	107.44	94.68	181.3**
ΔIsc following forskolin ileum	65.03	117.6	156.0	200.9
Day 21				
		116.6	32.45	110.7
ΔIsc following carbachol colon	36.95	41.25	49.15	140.4**
	50.08			
Day 7			73.11	59.81
Day 21		86.34**		
	20.89			
ΔIsc following carbachol ileum				
Day 21				

*Indicates significantly different from crofelemer/buffer control group (Two-Way ANOVA with Tukey post-hoc test, $p < 0.05$)

** Indicates significantly different from water/buffer control group (Two-Way ANOVA with Tukey post-hoc test, $p < 0.05$)

Table 2 (Continued) **Report Title:** Pf1 main study

Small intestinal and colonic mucous cells

	Male			
Daily Dose (mg/kg/day)	**0D, 0C**	**0D, 25C**	**7.5D, 0C**	**7.5D, 25C**
	Group Mean			
Jejunum mucous cells (mean/crypt)				
Day 7	20.32	17.31	14.17	14.51
Day 21	20.66	19.00	13.42	15.30
Colon mucous cells (mean/crypt)				
Day 7	380.5	318.0	348.3	338.5
Day 21	312.2	332.8	366.2	353.7

Table 2 (Continued)

Report Title: Pf1 main study

Small intestinal and colonic morphometry

	Male			
Daily Dose (mg/kg/day)	**0D, 0C**	**0D, 25C**	**7.5D, 0C**	**7.5D, 25C**
	Group Mean			
Jejunum villus height				
(µ)	526.9	481.1	357.5*	263.8*
Day 7	470.6	547.1	286.2*	405.2
Day 21				
Jejunum crypt depth				
(µ)	145.4	129.8	138	113.1*
Day 7	128.6	124.6	106.7	118
Day 21				
Colon crypt depth (µ)				
Day 7	197.6	211.2	191	185.3
Day 21	210.5	196.5	205.2	236.1

H&E scores jejunum				
Day 7	0.0	1.33	1.5	0.83
Day 21	0.83	1.33	1.67	0.67
H&E scores colon				
Day 7	0.5	0.17	0.4	0.5
Day 21	1.33	1.5	2	0.83

* Indicates significantly different from water/buffer control group (Two-Way ANOVA with Tukey post-hoc test, $p < 0.05$)

Table 2 (Continued)

Report Title: Pf1 main study

Small intestinal and colonic inflammation (MPO and IL-1β)

	Male			
Daily Dose (mg/kg/day)	**0D, 0C**	**0D, 25C**	**7.5D, 0C**	**7.5D, 25C**
	Group Mean			
Jejunum MPO cell count (mean/1mm^2)				
Day 7	17.85	26.43	13.32	42.45*
Day 21	19.87	25.7	28.57	25.94
Colon MPO cell count (mean/1mm^2)				
Day 7	2.061	4.817	11.27	9.90
Day 21	7.162	5.940	10.58	14.25

Jejunum IL-1 β staining intensity				
Day 7	3.333	5.000	5.667	5.333
Day 21	4.667	5.833	6.167	5.333
Colon IL-1 β staining intensity				
Day 7	4.333	3.833	3.833	3.000
Day 21	3.333	4.833	5.167	5.167

* Indicates significantly different from water/buffer control group (Two-Way ANOVA with Tukey post-hoc test, $p < 0.05$)

Table 2 (Continued)

Report Title: Pf1

Small intestinal and colonic apoptosis and proliferation

	Male			
Daily Dose (mg/kg/day)	**0D, 0C**	**0D, 25C**	**7.5D, 0C**	**7.5D, 25C**
	Group Mean			
Jejunum apoptotic cell count (mean/crypt)				
	0.04	0.04	0.11	0.078
Day 7	0.1	0.1556	0.2444	0.2111
Day 21				
Colon apoptotic cell count (mean/crypt)				
Day 7	1.2	0.61	1.278	1.1
Day 21	0.8222	0.9600	0.9444	1.333

Jejunum proliferative cell count (mean/crypt)				
	20.5	21.89	20.14	21.62
Day 7	22.7	19.67	18.82	18.31
Day 21				
Colon proliferative cell count (mean/crypt)				
	14.31	17.49	13.12	16.78
Day 7	16.22	15.27	11.91	14.56
Day 21				

End of Results

DETAILS OF TEST FACILITY, PERSONNEL, AND ARCHIVING

Sponsor Pfizer

Test Facility School of Medical Sciences

The University of Adelaide

Frome Rd, Adelaide, South Australia, 5000 Australia

Study Number Pf1

Principal Study Personnel Ysabella Van Sebille, PhD candidate, University of Adelaide

Joanne Bowen, PhD, University of Adelaide.

Dorothy Keefe, Professor of Cancer Medicine, Royal Adelaide Hospital.

The address of study personnel listed is the same as the Test Facility unless otherwise specified.

Study Director Dr Joanne Bowen, PhD

Technical Support Ysabella Van Sebille

Animal Husbandry The University of Adelaide Animal House staff

Test Article Formulation N/A

Test Formulation Analysis N/A

Ophthalmoscopy N/A

Clinical Pathology Ysabella Van Sebille

Histotechnology Ysabella Van Sebille

Pathology Ysabella Van Sebille

Peer Review Pathology N/A

Platform Technology and Science N/A

Drug Pharmacokinetics N/A

Veterinary Services Laboratory Animal Services, The University of Adelaide

Statistical Analysis Ysabella Van Sebille

Report Writing Ysabella Van Sebille

Archival of Records

Data, left over samples, and reports will be stored in the School of Medical Sciences, The University of Adelaide.

INTRODUCTION

PF-00299804 (Dacomitinib) is an irreversible pan-HER tyrosine kinase inhibitor that is currently in clinical trials for the treatment of non-small cell lung cancer and head and neck squamous cell cancer. The most common adverse event reported is diarrhoea, although the underlying cause of this side effect is currently unknown. Despite promising response data, the frequency of diarrhoea is higher compared to treatment with 1st generation HER inhibitors and is a dose limiting toxicity impeding optimal treatment. All doses and concentrations are expressed in terms of the parent compound, which for the purpose of this report is referred to as DACOMITINIB.

Crofelemer is produced from the plant, *Croton lechleri* (active component oligomeric proanthocyanidin), and inhibits both cAMP cystic fibrosis (CFTR) and calcium activated (CaCC) chloride channels. If inhibition of HER signaling results in increased mucosal chloride secretion, this agent may be effective at reducing dacomitinib-induced diarrhoea. Crofelemer is currently in clinical trials for treatment of secretory diarrhoea of multiple different etiologies and has recently been FDA approved for the treatment of diarrhoea in HIV/AIDS patients on anti-retroviral therapy. It is not systemically absorbed, only acting locally on the gastrointestinal tract to modify water balance without affecting motility. As such, this agent is potentially an effective management approach to dacomitinib-induced diarrhoea.

Objective

The objective of the study was to determine the gastrointestinal changes induced by dacomitinib and assess the efficacy of chloride secretion inhibition with crofelemer in a 21 day oral administration study in rats.

Rationale for Selection of Dose

Dacomitinib and crofelemer doses were selected based on experiments conducted in our laboratory.

Dacomitinib was administered at 7.5 mg/kg via daily oral gavage, which induced mild to severe diarrhoea without mortality and was deemed appropriate for all investigations. Crofelemer was given daily via oral gavage at 10, 25 and 50 mg/kg doses and were compared in different treatment schedules to determine the optimal dose. Combination of dacomitinib at 7.5 mg/kg and crofelemer at 25 mg/kg was most effective, decreasing the number of days with diarrhoea from 19 to 9. Previous research in mice has shown that 30 mg/kg crofelemer is effective at reducing cholera toxin-induced water accumulation in the intestines. As such, it seemed feasible that 25 mg/kg crofelemer in our pilot study reduced diarrhoea by preventing water accumulation in the intestines following dacomitinib treatment. This dose and treatment schedule was considered to best reflect the clinical setting and so was chosen for subsequent experiments.

Rationale for Selection of Species and Route of Administration

The rat was selected because it is a standard rodent species recognised by international regulatory agencies for use in safety evaluation studies. The Crl:WI(Han) rat was chosen because of the knowledge of this strain's general pathology and response to HER TKI's. Male rats were used in this study to be consistent with previous experiments that have shown that male Wistar rats effectively metabolise HER TKI's.

The oral route was selected for dacomitinib and crofelemer because this is the intended route of administration to humans. For dacomitinib, this route of administration has been used

extensively in preclinical studies, and the pharmalogical response is well documented. For crofelemer, previous studies in rats have also preferred this route of administration.

This study did not replicate any known previous work.

Regulatory Guidelines

N/A

MATERIALS AND METHODS

Test Article and Dose Preparation

PF-00299804 (Dacomitinib) was supplied by Pfizer and was stored at room temperature (18°C) and protected from light.

Dacomitinib at concentration of 2 mg/mL (as active moiety) in methylcellulose buffer vehicle was prepared daily and used immediately. The vehicle was prepared weekly and stored at refrigerated temperature (4°C) protected from light. Crofelemer was in tablet form and stored at room temperature protected from light in a sterile container. Crofelemer was ground and diluted with sterile distilled water to 5 mg/ml immediately before use.

Fluorescein isothocyanate dextran (FITC) 2-5 kDa made at a solution of 120 mg/ml was administered via oral gavage at a dose of 600 mg/kg, 2 hours prior to kill to assess gut barrier permeability.

The compounds, vehicle components, suppliers, and batch numbers used are as follows.

Material	Batch Number	Supplier
hydroxypropylmethylcellulose	067K0012	Sigma
Crofelemer (Fulyzaq)	3106372	Salix

Dacomitinib	Pfizer
Fluorescein isothocyanate (FITC) dextran	BCBN601N Sigma

Animals and Maintenance

Male Crl:WI(Han) rats were obtained from The University of Adelaide, Waite Campus breeding facility, and randomly allocated to study groups. The rats were housed in groups of 2 to 6 (of the same treatment arm) in individually ventilated cages with paper litter. Following randomisation, rats were acclimatised to local housing conditions for a minimum of 7 days prior to the first day of dosing. On Day 1 of treatment, the rats were approximately 6 - 8 weeks old and weighed on average 193 g to 233 g.

Standard pellet rodent chow and filtered water were available ad libitum. If rats were considered to be experiencing treatment-related toxicity (e.g., diarrhoea, weight loss, stress marks) they were allowed soaked chow in addition, or in severe cases (n = 1) were gavaged lectade oral rehydration therapy (Jurox) (glycine, citric acid, potassium phosphate monobasic, potassium citrate, sodium chloride, glucose). Available information on the diet used and results from periodic analysis of the water in this facility does not indicate the presence of any substance at a concentration likely to influence the outcome of the study.

The environmental controls were set to maintain temperature within the range 19 to 23 °C and relative humidity within the range 45 % to 70 %; with a 12 - hour light and 12 - hour dark cycle. A general check including availability of food and water and environmental conditions was performed up to thrice daily. Clinical record sheets were filled in during each check. The clinical sheets requested information on piloerection, reluctance to move, reduced food/water intake,

diarrhoea and weight loss. Each category was scored from 0 to 3 (0 = none, 1 = mild, 2 = moderate, 3 = severe). Scores of 12 or above required the rat to be checked 4 times daily and veterinary advice was sought regarding the removal of the rat from the study.

STUDY DESIGN

For each experiment, all rats were randomly allocated to group by randomize.org. Rats were identified by a unique animal number written with an indelible marker on the tail.

During the 21 day treatment period, rats received daily oral doses of dacomitinib or vehicle at a constant dose volume of approximately 5 mL/kg at 9 am. Individual dose volumes were adjusted daily according to body weight. The first day of dosing was designated Day 0, days in the pre-treatment period were assigned negative numbers. The final dose was given on the day before scheduled necropsy, or in the case of the additional study on the same day as necropsy. The terminal necropsy was conducted on Days 7 and 21.

Deviations from dose regimen:

The following table summarises study group assignment and dose information.

Table of study outline

Group Number	**Dose (mg/kg/day)**	**Dose Concentration (mg/mL)**	**Number/Sex**
Pf1			

1 – Water vehicle control 2 – Methylcellulose Buffer vehicle control	1 ml 1 ml	NA NA	12M
1 – Water vehicle control 2 – Dacomitinib	1 ml 7.5	NA 2	12M
1 – Crofelemer 2 – Methylcellulose Buffer vehicle control	25 1 ml	5 NA	12M
1 – Crofelemer 2 – Dacomitinib	25 7.5	5 2	12M

MEASUREMENTS AND OBSERVATIONS

Mortality

A viability check was performed near the start and end of each working day. If rats appeared excessively toxic, checks increased to thrice daily. A necropsy was performed on any animals

that were killed early during the treatment period, but these animals were not included in final analysis.

Clinical Observations

A check of the condition and behaviour of all animals was made daily throughout the treatment period. During the treatment period, all animals were examined and clinical signs recorded twice daily. Detailed clinical examinations were performed prior to initiation of dosing, during days 0 - 21 and on the day of necropsy.

Where identical findings (including no abnormalities detected) were recorded for an animal more than once on the same day, only one instance of the finding has been reported.

Mild diarrhoea was defined as soft stools (G1), moderate diarrhoea as loose stools with perianal staining of fur (G2), and severe diarrhoea as watery stools +/- mucous with fur staining incorporating hind legs (G3).

Body Weight

The animals were weighed at 9 am once daily during the treatment period and on the day of necropsy.

Food Consumption

Animals were allowed *ad libitum* access to standard rat chow and water. Food consumption was not recorded.

Clinical Pathology

Blood was collected at scheduled necropsy by cardiac puncture under deep isoflurane anaesthesia. Serum was separated and biochemical analysis performed at an external facility (Institute of Medical and Veterinary Science, The Royal Adelaide Hospital).

Clinical Chemistry

Samples for clinical chemistry were collected into serum tubes without anticoagulant. The following parameters were measured from serum samples.

Alanine aminotransferase	Urea
Aspartate aminotransferase	Creatinine
Alkaline Phosphatase	Phosphate
Lactate dehydrogenase	Bicarbonate
Total bilirubin	Sodium
Glucose	Potassium
Total protein	Gamma-glutamyl transpeptidase
Globulin	Anion Gap

Fluorescein isothocyanate dextran

Fluorescein isothocyanate dextran (FITC) 2-5 kDa made at a solution of 120 mg/ml was administered via oral gavage at a dose of 600 mg/kg, 2 hours prior to kill. Levels of FITC were determined using fluorescent reading conducted on serum samples collected at necropsy to assess gut barrier permeability.

Terminal Procedures

After 7 and 21 days of treatment animals were killed by exsanguination under deep isoflurane anaesthesia followed by cervical dislocation. 5 mL of blood without anticoagulant for serum together with tissue samples from the digestive tract were obtained from all animals.

Organ Weights

The following organs were weighed:

Small intestine	Liver

Large intestine	Spleen	
Stomach (empty)	Kidney	

Tissues Fixed and Examined

Following a detailed external and internal examination, the tissues highlighted below were taken from each animal and preserved in either: 10% neutral buffered formalin (NBF), snap frozen in liquid nitrogen (SF), frozen in RNA later (RNA) (Sigma Aldrich), or placed in Ringers with indomethacin (R) (composition in mmol L−1: NaC1 115.4; KCl 5; MgCl2 1.2; NaH2PO4 0.6; NaHCO3 25; CaCl2 1.2 and glucose 10).

Tissues Fixed	Tissues Examined	Tissues Fixed	Tissues Examined
Adrenals	X	Pituitary	X
Animal identification		Preputial/clitoral gland	X
Aorta (thoracic)	X	Prostate	X
Brain	X	Rectum	X
CAECUM	NBF	Salivary gland -	X
Cervix	X	mandibular	X
COLON	NBF, R, SF, RNA	sublingual	X
DUODENUM	NBF, SF, RNA	parotid	X
Epididymides	X	Sciatic nerve	X
Eyes/Optic nerves	X	Seminal vesicles	X
Femur (Femoro-tibial joint)	X	Skeletal muscle (hindlimb)	X
Harderian glands	X	**SKIN**	NBF
HEART	NBF	Spinal column -	X

Tissues Fixed	Tissues Examined	Tissues Fixed	Tissues Examined
ILEUM	NBF, R, SF, RNA	spinal cord (cervical)	X
[Injection site(s)	X	spinal cord (thoracic)	X
JEJUNUM	NBF, SF, RNA	spinal cord (lumbar)	X
KIDNEYS	NBF	**SPLEEN**	NBF
Larynx	X	Sternum with bone marrow	X
LIVER [and gallbladder]	NBF	**STOMACH**	NBF
LUNG	NBF	Testes	X
Lymph node -	X	Thymus/Thymic area	X
mandibular	X	Thyroid	X
mesenteric	X	**TISSUES SHOWING MACROSCOPIC**	X
Mammary gland (inguinal)	X	**OBSERVATIONS**	NBF
Nasal cavities and nasopharynx (with	X	**TONGUE**	NBF
skull)	X	Trachea	X
OESOPHAGUS	NBF	**URINARY BLADDER**	NBF
ORAL MUCOSA	NBF	Uterus	X
Pancreas	X	Vagina	X
Parathyroids	X	Tibial long bone	

Samples of the jejunum and colon tissues fixed in NBF were processed to paraffin wax, sectioned, stained with haematoxylin and eosin, alcian blue periodic acid Schiff (AB-PAS) or immunohistochemistry and examined microscopically for all animals killed at the end of the dosing period.

Specialized immunohistochemical staining (caspase-3, Ki-67, MPO, IL-1β) were applied to additional sections of the jejunum and colon using a DAKO reagents on an automated machine (AutostainerPlus Dako, Denmark) following standard procedures supplied by the manufacturer (Flex Plus detection system, Dako, Denmark).

All slides were scanned using a NanoZoomer and analysed with NanoZoomer Digital Pathology Software version 2.3.14. All assessments were done in a blinded fashion.

Colon and Ileum pieces were placed in Ringers solution with indomethacin (R), and immediately had the muscularis layer stripped via microdissection while remaining in R and being gassed with carbogen (95 % O2 – 5 % CO2) to maintain tissue integrity. It is important to remove the muscularis layer in Ussing chamber experiments to ensure that results can be solely attributed to mucosal chloride secretion.

Gastrointestinal Electrogenic Ion Transport

Once muscularis was removed, samples were mounted in Ussing chambers. The tissue samples were bathed with 4 ml of carbogen-gassed R solution (no indomethacin) on each side. Each reservoir was gassed with 95 % O2 - 5 % CO2 and kept at constant temperature of 37 °C. Electrogenic ion transport was monitored continuously as short-circuit current (Isc) by using an automated multichannel voltage/current clamp apparatus (VCC MC8) (Physiologic Instruments) linked through Acquire Analyze 2.3 computer program. Baseline readings were recorded to assess baseline differences in electrophysiological function. Forskolin was administered at a concentration of 10μM to the basolateral chamber to elevate levels of cAMP to activate CFTR chloride channels. Carbachol was administered at a concentration of 100 μM to the basolateral chamber to elevate levels of calcium to activate the Calcium activated chloride channels.

Material	Batch Number	Supplier
Indomethacin	BCBK0293V	Sigma

Forskolin	SLB3902V	Sigma
Carbachol	BCBG1471V	Sigma

Computer Systems

The computer systems that were used on this study to acquire and quantify data include: Windows (Word, Excel), Prism version 6, NanoZoomer Digital Pathology, DAKO autostainer software, Acquire and Analyse (Physiologic Instruments), Gen 5.

Analysis of Data

Numeric data for body weights, body weight changes, organ weights, and clinical pathology are expressed as the arithmetic mean for each group. The test article groups were compared with the control groups.

The assumptions of equality of variance for each group and normally distributed data were tested using Tukey's test after performing the 2 way analysis of variance (ANOVA) for body weights, organ weights, clinical biochemistry, histopathology, goblet cells, Ki-67, caspase-3, IL-1β, MPO, Isc, and FITC. Chi squared test was performed for diarrhoea scores.

The numerical data presented in this report were generated by different computer systems. When performing calculations, these systems may round numbers differently or may not report values to the same number of significant digits. Because of these differences, means or standard

deviations in tables and appendices may differ slightly, and recalculation of derived values from individual data presented in this report will, in some instances, yield minor variation.

RESULTS

Noteworthy findings are described in this section. No specific mention is made of minor differences between treated and control groups if considered not related to test article administration.

Clinical Observations

Clinical observations were conducted twice daily during the treatment period.

The most commonly recorded clinical observations throughout the experiments were loose faeces. Diarrhoea severity ranged from mild (grade 1) to severe (grade 3). Diarrhoea (grade1 - 3) occurred in 100 % of water and dacomitinib and crofelemer and dacomitinib treated rats. Approximately 50 % of rats treated with combination crofelemer and dacomitinib had severe diarrhoea (grade 3: severe diarrhoea as watery stools +/- mucous with fur staining incorporating hind legs). Approximately 30 % of rats treated with dacomitinib only had severe diarrhoea. Combination of crofelemer and dacomitinib caused significantly ($p = 0.0003$) worse diarrhoea than dacomitinib alone.

The second most common clinical observations were piloerection and red discolouration of the fur around the nose and eyes. These signs indicate stress in the animal and were most common in the combination groups.

Although rare (n = 2), other clinical observations included skin toxicity (pictured below), characterised by hair loss, and red inflamed skin. Animals displaying skin toxicity were treated with crofelemer and dacomitinib. This clinical observation preceded removal of the rats from the study due to excessive weight loss. All other clinical observations were rare.

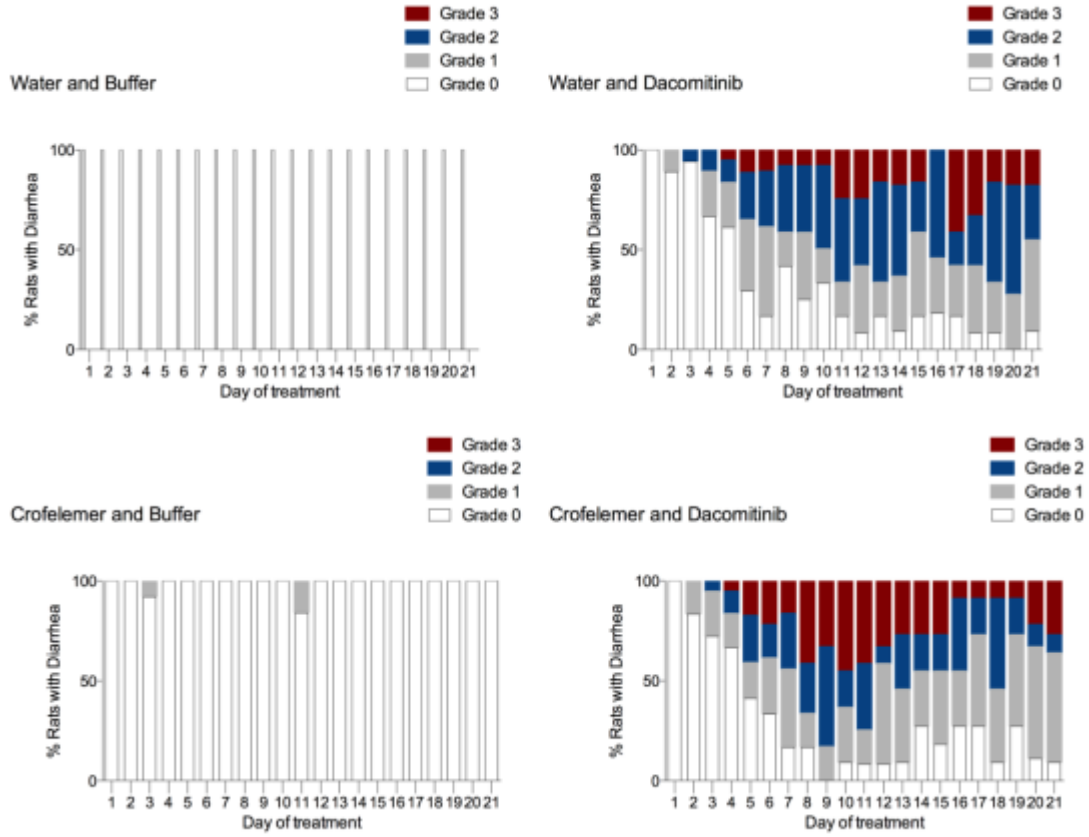

Body Weight

The third most common clinical observation was weight loss. From day 10 – 21 rats treated with crofelemer and dacomitinib had significantly less weight gained compared to controls ($p < 0.0340$). From day 13 – 21 rats treated with dacomitinib alone had significantly less weight gained compared to controls ($p < 0.00167$). A number of rats treated with crofelemer and dacomitinib (n = 4) and rats treated with dacomitinib alone (n = 1) were removed from the study due to excessive weight loss of > 15 %, due to ethical guidelines.

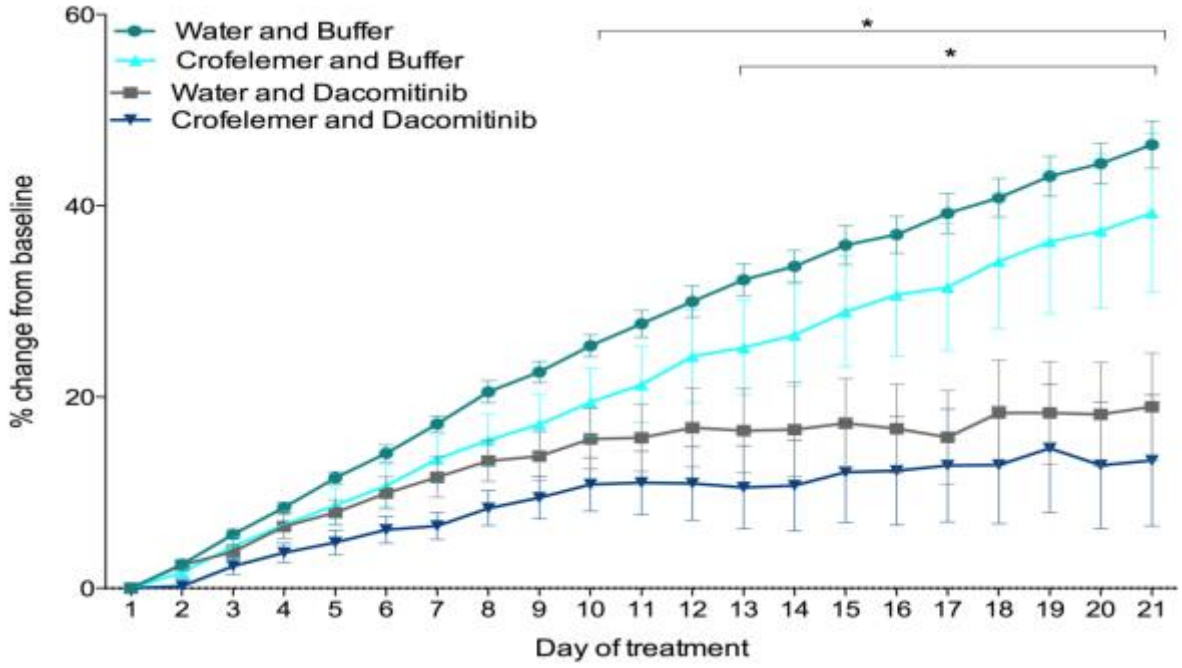

Clinical Chemistry

All serum biochemistry and liver enzyme results are shown in the summary section, table 2. Serum biochemistry and liver enzyme analysis showed mixed results. Liver enzymes were increased in rats treated with dacomitinib. ALP was significantly increased in rats treated with crofelemer and dacomitinib and dacomitinib alone compared to water and buffer control rats after 7 days of treatment. ALT was significantly increased after 21 days of treatment in rats treated with crofelemer and dacomitinib compared to water and buffer control rats.

Urea, creatinine and albumin levels were significantly different at 21 days post treatment in rats treated with crofelemer and dacomitinib and dacomitinib alone compared to control rats treated with water and buffer. The anion gap was increased at 21 days post treatment in rats treated with crofelemer and dacomitinib and dacomitinib alone compared to control rats treated with water and buffer. LD was significantly increased in rats treated with crofelemer and dacomitinib compared to control rats treated with water and buffer at 21 days.

Organ Weights

All data for organ weights is shown in summary section, table 2.

Stomach, small intestine, large intestine, kidneys, liver and spleen were weighed and compared as total weight.

No differences were noted in large intestine and kidney weights. Spleen weights were significantly less in rats treated with dacomitinib alone ($p = 0.0018$) and combination crofelemer and dacomitinib ($p = 0.0091$) compared to water and buffer treated control rats. Liver weights were significantly less in rats treated with dacomitinib alone ($p < 0.0001$) and combination crofelemer and dacomitinib ($p < 0.0001$) compared to water and buffer treated control rats. Small intestine weights were significantly less in rats treated with dacomitinib alone ($p = 0.0017$) and combination crofelemer and dacomitinib ($p = 0.0134$) compared to water and buffer treated control rats. Stomach weights were significantly less in rats treated with dacomitinib alone ($p = 0.0089$) compared to water and buffer treated control rats.

Terminal Necropsy

Groups of rats were killed at 7 days and 21 days of treatment. Macroscopic pathology was more frequently observed in rats treated with dacomitinib alone or combination crofelemer and dacomitinib. The most common pathology was distended, bloated caecum and large intestines. Inflamed, vascular intestines were also observed in a number of rats.

Gastrointestinal Permeability

Fluorescein isothocyanate dextran (FITC) 2-5 kDa made at a solution of 120 mg/ml was administered via oral gavage at a dose of 600 mg/kg, 2 hours prior to kill. Levels of FITC were determined using fluorescent reading conducted on serum samples collected at necropsy to assess gut barrier permeability. Rats treated with combination crofelemer and dacomitinib had significantly increased serum levels of FITC dextran compared to water and buffer treated control rats ($p = 0.0202$) and crofelemer and buffer treated rats ($p = 0.0172$).

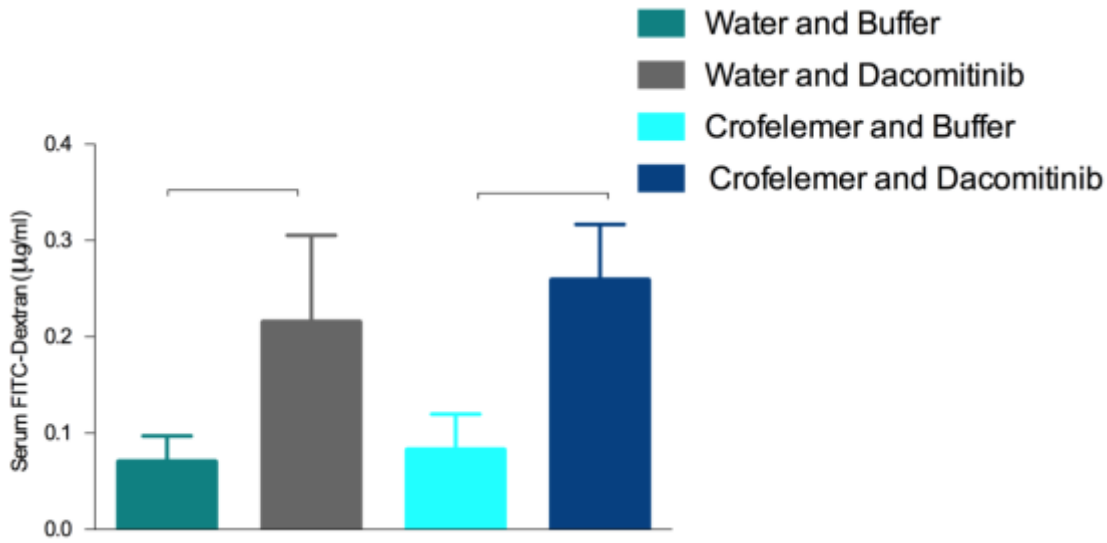

Gastrointestinal Electrogenic Ion Transport

Samples of colon and ileum were mounted in Ussing chambers to record gastrointestinal electrogenic ion transport as short circuit current (Isc). Baseline readings were recorded to assess baseline differences in electrophysiological function. Baseline Isc in the colon was significantly higher in rats treated with combination crofelemer and dacomitinib compared to dacomitinib alone ($p = 0.0445$), and crofelemer alone ($p = 0.0145$) at 7 days, and at 21 days compared to crofelemer alone ($p = 0.0078$). Baseline conductance in the colon was significantly higher in rats treated with combination crofelemer and dacomitinib compared to crofelemer alone at 21 days ($p = 0.0409$). Samples of ileum from rats treated with combination crofelemer and dacomitinib had

significantly increased baseline conductance compared to water and buffer control rats ($p = 0.0030$), crofelemer alone rats ($p = 0.0077$) and dacomitinib alone rats ($p = 0.0282$) at 21 days. No significant differences were noted in baseline voltage or resistance in ileum or colon samples. Forskolin was administered at a concentration of 10μM to the basolateral chamber to elevate levels of cAMP to activate CFTR chloride channels. No differences were noted between groups in ileum samples following forskolin administration. The colon samples of rats treated with combination crofelemer and dacomitinib for 21 days had significantly increased Isc following forskolin administration compared to water and buffer control rats ($p = 0.0087$) and dacomitinib alone rats ($p = 0.0201$).

Carbachol was administered at a concentration of 100μM to the basolateral chamber to elevate levels of calcium to activate the Calcium activated chloride channels. No differences were noted between groups in ileum samples following carbachol administration. The colon samples of rats treated with combination crofelemer and dacomitinib for 21 days had significantly increased Isc following carbachol administration compared to water and buffer control rats ($p = 0.0020$), crofelemer alone rats ($p = 0.0006$), and dacomitinib alone rats ($p = 0.0022$).

Microscopic Observations

Histopathological analysis included investigation of colon and jejunum paraffin fixed samples. Specific stains included: haematoxylin and eosin (H&E) to asses anatomical derangement, alcian blue periodic acid Schiff (AB-PAS) to asses mucin changes, immunohistochemistry with a variety of antibodies to asses apoptosis (Caspase-3), proliferation (Ki-67), and inflammation (MPO and IL-1β).

The jejunum and colon were assessed for changes in morphometry in H&E stained sections. Specifically, villus height and crypt depth were measured and a validated injury score was used to assess damage. Briefly, this score includes evaluation of brush border and surface enterocyte

disruption, crypt loss and architectural disruption, disruption of crypt cells, infiltration of polymorphonuclear cells and lymphocytes, dilation of lymphatics and capillaries, oedema, villus fusion and villus atrophy. There was no significant difference in crypt depth between groups in the colon or jejunum at 21 days. At 7 days, rats treated with combination crofelemer and dacomitinib had significantly decreased jejunum crypts compared to water and buffer control rats ($p = 0.00185$). Villus height was significantly decreased at 7 days in rats treated with dacomitinib alone ($p = 0.0009$) and combination crofelemer and dacomitinib ($p < 0.0001$) compared to water and buffer controls. At 21 days dacomitinib alone ($p = 0.0003$) and combination crofelemer and dacomitinib ($p = 0.0065$) had significantly decreased villus heights compared to controls. There was no difference in injury scores between groups in the colon or jejunum at either time point.

Changes in mucin secretion was analysed using AB-PAS stained sections of the colon and jejunum. The number of positively stained cells were counted. No significant differences were noted in either the colon or the jejunum at either time point.

Apoptosis was analysed using caspase-3 stained sections of the colon and the jejunum. The number of positively stained cells were counted. No significant differences were noted in either the colon or the jejunum at either time point.

Proliferation was analysed using Ki-67 stained sections of the colon and the jejunum. The number of positively stained cells were counted. No significant differences were noted in either the colon or the jejunum at either time point.

Inflammation was assessed using MPO and IL-1β stained sections of the colon and the jejunum. MPO is a marker of granulocytes; the number of positively stained cells were counted in the colon and the jejunum. There were no significant differences in the number of MPO positively stained cells between groups in colon samples at either time point. In jejunum samples, the number of MPO positively stained cells was significantly increased in rats treated with

combination crofelemer and dacomitinib compared to water and buffer control rats at 7 days ($p = 0.0259$). There were no significant differences in the number of Il-1 β positively stained cells between groups in jejunum or colon samples at either time point.

DISCUSSION

The purpose of these experiments was to develop a rat model of dacomitinib-induced diarrhoea that could be interrogated for mechanisms of diarrhoea and be used to assess chloride channel inhibition as an intervention. This study was conducted over two phases; the first phase aimed to determine the optimal dose of dacomitinib and crofelemer administration, the second phase aimed to determine the effect of concurrent crofelemer on dacomitinib-induced diarrhoea. Crofelemer administered alone did not induce diarrhoea and was safe and well tolerated.

We were successful in designing a model that reflects the clinical picture by inducing moderate diarrhoea in all rats when treated with 7.5 mg/kg dacomitinib. At a dose of 7.5 mg/kg, dacomitinib induced diarrhoea in a pattern whereby diarrhoea had a slow onset, increasing in frequency and severity as the study progressed. A similar pattern was noted in rats treated with combination crofelemer and dacomitinib. Diarrhoea that occurred in the first 3 days of the experiment was possibly due to restraint stress as dacomitinib-induced diarrhoea occurred more predominantly from day 5 of treatment. During this experiment, diarrhoea in the combination crofelemer and dacomitinib treated rats occurred at an increased frequency and severity than all other groups. Inhibition of chloride channels with crofelemer did not effectively treat diarrhoea.

Body weight of rats is a frequently used measure of health. Rats treated with dacomitinib alone or combination crofelemer and dacomitinib had significantly less weight gain from baseline indicating that rats in these groups had increased toxicity. Combination crofelemer and dacomitinib rats had significantly lower body weights than controls from day 10 onwards, whereas dacomitinib alone rats did not have significantly lower body weights until day 13. This

suggests that crofelemer induced dacomitinib induced-toxicity earlier than when dacomitinib is administered alone.

Liver enzymes were increased in rats treated with dacomitinib. ALP and ALT was significantly increased in rats treated with dacomitinib alone and combination crofelemer and dacomitinib rats compared to control rats. This suggests that dacomitinib causes liver dysfunction, further supported, as liver weights were significantly lighter in rats from these groups. Urea, creatinine and albumin levels were significantly different at 21 days post treatment in rats treated with dacomitinib alone and combination crofelemer and dacomitinib rats compared to control rats, suggesting that dacomitinib causes renal dysfunction. The anion gap was increased at 21 days post treatment in rats treated with dacomitinib alone and combination crofelemer and dacomitinib rats compared to control rats, this may suggest renal dysfunction, or could be a result from the severe diarrhoea. LD was significantly increased in rats treated with crofelemer and dacomitinib compared to control rats suggesting tissue injury. No differences were noted in serum chloride concentrations.

FITC dextran is a fluorescent-labelled sugar that is administered via oral gavage 2 hours prior to blood collection to assess gastrointestinal barrier permeability. Levels of FITC were determined using fluorescent reading conducted on serum samples collected at necropsy. Rats treated with combination crofelemer and dacomitinib had significantly increased serum levels of FITC dextran compared to water and buffer treated control rats. This indicates that rats treated with combination crofelemer and dacomitinib had decreased barrier function. This is further confirmed in Ussing chamber experiments, where ileum and colon samples from rats treated with crofelemer and dacomitinib showed increased baseline conductance, suggesting that rats from this group had increased gastrointestinal permeability. This is consistent with gastrointestinal

toxicity induced by traditional chemotherapy. Further investigations are needed to determine the cause of the increased permeability.

Ussing chamber experiments were conducted on distal portions of the colon and the ileum to investigate *ex vivo* the electrogenic transport of the gastrointestinal mucosa. Short circuit current (Isc) is a measure of chloride secretion across the epithelium. In these experiments, baseline Isc was decreased in rats treated with crofelemer alone, indicating that when given in isolation, crofelemer is effective at inhibiting chloride secretion. However, when given in combination with dacomitinib, this effect is lost as Isc is increased. Forskolin and carbachol were administered to assess CFTR and CaCC chloride channels. Colon samples of rats treated with combination crofelemer and dacomitinib had significantly increased Isc following both forskolin and carbachol administration, suggesting that this treatment increases chloride secretion via the both chloride channels. Results from Ussing chamber experiments do not indicate that dacomitinib-induced diarrhoea is due to secretory mechanisms, as dacomitinib alone treated rats did not have an increase in baseline Isc, or in reaction to forskolin or carbachol administration. This explains why crofelemer is not effective at inhibiting dacomitinib-induced diarrhoea, but does not address why crofelemer worsens dacomitinib-induced diarrhoea.

This study found mixed results in tissue pathology. Histopathological analysis did not suggest an increased mucin secretion or an inflammatory component to be responsible for the clinical measures of gastrointestinal toxicity noted. All rats treated with dacomitinib (alone, or in combination with crofelemer) had decreased villus height, suggesting dacomitinib induces atrophy of the small intestine. This is further supported as rats in these groups had significantly lighter small intestine weights. Contrary to the study hypothesis, and the currently available literature, these results imply that dacomitinib may cause small intestinal atrophy. Decreased surface area of the small intestine caused by said atrophy can lead to diarrhoea due to an inability

to control solute absorption and secretion. These characteristics are consistent with traditional chemotherapy-induced gut toxicity, and inconsistent with previously published preclinical studies of oral small molecule TKIs. Nevertheless, no differences were noted in apoptosis, proliferation or injury scores, which is inconsistent with typical small intestinal atrophy/damage caused by traditional chemotherapy.

The mechanisms underlying development of diarrhoea in this model require more investigation. The results from this study are inconclusive as to whether the mechanism of dacomitinib-induced diarrhoea is due to small intestinal atrophy, or chloride secretion. Theoretical causes may include that unabsorbed dacomitinib acts as an irritant within the small and large intestine, causing activation of neural and immune signals that lead to increased motility as a reflex for removal of the stimulus. Further studies are needed to determine changes in expression and function of membrane channels, which control solute and water movement along the length of the tract in response to dacomitinib.

CONCLUSION

In conclusion, the findings from this study support the Albino Wistar rat as an appropriate choice to model dacomitinib-induced diarrhoea. We have shown that combining crofelemer with dacomitinib causes worse diarrhoea compared to either alone, indicating that it is unlikely that dacomitinib induces diarrhoea due to secretory mechanisms. Further research is required to understand the mechanisms of dacomitinib-induced diarrhoea to best target interventions.

PART 2

IN VITRO STUDY		**Compound:**	**Dacomitinib (PF-00299804)**
Information Type:	In Vitro interrogation		

Title:	Part 2: Investigating the effect of dacomitinib on chloride secretion in colonic epithelial cells– In vitro study

Table 1

Report Title: Part 2 in vitro study

Baseline Short circuit current (Isc)

Dose dacomitinib (D) & crofelemer (C) µM	**0D, 0C**	**0D, 10C**	**1D, 0C**	**1D, 10C**
Baseline Isc ($\mu A/cm^2$)	**Group mean**			
5 minutes	7.481	9.387**	36.08*	6.707**
20 minutes			30.54*	9.175**
60 minutes			6.851	
90 minutes			5.383	
3 hours			3.354	
6 hours			11.04	
24 hours			9.948	
48 hours			15.31	

* Indicates significantly different from DMSO control group (One-Way ANOVA, $p < 0.0001$)

** Indicates significantly different from dacomitinib group (One-Way ANOVA, $p < 0.0001$)

Table 2

Report Title: Part 2 in vitro study

Baseline Resistance

Dose dacomitinib (D) & crofelemer (C) µM	**0D, 0C**	**0D, 10C**	**1D, 0C**	**1D, 10C**
Baseline Resistance (Ohms/cm^2)	**Group mean**			
5 minutes	554.4	956.5	717.1**	1659*
20 minutes			604.7**	1130*
60 minutes			911.7	
90 minutes			430.5	
3 hours			591.9	
6 hours			559.7	
24 hours			757.1	
48 hours			708.2	

* Indicates significantly different from DMSO control group (One-Way ANOVA, $p < 0.0003$)

** Indicates significantly different from crofelemer/dacomitinib group (One-Way ANOVA, $p < 0.0001$)

Table 3

Report Title: Part 2 in vitro study

Baseline Conductance

Dose dacomitinib (D) & crofelemer (C) μM	0D, 0C	0D, 10C	1D, 0C	1D, 10C
Baseline Conductance (mS/cm^2)	**Group mean**			
5 minutes	2.204	1.158	1.540	0.6220*
20 minutes			1.663	0.8856*
60 minutes			1.136	
90 minutes			2.375	
3 hours			2.024	
6 hours			1.839	
24 hours			1.509	
48 hours			1.763	

* Indicates significantly different from DMSO control group (One-Way ANOVA, $p < 0.005$)

Table 4

Report Title: Part 2 in vitro study

Δ Isc after forskolin

Dose dacomitinib				

(D) & crofelemer (C) µM	**0D, 0C**	**0D, 10C**	**1D, 0C**	**1D, 10C**
Δ Isc after forskolin ($\mu A/cm^2$)	**Group mean**			
5 minutes	16.70	14.45	2.164*	14.68
20 minutes			4.551*	3.471*
60 minutes			16.28	
90 minutes			14.02	
3 hours			23.59	
6 hours			7.481	
24 hours			19.95	
48 hours			12.28	

* Indicates significantly different from DMSO control group (One-Way ANOVA, $p < 0.05$)

Table 5

Report Title: Part 2 in vitro study

Δ Isc after carbachol

Dose dacomitinib (D) & crofelemer (C) µM	**0D, 0C**	**0D, 10C**	**1D, 0C**	**1D, 10C**
Δ Isc after carbachol ($\mu A/cm^2$)	**Group mean**			

5 minutes	107	28.60*	96.58***	16.81*,**
20 minutes			145.1***	12.50*,**
60 minutes			97.36***	
90 minutes			132.5***	
3 hours			141.6***	
6 hours			90.67***	
24 hours			139.2***	
48 hours			107.6***	

* Indicates significantly different from DMSO control group (One-Way ANOVA, $p < 0.0001$)

** Indicates significantly different from dacomitinib group (One-Way ANOVA, $p < 0.0001$)

*** Indicates significantly different from crofelemer group (One-Way ANOVA, $p < 0.05$)

Table 6

Report Title: Part 2 in vitro study

Baseline Isc in presence of tetraethylammonium chloride pre-treatment

Dose dacomitinib (D) µM & Tetraethylammonium (T) mM	**0D, 0T**	**0D, 1T**	**1D, 0T**	**1D, 1T**
Baseline Isc ($\mu A/cm^2$)	**Group mean**			
5 minutes	7.481*,**	19.20*,***	36.08**,***	27.25**, ***

20 minutes		18.67*,***	30.54***	5.066*, **

* Indicates significantly different from dacomitinib group (One-Way ANOVA, $p < 0.0001$)

** Indicates significantly different from tetraethylammonium group (One-Way ANOVA, $p < 0.005$)

*** Indicates significantly different from DMSO control group (One-Way ANOVA, $p < 0.005$)

Table 7

Report Title: Part 2 in vitro study

Baseline resistance in presence of tetraethylammonium chloride pre-treatment

Dose dacomitinib (D) µM & Tetraethylammonium (T) mM	**0D, 0T**	**0D, 1T**	**1D, 0T**	**1D, 1T**
Baseline Resistance (Ohms/cm^2)	**Group mean**			
5 minutes	555.4*	759.2	717.1	636.6
20 minutes		682.2*	604.7*	1179

* Indicates significantly different from dacomitinib + tetraethylammonium 20 minute group (One-Way ANOVA, $p < 0.005$)

Table 8

Report Title: Part 2 in vitro study

Baseline conductance in presence of tetraethylammonium chloride pre-treatment

Dose dacomitinib (D) µM & Tetraethylammonium (T) mM	0D, 0T	0D, 1T	1D, 0T	1D, 1T
Baseline Conductance (mS/cm^2)	**Group mean**			
5 minutes	2.204	1.360	1.540	1.653
20 minutes		1.666	1.663*	1.177

* Indicates significantly different from DMSO vehicle control group (One-Way ANOVA, $p < 0.05$)

Table 9

Report Title: Part 2 in vitro study

Δ Isc after forskolin in the presence of tetraethylammonium chloride <u>pre-treatment</u>

Dose dacomitinib (D) µM & Tetraethylammonium (T) mM	0D, 0T	0D, 1T	1D, 0T	1D, 1T
Δ Isc after forskolin ($\mu A/cm^2$)	**Group mean**			
5 minutes	16.70	5.08*	6.133*	9.258
20 minutes		8.618*	4.551*	13.06**

* Indicates significantly different from DMSO vehicle control group (One-Way ANOVA, $p < 0.005$)

** Indicates significantly different from dacomitinib group (One-Way ANOVA, $p < 0.001$)

Table 10

Report Title: Part 2 in vitro study

Δ Isc after carbachol in the presence of tetraethylammonium chloride pre-treatment

Dose dacomitinib (D) µM & Tetraethylammonium (T) mM	**0D, 0T**	**0D, 1T**	**1D, 0T**	**1D, 1T**
Δ Isc after carbachol (µA/cm²)	**Group mean**			
5 minutes	107	90.51	96.58	112.2
20 minutes		118	145.1	125

Table 11

Report Title: Part 2 in vitro study

Baseline Isc in the presence of tetraethylammonium chloride post-treatment

Dose dacomitinib (D) µM	**0D, 0T**	**0D, 1T**	**1D, 0T**	**1D, 1T**

& Tetraethylammonium (T) mM				
Baseline Isc (µA/cm^2)	**Group mean**			
5 minutes	7.481*,**	19.20	36.08	4.174*,**
20 minutes		18.67**	30.54	5.968*,**

* Indicates significantly different from DMSO + Tetraethylammonium group (One-Way ANOVA, $p < 0.005$)

** Indicates significantly different from dacomitinib group (One-Way ANOVA, $p < 0.001$)

Table 12

Report Title: Part 2 in vitro study

Baseline Resistance in the presence of tetraethylammonium chloride post-treatment

Dose dacomitinib (D) µM & Tetraethylammonium (T) mM	**0D, 0T**	**0D, 1T**	**1D, 0T**	**1D, 1T**
Baseline Resistance (Ohms/cm^2)	**Group mean**			
5 minutes	554.4*	759.2	717.1*	1211
20 minutes		682.2*	604.7*	1125

* Indicates significantly different from dacomitinib group (One-Way ANOVA, $p < 0.003$)

Table 13

Report Title: Part 2 in vitro study

Baseline conductance in the presence of tetraethylammonium chloride post-treatment

Dose dacomitinib (D) µM & Tetraethylammonium (T) mM	**0D, 0T**	**0D, 1T**	**1D, 0T**	**1D, 1T**
Baseline Conductance (mS/cm^2)	**Group mean**			
5 minutes	2.204	1.360	1.540	0.8957*
20 minutes		1.666	1.663	0.9492*

* Indicates significantly different from DMSO group (One-Way ANOVA, $p < 0.0005$)

Table 14

Report Title: Part 2 in vitro study

Δ Isc after forskolin in the presence of tetraethylammonium chloride post-treatment

Dose dacomitinib (D) µM & Tetraethylammonium (T) mM	**0D, 0T**	**0D, 1T**	**1D, 0T**	**1D, 1T**
Δ Isc after forskolin	**Group mean**			

(µA/cm²)				
5 minutes	16.70	5.080*,**	6.133*,**	16.42
20 minutes		8.618*	4.551*	6.544*

* Indicates significantly different from DMSO vehicle control group (One-Way ANOVA, $p < 0.003$)

** Indicates significantly different from dacomitinib + tetraethylammonium group (One-Way ANOVA, $p < 0.002$)

Table 15

Report Title: Part 2 in vitro study

Δ Isc after carbachol in the presence of tetraethylammonium chloride post-treatment

Dose dacomitinib (D) µM & Tetraethylammonium (T) mM	**0D, 0T**	**0D, 1T**	**1D, 0T**	**1D, 1T**
Δ Isc after carbachol (µA/cm²)	**Group mean**			
5 minutes	107	90.51	96.58	139.7
20 minutes		118	145.1	93.74*

* Indicates significantly different from dacomitinib group (One-Way ANOVA, $p < 0.05$)

END OF RESULTS

DETAILS OF TEST FACILITY, PERSONNEL, AND ARCHIVING

Sponsor Pfizer

Test Facility School of Medical Sciences

The University of Adelaide

Frome Rd, Adelaide, South Australia, 5000 Australia

Study Number Pf1

Principal Study Personnel Joanne Bowen, PhD, University of Adelaide.

Dorothy Keefe, Professor of Cancer Medicine, Royal Adelaide Hospital.

The address of study personnel listed is the same as the Test Facility unless otherwise specified.

Study Director Dr Joanne Bowen, PhD

Technical Support Ysabella Van Sebille

Animal Husbandry N/A

Test Article Formulation N/A

Test Formulation Analysis N/A

Ophthalmoscopy N/A

Clinical Pathology N/A

Histotechnology N/A

Pathology N/A

Peer Review Pathology N/A

Platform Technology and Science Ysabella Van Sebille

Drug Pharmacokinetics N/A

Veterinary Services N/A

Statistical Analysis Ysabella Van Sebille

Report Writing Ysabella Van Sebille

Archival of Records

Data, left over samples, and reports will be stored in the School of Medical Sciences, The University of Adelaide.

INTRODUCTION

Part 1 of this report indicated that the most common adverse event of dacomitinib treatment in rats is diarrhoea. Despite promising response data, the underlying cause of this side effect was not evident in the preclinical (PART 1) component of this study. Therefore, PART 2 was conducted in vitro to further investigate the potential role of chloride secretion on dacomitinib-induced diarrhoea. All doses and concentrations are expressed in terms of the parent compound, which for the purpose of this report is referred to as DACOMITINIB.

Crofelemer is produced from the plant, *Croton lechleri* (active component oligomeric proanthocyanidin), and inhibits both cAMP cystic fibrosis (CFTR) and calcium activated (CaCC) chloride channels. It was hypothesized that If inhibition of HER signaling results in increased intestinal chloride secretion, this agent may be effective at reducing dacomitinib-induced diarrhoea, however PART 1 of this study indicated that crofelemer is not effective at attenuating dacomitinib-induced diarrhoea.

Objective

The objective of the study was to interrogate and correlate changes induced by dacomitinib in PART 1 in an in vitro model.

Rationale for Selection of Dose

Dacomitinib and crofelemer doses were selected based on previous literature.

Dacomitinib was administered at 1 μM in both Ussing chambers (5, 20, 60, 90 minutes) and in Transwells (3, 6, 24, 48 hours) via apical routes to mimic the clinical oral administration. It has previously been described that doses above 1 μM of dacomitinib are where off-targeting or non-specific effects manifest, based on enzymatic analysis (Ather, 2013). Effects at or below 1 μM are therefore more likely to be due to the specific effect of dacomitinib on the HER receptors.

Crofelemer was administered at 10 μM in Ussing chambers (5 and 20 minutes) via apical routes to mimic the clinical oral administration. Crofelemer was only administered at 5 and 20 minute time points, as these times were where most dacomitinib induced chloride secretion was observed. The dose of crofelemer was based on previous research that has shown that 10 μM crofelemer is effective at inhibiting chloride secretion in T84 cells (Tradtrantip, 2014).

Ather F, Hamidi H, Fejzo MS, Letrent S, Finn RS, et al. (2013) Dacomitinib, an Irreversible Pan-ErbB Inhibitor Significantly Abrogates Growth in Head and Neck Cancer Models That Exhibit Low Response to Cetuximab. PLoS ONE 8(2).

Tradtrantrip L, Namkung W, Verkman AS. (2010) Crofelemer, an Antisecretory Antidiarrhoeal Proanthocyanidin Oligomer Extracted from Croton lechleri, Targets Two Distinct Intestinal Chloride Channels. Mol Pharmacol 77(1).

Rationale for Selection of Cells for in vitro Experiments

T84 cells are a representative cell line of colonic epithelium. This cell line has previously been shown to reliably replicate the chloride secretory mechanisms of the intact intestine permitting a detailed examination of intracellular mechanisms intrinsic to the epithelium that regulates the secretory diarrhoea mechanism.

MATERIALS AND METHODS

Test Article and Dose Preparation

PF-00299804 (Dacomitinib) was supplied by Pfizer and was stored at room temperature (18°C) and protected from light. Dacomitinib is soluble in dimethyl sulfoxide (DMSO) at 19 mg/ml; 2.4734 μL aliquots of dacomitinib in DMSO were added to 2 ml of appropriate vehicle (Ringers for Ussing treatment, Media for Transwell treatment), to create a 50 μM concentration. Appropriate volumes were added to either Transwells (3, 6, 24 and 48 hour treatments) or Ussing chambers (5, 20, 60 and 90 minutes) to reach a final concentration of 1 μM. The vehicles were prepared daily. Exposure of DMSO to cells did not exceed 0.01%. The same concentration of DMSO was used as a vehicle control.

Crofelemer was in tablet form and stored at room temperature protected from light in a sterile container. Crofelemer was ground and diluted with DMSO to 21 mg/ml (10 mM) immediately before use, 5 μL of this was added to 5 ml of Ringers in Ussing chambers to reach a desired concentration of 10 μM.

The compounds, vehicle components, suppliers, and batch numbers used are as follows.

Material	Batch Number	Supplier
Dulbecco's Modified Eagle's Medium F-12 Ham (D8437)	RNBD6086	Sigma

Normocin	NOL-37-04	Invitrogen
Penicillin/Gentamicin/Fungizone	AF-28	IMVS Media Production Unit
Foetal Bovine Serum (FBS)	12768	Bovogen
L-glutamine	GLUT-65	IMVS Media Production Unit
Dimethyl Sulfoxide (DMSO)	SHBD9856V	Sigma
Snapwell polyester Transwells	10915014	Corning Costar
Crofelemer (Fulyzaq)	3106372	Salix
Dacomitinib	PF-00299804	Pfizer

Cell Preparation and Maintenance

Cryopreserved T84 cells (passage 5-15) derived from a human colorectal carcinoma were obtained from Culture Collections (Porton Down, UK; 88021101). The T84 cell line retained its original morphology and growth characteristics over the range of passages used.

Cells were thawed in a 37°C water bath and maintained in a 75 cm2 or 150 cm2 sterile cell culture flask (Corning Life Sciences, MA, USA) at 37°C with 5 % CO2. T84 cell culture media was Dulbecco's Modified Eagle Medium/Ham's F-12 Nutrient Mixture containing 15 mM HEPES, L-glutamine and sodium bicarbonate, supplemented with 1 % penicillin/gentamicin+fungizone, 10 % foetal bovine serum and 1 mM l-glutamine (complete DMEM). Experimental cell cultures were grown in sterile, multi-well tissue culture plates under identical growth conditions. Cell lines were routinely passaged when culture monolayers reached approximately 80 % confluence at subculture ratios between 1:3 and 1:6 in fresh growth medium. Cells were detached by aspirating growth medium, washing with 1X phosphate

buffered saline (PBS; pH 7.4) and incubating with 3 ml of trypsin-EDTA for 10 min at 37°C. The reaction was then quenched by the addition of growth medium. Cells were centrifuged at 300 g for 5 min, supernatant removed and cells resuspended in fresh, complete DMEM. Cell counts were conducted using an automated cell counter (BioRad, NSA, Australia) and were seeded into 1.12 cm^2, 0.4 mm pore polyester Transwell inserts (Corning Life Sciences, MA, USA; CLS3801). T84 cells were seeded at a density of 100,000 cells/cm^2. Cell culture media in both the apical and basolateral chambers was changed every 48 hours. Transepithelial electrical resistance (TEER) was measured daily using am EVOM2 epithelial volt-ohm-meter with chopstick electrodes (World Precision Instruments, Sarasota, FL, USA) for 1 week during the growth period and area adjusted for analysis using the following formula; TEER monolayer (W/cm2) = [raw TEER (W) – TEER blank (W)]/area of membrane (cm2). All experiments were repeated eight times.

STUDY DESIGN

Ion channel analysis: To test whether dacomitinib increased intestinal epithelial cell Cl^- secretion, short-circuit current (Isc) was measured in T84 cells in symmetrical physiological solutions in Ussing chambers. T84 monolayers were grown on polyester Transwell membranes and once adequate resistance was reached (determined by TEER of > 1000 Ω □ cm), were then treated with 1 µM dacomitinib, DMSO (negative control) and mounted into Ussing chambers. Exposure time of T84 monolayers to dacomitinib included 5, 20, 60, and 90 minutes (administration in Ussing chambers), and 3, 6, 24 and 48 hours (administration in Transwell). Inserts were mounted into sliders and bathed in Ringers solution (R) (composition in mmol/L: NaCl 115.4; KCl 5; $MgCl_2$ 1.2; NaH_2PO_4 0.6; $NaHCO_3$ 25; $CaCl_2$ 1.2 and glucose 10) continuously gassed with carbogen. Short circuit current and resistance were measured throughout the experiment set up using Acquire and Analyse software (Physiologic Instruments).

Peak activity of dacomitinib-induced chloride secretion was assessed, and crofelemer was administered at these times points.

The following table summarises study design.

Exposure time to dacomitinib or DMSO control	Administered Forskolin	Administered Carbachol	Administered Tetraeyhtlammonium (+Forskolin) (+Carbachol)	Administered Crofelemer (+Forskolin) (+Carbachol)
5 minutes	n=8	n=8	n=8 (pre-treatment tetraethylammonium) n=8 (post-treatment tetraethylammonium)	n=8
20 minutes	n=8	n=8	n=8 (pre-treatment tetraethylammonium) n=8 (post-treatment tetraethylammonium)	n=8
60 minutes	n=8	n=8	Time course discontinued	Time course discontinued
90 minutes	n=8	n=8	Time course discontinued	Time course discontinued
3 hours	n=8	n=8	Time course discontinued	Time course discontinued
6 hours	n=8	n=8	Time course discontinued	Time course discontinued
24 hours	n=8	n=8	Time course discontinued	Time course discontinued

48 hours	n=8	n=8	Time course discontinued	Time course discontinued

MEASUREMENTS AND OBSERVATIONS

Monolayer Integrity

A viability check was performed prior to monolayer treatment and mounting in Ussing chambers to assess the integrity of the monolayer. If monolayers had a TEER of < 1000 Ω □ cm they were excluded from the study, as reliable results could not be assured.

Epithelial Electrogenic Ion Transport

T84 monolayers on Transwells were bathed with 5 ml of carbogen-gassed ringers solution on each side. Each reservoir was gassed with 95 % O2 - 5 % CO2 and kept at constant temperature of 37°C. Electrogenic ion transport was monitored continuously as short-circuit current (Isc) by using an automated multichannel voltage/current clamp apparatus (VCC MC8) (Physiologic Instruments) linked through Acquire Analyze 2.3 computer program. Baseline readings were recorded to assess baseline differences in electrophysiological function. Amiloride was administered at a concentration of 20 μM to the apical chamber to inhibit the epithelial sodium channel (ENaC). This priming step was conducted in all experiments to inhibit sodium reabsorption, so that all results can be solely attributed to the movement of ions in a luminal direction. Forskolin was administered at a concentration of 10 μM to the basolateral chamber to elevate levels of cAMP to activate CFTR chloride channels. Carbachol was administered at a concentration of 100 μM to the basolateral chamber to elevate levels of calcium to activate the CaCC. Tetraethylammonium was administered at a concentration of 1 mM to the basolateral chamber to inhibit basolateral potassium channels.

Material	Batch Number	Supplier
Amiloride	BCBC4358V	Sigma
Tetraethylammonium	BCBF2894V	Sigma
Forskolin	SLB3902V	Sigma
Carbachol	BCBG1471V	Sigma

Computer Systems

The computer systems that were used on this study to acquire and quantify data include: Windows (Word, Excel), Prism version 6, Acquire and Analyse 2.3 (Physiologic Instruments).

Analysis of Data

Numeric data for delta short circuit current, baseline resistance, conductance, short circuit current, and voltage are expressed as the arithmetic mean for each group. The test article groups were compared with the DMSO control groups. All baseline readings are an average of each monolayer over 5 minutes. All data has been area adjusted (1.12 cm^2) The assumptions of equality of variance for each group and normally distributed data were tested using Tukey's test after performing the 1-way analysis of variance (ANOVA).

RESULTS

Noteworthy findings are described in this section. No specific mention is made of minor differences between groups if considered not related to test article administration.

Determining optimal time point to investigate dacomitinib-induced chloride secretion

All measurements were taken using Acquire and Analyse linked to Physiological systems Ussing chambers.

To test whether dacomitinib induced intestinal chloride secretion, short circuit current (Isc) was measured in T84 cell monolayers in symmetrical physiological solutions. Analysis began with T84 monolayers treated with dacomitinib only, to determine the optimal time point to further investigate precise mechanisms. Dacomitinib was exposed to T84 monolayers at 5, 20, 60 and 90 minutes, and 3, 6, 24 and 48 hours. Baseline chloride secretion was significantly increased ($p < 0.0001$) compared to controls in cells that had 5 and 20 minutes exposure time to dacomitinib. Baseline resistance and conductance were also measured, however the results of this are not considered noteworthy. All further experiments were conducted at 5 and 20 minute time points.

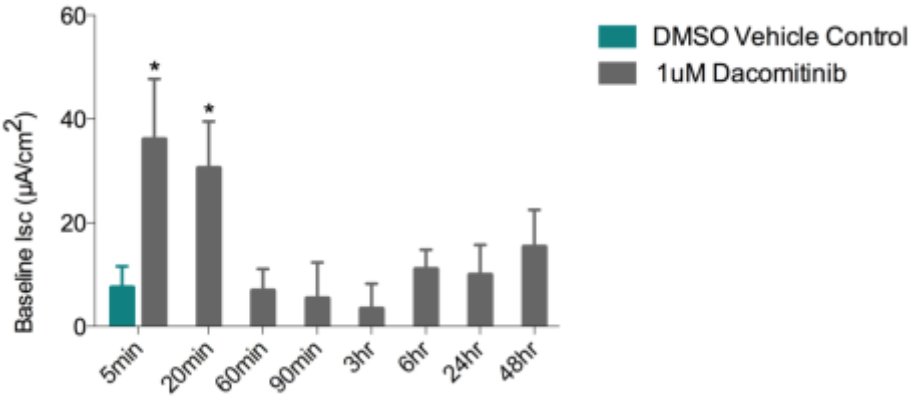

* Indicates significantly different from DMSO vehicle control (One-Way ANOVA, $p < 0.0001$)

Investigating dacomitinib-induced chloride secretion via the CFTR and CaCC chloride channels

To test the effect of dacomitinib on the CFTR chloride channel, delta values of short circuit current were measured following the administration of cAMP agonist forskolin. Exposure to dacomitinib did not increase chloride secretion specifically via the CFTR chloride channel, as there was a significantly decreased response to CFTR chloride channel activation with administration of forskolin compared to controls ($p < 0.05$).

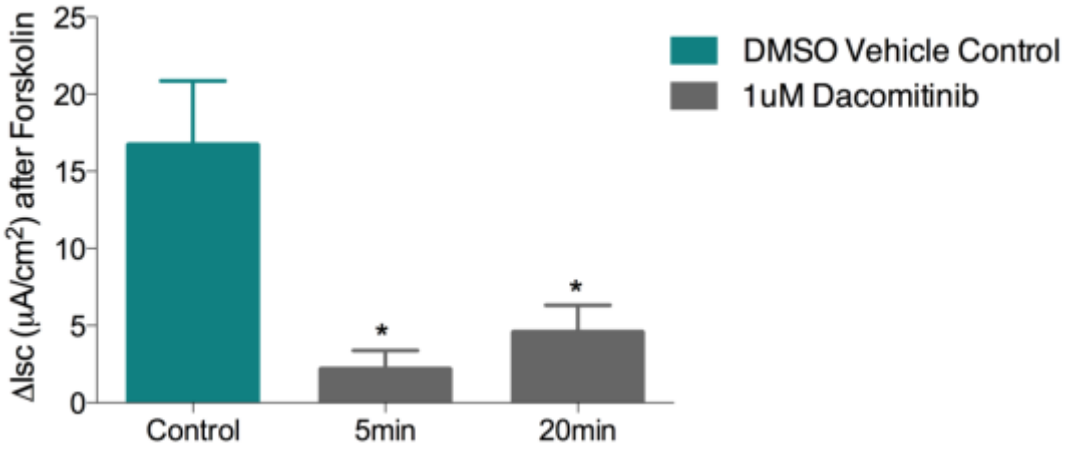

*Indicates significantly different from DMSO vehicle control (One-Way ANOVA, $p < 0.05$)

To test the effect of dacomitinib on the calcium activated chloride channel, delta values of short circuit current were measured following the administration of calcium agonist carbachol. Exposure to dacomitinib did not increase chloride secretion specifically via the CaCC, as there was no significant difference in response to CaCC activation with administration of carbachol compared to controls ($p > 0.05$).

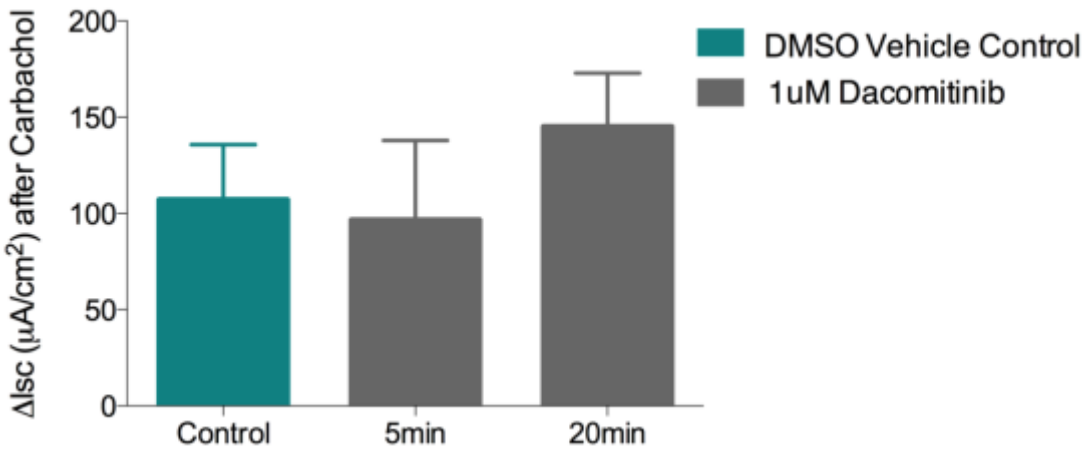

Investigating the effect of dacomitinib-induced chloride secretion via the potassium channel

Given the role of the HER receptors on inhibiting the basolateral potassium channel, tetraethylammonium was administered to inhibit this channel. Treatment included both pre and post exposure to dacomitinib, with no significant differences noted in treatment schedule. The presence of tetraethylammonium did not change the effect of dacomitinib on short circuit current described in sections 14.1, and 14.2.

Investigating the effect of crofelemer on inhibiting dacomitinib-induced chloride secretion

To assess if crofelemer was effective at inhibiting dacomitinib-induced intestinal chloride secretion, baseline short circuit current was assessed at key time points. Baseline short circuit current indicated that crofelemer significantly attenuated dacomitinib-induced intestinal chloride secretion ($p < 0.0001$) supporting the study hypothesis.

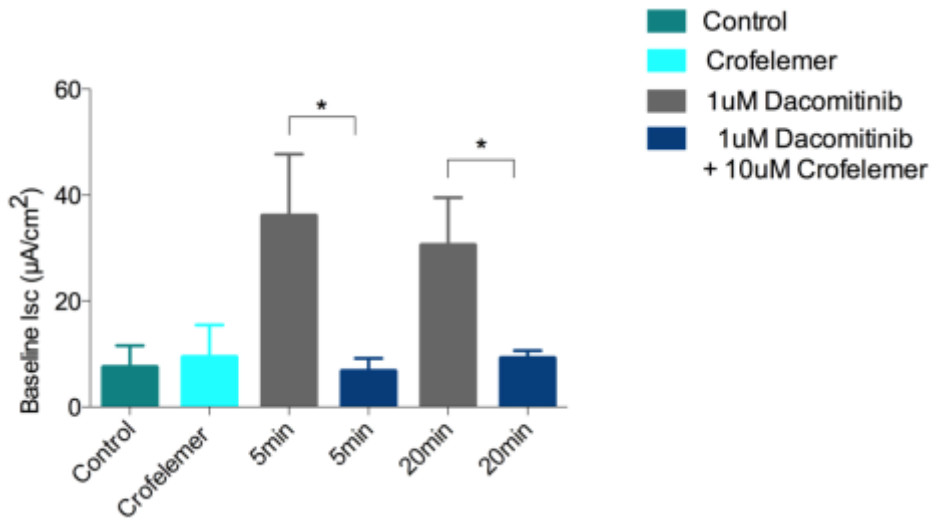

*Indicates significance (One-Way ANOVA, $p < 0.00001$)

To assess if the decrease in baseline short circuit current induced by crofelemer was due to CFTR chloride channels, the cAMP agonist forskolin was applied to activate the CFTR chloride channels, and the delta Isc recorded. Results indicated that crofelemer does not decrease chloride secretion via the CFTR chloride channel. At the 5 minute time point, the inhibitory action of crofelemer on dacomitinib induced chloride secretion was lost, and was significantly higher ($p = 0.0023$). Crofelemer administered alone did not change ($p > 0.05$) chloride secretion via the CFTR chloride channel.

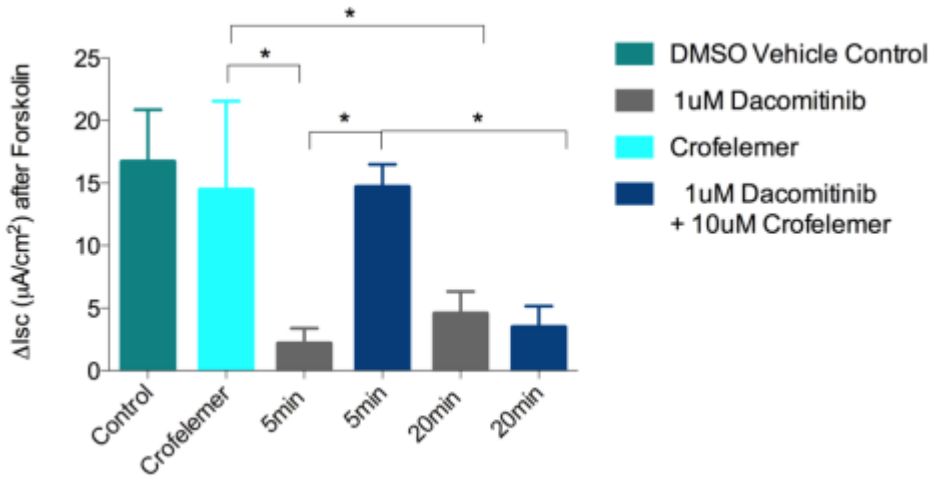

*Indicates significance (One-Way ANOVA, $p < 0.00001$)

To assess if the decrease in baseline short circuit current induced by crofelemer was due to CaCC, the calcium agonist carbachol was applied to activate the calcium activated chloride channels, and the delta Isc recorded. Crofelemer exposed cells had a decreased response to carbachol compared to controls ($p < 0.0001$). These results indicate that crofelemer works primarily via the CaCC, consistent with the literature. Response to carbachol was significantly decreased in cells exposed to dacomitinib/crofelemer combination compared to dacomitinib alone at both time points ($p < 0.0001$), suggesting that changes seen in baseline short circuit current are due to inhibition of CaCC and not CFTR.

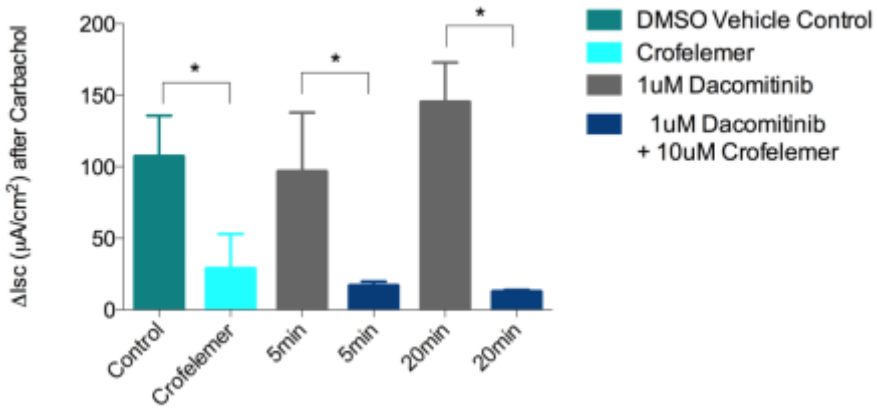

*Indicates significance (One-Way ANOVA, $p < 0.00001$)

DISCUSSION

The purpose of these experiments was to investigate the mechanisms of dacomitinib-induced diarrhoea by investigating intestinal chloride secretion. The first component of the in vitro arm (PART 2) of this study aimed to determine the optimal time to investigate dacomitinib-induced intestinal chloride secretion, the second component aimed to investigate the mechanisms of chloride secretion, and the effect of inhibiting chloride secretion with crofelemer.

We were successful in determining the optimal time to investigate dacomitinib-induced chloride secretion. After 5 and 20 minutes of exposure to dacomitinib, T84 monolayers had significantly increased chloride secretion. This effect was lost at exposure times exceeding 20 minutes. Therefore, only these time points were continued for all other investigations. The results of this study indicate that dacomitinib increases intestinal chloride secretion. However, this is inconsistent with the in vivo (PART 1) aspect of the study. This may be due to timing, as in vivo secretory analysis occurred a number of hours after dacomitinib treatment. The in vitro aspect of this study showed that dacomitinib significantly increased chloride secretion, but not when exposure exceeds 20 minutes. This suggests that the effect of dacomitinib on intestinal chloride secretion is immediate and transient.

The cellular secretory targets of dacomitinib were further investigated, focusing on the principal luminal membrane determinants of intestinal fluid secretion by administering forskolin and carbachol. We found that dacomitinib induced chloride secretion via the apical membrane calcium-stimulated Cl^- channels, but not the cAMP-stimulated CFTR Cl^- channels. In normal physiological conditions, the HER receptors negatively regulate basolateral K^+ channels, therefore these channels were inhibited with tetraethylammonium to assess the role of this ion channel in dacomitinib-induced intestinal chloride secretion. The baseline effects seen following dacomitinib treatment did not change when K^+ channels were inhibited, suggesting that this ion channel is not involved in dacomitinib-induced chloride secretion.

Crofelemer was administered at key time points, when dacomitinib-induced intestinal chloride secretion was most increased. When crofelemer was administered to T84 monolayers that had been exposed to dacomitinib, baseline chloride secretion was significantly reduced. This is consistent with the study hypothesis. However, this result

was lost when implemented in the in vivo setting, suggesting that the cellular secretory processes of dacomitinib and crofelemer are not translatable into a fully functioning physiological setting. The administration of forskolin and carbachol indicated that crofelemer inhibited chloride secretion predominantly via the CaCC, which is consistent with previous literature on crofelemer and optimal for dacomitinib-induced intestinal chloride secretion; given that we determined that this was driven predominantly via the CaCC.

CONCLUSION

The mechanisms underlying development of diarrhoea in this model require further investigation. The hypothesis of this study was that dacomitinib-induced diarrhoea is driven by intestinal chloride secretion; because in normal physiological settings HER receptors negatively regulate the principal chloride channels, and so when dacomitinib inhibits these receptors, the negative regulation is lost. The in vitro component of this study supported this hypothesis, and was able to attenuate the increased chloride secretion with crofelemer, identifying the CaCC as the primary channel for this. However, this did not translate in the in vivo component of the study. Nevertheless given the in vitro findings, this hypothesis should not be discounted.